

Catalytic Dehydrogenative Cross-Coupling: Forming Carbon–Carbon Bonds by Oxidizing Two Carbon–Hydrogen Bonds

Charles S. Yeung and Vy M. Dong*

Department of Chemistry, University of Toronto, 80 St. George Street, Toronto, Ontario, Canada M5S 3H6

CONTENTS

1. Introduction	1215
2. Cross-Coupling via a Heck-Type Mechanism	1216
2.1. Recent Advances in Arene–Alkene Coupling	1216
2.2. Intramolecular Arene–Alkene Coupling	1224
2.3. Arene–Benzoquinone Coupling	1224
2.4. Arene–Alkene Coupling Catalyzed by Metals Other than Palladium	1227
2.5. Alkene–Alkene Cross-Coupling	1230
2.6. Enolate–Alkene Coupling	1233
2.7. Miscellaneous Examples	1234
3. Cross-Coupling of Two Arenes Catalyzed by Palladium	1235
3.1. Intermolecular Biaryl Bond Formation	1236
3.2. Intramolecular Biaryl Bond Formation	1244
3.3. Miscellaneous Examples	1247
4. Cross-Coupling via Ionic Intermediates	1247
4.1. α -Functionalization of Amines	1248
4.2. α -Functionalization of Ethers	1255
4.3. Allylic C–H Bond Functionalization	1256
4.4. Benzylic C–H Bond Functionalization	1257
4.5. Biaryl Bond Formation	1260
4.6. Miscellaneous Examples	1262
5. Cross-Coupling via Radical Intermediates	1262
5.1. Biaryl Bond Formation	1263
5.2. α -Arylation of Aldehydes by Organo-SOMO Catalysis	1266
5.3. Enolate–Enolate Cross-Coupling	1266
5.4. Functionalization of Simple Alkanes	1271
6. Enzyme-Catalyzed Oxidative Coupling	1274
7. Other Mechanisms for Cross-Coupling	1277
7.1. Indole Synthesis by Intramolecular Coupling	1277
7.2. Sonogashira-Type Cross-Coupling	1279
7.3. Cross-Coupling Aldehydic C–H Bonds	1283
7.4. Miscellaneous Examples	1285
8. Conclusions and Outlook	1285
Author Information	1286
Biographies	1286
Acknowledgment	1286

Abbreviations	1286
References	1288

1. INTRODUCTION

Inspired by the need for green and sustainable chemistry,¹ synthetic chemists seek more efficient ways to construct carbon–carbon (C–C) bonds, the essential link in all organic molecules.² In recent years, building a carbon–carbon linkage directly from two simple carbon–hydrogen (C–H) bonds has emerged as an attractive and challenging goal in catalysis (Figure 1). Tandem oxidation of C–H bonds allows use of simple (i.e., less functionalized) reagents and often reduces the number of steps to the target molecule.³ The benefits of this strategy include lower cost and less waste, but the challenges to achieving oxidative cross-coupling are many. Despite being termed *catalytic dehydrogenative cross-coupling* (CDC),⁴ hydrogen gas is not usually the byproduct of these transformations. The thermodynamics of making a C–C bond with loss of H₂ is typically unfavorable and thus requires an external driving force, namely, an appropriate sacrificial oxidant. Other challenges include overcoming the low reactivity of C–H bonds, achieving site selective functionalization of one C–H bond in the presence of all others, and outcompeting dimerization.⁵ Yet, examples of oxidative cross-coupling have been demonstrated—a survey of the literature reveals isolated reports dating back to the early 1960s and a steady increase in accounts over the last 10 years.

In the following article, we review transformations that can be categorized as catalytic dehydrogenative cross-couplings. These couplings are arranged by their proposed mechanisms,⁶ including those that involve Heck-type processes,⁷ direct arylations,^{8,9} ionic intermediates,⁴ or radical intermediates. Our goal is to highlight the scope and limits of this general strategy, as well as its specific application in asymmetric catalysis and natural product synthesis. Oxidative C–C bond formation has been achieved by various catalysts, including transition metals, organocatalysts, the combined use of metal and organocatalysts, and enzymes. It is a topic that spans different modes of activation and a challenge that will continue to drive discoveries in organic chemistry. We hope this review will serve as a handy reference for chemists interested in using catalytic dehydrogenative coupling in multistep synthesis

Special Issue: 2011 Frontiers in Transition Metal Catalyzed Reactions

Received: August 24, 2010

Published: March 09, 2011

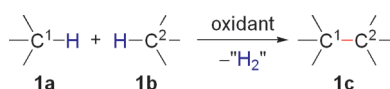


Figure 1. General scheme for oxidative C–C cross-coupling.

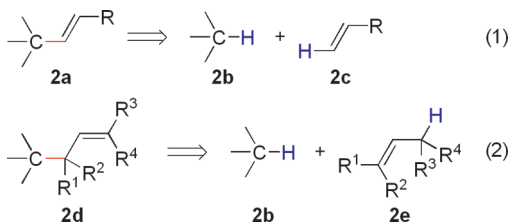


Figure 2. General cross-couplings via Heck-type mechanisms.

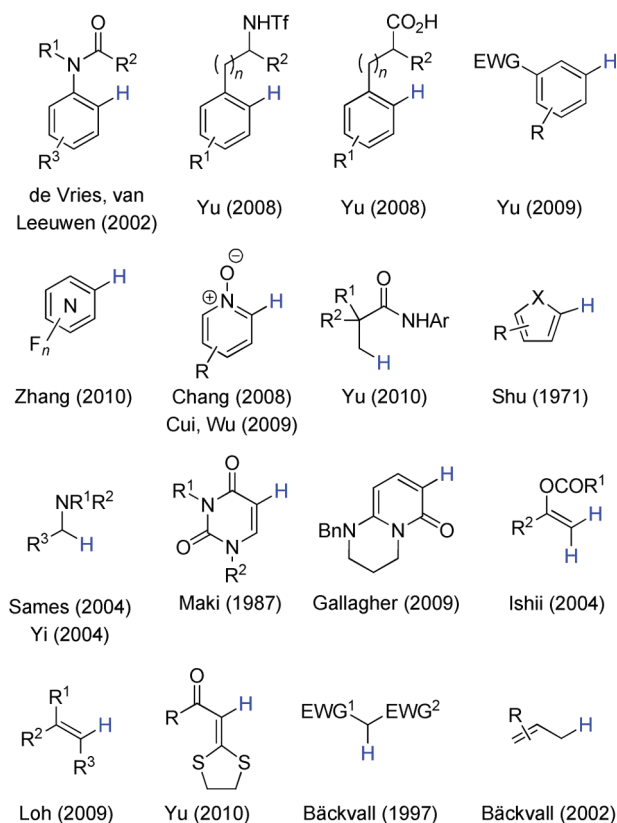
Substrates

Figure 3. Overview of cross-couplings via Heck-type mechanisms.

and those interested in inventing greener methods for C–C bond construction.

2. CROSS-COUPLING VIA A HECK-TYPE MECHANISM

Olefins represent basic building blocks, and stereoselective methods for their preparation are highly valued. A promising method for making alkenes combines C–H bond functionalization with a Heck-type alkenylation (Figure 2).¹⁰ In this process, a transition metal promotes selective C–H bond activation to generate an organometallic complex with a M–C bond that can subsequently insert into C=C double bonds, yielding an intermediate that undergoes β -H elimination to furnish the desired

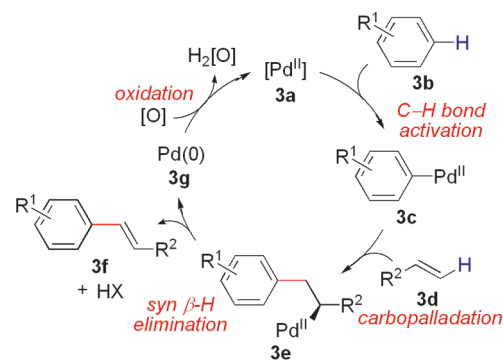
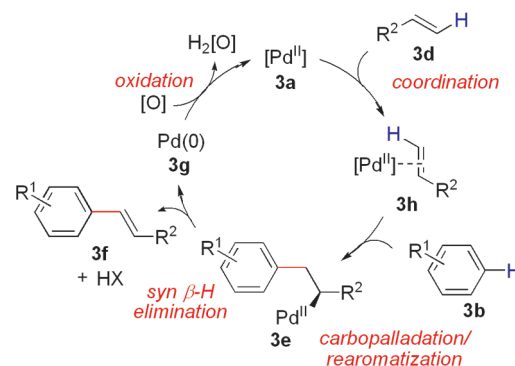
a) Oxidative Heck-type alkenylation by C–H palladation**b) Oxidative Heck-type alkenylation by intermolecular carbopalladation**

Figure 4. General mechanisms for Pd-catalyzed oxidative C–C cross-coupling involving Heck-type alkenylation.

product (Figure 2, eq 1). The regioselectivity for C–H functionalization of the alkene partner can be predicted based on the well-established mechanism of the Heck reaction. Depending on the olefin substrate chosen, β -H elimination can also occur with translocation of the C=C double bond (Figure 2, eq 2). Figure 3 depicts different substrates that cross-couple to alkenes, including arenes bearing Lewis basic groups (e.g., amides, carboxylates), electron-rich heteroarenes, other alkenes, and substrates with reactive sp^3 C–H bonds.

In oxidative Heck-type alkenylations, palladium salts have been the catalyst of choice. Fujiwara and co-workers reported initial accounts on Pd-mediated cross-coupling between arenes and olefins in the late 1960s.¹¹ As shown in Figure 4a, the mechanism involves the electrophilic palladation of arene ring 3b with a Pd(II) catalyst to generate arylpalladium intermediate 3c. Subsequent carbopalladation of olefin 3d leads to alkylpalladium complex 3e that undergoes $\text{syn-}\beta$ -H elimination to yield styrenyl product 3f and Pd(0) (3g). The final step of the catalytic cycle is oxidation of Pd(0) to Pd(II), using Cu salts, Ag salts, benzoquinone, O_2 , and peroxides, among other oxidants examined.^{7,12} In an alternative mechanism, the Pd(II) catalyst is proposed to coordinate to the olefin, which enhances its electrophilicity and propensity to undergo nucleophilic addition with electron-rich aromatic rings (Figure 4b).¹³ Intermediate 3e is also intercepted in this pathway.

2.1. Recent Advances in Arene–Alkene Coupling

Oxidative arene alkenylations has been reviewed,⁷ and selected recent examples will be discussed here. In 2002, the groups of de Vries and van Leeuwen reported an exceptionally mild

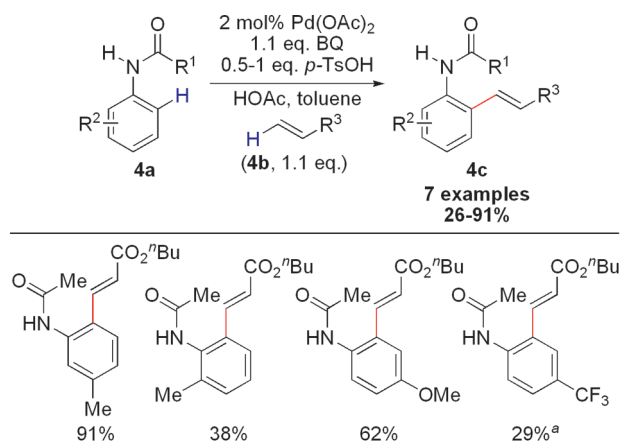


Figure 5. Pd-catalyzed oxidative *ortho*-alkenylation of anilides at room temperature.¹⁴

^aYield determined by GC.

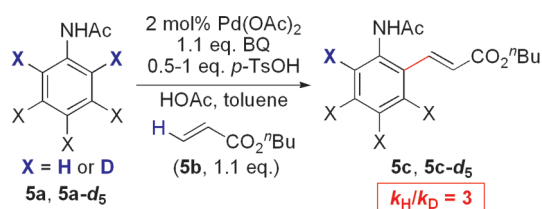


Figure 6. Kinetic isotope effect study for Pd-catalyzed oxidative *ortho*-alkenylation of anilides at room temperature.¹⁴

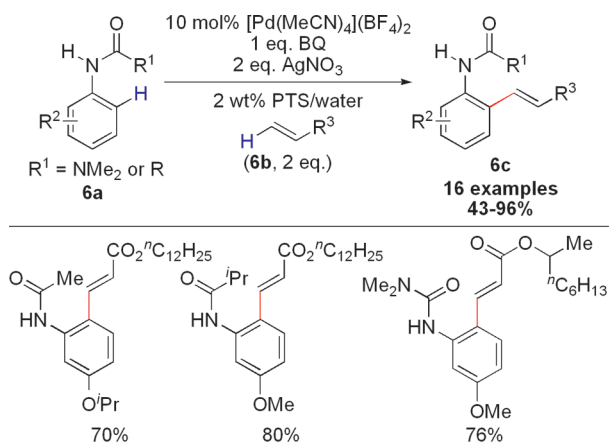


Figure 7. Pd-catalyzed *ortho*-alkenylation of anilides at room temperature in water.¹⁵

oxidative Heck-type olefination that uses amide directing groups to control reactivity and regioselectivity (Figure 5).¹⁴ Selective *ortho*-alkenylation of anilides (**4a**) takes place under palladium catalysis, whereas other metal complexes, including $\text{Ru}_3(\text{CO})_{12}$, $[\text{RuCl}_2(p\text{-cymene})]_2$, PtCl_2 , $\text{Ni}(\text{OAc})_2$, PdCl_2 , and $\text{Pd}(\text{PPh}_3)_2\text{Cl}_2$, are ineffective. Whereas the addition of inorganic acids is detrimental to reaction efficiency, p -toluenesulfonic acid has a large beneficial effect, because counterion exchange produces $\text{Pd}(\text{OTs})_2$ (**7a**), a highly electrophilic catalyst capable of undergoing facile C–H palladation. As such, coordinating solvents

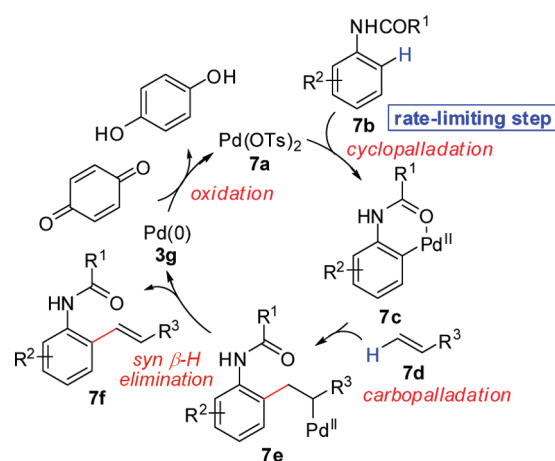


Figure 8. Proposed mechanism for Pd-catalyzed *ortho*-alkenylation of anilides.

(e.g., NMP) hamper the desired reaction. Benzoquinone is the optimal oxidant, superior to both $\text{Cu}(\text{OAc})_2$ and H_2O_2 , and may additionally play a role as a ligand for palladium. A free N–H bond on the amide functionality is crucial—protected anilides (e.g., N–Me) exhibit no observed reactivity. de Vries and van Leeuwen conducted competition experiments revealing that electron-rich anilides react at a faster rate than electron-deficient ones ($\rho^+ = 2.2$). A large kinetic isotope effect on the anilide cross-coupling partner was measured ($k_{\text{H}}/k_{\text{D}} = 3$) (Figure 6). To further study this mechanism, the authors prepared a palladacycle derived from an anilide coupling partner via *ortho*-C–H activation and found that this palladium complex displays higher reaction rates than *in situ* generated catalysts. On the basis of this data, the authors proposed that electrophilic palladation of the anilide starting material **7b** is the turnover-limiting step (Figure 8). The resulting palladacycle **7c** undergoes carbopalladation to install the new C–C bond and subsequent $\beta\text{-H}$ elimination to furnish the *ortho*-alkenylation product **7f**. Lipshutz and co-workers reported a similar reaction using cationic Pd catalysts in water in the presence of a suitable surfactant, with PTS (i.e., polyoxyethanyl α -tocopheryl sebacate) being superior to Brij 35, Triton X-100, and Solutol (Figure 7).¹⁵ Both amide and urea directing groups promote this oxidative *ortho*-alkenylation.

Lloyd-Jones, Booker-Milburn, and co-workers demonstrated that intermolecular oxidative cross-coupling between phenylureas (**8a**) and dienes (**8b**) affords indoline products by *ortho*-alkenylation followed by cyclization (**8c**, Figure 9).¹⁶ In this *interrupted* Heck reaction, carbopalladation yields a Pd π -allyl intermediate **9b** that can undergo nucleophilic displacement as highlighted in Figure 10. Although oxidative conditions are used for this transformation, overoxidation to the corresponding indoles is not observed. The authors note that Ac_2O is added to keep the conditions anhydrous; accordingly, 3A MS can be used instead without changing the overall catalytic efficiency. The highly electrophilic species $\text{Pd}(\text{OTs})_2$ is proposed to be the active catalyst for this cyclization. In the case where either R^2 or $\text{R}^3 = \text{H}$ (see Figure 9), Lloyd-Jones and Booker-Milburn observe a second cyclization event by a conjugate addition mechanism to afford tricyclic product **8d** as a single diastereomer. In this reaction, one C–C bond and two C–N bonds are formed at the expense of two C–H bonds, a C=C double bond, and benzoquinone.

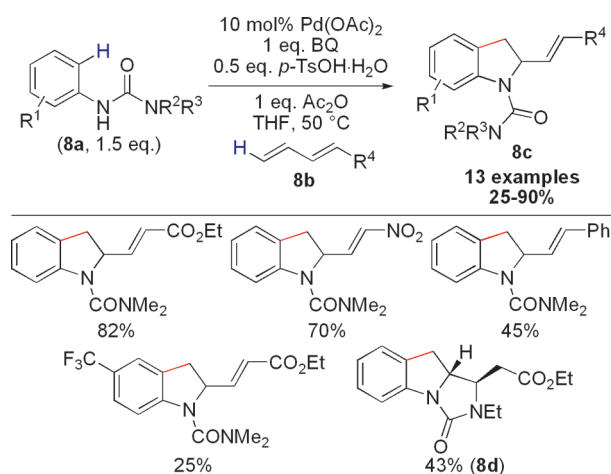


Figure 9. Pd-catalyzed *ortho*-alkenylation of ureas toward indoline synthesis.¹⁶

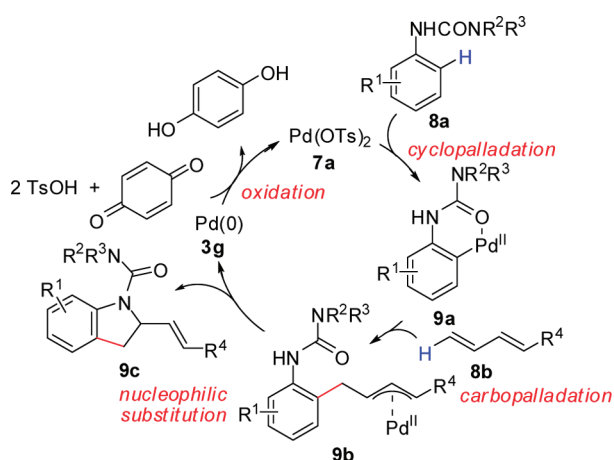


Figure 10. Proposed mechanism for Pd-catalyzed *ortho*-alkenylation of ureas toward indoline synthesis.

A related alkenylation of homobenzyl- and bishomobenzylamides (**10a**) was reported by the Yu group to provide pharmaceutically relevant motifs (Figure 11).¹⁷ It is proposed that cyclopalladation initiates this transformation: homobenzylamides form a six-membered palladacycle, whereas bishomobenzylamides result in a seven-membered palladacycle. When methyl vinyl ketone is the olefin partner, an intramolecular conjugate addition reaction results in tetrahydroisoquinoline products (e.g., **10d**); this tandem C–C bond dehydrogenation/cyclization occurs with excellent diastereoselectivity and complements traditional Pictet–Spengler and Bischler–Napieralski reactions.¹⁸ Yu's olefination shows high compatibility with functional groups—even a sensitive C–OTf can be tolerated under these mild conditions (e.g., **10d**).¹⁷ Triflimide **11a** can undergo difunctionalization via C–H alkenylation of both C2 and C4 positions (Figure 12) to make useful tryptophan analogues by a late-stage C–H oxidation.¹⁹

In a complementary oxidative coupling of phenylacetic acids (**12a**) and olefins (**12b**), Yu proposes that weak interactions between the C=O of the carboxylate and Pd(OAc)₂ promote *ortho*-C–H bond functionalization (Figure 13).²⁰ These mild conditions afford functionalized phenylacetic acid derivatives in

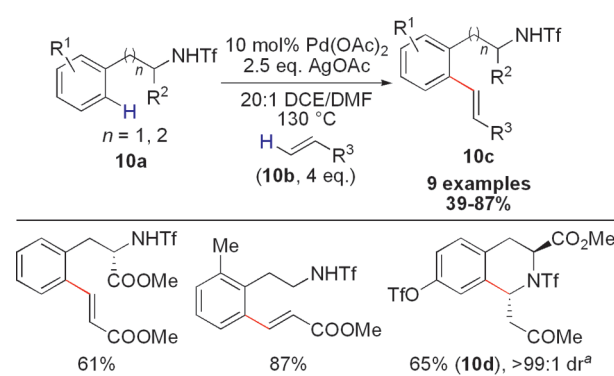


Figure 11. Pd-catalyzed *ortho*-alkenylation of homoallyl- and bishomoallylamides.¹⁷

^aReaction conducted in 10:1 DCE/DMF.

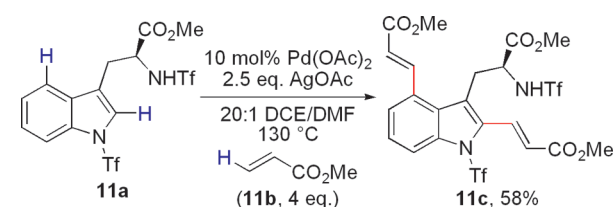


Figure 12. Pd-catalyzed bisalkenylation of (*S*)-tryptophan *N*-triflimide methyl ester.¹⁷

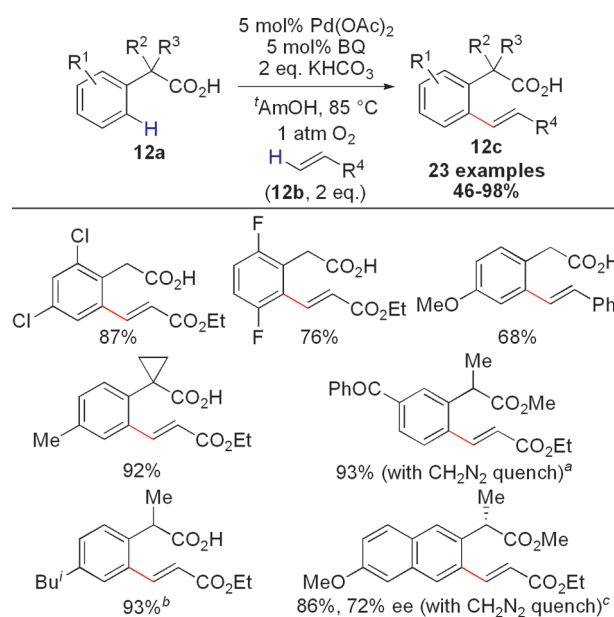


Figure 13. Pd-catalyzed *ortho*-alkenylation of phenylacetic acids.²⁰

^aProduct derived from *ortho*-alkenylation of ketoprofen.

^bProduct derived from *ortho*-alkenylation of ibuprofen.

^cProduct derived from *ortho*-alkenylation of naproxen.

moderate to excellent efficiencies with broad functional group compatibility. Nonsteroidal anti-inflammatory drugs (NSAIDs) ketoprofen, ibuprofen, and naproxen react smoothly with a range of alkene coupling partners. Optically pure naproxen (97% ee) affords the olefination product with an eroded enantiomeric excess (72% ee). Substituting KHCO₃ with Li₂CO₃, however,

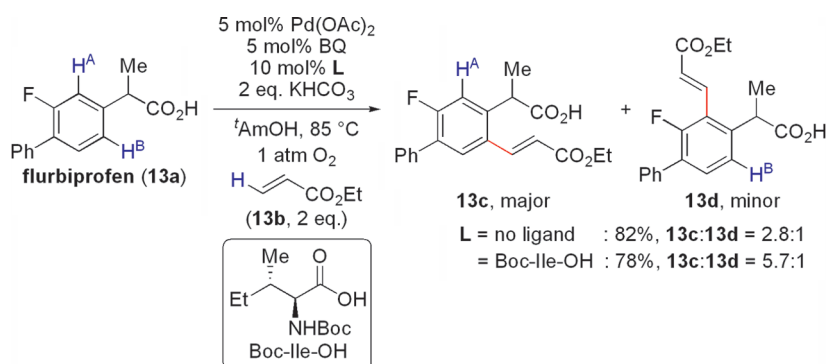


Figure 14. Pd-catalyzed regioselective *ortho*-alkenylation of flurbiprofen (**13a**).²⁰

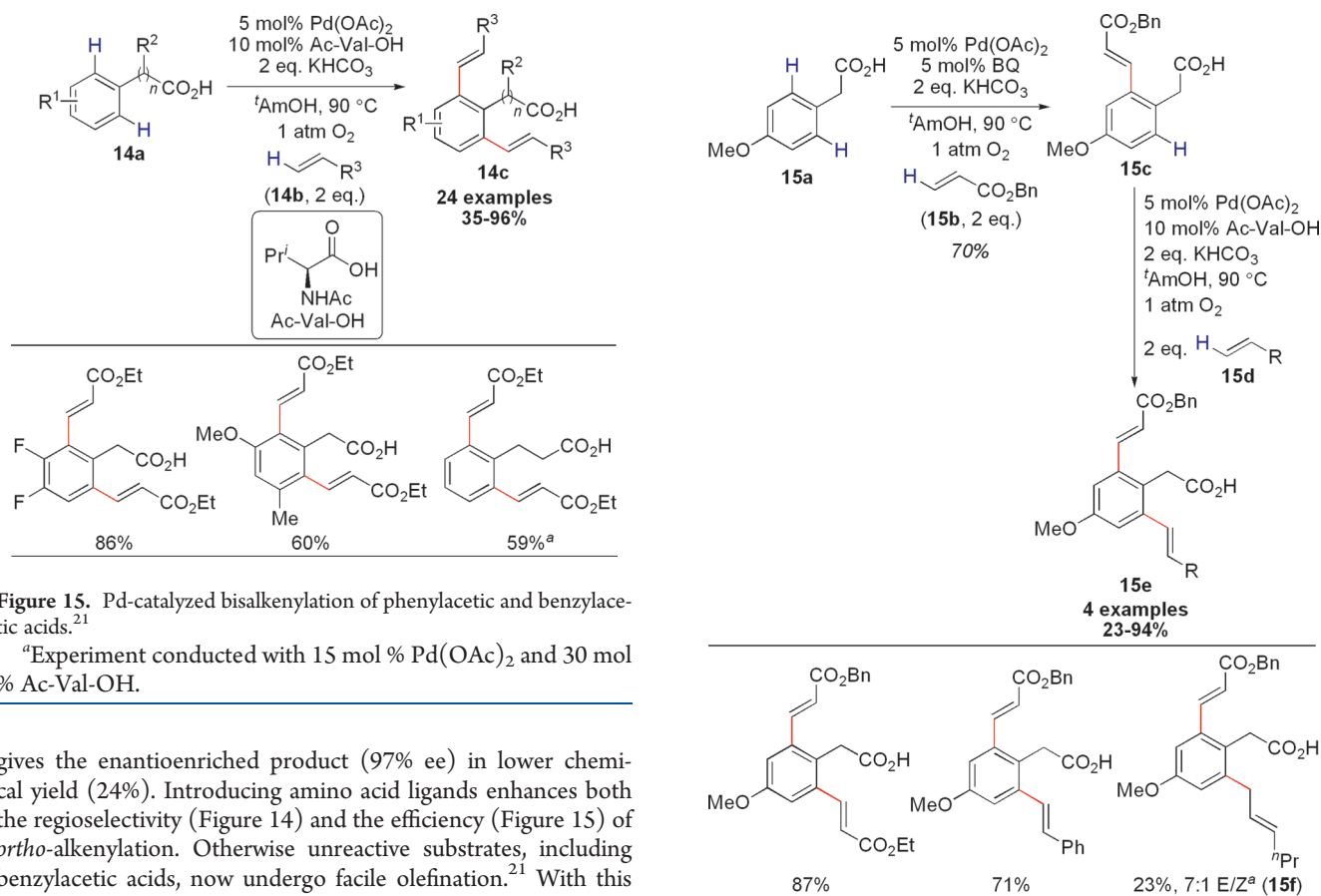


Figure 15. Pd-catalyzed bisalkenylation of phenylacetic and benzylacetic acids.²¹

^aExperiment conducted with 15 mol % Pd(OAc)₂ and 30 mol % Ac-Val-OH.

gives the enantioenriched product (97% ee) in lower chemical yield (24%). Introducing amino acid ligands enhances both the regioselectivity (Figure 14) and the efficiency (Figure 15) of *ortho*-alkenylation. Otherwise unreactive substrates, including benzylacetic acids, now undergo facile olefination.²¹ With this approach, the naphthoic acid cores of both neocarzinostatin and kedarcidin were prepared.²⁰ Iterative C–H bond alkenylation with different olefin coupling partners is also possible (Figures 16 and 17): in a two-step sequence, Pd catalysis provides phenylacetic acids with different *ortho*-alkene substituents.²¹ Terminal alkenes typically undergo coupling at the terminal C–H bond, but unactivated olefins such as 1-hexene afford unique nonconjugated products resulting from a different β -H elimination (e.g., **15f**). Isomerization to the more thermodynamically favorable conjugated system is not observed.

Yu's oxidative alkenylations can be performed with catalyst loadings as low as 0.2 mol % for electron-deficient phenylacetic acids with TON = 455 in the presence of Ac-Ile-OH (Figure 18).²² This olefination is a rare example of *ligand-accelerated* catalysis in oxidative couplings, and one that operates at practical catalyst loadings (Figure 19). In contrast to other Heck reactions, this

Figure 16. Iterative Pd-catalyzed bisalkenylation of 4-methoxyphenylacetic acid.²¹

^a1 equiv 1-hexene was used as the Heck acceptor in the second iteration.

reaction is more green and generates water (formed via reduction of O₂) as the only waste product.

The Yu group performed mechanistic studies to better understand the high reactivities afforded by protected amino acid ligands.²² A competition study between 2-(2-(trifluoromethyl)phenyl)acetic acid (**17a**) and 2-*o*-tolylacetic acid (**19a**) reveals preferential alkenylation of the more electron-rich phenylacetic acid. However, in the presence of Ac-Ile-OH, this selectivity is reversed (Figure 20). Initial rate studies for oxidative olefinations of **17a** and **19a** revealed a similar trend. In an intermolecular

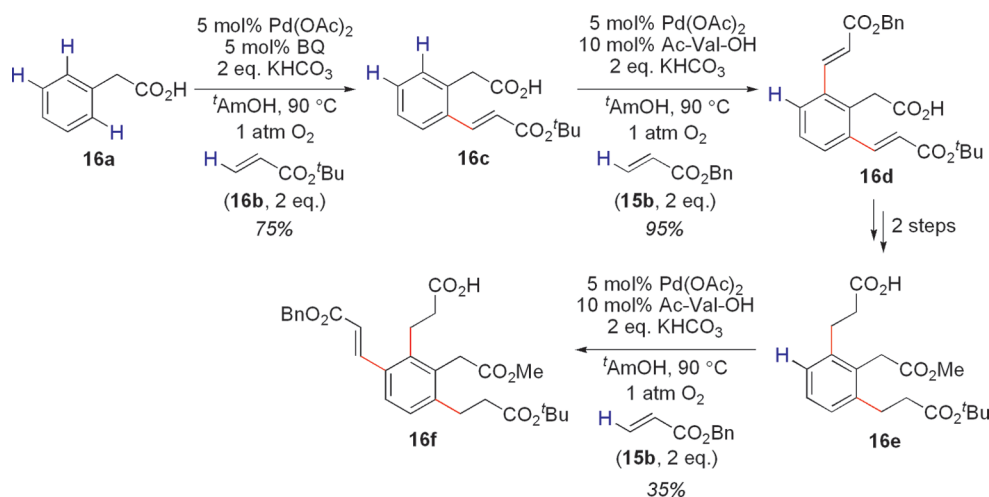


Figure 17. Iterative Pd-catalyzed trisalkenylation of phenylacetic acid (**16a**).²¹

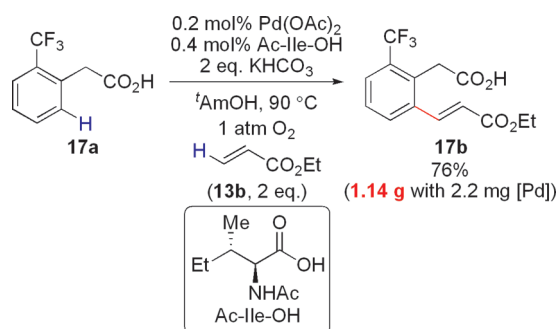


Figure 18. Pd-catalyzed *ortho*-alkenylation of 2-(2-(trifluoromethyl)phenyl)acetic acid (**17a**) at low catalyst loadings.²²

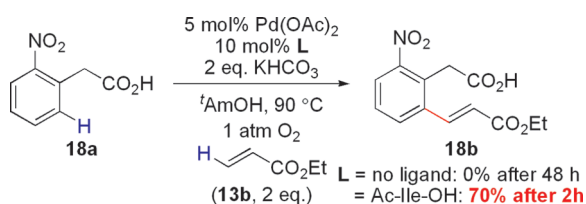
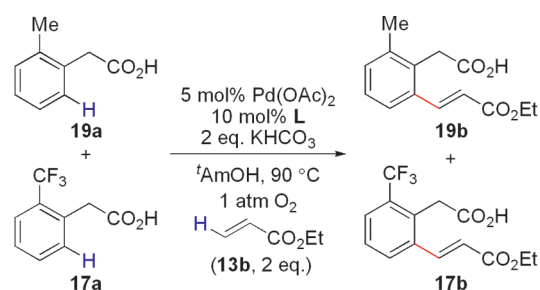


Figure 19. Pd-catalyzed *ortho*-alkenylation of 2-(2-nitrophenyl)acetic acid (**18a**) using a protected amino acid ligand.²²

kinetic isotope effect study, the authors found a strong dependence of $k_{\text{H}}/k_{\text{D}}$ on the ligand (Figure 21). On the basis of these investigations, Yu and co-workers proposed a *ligand-assisted* C–H activation mechanism that depends on the coordination mode adopted by the protected amino acid (Figure 22). Under bidentate coordination, the Pd(II) center is coordinatively saturated and deprotonation can occur by either an external base (e.g., acetate, bicarbonate) or by the Lewis basic C=O group of the amino acid ligand (e.g., amide, carbamate). Alternatively, under monodentate coordination, the Pd(II) center remains ligated to an acetate and intramolecular C–H deprotonation occurs. Palladacycle formation may involve agostic interactions²³ or may occur through concerted metalation deprotonation.²⁴ It is unknown whether Ac-Ile-OH adopts bidentate or monodentate coordination.



L = no ligand (after 120 min): 3% **19b**, 14% **17b** ($k_{19\text{b}}/k_{17\text{b}} = 0.22$)^a
 = Ac-Ile-OH (after 10 min): 40% **19b**, 21% **17b** ($k_{19\text{b}}/k_{17\text{b}} = 1.87$)^{b,c}

Figure 20. Competition study for Pd-catalyzed alkenylation of phenylacetic acids.²²

^aIndependently determined initial rates give $k_{19\text{b}}/k_{17\text{b}} = 0.37$.

^bIndependently determined initial rates give $k_{19\text{b}}/k_{17\text{b}} = 1.38$.

^cUsing Boc-Val-OH, 18% **19b** and 21% **17b** was observed ($k_{19\text{b}}/k_{17\text{b}} = 0.58$). Although the reaction exhibits significant ligand acceleration, the authors hypothesize that the moderate change in selectivity using the different protected amino acid ligands can be attributed to the different steric and electronic properties of the protecting groups (i.e., Boc versus Ac). Independently determined initial rates give $k_{19\text{b}}/k_{17\text{b}} = 0.90$.

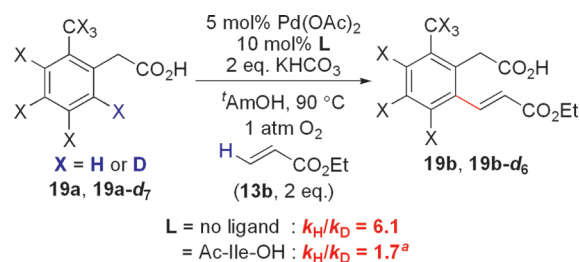
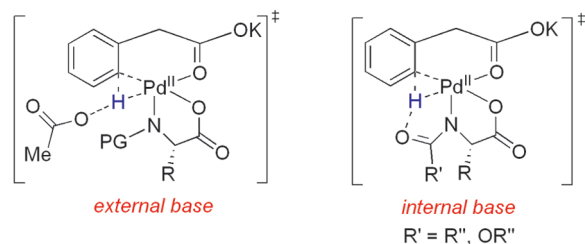


Figure 21. Kinetic isotope effect study for Pd-catalyzed oxidative *ortho*-alkenylations of phenylacetic acids.²²

^aUsing Boc-Val-OH, $k_{\text{H}}/k_{\text{D}} = 5.5$. Although the reaction exhibits dramatic ligand acceleration, the authors hypothesize that the moderate change in selectivity using the different protected amino acid ligands can be attributed to the different steric and electronic nature of the protecting groups (i.e., Boc versus Ac).

Bidentate coordination of protected amino acid



Monodentate coordination of protected amino acid

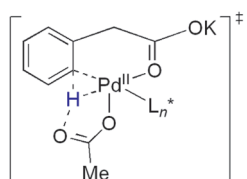


Figure 22. Proposed transition states for Pd-catalyzed oxidative *ortho*-alkenylations of phenylacetic acids promoted by protected amino acid ligands. Adapted with permission from ref 22. Copyright 2010 American Chemical Society.

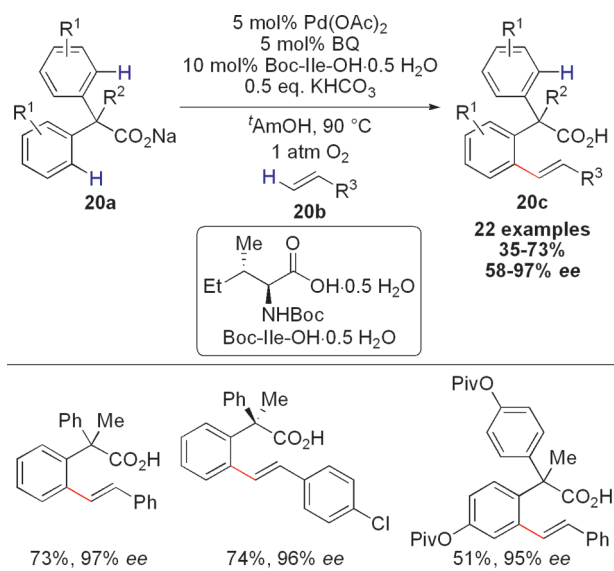


Figure 23. Enantioselective Pd-catalyzed *ortho*-alkenylation of diphenylacetic acids.²⁵

In Yu's *ortho*-alkenylations, ligands can be used to enhance rate and regioselectivity, as well as to control enantioselectivity. With a chiral amino acid, diphenylacetate sodium salt **20a** undergoes an asymmetric Heck-type desymmetrization to afford **20b** (Figure 23) in modest to excellent enantioselectivities (see Figure 24 for a model for enantioinduction).²⁵ Yu's asymmetric transformation provides valuable enantioenriched carboxylic acids bearing stereogenic quaternary carbons, but products with an α -proton are prone to racemize under these conditions. The carboxylic acid group can remain intact in this coupling, but when an acrylate is used instead of a styrene, in situ cyclization by Michael addition gives a six-membered lactone instead (not shown).²⁵

The Yu lab reported Pd-catalyzed olefination of electron-deficient arenes **21a** that occurs with *meta*-selectivity (Figure 25).^{26,27} Pyridine ligands, which are known to promote oxidation of Pd(0), were chosen for this transformation.²⁶ Common pyridine ligands

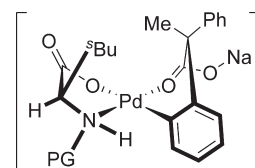


Figure 24. Proposed model for enantioinduction for enantioselective (Boc-Ile-OH)Pd-catalyzed *ortho*-alkenylation of diphenylacetic acids. Adapted with permission from ref 25. Copyright 2010 American Chemical Society.

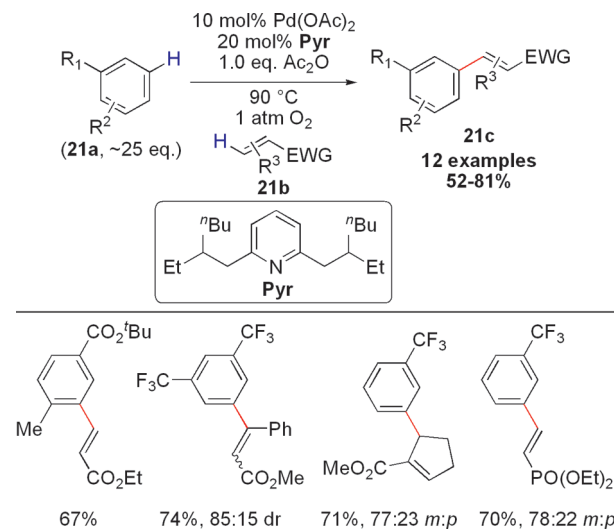


Figure 25. Pd-catalyzed *meta*-alkenylation of electron-deficient arenes.²⁶

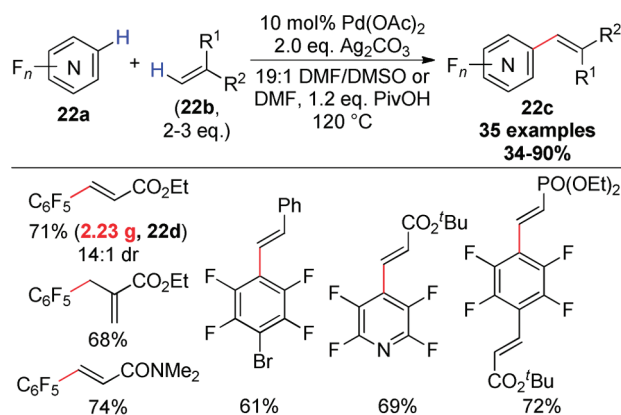
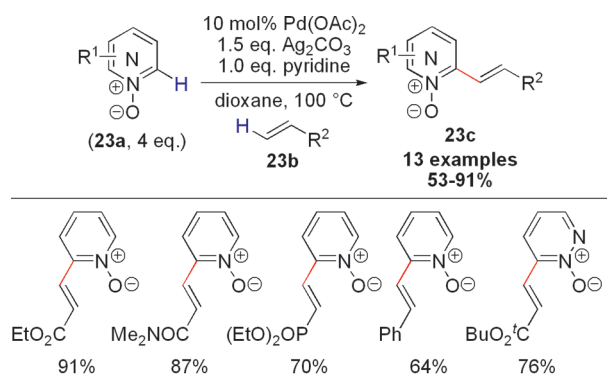
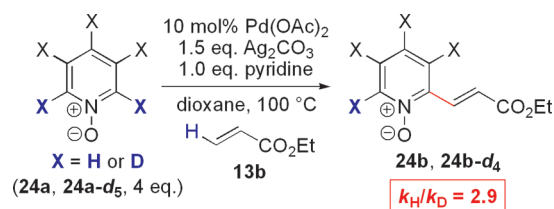
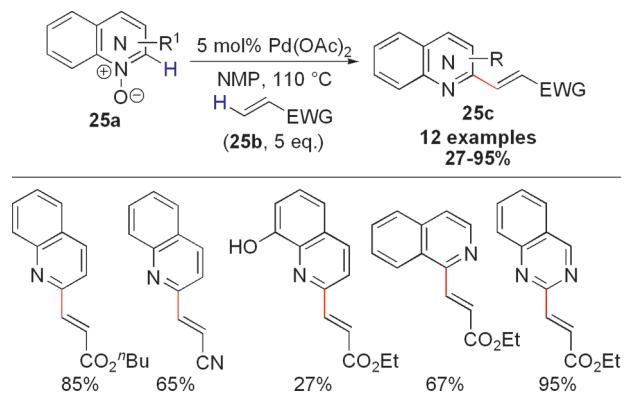


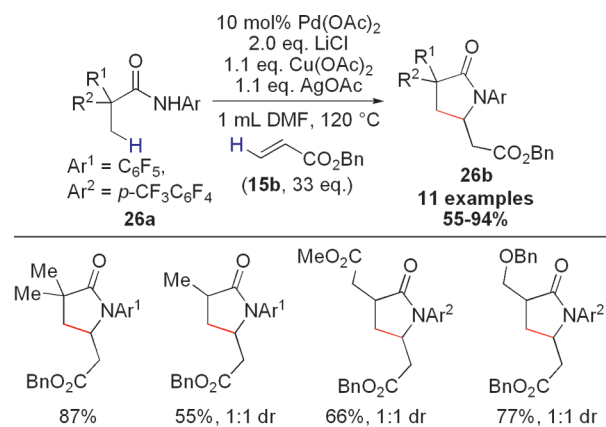
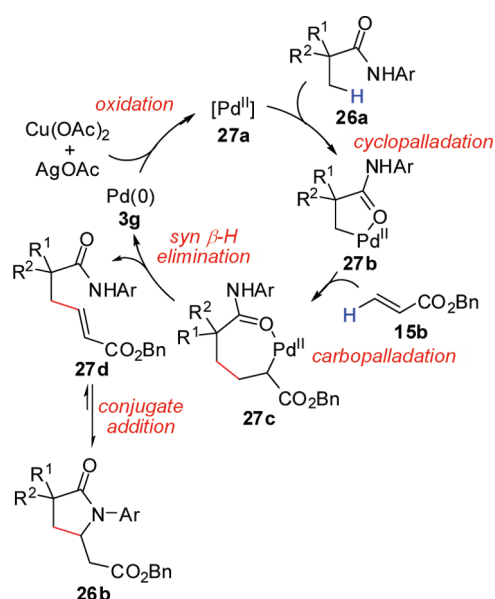
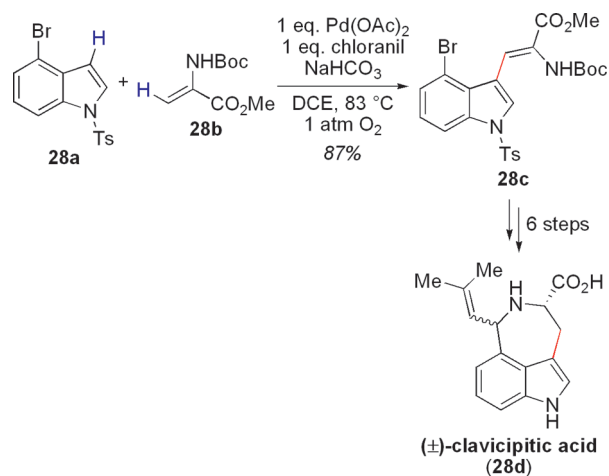
Figure 26. Pd-catalyzed alkenylation of perfluorinated arenes.²⁹

resulted in low reactivities, however, likely because strong Pd–N coordination disfavors productive association with the electron-deficient arene partners. To this end, Yu envisioned a novel ligand **Pyr** with steric encumbrance at the exterior of the ligand (i.e., removed from the Lewis basic N atom). In this design, a strong Pd–N interaction is maintained while imparting the necessary destabilization in dimers required to promote substrate coordination. In contrast, ligands bearing steric bulk in the immediate vicinity of the Pd(II) center (e.g., 2,6-di-*tert*-butylpyridine), as well as those exhibiting decreased electron density at the N (e.g., ethyl nicotinate), led to catalyst decomposition (i.e., palladium black formation). In the presence of **Pyr**, arenes bearing electron-withdrawing groups (e.g.,

Figure 27. Pd-catalyzed alkenylation of pyridine *N*-oxides.³⁰Figure 28. Kinetic isotope effect study for Pd-catalyzed alkenylation of pyridine *N*-oxides.³⁰Figure 29. Pd-catalyzed alkenylation of quinoline *N*-oxides in the absence of external oxidants.³¹

trifluoromethyl, nitro, ester, ketone) were able to coordinate to the Pd catalyst and undergo sp^2 C–H bond activation. Oxidative alkenylation occurs regioselectively due to enhanced acidity of the C–H bonds *meta* to the electron-withdrawing groups. Alternatively, *meta*-selectivity may be attributed to an electrophilic substitution mechanism. Ac₂O is necessary for this reaction and cannot be replaced with molecular sieves, which suggests that this additive helps convert H–Pd–OAc to Pd(OAc)₂ under aerobic conditions.^{7,12}

Extending oxidative coupling to perfluoroarenes is considered nontrivial because C–H activation results in an intermediate bearing a strong Pd–Ar_F bond, and this complex may be too stable for catalysis.²⁸ Zhang and co-workers have shown, however, that perfluorinated arenes 22a will undergo Pd-catalyzed alkenylation (Figure 26).²⁹ Ag₂CO₃ functions as both a base and an oxidant. Other Pd catalysts (e.g., PdCl₂, Pd(TFA)₂,

Figure 30. Pd-catalyzed alkenylation of sp^3 C–H bonds.³²Figure 31. Proposed mechanism for Pd-catalyzed alkenylation of sp^3 C–H bonds.Figure 32. Total synthesis of (±)-clavicipitic acid via a Pd-mediated C3 alkenylation of an indole derivative.³⁵

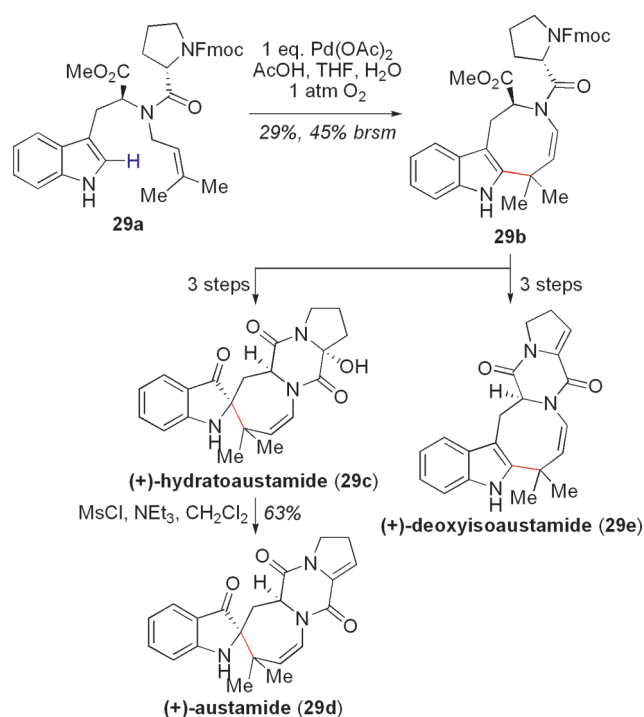


Figure 33. Total synthesis of (+)-hydratoaustamide (29c), (+)-austamide (29d), and (+)-deoxyisoaustamide (29e) via intramolecular oxidative indole–alkene Heck-type olefinations.³⁷

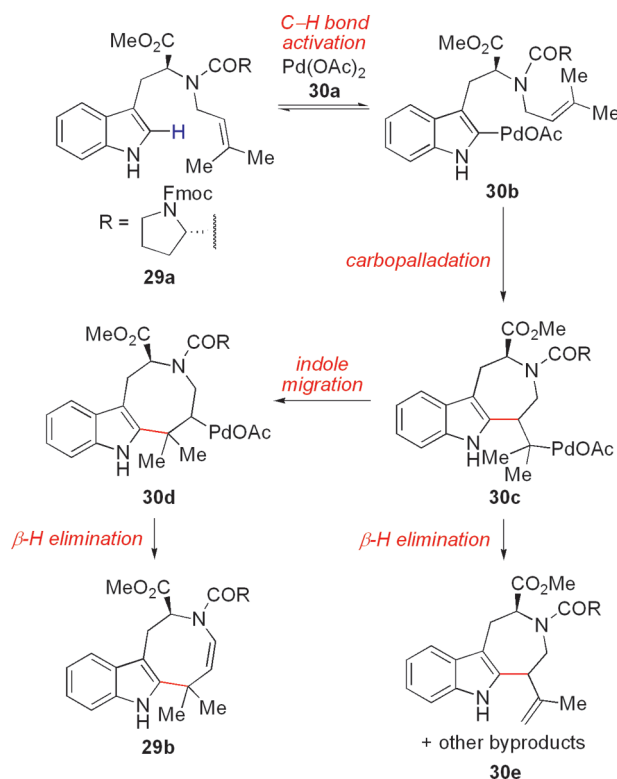


Figure 34. Proposed mechanism for intramolecular oxidative indole–alkene Heck-type olefinations.³⁷

Pd₂(dba)₃ and oxidants (e.g., Cu(OAc)₂, Oxone, benzoquinone, PhI(OAc)₂, O₂) were ineffective. Zhang's dehydrogenative cross-coupling accommodates a wide range of alkenes (22b),

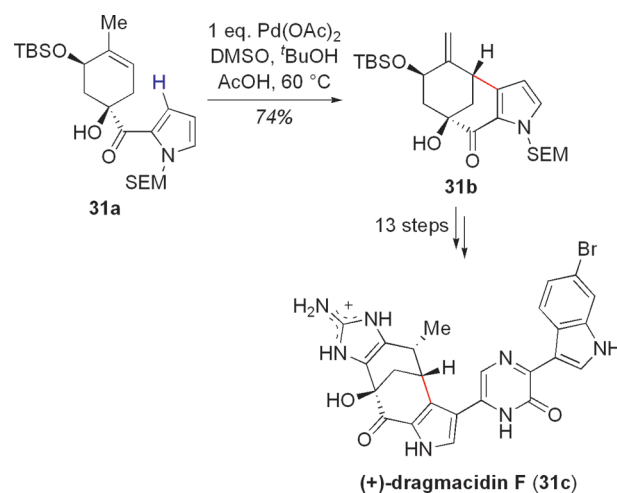


Figure 35. Total synthesis of (+)-drarmacidin F (31c) via an intramolecular oxidative indole–alkene Heck-type olefination.³⁸

including acrylates, acrylamides, and vinylphosphates, and Lewis basic functionalities, including pyridines, were tolerated. With this approach, the authors performed a 2 g scale synthesis of (*E*)-ethyl 3-(perfluorophenyl)acrylate (22d) in 71% yield from commercially available pentafluorobenzene and ethyl acrylate.

Chang and co-workers reported the analogous oxidative coupling between pyridine *N*-oxides (23a) and alkenes (23b) with Ag₂CO₃ as the sacrificial oxidant (Figure 27).³⁰ Pyridine *N*-oxide (24a) is observed to form a 1:1 coordination complex with palladium via O-binding. Yet, this palladium complex is catalytically inactive under the reaction conditions, which suggests that this coordination is nonproductive. Studies with deuterium-labeled pyridine *N*-oxide (24a-*d*₅) revealed a primary kinetic isotope effect (Figure 28). Subsequently, the groups of Cui and Wu demonstrated that quinoline *N*-oxides (25a) undergo an olefination in the *absence* of external oxidants to afford 2-alkenylquinolines (25c, Figure 29).³¹ The addition of metal salts, for example, Ag₂O, leads to decreased reaction efficiencies. When a mixture of quinoline *N*-oxide and 2-alkenylquinoline *N*-oxide is treated with Pd₂(dba)₃, only the latter is reduced to the corresponding quinoline. 2-Alkenylquinoline *N*-oxides are thus terminal oxidants in Cui and Wu's coupling. Azine *N*-oxide alkenylation occurs via rate-limiting C–H activation of the pyridine or quinoline *N*-oxide, alkene carbopalladation, β-H elimination, and oxidation of Pd(0) to Pd(II). Either Ag₂CO₃ or the 2-alkenylquinoline *N*-oxide product formed in situ acts as the terminal electron acceptor.

Although functionalizing sp³-hybridized C–H bonds is challenging, Yu and co-workers recently demonstrated the first example of alkane olefination (Figure 30).³² Amide-assisted cyclopalladation of propionamides 26a generates five-membered metallacycle 27b, which undergoes carbopalladation to form 27c. This seven-membered palladacycle (27c) β-hydride eliminates to form 27d, which cyclizes to afford 26b (Figure 31). Lactamization of 27d (by hydroamination) produces a 1:1 mixture of diastereomers. A combination of Cu(OAc)₂ and AgOAc oxidants provides the best yields. LiCl serves as a source of chloride anions that stabilize Pd(0) and aid formation of chloride-bridged bimetallic palladium species, complexes known to undergo carbopalladation with ease.³³ In Yu's transformation, substrates bearing β-hydrogens (i.e., if R¹ = H or R² = H) are accommodated, and olefination of cyclopropane C–H bonds is also possible (not shown).³²

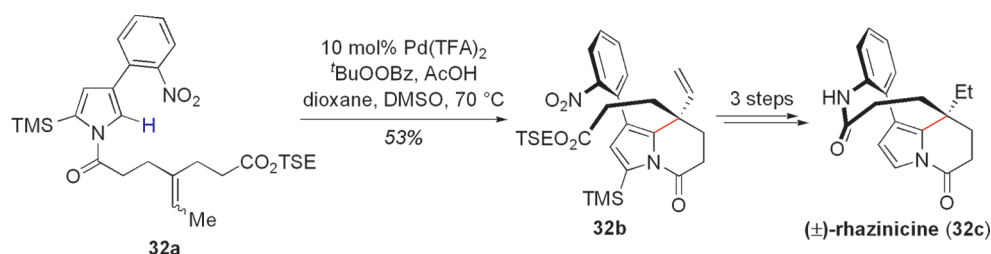


Figure 36. Total synthesis of (±)-rhazinicine via a Pd-catalyzed intramolecular oxidative pyrrole–alkene Heck-type olefination.³⁹

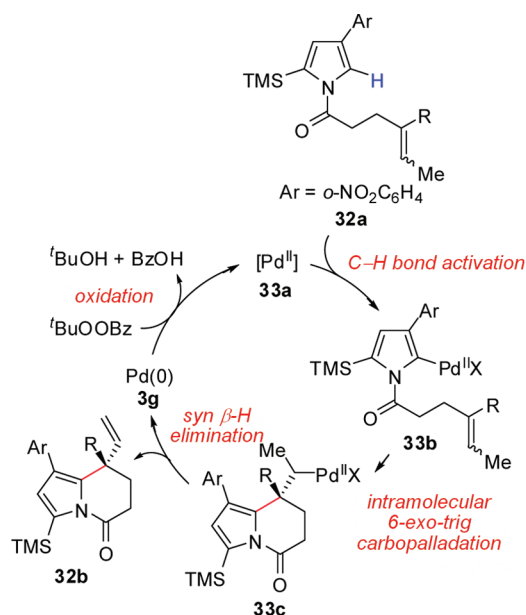


Figure 37. Proposed mechanism for Pd-catalyzed intramolecular oxidative pyrrole–alkene Heck-type olefination.

Electron-rich heteroaromatic compounds undergo intermolecular oxidative Heck couplings.³⁴ Ergot alkaloid (±)-clavicipitic acid (**28d**) (isolated as a mixture of diastereomers) was synthesized using this approach (Figure 32).³⁵ In 1995, Yokoyama and Murakami reported a Pd-mediated indole–dehydroamino acid ester cross-coupling that afforded 3-vinylindole derivative **28c** in 87% yield and high regioselectivity. In Yokoyama's synthesis, stoichiometric Pd is used because catalytic amounts resulted in poor yield (cf. 38%). Chloranil, a benzoquinone derivative, was the sacrificial oxidizing agent. Other oxidants, including DDQ, MnO₂, Ag₂CO₃, Co(salen)₂, and Cu(OAc)₂, were less efficient. The C–Br bond of **28a** remains intact during indole palladation and serves as a handle for further manipulations.

2.2. Intramolecular Arene–Alkene Coupling

Intramolecular alkenylations are well precedented³⁶ and have been applied to total synthesis. Baran and Corey achieved the syntheses of (+)-hydratoaustamide (**29c**), (+)-austamide (**29d**), and (+)-deoxyisoaustamide (**29e**) from (*S*)-tryptophan methyl ester derivative **29a** via a challenging eight-membered ring closure using the Fujiwara–Moritani reaction (Figures 33 and 34).³⁷ The key step in the synthesis proceeds in a modest 29% yield, 45% brsm (based on recovering starting material) due to competing seven-membered ring formation (affording a side-product that also arises from dehydrogenative coupling). The

presence of the methyl ester group on the backbone helps to promote the desired cyclization. To probe the mechanism, the authors prepared an arylmercury reagent (by C2 mercuration of the starting material with HgCl₂) and found that it undergoes intramolecular coupling with similar efficiencies. Corey's proposed mechanism for his indole–alkene coupling involves indole palladation to give arylpalladium **30b**, which then undergoes alkene insertion to yield benzazepine **30c**. Ring expansion by indole migration and subsequent β-H elimination liberates product **29b** as shown in Figure 33. Alternatively, β-H elimination from seven-membered cycloalkylpalladium complex **30e** results in byproduct formation.

Stoltz and co-workers used a similar oxidative pyrrole–alkene Heck-type olefination in their synthesis of (+)-dragmacidin F (**31c**), an alkaloid extracted from the Mediterranean sponge *Halicortex* sp. that displays potent activity against HIV-1 (Figure 35).³⁸ In these studies, the more conventional aromatic halide coupling partner (i.e., a bromopyrrole derivative) led to competitive byproduct formation. Electrophilic palladation of the pyrrole ring is believed to occur prior to intramolecular *cis*-carbopalladation. Cyclization takes place exclusively on the face closest to the pyrrole.

The Gaunt group achieved the synthesis of (±)-rhazinicine (**32c**) using an intramolecular dehydrogenative coupling as the key step (Figure 36).³⁹ Pd-catalyzed cyclization affords a single regioisomer—a tetrahydroindolizine ring system bearing a quaternary carbon stereocenter. Pd(TFA)₂ is superior to Pd(OAc)₂ in this transformation (Figure 37). The Trauner group reported a related strategy toward (±)-rhazinal (**34c**) with *tert*-butylhydroperoxide as the oxidant (Figure 38).⁴⁰ The reaction could be conducted under an aerobic atmosphere in the absence of this peroxide if desired.

Enantioselective variants of Ferreira and Stoltz's oxidative cyclizations^{36b} have been investigated by Oestreich and co-workers (Figure 39).⁴¹ Indoles **35a,c** and pyrrole **35e** undergo 5-*exo*-trig cyclizations in the presence of palladium, PyOx-X (a chiral pyridine–oxazoline ligand), and an oxidant (e.g., *t*BuOOBz, benzoquinone, O₂) with moderate enantiomeric excesses. Oestreich found that subjecting the (*E*)-isomer of the alkene starting material to the chiral catalyst favors one enantiomer of the annulated product, whereas the (*Z*)-isomer produces the opposite enantiomer. This stereospecific dehydrogenative coupling is currently limited to making enantioenriched five-membered rings.

2.3. Arene–Benzoquinone Coupling

In comparison to other olefins, benzoquinones are highly electrophilic and exhibit redox activity (i.e., they can undergo oxidation state changes during the course of the reaction). Yet, benzoquinone derivatives will undergo formal oxidative

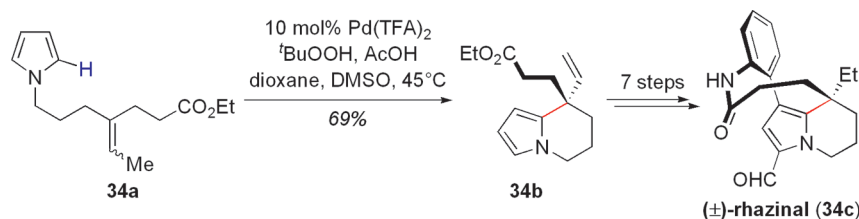


Figure 38. Total synthesis of (±)-rhazinal via a Pd-catalyzed intramolecular oxidative pyrrole–alkene Heck-type olefination.⁴⁰

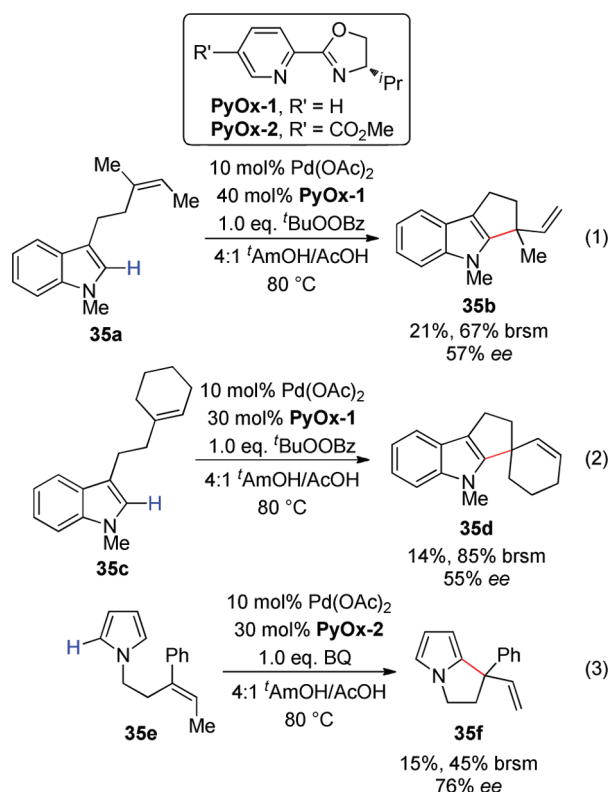


Figure 39. Enantioselective Pd-catalyzed intramolecular oxidative indole–alkene and pyrrole–alkene Heck-type olefinations.⁴¹

cross-coupling with aromatic C–H bonds. The Pd-mediated coupling of arenes and heteroarenes with quinones was first reported in 1981 by Itahara.⁴² Later, a catalytic variant was found using $\text{Na}_2\text{S}_2\text{O}_8$ as the stoichiometric oxidant.⁴³ Catalyst loadings as low as 0.8 mol % promote the desired oxidative coupling. Persulfate salts such as $\text{Na}_2\text{S}_2\text{O}_8$ are better oxidants than $\text{Cu}(\text{OAc})_2$, FeCl_3 , KMnO_4 , and $\text{K}_2\text{Cr}_2\text{O}_7$.

Intramolecular coupling between an aniline and benzoquinone provides straightforward access to the carbazomycins, a class of antibiotics and antioxidants.⁴⁴ Knölker and co-workers reported cyclizations of benzoquinone-tethered anilines (**36a**) as key steps for the syntheses of carbazomycins G (**36c**) and H (**36d**) and carbazoquinocin C (**36e**, Figure 40). Stoichiometric (1 equiv) and catalytic (0.1–0.3 equiv) amounts of palladium yield similar results. These reactions are more efficient, however, in air than under argon, and it is believed that atmospheric O_2 may be an auxiliary oxidant for this dehydrogenative cyclization.

Indol-3-ylbenzoquinones are structural motifs common in natural products. Electron-rich aromatic heterocycles, such as

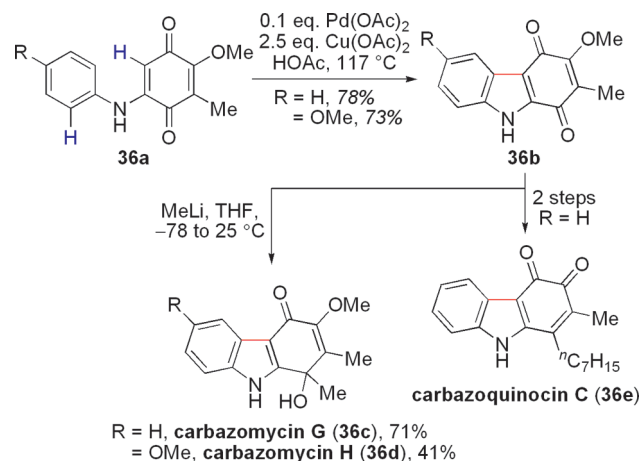


Figure 40. Total synthesis of carbazomycins G (**36c**) and H (**36d**) and carbazoquinocin C (**36e**) via intramolecular oxidative aniline–alkene Heck-type olefinations.⁴⁴

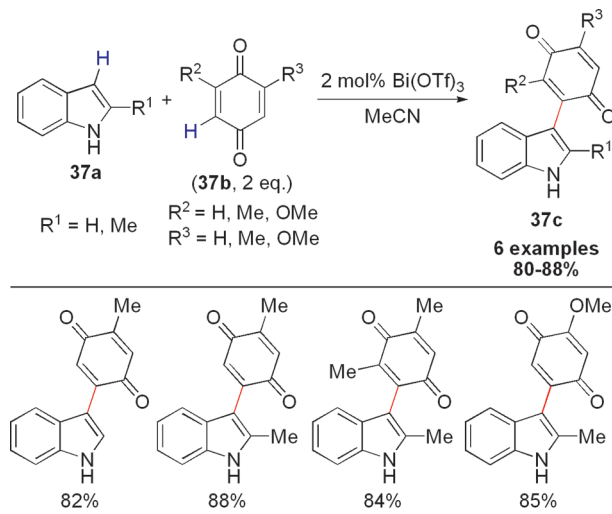


Figure 41. Bicatalyzed C3 alkenylation of indoles with benzoquinone.⁴⁷ The second equivalent of quinone acts as the terminal oxidant.

indoles, will undergo Michael addition to benzoquinones to afford these motifs in the *absence* of any transition metal catalyst.⁴⁵ Nucleophilic addition between indoles and benzoquinones (i.e., electrophilic aromatic substitution⁴⁶) generates hydroquinone intermediates that can reoxidize to yield indol-3-ylbenzoquinones. The oxidant used can be an external additive or the quinone starting material itself. Because of the inherent nucleophilicity of the C3 position of indoles, this oxidative coupling occurs with high regioselectivity. Lewis and protic acid

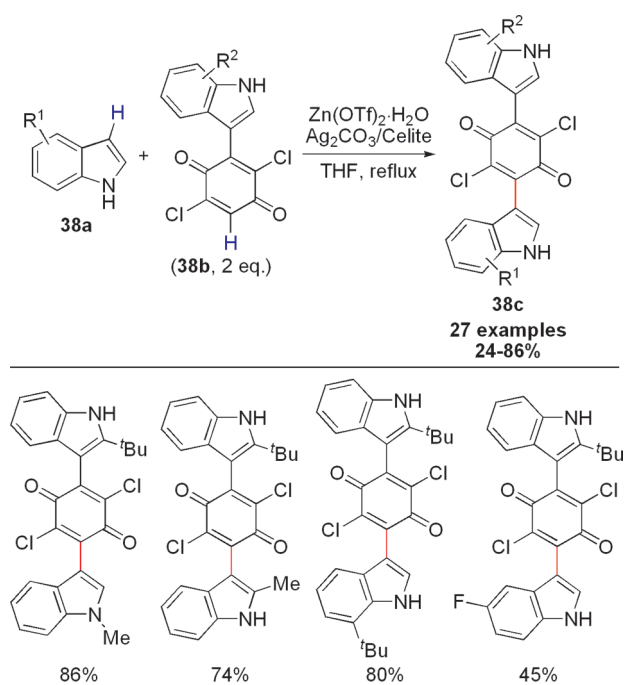


Figure 42. Zn-mediated C3 alkenylation of indoles with benzoquinone.⁴⁸ The second equivalent of quinone acts as the terminal oxidant.

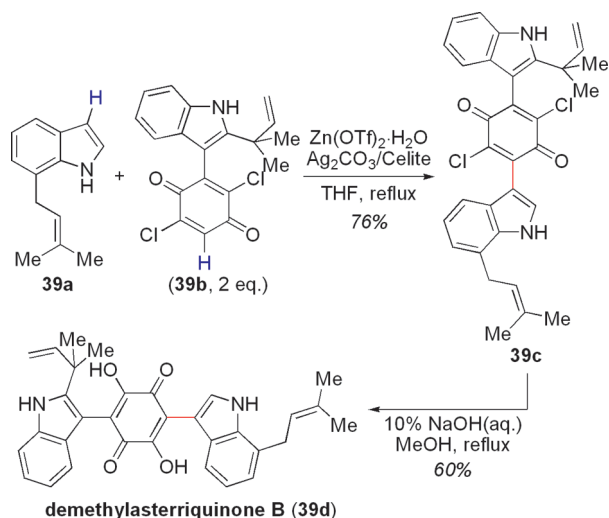


Figure 43. Total synthesis of demethylasterriquinone B (**39d**) via a Zn-mediated C3 alkenylation of indoles with benzoquinone.⁴⁸ The second equivalent of quinone acts as the terminal oxidant.

catalysts are typically used to improve reaction efficiency and generality. In 2003, Yadav and co-workers reported dehydrogenative couplings using $\text{Bi}(\text{OTf})_3$ (Figure 41).⁴⁷ Later, Pirrung and co-workers demonstrated that stoichiometric amounts of $\text{Zn}(\text{OTf})_2 \cdot \text{H}_2\text{O}$ and Ag_2CO_3 on Celite promote intermolecular indole–benzoquinone coupling (Figure 42).⁴⁸ While $\text{Dy}(\text{OTf})_3$ is also effective, other Lewis acids, such as $\text{BF}_3 \cdot \text{OEt}_2$, $\text{Cu}(\text{OTf})_2$, and $\text{Sc}(\text{OTf})_3$, fail to yield any indol-3-ylbenzoquinone products (**38c**). Demethylasterriquinone B (**39d**) was prepared by this route (Figure 43).

In water, $\text{In}(\text{OTf})_3$ is an excellent catalyst for oxidative arene–benzoquinone olefinations in the absence of external oxidants

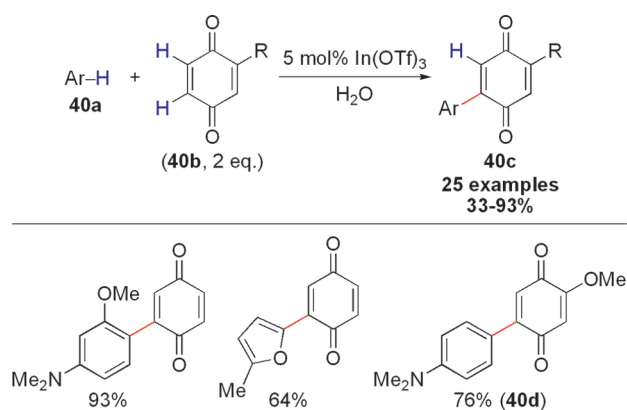


Figure 44. In-catalyzed intermolecular oxidative arene–benzoquinone olefination.⁴⁹ The second equivalent of quinone acts as the terminal oxidant.

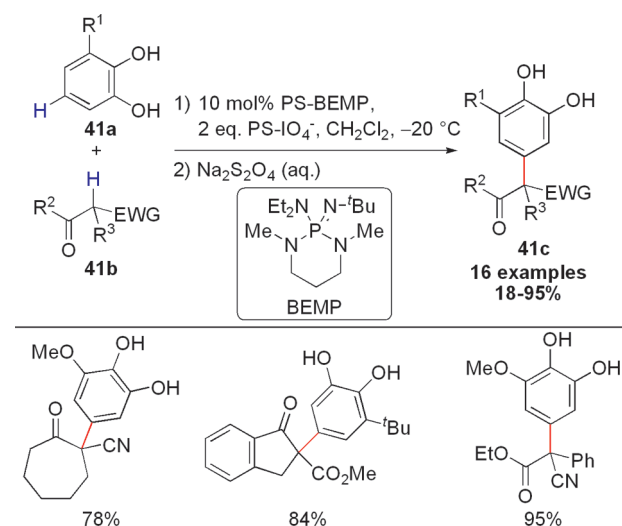


Figure 45. Organocatalytic oxidative alkylation of catechols with carbon-based nucleophiles.⁵⁰ The conjugate addition between quinone **42a** and **41b** is subject to nucleophilic catalysis with BEMP (not shown).

(Figure 44).⁴⁹ Li and co-workers found that HOTf displays comparable catalytic activity and suggest that $\text{In}(\text{OTf})_3$ may be a source of HOTf. If the benzoquinone starting material bears Lewis basic groups (e.g., OMe), chelation control provides cross-coupling products regioselectively (e.g., **40d**).

In a similar approach, the Dixon group reported an organocatalytic two-step process for dehydrogenative C–C bond formation using catechols as the coupling partners (Figure 45).⁵⁰ In the first step, the catechol starting material (**41a**) is converted to its corresponding *o*-quinone (**42a**) via oxidation (Figure 46). In the second step, Michael addition of a stabilized enolate (**41b**) generates the new C–C bond. Finally, a reductive workup procedure restores the catechol oxidation state. The overall transformation, thus, involves formal oxidative coupling of a phenol C–H bond. While sodium periodate (NaIO_4) works, the oxidant of choice is polymer-supported periodate (PS-IO_4^-).⁵¹ Dixon's transformation requires the addition of an organic base (e.g., BEMP) that also acts as a nucleophilic catalyst.⁵⁰ The products of this cross-coupling contain quaternary carbons; as such, the authors prepared (\pm)-powelline (**43d**) and (\pm)-buphanidine

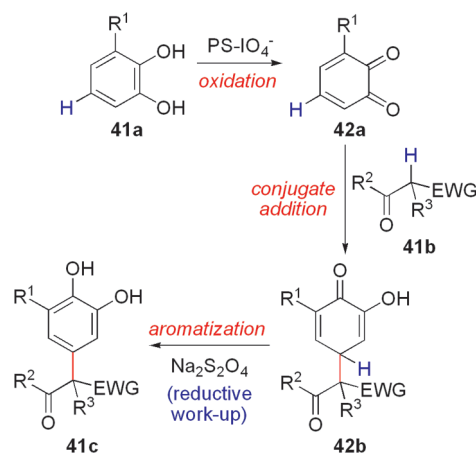


Figure 46. Proposed mechanism for organocatalytic oxidative alkylation of catechols with carbon-based nucleophiles.⁵⁰

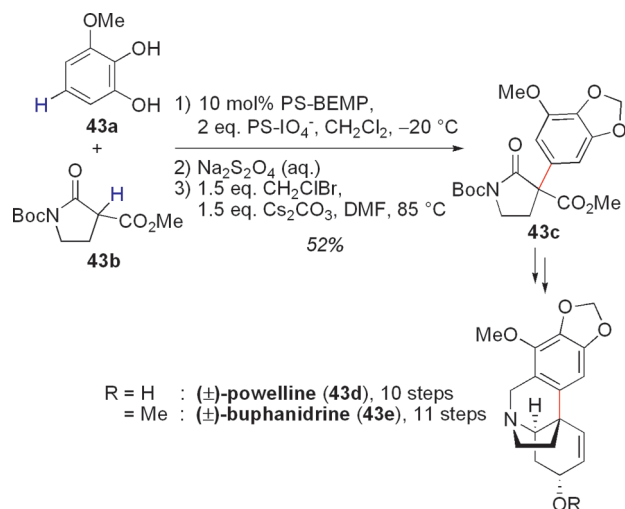


Figure 47. Total synthesis of (±)-powelline (43d) and (±)-buphanidrine (43e) via organocatalytic oxidative alkylation of catechols with carbon-based nucleophiles.⁵⁰

(43e), crinane-type *Amaryllidaceae* alkaloids (Figure 47). An asymmetric variant using organocatalysts derived from cinchona alkaloids has been achieved with moderate to good enantiocontrol (CA-x; Figure 48).

2.4. Arene–Alkene Coupling Catalyzed by Metals Other than Palladium

Besides palladium, other transition metal catalysts have been reported for the Fujiwara–Moritani reaction. Rh complexes were first shown to catalyze the oxidative Heck-type alkenylations in the late 1970s.^{52–54} Most of these examples, however, were low yielding and limited in scope. Copper salts and O₂ were the terminal oxidants,⁵³ and photolysis was applied in some cases, rather than thermal heating.⁵⁴ A rare example of Rh-catalyzed alkenylation of sp² C–H bonds was achieved by Ueura, Satoh, and Miura in 2007 (Figure 49).⁵⁵ Using a mixed Rh/Cu system at low catalyst loadings, olefination of benzoic acid (45a) results in *ortho*-alkenylated lactones, which arise from di-*ortho*-substitution and subsequent intramolecular Michael addition. This reaction involves four independent C–H bonds undergoing concomitant functionalization with oxygen as the sacrificial oxidant.

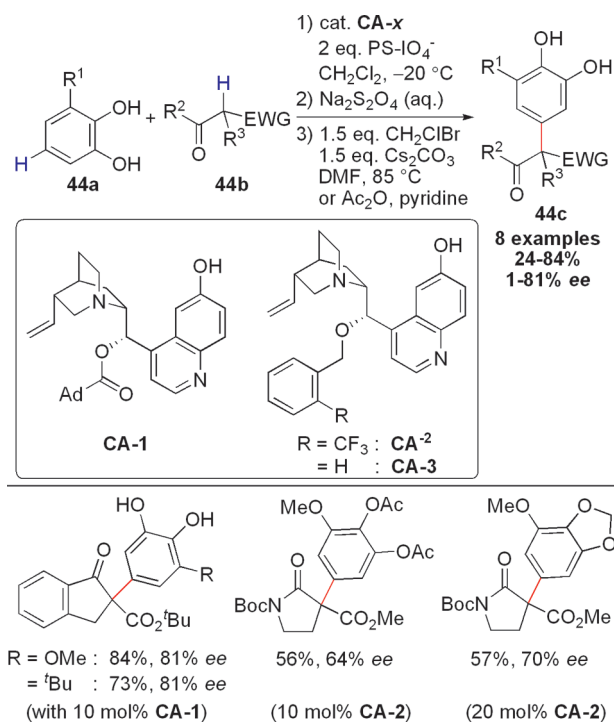


Figure 48. Enantioselective cinchona alkaloid-catalyzed oxidative alkylation of catechols with carbon-based nucleophiles.⁵⁰

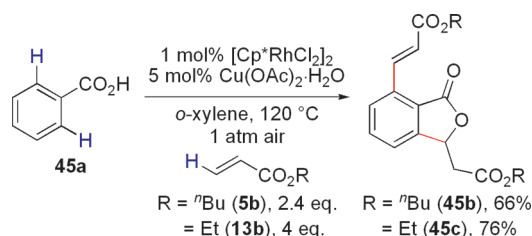


Figure 49. Rh/Cu-catalyzed bis-*ortho*-alkenylation of benzoic acid (45a).⁵⁵

Tandem oxidative alkenylation/intramolecular Michael addition has been extended to benzamide substrates (46a) for the synthesis of phthalimides (46b, Figure 50).⁵⁶ Remarkably, oxidative functionalization is selective for the more hindered C–H bond (e.g., 46d,e). Using less electron-deficient alkenes such as styrenes, cyclization is not observed. With heteroaryl-derived amides (47a), Rh-catalyzed dehydrogenation occurs in the absence of cyclization predominantly (Figure 51). Li and co-workers reported that isoquinolin-1(2*H*)-one (48a) could undergo *ortho*-olefination followed by *intermolecular* Michael addition (Figure 52).

The Satoh and Miura groups demonstrated that catalytic amounts of (Cp*RhCl₂)₂ effect the oxidative *ortho*-alkenylation of *N*-phenylpyrazoles, 2-phenylpyridines, and 1-phenylimidazoles (49a, Figure 53).⁵⁷ With Cu(OAc)₂·H₂O as the oxidant, *mono*- and *di*olefination occur. Although stoichiometric amounts of copper are required to turn over the Rh catalyst, as little as 10 mol % of Cu(OAc)₂ under aerobic conditions can be used instead. This reaction can produce differentially functionalized *ortho*-alkenylated products by sequential addition of olefin coupling partners (Figure 54). The proposed mechanism involves a

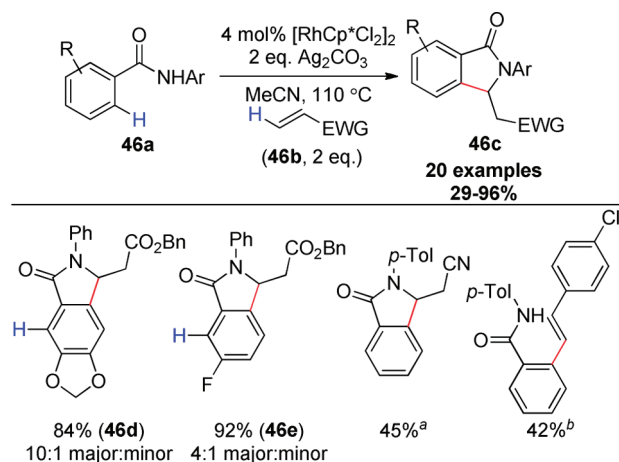


Figure 50. Rh-catalyzed intermolecular oxidative *ortho*-alkenylation/hydroamination of benzamides.⁵⁶

^aThe starting material was recovered in 39% yield.

^bThe intramolecular Michael reaction was not observed.

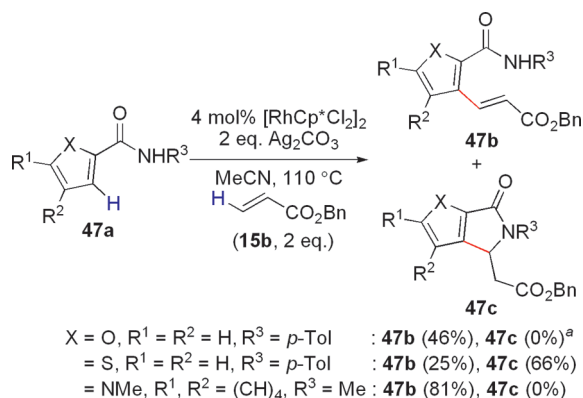


Figure 51. Rh-catalyzed intermolecular oxidative *ortho*-alkenylation of heteroarylcarboxamides.⁵⁶

^aThe starting material was recovered in 44%.

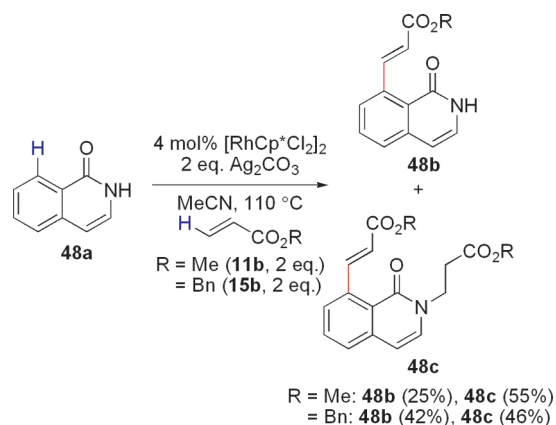


Figure 52. Rh-catalyzed intermolecular oxidative *ortho*-alkenylation of isoquinolin-1(2H)-one.⁵⁶

Rh(III/I) catalytic cycle similar to that proposed for Pd(II/0): C–H activation, carbometalation, β -H elimination, and then

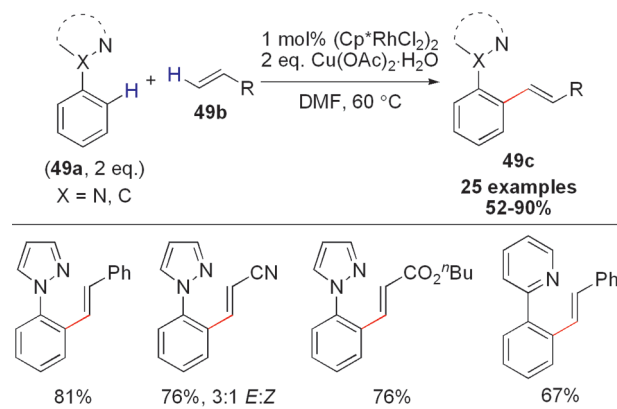


Figure 53. Rh-catalyzed intermolecular oxidative *mono*- and *di-ortho*-alkenylation of *N*-phenylpyrazoles, 2-phenylpyrroles, and 1-phenylimidazoles.⁵⁷

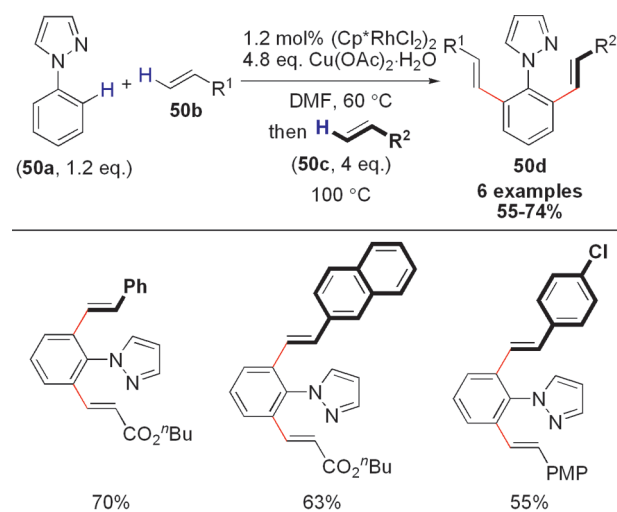


Figure 54. Rh-catalyzed iterative intermolecular oxidative *di-ortho*-alkenylation of *N*-phenylpyrazoles.⁵⁷

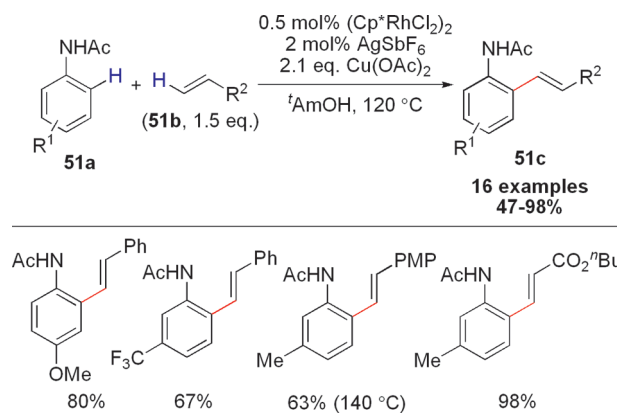


Figure 55. Rh-catalyzed intermolecular oxidative *ortho*-alkenylation of anilides.⁵⁸

catalyst oxidation. Patureau and Glorius achieved a related Rh-catalyzed *ortho*-alkenylation of anilides using a cationic rhodium salt (**51a**, Figure 55).⁵⁸ The challenging *ortho*-ethenylation reaction

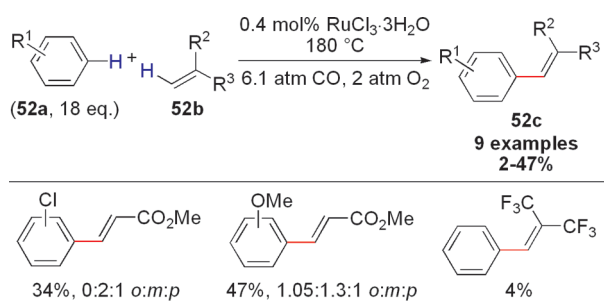


Figure 56. Ru-catalyzed intermolecular oxidative arene–alkene Heck-type olefination.⁵⁹

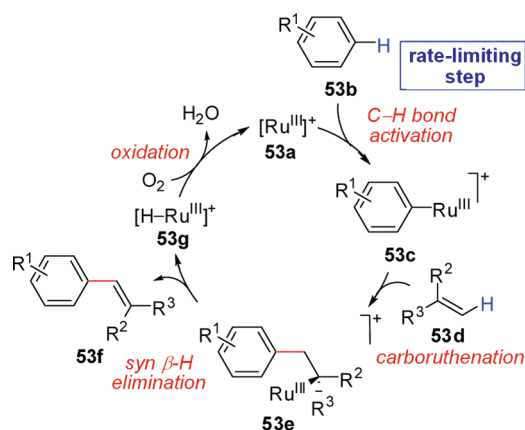


Figure 57. Proposed mechanism for Ru-catalyzed intermolecular oxidative arene–alkene Heck-type olefination.⁵⁹

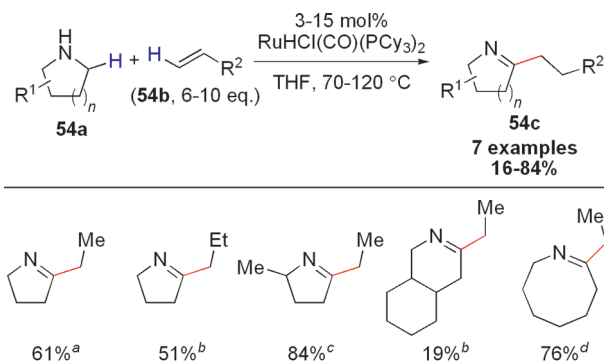


Figure 58. Ru-catalyzed α -alkenylation of cyclic amines toward the synthesis of α -alkylamines.⁶¹

^aReaction conducted with 5 mol % $\text{RuHCl}(\text{CO})(\text{PCy}_3)_2$ at 80 °C.

^bReaction conducted with 10 mol % $\text{RuHCl}(\text{CO})(\text{PCy}_3)_2$ at 120 °C.

^cReaction conducted with 10 mol % $\text{RuHCl}(\text{CO})(\text{PCy}_3)_2$ at 80 °C.

^dReaction conducted with 3 mol % $\text{RuHCl}(\text{CO})(\text{PCy}_3)_2$ at 70 °C.

was realized using an ethylene atmosphere at elevated pressures (2 bar, 4 mol % $[\text{Rh}]$, dioxane). In Glorius' reaction, *N*-methyl-substituted tertiary amides react with lower efficiency (13% yield) than corresponding secondary amides.

In 2001, Milstein and co-workers demonstrated that coupling arenes (**52a**) and alkenes (**52b**) can be achieved using Ru catalysts (Figure 56).⁵⁹ Although a CO atmosphere is required, a range of ruthenium salts (e.g., $\text{RuCl}_3 \cdot 3\text{H}_2\text{O}$, $[\text{Ru}(\text{CO})_3\text{Cl}_2]_2$,

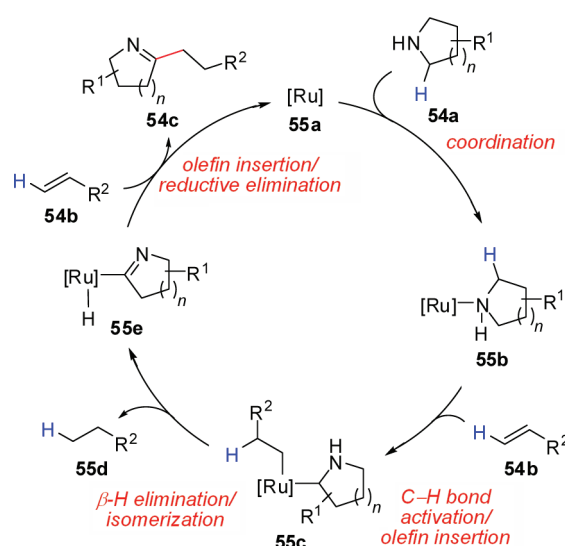


Figure 59. Proposed mechanism for Ru-catalyzed α -alkenylation of cyclic amines toward the synthesis of α -alkylamines.⁶¹

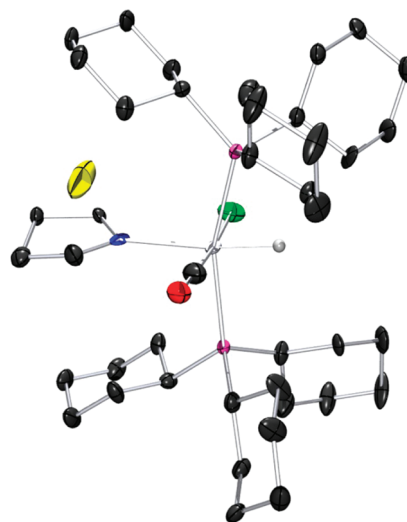


Figure 60. ORTEP plot of cationic Ru–H complex derived from pyrrolidine and $\text{RuHCl}(\text{CO})(\text{PCy}_3)_2$. All H atoms, except the Ru–H, have been omitted for clarity. Anisotropic displacement ellipsoids are shown at the 50% probability level. The POV-Ray drawing was created from coordinates obtained from Yi et al.⁶¹ Legend: black = carbon, red = oxygen, blue = nitrogen, silver = ruthenium, white = hydrogen, green = chlorine, violet = phosphorus, and yellow = sodium.

$[(\eta^6\text{-C}_6\text{H}_6)\text{RuCl}_2]_2$, $\text{Ru}(\text{NO})\text{Cl}_3 \cdot 5\text{H}_2\text{O}$, and $\text{Ru}(\text{F}_6\text{-acac})_2$) enable catalysis except $\text{Ru}_3(\text{CO})_{12}$, which exhibits low activity. The authors observed that chloride anions (e.g., CuCl_2 or CsCl) and amine bases (e.g., lutidine) inhibit catalysis by coordination to the Ru complex. Carbon monoxide, on the other hand, is proposed to stabilize cationic Ru species; indeed, Ru–CO stretches can be observed by in situ IR spectroscopy. Radical and heterogeneous catalysis is ruled out because galvinoxyl (a radical inhibitor) and Hg have no effect on reaction efficiency. The authors propose a mechanism involving cationic ruthenium intermediates as depicted in Figure 57. First, C–H bond activation of unactivated arene **53b** occurs to form **53c**, which carbometallates olefin **53d**. The resulting complex **53e** undergoes β -H

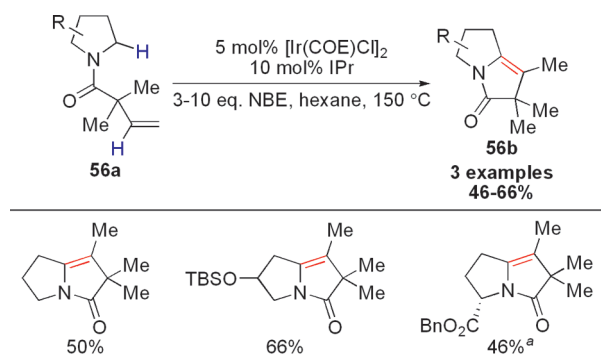


Figure 61. Ir-catalyzed intramolecular dehydrogenative oxidative pyrrolidine-alkene Heck-type olefinations.⁶²

“3,3-Dimethyl-1-butene (TBE) was used as the hydrogen acceptor.

elimination to liberate product **53f** and ruthenium hydride **53g** (which is reoxidized). Milstein favors an electrophilic metalation of arene **52a**⁶⁰ because electron-rich arenes react faster than electron-deficient arenes ($\rho = -1.16$ for σ_{para}), and benzene reacts faster than its deuterated analogue ($k_{\text{H}}/k_{\text{D}} = 2$).

Most dehydrogenative Heck-type cross-couplings occur with hazardous byproduct formation (e.g., copper and silver salts). In contrast, Yi and co-workers reported one of the first dehydrogenative couplings where 1 equiv of H_2 is generated, as exemplified by his $\text{RuHCl}(\text{CO})(\text{PCy}_3)_2$ -catalyzed cyclic amine α -alkenylation (**54a**) reaction (Figure S8).⁶¹ The proposed mechanism involves coordination of **54a** to Ru (**55a**), followed by α -C–H activation (of an sp^3 -hybridized C–H bond) to generate a ruthenium hydride that is immediately trapped by the olefin (**54b**, Figure S9). Intermediate **55c** undergoes β -H elimination and isomerization, liberating 1 equiv of alkane **55d**. The resulting α -ruthenated imine complex **55e** is the formal α -C–H activation product of a cyclic imine. Insertion across a second equiv of alkene **54b**, followed by reductive elimination, yields **54c**. In support of this proposal, the Yi group isolated a catalytically competent ruthenium hydride pyrrolidide (Figure 60). The equiv of H_2 that is formed in the reaction reduces excess equiv of the alkene starting material. Byproducts from overreduction to α -alkylated amines were observed, and competing *N*-alkylation can also take place. For a mechanistically distinct approach to α -functionalization of amines, see section 4.1.

Concurrently, an intramolecular dehydrogenative coupling was achieved by Sames and co-workers as depicted in Figure 61.⁶² In this reaction, $[\text{Ir}(\text{COE})\text{Cl}]_2$ promotes the oxidative cyclization of *N*-acylated pyrrolidines **56a** to give bicyclic 2,3-dihydro-1*H*-pyrrolizin-5(6*H*)-one derivatives **56b**. 5-*exo*-Cyclization is favored over competing 6-*endo*-cyclization. While various *Rh* catalysts resulted in unproductive intramolecular transfer hydrogenation reactions, *Ir* complexes catalyze the desired sp^3 C–H bond activation and olefin insertion sequence. *N*-Heterocyclic carbene (NHC) ligand IPr (i.e., *N,N'*-bis(2,6-di-*iso*-propylphenyl)imidazolyl carbene) performs better than other phosphine ligands tried. Sames and co-workers propose a mechanism that parallels the well-accepted Heck-type addition/elimination sequence within an Ir(I/III) catalytic cycle (Figure 62). During catalysis, liberation of 1 equiv of H_2 forms catalytically inactive Ir(III) complex **57d**. Hence, norbornene (NBE) is critical as a hydrogen acceptor because it reduces Ir(III) back to catalytically

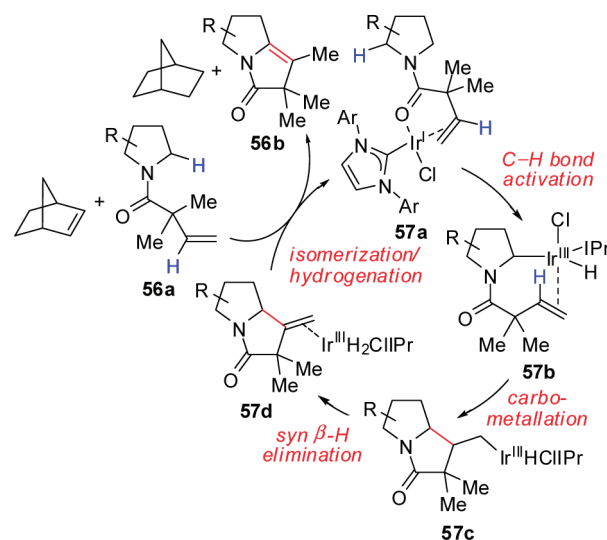


Figure 62. Proposed mechanism for Ir-catalyzed intramolecular dehydrogenative oxidative pyrrolidine-alkene Heck-type olefination.⁶² Ar = DIIP.

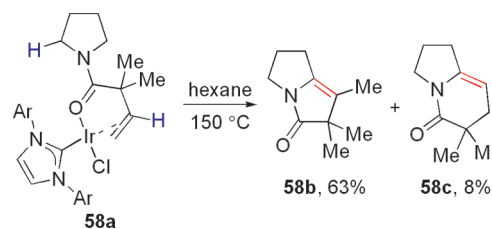


Figure 63. Stoichiometric study for Ir-catalyzed intramolecular dehydrogenative oxidative pyrrolidine-alkene Heck-type olefination.⁶² Ar = DIIP.

active Ir(I) (**57a**); additionally, NBE suppresses the aforementioned transfer hydrogenation process. Substrate-bound Ir complex **58a** converts smoothly to cyclized product **58b** upon heating (Figure 63).

It is worthwhile to mention that couplings between arenes and benzoquinones are also catalyzed by metals other than palladium (see section 2.3). In these examples, the metal salt typically acts as a Lewis acid catalyst rather than being intimately involved in C–H bond activation.^{47,48} For related indole syntheses by intramolecular cyclizations of *N*-arylenamines via non-Heck-type pathways, see section 7.1.

2.5. Alkene–Alkene Cross-Coupling

In comparison to arene–alkene Heck-type olefinations, alkene–alkene couplings are much less common because of difficulties associated in promoting desired *cross*-coupling over homocoupling and a relatively limited understanding in the mechanism of alkene C–H bond palladation. In addition to discovering that simple arenes can react with benzoquinones in the presence of palladium salts,⁴² Itahara reported that *N*-methylpyridone and 4*H*-pyran-4-one are suitable substrates for dehydrogenative bond formation with olefins.⁴³ (Although these coupling partners can also be classified as heterocycles, we will cover them within the context of alkene–alkene cross-coupling because they are more similar to acrylates than electron-rich heteroaromatic compounds). *N*-Methylpyridone alkenylation

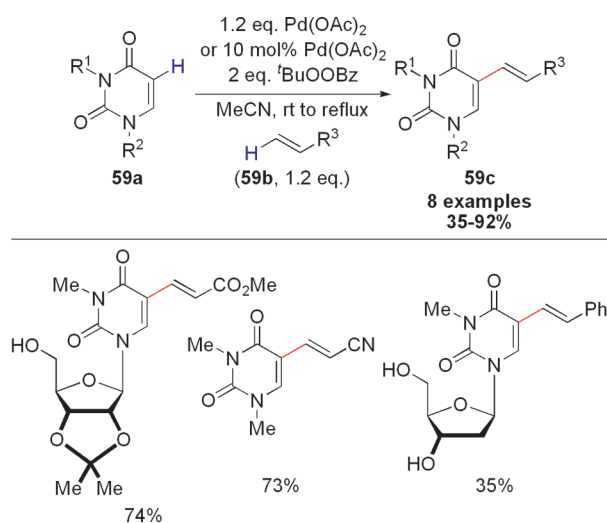


Figure 64. Pd-catalyzed intermolecular oxidative pyrimidone–alkene Heck-type olefination.⁶³

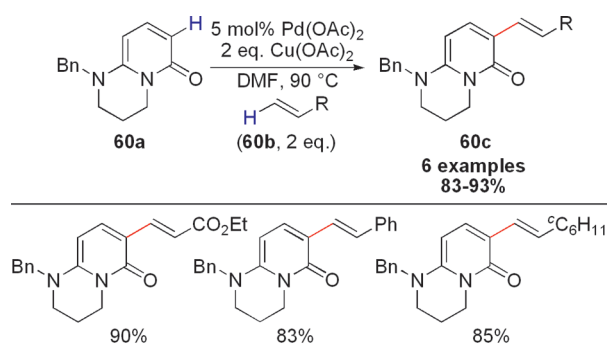


Figure 65. Pd-catalyzed intermolecular oxidative pyridone–alkene Heck-type olefination.⁶⁴

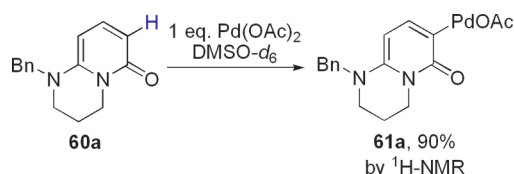


Figure 66. Stoichiometric palladation of pyridone derivative en route to oxidative Heck-type olefination.⁶⁴

occurs with competing C3- and C5-functionalization. Subsequent to this work, Pd-catalyzed functionalization of pyrimidones (59a), structural motifs found in uracil derivatives, was achieved with excellent regio- and diastereocontrol (Figure 64).⁶³ Alkene–alkene oxidative cross-coupling was next extended to include C6-substituted pyridones (60a) by Cheng and Gallagher (Figure 65).⁶⁴ The authors obtained NMR spectroscopic evidence for the existence of alkenylpalladium complex 61a (obtained from starting material 60a). This result supports C–H palladation as the first step in the catalytic cycle for alkene–alkene dehydrogenation (Figures 66 and 67). The presence of an electron-donating substituent at C6 favors regioselective alkenylation at C3.

Cross-coupling between two acyclic alkenes remained elusive until the work of Ishii and co-workers. In this vinylcarboxylate–

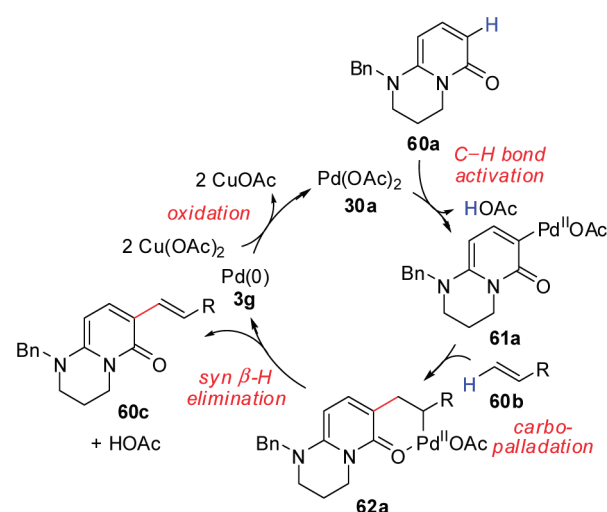


Figure 67. Proposed mechanism for Pd-catalyzed intermolecular oxidative pyridone–alkene Heck-type olefination.⁶⁴

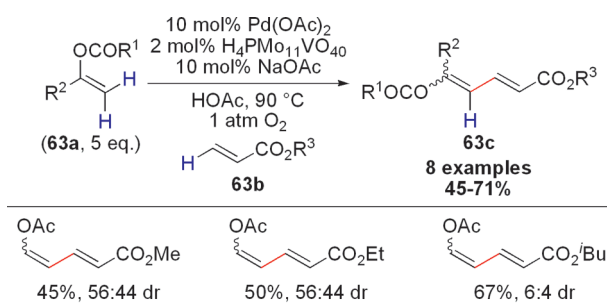


Figure 68. Pd-catalyzed intermolecular oxidative vinylcarboxylate–acrylate Heck-type olefination.⁶⁵

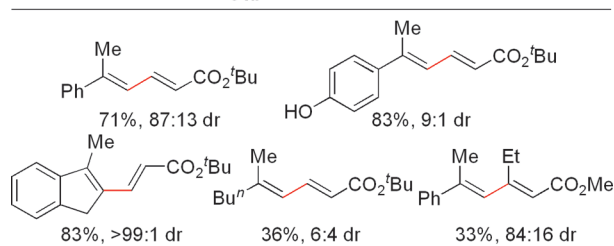
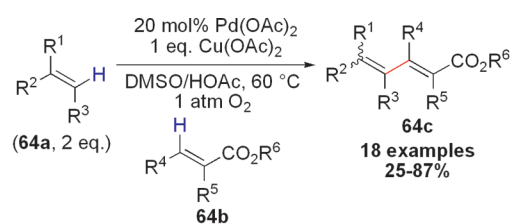
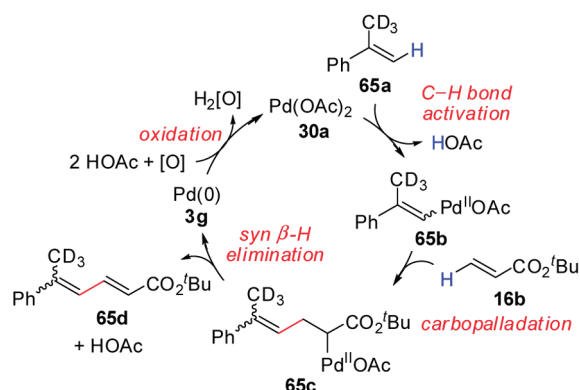


Figure 69. Pd-catalyzed intermolecular oxidative alkene–acrylate Heck-type olefination.⁶⁶

acrylate dehydrogenation, palladium catalysis affords diene products (63c) in the presence of vanadomolybdophosphoric acid and an O₂ atmosphere (Figure 68).⁶⁵ Unfortunately, the olefin geometry of products 63c is not well controlled. Following this account, the Loh group achieved a Pd-catalyzed alkene–acrylate cross-coupling with enhanced substrate scope and enhanced diastereoselectivities (Figure 69).⁶⁶ Replacing Pd(OAc)₂ with

a) Oxidative alkene cross-coupling by C–H palladation



b) Oxidative alkene cross-coupling by acetoxypalladation

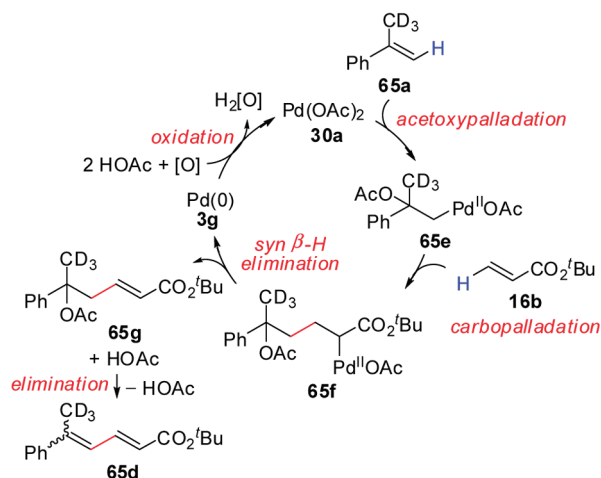


Figure 70. Possible mechanisms for Pd-catalyzed intermolecular oxidative alkene–acrylate Heck-type olefination (i.e., cross-coupling of α -CD₃-styrene (**65a-d₃**) and *tert*-butyl acrylate (**16b**)).⁶⁶

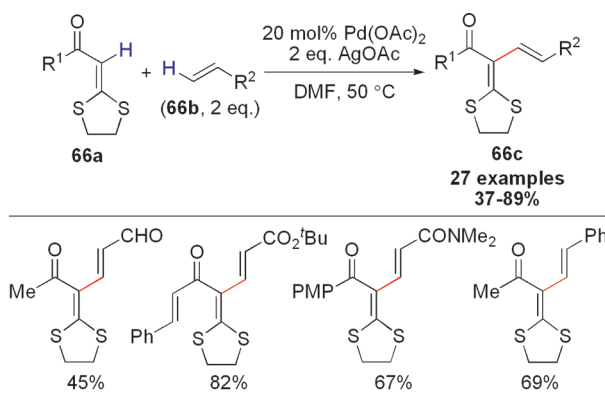


Figure 71. Pd-catalyzed intermolecular alkene–alkene oxidative cross-coupling.⁶⁷

PdCl₂ or Pd(TFA)₂ leads to decreased reactivities; Pd(PPh₃)₂Cl₂, on the other hand, is not an effective catalyst and phosphine ligands inhibit catalysis completely. The combination of Cu(OAc)₂ and O₂ is the best oxidant for Loh's coupling. In this reaction, selectivity for (*E*)-dienes (**63c**) is improved over Ishii's original work, and both simple alkenes and styrenes can participate in this coupling. Loh performed a deuterium labeling study and found that α -CD₃-styrene (**65a**) couples without

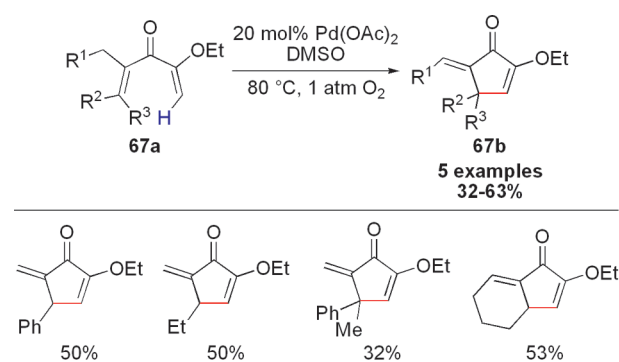


Figure 72. Pd-catalyzed intramolecular oxidative alkene–alkene Heck-type olefination.⁶⁸

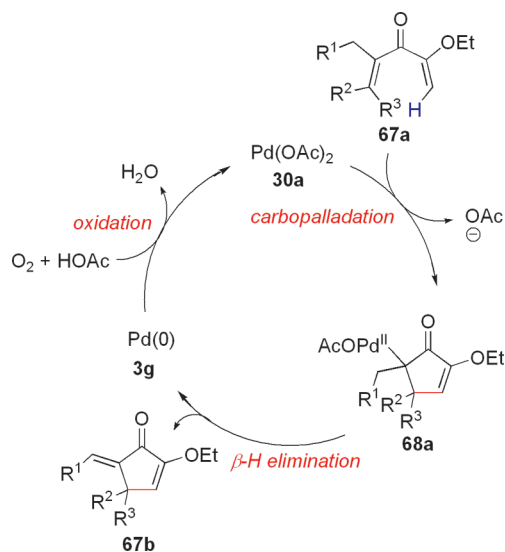


Figure 73. Proposed mechanism for Pd-catalyzed intramolecular oxidative alkene–alkene Heck-type olefination.⁶⁸

scrambling of the deuterium atoms—this result suggests that Pd π -allyl complexes are not intermediates (Figure 70). Instead, a Pd–C bond generated from styrene **65b** is proposed to undergo either direct C–H activation (Figure 70a) or acetoxypalladation (Figure 70b) to generate an organopalladium intermediate **65c** or **65f**, respectively, both of which can participate in Heck-type olefination (i.e., carbopalladation and β -H elimination).

The Yu group reported a complementary oxidative alkenylation with cyclic dithiane directing groups (Figure 71).⁶⁷ Although O₂ is not a suitable oxidant, Yu's reaction can be conducted under air with Cu(OAc)₂, benzoquinone, or PhI(OAc)₂. Replacing Pd(OAc)₂ with PdCl₂, Pd(PPh₃)₂Cl₂, or Pd(PPh₃)₄, however, decreased reaction efficiencies. Yu and co-workers synthesized a number of 1,3-butadienes (**66c**) bearing various functional groups, including aldehydes and aryl bromides. The S atoms of the cyclic dithiane direct selective C–H activation of **66a**, while minimizing reactivity at other olefinic C–H bonds. The diethylthiane derivative, however, is unreactive to dehydrogenative coupling (<5% yield).

Cyclizations by oxidative alkene–alkene cross-coupling have been disclosed by the Tius group. In particular, an oxidative Heck variant of the Nazarov reaction affords cyclopentenone products **67b** in moderate yields (Figure 72).⁶⁸ In the traditional

Nazarov reaction, divinyl ketones cyclize in the presence of Lewis acids;⁶⁹ Tius' variation involves the Pd-catalyzed intramolecular coupling of electronically differentiated cross-conjugated ketones in the presence of a sacrificial oxidant (e.g., O₂).⁶⁸ Intermolecular carbopalladation of the electron-deficient alkene occurs between the electron-rich vinyl group and the Pd(OAc)₂ catalyst. The resulting organopalladium intermediate undergoes β -H elimination to liberate product **67b** and expel Pd(0) (**3g**, Figure 73).

2.6. Enolate–Alkene Coupling

An alternative strategy for oxidative cross-couplings by Heck-type mechanisms is the direct addition of enolates to alkenes. Olefin coordination to palladium results in enhanced electrophilicity of the C=C double bond. In 1997, Bäckvall and co-workers reported an intramolecular oxidative enolate–alkene coupling, an olefination in which a diene was functionalized with an enolate stabilized by sulfone, nitro, and ester functionalities (Figure 74).⁷⁰ Reaction yields, however, were low because of competing diene carboxygenation (i.e., formal addition of a C–O bond across a C=C double bond). Although this transformation can be considered an early example of dehydrogenative allylic alkylation, its mechanism does not involve allylic C–H bond oxidation (see section 2.3).

Bäckvall's work was extended to simple alkenes by Widenhoefer and co-workers, who used stoichiometric amounts of a CuCl₂ oxidant (Figure 75).^{71,72} Cyclohexenone (**70b**) formation is possible for β -diketones and β -ketoesters attached to olefins (**70a**), both with and without substituents on the tether. Although the mechanism differs depending on the substrate, it is generally accepted that alkene carbopalladation between enolate and Pd catalyst occurs. This reaction can follow one of two pathways: (1) formation of alkylpalladium complex **71b** via carbopalladation, followed by olefin insertion, or (2) direct nucleophilic addition to the C=C double bond coordinated to the Pd catalyst (see Figure 76).

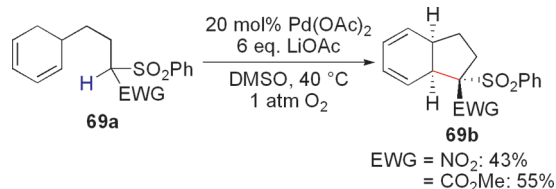


Figure 74. Pd-catalyzed intramolecular enolate–diene Heck-type olefination.⁷⁰

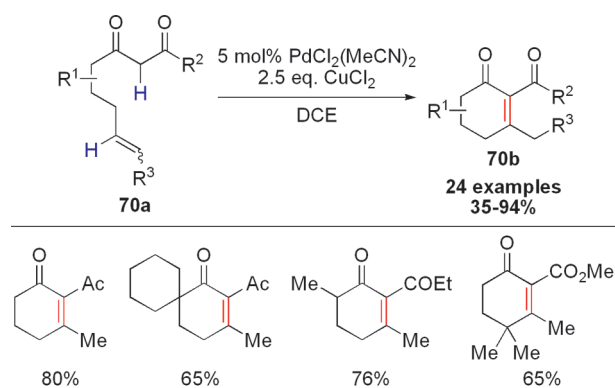


Figure 75. Pd-catalyzed intramolecular enolate–alkene Heck-type olefination.^{71,72}

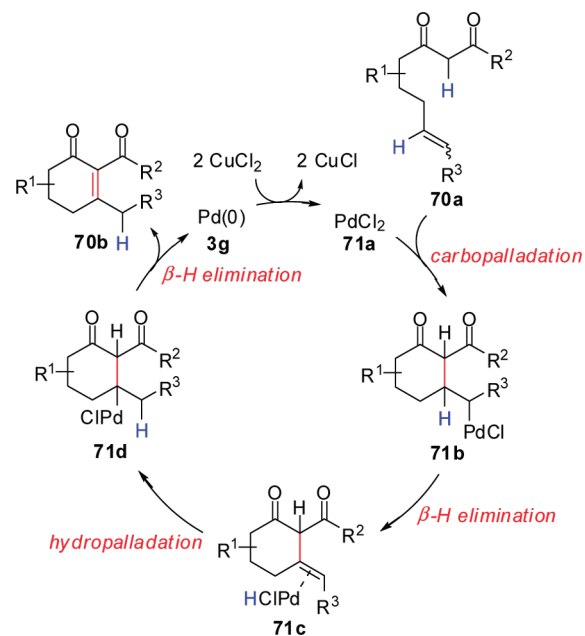


Figure 76. Proposed mechanism for Pd-catalyzed intramolecular enolate–alkene Heck-type olefination.⁷²

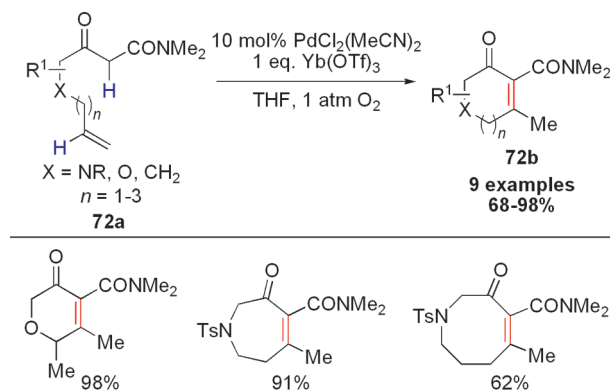


Figure 77. Pd-catalyzed intramolecular β -ketoamide–alkene Heck-type olefination.⁷³

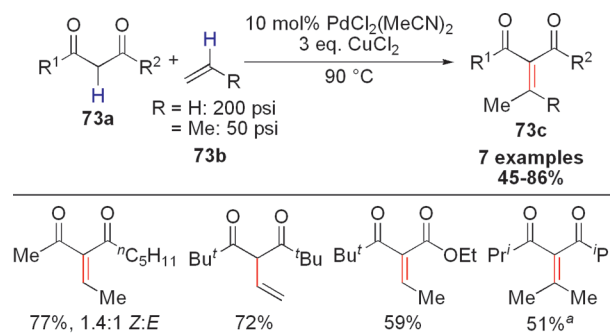


Figure 78. Pd-catalyzed intermolecular oxidative enolate–alkene Heck-type olefination.⁷⁴

^a1 equiv EuCl₃, 100 °C.

The resulting alkylpalladium complex **71b** undergoes β -H elimination to generate another palladium-bound alkene **71c**. Hydropalladation (i.e., reinsertion) with the opposite regiochemistry affords

alkylpalladium complex **71d**, which is subject to a second β -H elimination to generate Knoevenagel-type products **70b**.⁷²

Shortly thereafter, the Yang group achieved an intramolecular aerobic oxidative coupling between β -ketoamides and alkenes (Figure 77).⁷³ In addition to a Pd catalyst, the Lewis acid Yb(OTf)₃ is required to promote enolization of the β -ketoamide and subsequent dehydrogenative ring closure. This carbocyclization operates best to afford six-membered products (**72b**) but can be extended to seven- and eight-membered rings by prolong-

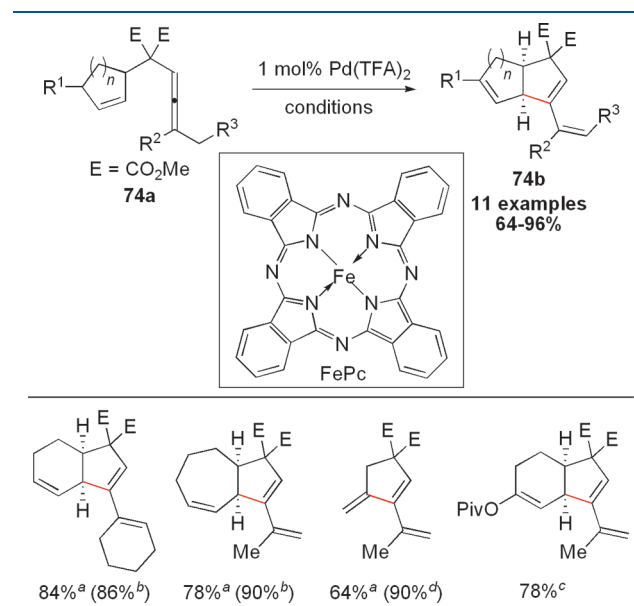


Figure 79. Pd-catalyzed intramolecular oxidative alkene-allene Heck-type olefination.^{75,76}

^aConditions: 2 equiv BQ, THF, reflux.

^bConditions: 4 mol % BQ, 1 mol % FePc, toluene, 95 °C.

^cConditions: 5 mol % Pd(TFA)₂, 20 mol % BQ, 5 mol % FePc, toluene, 95 °C.

^dConditions: 2 mol % Pd(OAc)₂, 2 equiv BQ, toluene, reflux.

ing reaction times. Oxygen serves as the oxidant in this reaction under copper-free conditions.

The only example of *intermolecular* vinylation of enolates was reported by Wang and Widenhoefer in 2004 (Figure 78).⁷⁴ In the presence of CuCl₂ and PdCl₂(MeCN)₂, activated methylenes **73a** including β -diketones and β -ketoesters undergo α -vinylation under elevated pressures of either ethylene or propylene gas (50–200 psi). The addition of a stoichiometric amount of EuCl₃, a Lewis acid, is required for propenylation. At low pressures, competing α -alkylation resulting from protonolysis (instead of β -H elimination) is observed. When propylene is chosen as the coupling partner, oxidative coupling occurs preferentially at the internal C–H bond, but competing protonolysis can lead to regioisomeric furan byproduct formation (not shown).⁷⁴

2.7. Miscellaneous Examples

Thus far, we have described the addition of arene, alkene, and enolate C–H bonds and palladium across C=C unsaturations as strategies for Heck-type dehydrogenations. Allylic C–H activation, on the other hand, remains an attractive alternative. Franzén and Bäckvall discovered an intramolecular oxidative carbocyclization between an alkene and allene catalyzed by palladium (Figure 79).⁷⁵ A range of cyclopentenones (**74b**) can be prepared by this strategy, including compounds bearing allylic acetate functionalities that are typically reactive to palladium salts. Benzoquinone is the sacrificial oxidant. The Bäckvall group further demonstrated that catalytic amounts of benzoquinone can be used in combination with iron phthalocyanine (FePc), an oxygen-activating macrocyclic metal complex based on a porphyrin framework.⁷⁶ This FePc co-oxidant is optionally attached to a resin for easy recovery and reuse. Bäckvall's coupling occurs through allylic C–H activation, followed by allene carbopalladation and β -H elimination (Figure 80).⁷⁵ Alternatively, palladation of the olefinic C=C bond and subsequent β -H elimination. When O₂ is the terminal oxidant, benzoquinone, FePc, and palladium participate in three interconnected catalytic cycles in a mechanism similar to those proposed for biologically relevant oxidative processes (Figure 81).⁷⁶ FePc exists in either the oxidized form (FePc_{ox}, **76b**) or the reduced form (FePc_{red}, **76a**) during catalysis.

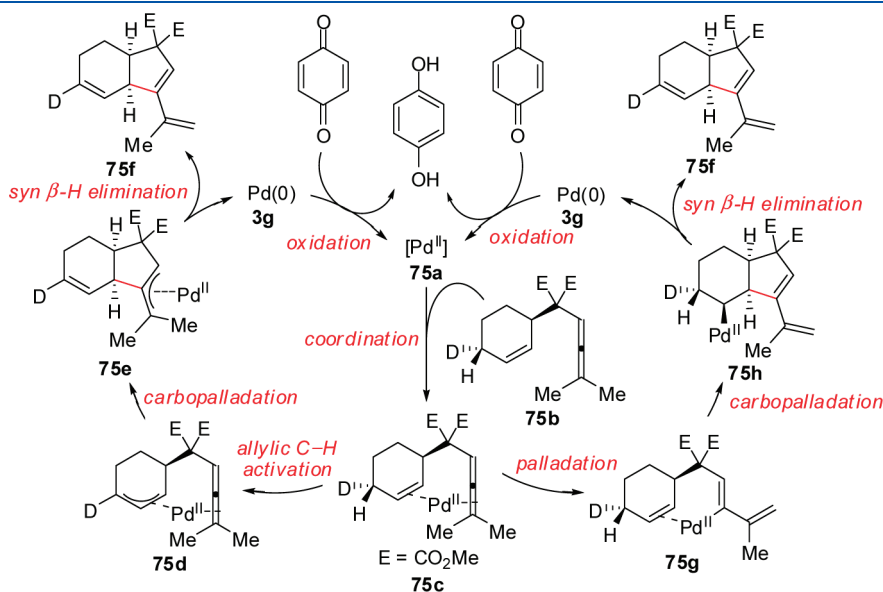


Figure 80. Proposed mechanism for Pd-catalyzed intramolecular oxidative alkene-allene Heck-type olefination of a D-labeled substrate **75b**.⁷⁵

3. CROSS-COUPLING OF TWO ARENES CATALYZED BY PALLADIUM

The biaryl motif is a common structure found in molecules relevant to fields ranging from medicinal chemistry to material science. Most cross-couplings (e.g., Suzuki, Negishi, Stille, Hiyama, Kumada) make C–C bonds by combining an aryl halide (or pseudohalide) with an appropriate organometallic reagent.⁷⁷ Although broadly applicable, these classical couplings require independent synthesis and isolation of aryl halide and arylmetal starting materials. Additionally, these reactions generate stoichiometric amounts of inorganic salts as byproduct. Direct arylation is an attractive alternative in which one coupling partner is a simple arene. As such, an sp^2 -hybridized C–H bond reacts instead of a C–X or C–M bond.⁹ In the cross-coupling of *two* simple arenes (known as tandem direct arylation or 2-fold C–H activation), neither the aryl halide nor the arylmetal coupling partner is required (Figure 82).⁸ To date, electron-rich arenes, arenes bearing pyridine, amide, carbamate, and other oxazoline directing groups, and pyridine *N*-oxides and other electron-deficient arenes can undergo oxidative biaryl C–C bond formation (Figure 83).

Palladium catalysis dominates in tandem direct arylation. In these dehydrogenations, two independent C–H activations take place (Figure 84). Depending on catalytic conditions and substrates involved, these two events occur through various mechanisms, such as cyclopalladation,⁷⁸ electrophilic metalation,⁶⁰ concerted metalation deprotonation (by either an internal or external base),²⁴ and σ -bond metathesis.⁷⁹ In reactions involving electron-rich heteroarenes, Heck-type pathways have also been

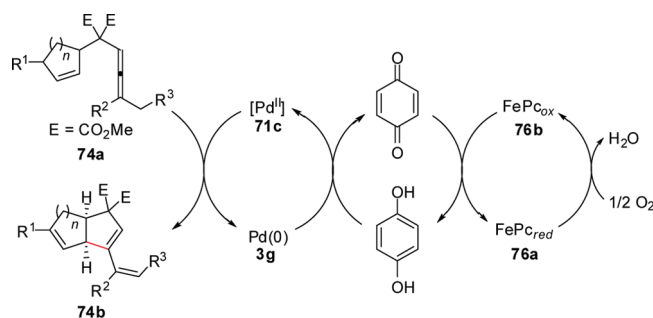
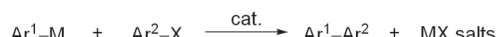


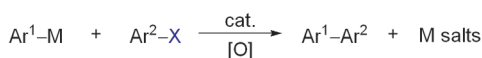
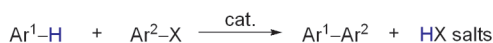
Figure 81. Triple-coupled catalytic system for Pd-catalyzed intramolecular oxidative alkene–allene Heck-type olefination.⁷⁶

a) Transition metal catalyzed cross-coupling



M = B(OR)₂, Suzuki
= ZnX, Negishi
= SnR₃, Stille
= SiR₃, Hiyama
= MgX, Kumada
X = halogen,
N₂⁺, OTf

b) Direct arylation



c) Tandem direct arylation

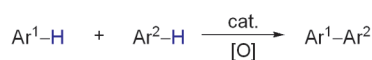


Figure 82. Generic scheme for cross-couplings of two arenes catalyzed by palladium.

Substrates

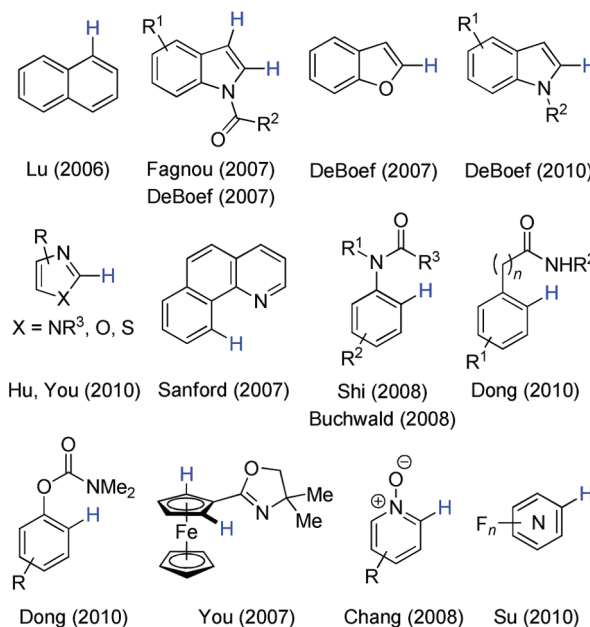


Figure 83. Overview of cross-couplings of two arenes catalyzed by palladium.

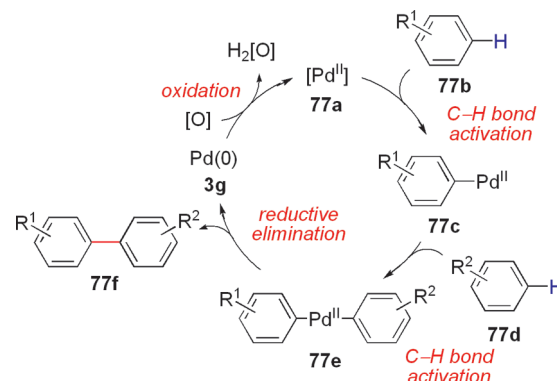


Figure 84. General mechanism for oxidative C–C cross-coupling involving direct arylation.

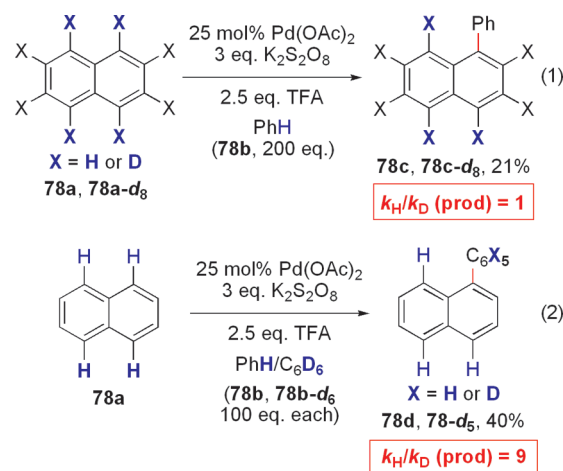


Figure 85. Kinetic isotope effect study for Pd-catalyzed oxidative arylation of naphthalene.⁸⁰

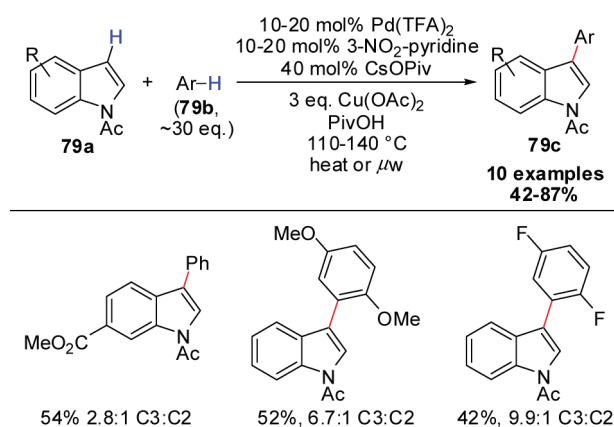


Figure 86. Pd-catalyzed oxidative C3 arylation of *N*-acetylindoles.⁸²

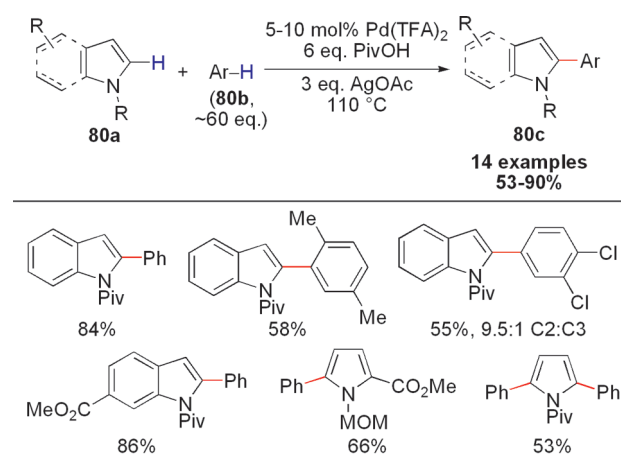


Figure 87. Pd-catalyzed oxidative C2 arylation of *N*-protected pyrroles and indoles.⁸³

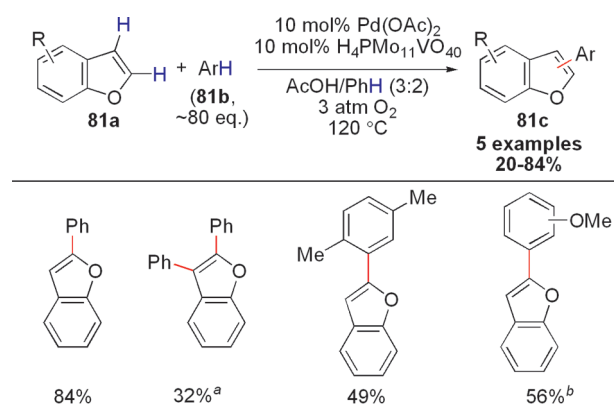


Figure 88. Pd-catalyzed oxidative C2 arylation of benzofurans.⁸⁴
^aUsing 2-phenylbenzofuran as the starting material, 2,3-diphenylbenzofuran was obtained in 20% yield.

^bThe arylation product was obtained in a 5:3:2 mixture of isomers.

suggested (see section 2). To achieve high regioselectivity, one of the coupling partners is usually an electron-rich arene or an arene bearing a directing group. Tandem C–H activation leads to diarylpalladium complex **77e** that ultimately undergoes reductive elimination to afford biaryl product **77f** and regenerate Pd(0) (**3g**).

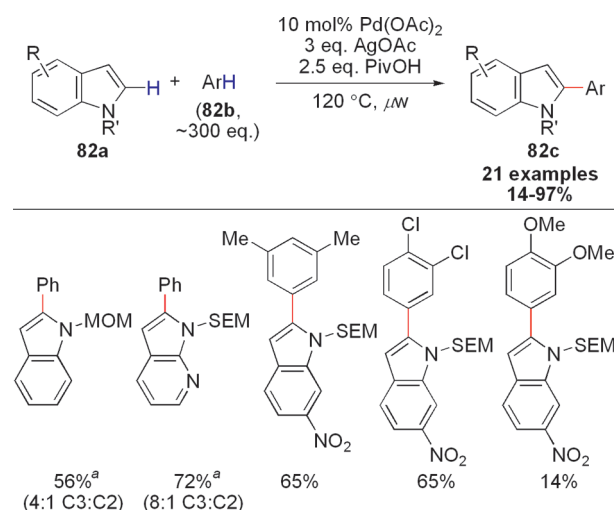


Figure 89. Pd-catalyzed oxidative C2 arylation of electron-rich *N*-protected indoles.⁸⁸

^aConventional heating was used.

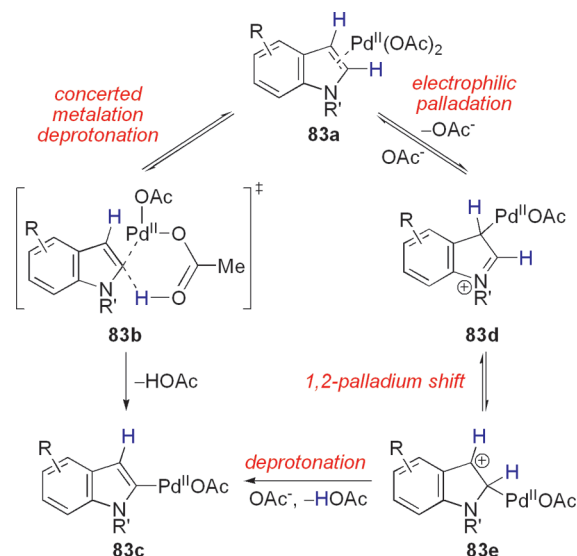
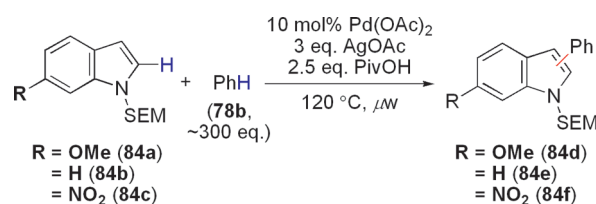


Figure 90. Proposed mechanisms for C2 palladation of *N*-protected indoles.⁸⁸



$$\frac{k_{84a}}{k_{84b}} = 1.34$$

$$\frac{k_{84b}}{k_{84c}} = 0.33$$

Figure 91. Competition study for Pd-catalyzed oxidative C2 arylation of electron-rich *N*-protected indoles.⁸⁸

3.1. Intermolecular Biaryl Bond Formation

One of the earliest accounts of regioselective arene *cross*-coupling was the contribution of Lu and co-workers in 2006. Dehydrogenative C–C bond formation was achieved between

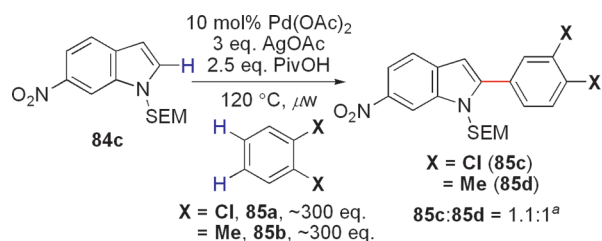


Figure 92. Intramolecular competition study for Pd-catalyzed oxidative C2 arylation of electron-rich *N*-protected indoles.⁸⁸

^aConducted with no PivOH.

^bConducted with 2.5 or 10 equiv PivOH.

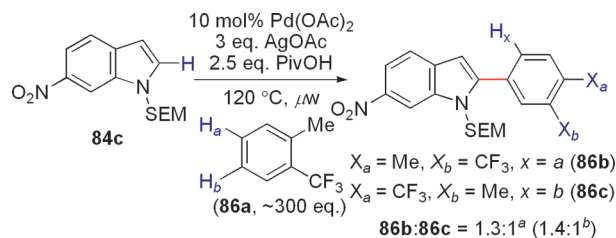


Figure 93. Intermolecular study for Pd-catalyzed oxidative C2 arylation of electron-rich *N*-protected indoles.⁸⁸

^aThe ratio of **86b**/**86c** was found to be unchanged with no PivOH, 2.5 equiv PivOH, or 10 equiv PivOH.

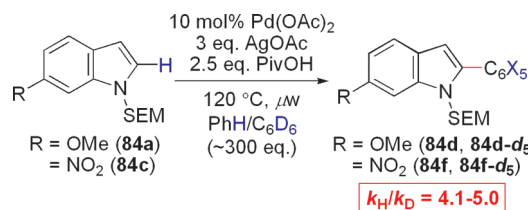


Figure 94. Kinetic isotope effect studies for Pd-catalyzed oxidative C2 arylation of electron-rich *N*-protected indoles.⁸⁸ Observed kinetic isotope effects (KIEs) were found to be relatively invariant with concentration of PivOH.

naphthalene and simple arenes using K₂S₂O₈ as the terminal oxidant.⁸⁰ Selective cross-coupling was achieved by optimizing the relative concentration of each arene starting material and the amount of trifluoroacetic acid (TFA). TFA is believed to enhance the electrophilicity of Pd(II) complexes, thus facilitating electrophilic palladations.⁸¹ Competition studies reveal no product kinetic isotope effect for the naphthalene coupling partner (**78a**, k_H/k_D (prod) = 1) but a large primary kinetic isotope effect for the simple arene coupling partners (**78b**, k_H/k_D (prod) = 9) (Figure 85).⁸⁰ Thus, two distinct C–H activation steps (involving different mechanisms) are implicated in this tandem direct arylation.

In 2007, Fagnou and co-workers published a seminal report on the oxidative cross-coupling of indoles and simple arenes. With Cu(OAc)₂ as the oxidant, C3 arylation of *N*-acetylindoles **79a** was achieved using **79b** as the solvent (Figure 86).⁸² The reaction tolerates electron-rich, -neutral, and -deficient simple arenes (**79b**). In contrast to *N*-acetylindoles, unprotected indoles and *N*-alkylindoles are inert under the same conditions. 3-Nitropyridine is added to this reaction and presumably plays an important role in stabilizing Pd(0) formed in the catalytic cycle. Although

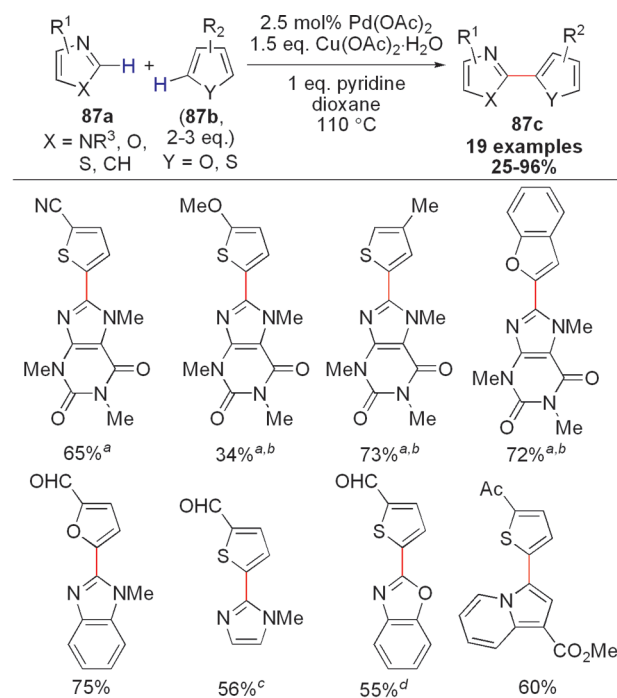


Figure 95. Pd-catalyzed oxidative 2-arylation of *N*-containing heterocycles.⁸⁹

^aArylation product derived from caffeine.

^b10 mol % CuCl was used as an additive.

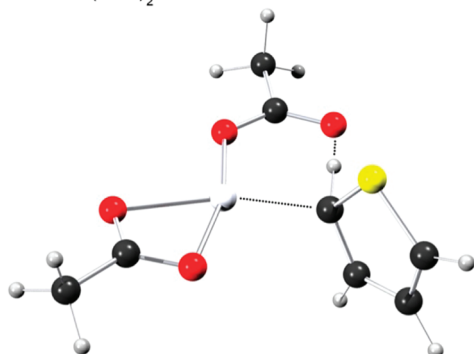
^cA second arylation occurring at C5 was observed (10% yield).

^d20 mol % CuCl and 20 mol % 1,10-phenanthroline was used as an additive, and the reaction was conducted in DMA.

conventional heating is effective, Fagnou favored microwave heating because this method enhanced the reaction rate. Choosing AgOAc as the terminal oxidant instead of Cu(OAc)₂, a reversal in regioselectivity and preference for C2 indole and pyrrole (**80a**) arylation is observed (Figure 87).⁸³ In the absence of Pd catalysts, Cu(OAc)₂ and AgOAc do not effect H/D exchange of either indole or pyrrole starting materials in AcOH-*d*₄. Using Pd(TFA)₂ with CsOAc, however, promotes C2 arylation. Additionally, C3 selectivity and palladium concentration is positively correlated (i.e., the ratio between 3-aryl- and 2-arylindole products increases with higher Pd catalyst loadings). To explain these findings, the authors propose higher-order Pd and/or Pd–Cu clusters that favor C3 arylation in the absence of external bases such as AgOAc; acetates are believed to prevent cluster formation, thus promoting cross-coupling at C2.

Concurrently, DeBoef and co-workers investigated the oxidative arylation of indoles and benzofurans with O₂ as the terminal oxidant (Figure 88).⁸⁴ Using O₂ is advantageous to other metal oxidants because C–C formation occurs with loss of water as the sole byproduct. Heteropolymolybdovanadic acid (H₄PMo₁₁VO₄₀) promoted oxidative arylation of benzofuran, favoring functionalization at C2. In a later study,⁸⁵ the DeBoef group observed that C2 and C3 regioselectivity depends on the oxidant chosen, because copper salts lead to the formation of polymetallic catalytically active clusters including Cu₂Pd(OAc)₆ and Cu₂Pd₄(OAc)₁₂.⁸⁶ Cu(OAc)₂ favors benzofuran arylation at C2, while AgOAc facilitates functionalization at C3.⁸⁵ Product kinetic isotope effects obtained for this reaction range from 1.9 to 4.0 and suggest that proton abstraction is the rate-limiting step. For indoles, C2 arylation predominates in the presence of copper,

a) Transition state model for thiophene palladation with $\text{Pd}(\text{OAc})_2$



b) Transition state model for *N*-methylimidazole palladation with $\text{Pd}(\text{OAc})(\text{thiophene})$

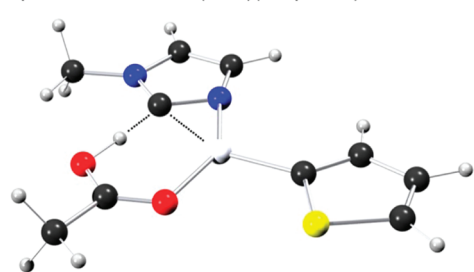


Figure 96. Transition state models for Pd-catalyzed oxidative 2-arylation of *N*-containing heterocycles. The POV-Ray drawing was created from coordinates obtained from Xi et al.⁸⁹ Legend: black = carbon, red = oxygen, blue = nitrogen, white = hydrogen, yellow = sulfur, and silver = palladium.

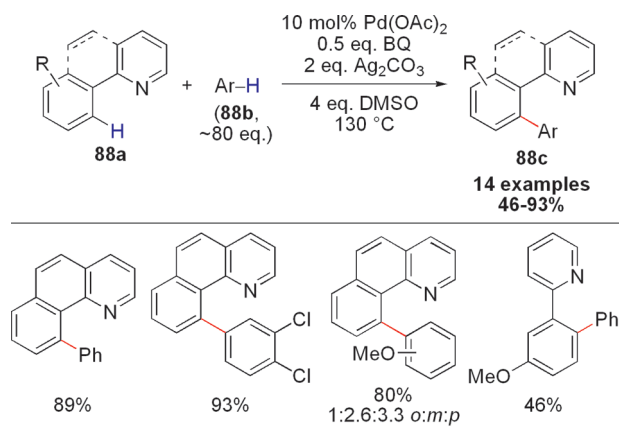


Figure 97. Pd-catalyzed oxidative arylation of benzo[*h*]quinoline and 2-phenylpyridines.⁹⁰

while C3 arylation is favored with silver, in agreement with Fagnou's work (vide supra). A proton abstraction mechanism is also consistent with the product kinetic isotope effects measured for indole arylation (2.4–4.0). It is important to note that the mechanistic intricacies concerning Pd-catalyzed functionalization of indoles, however, remain a subject of debate and can vary from reaction to reaction.^{13,87}

The DeBoef group demonstrated that electron-rich indoles are excellent cross-coupling partners in tandem direct arylations (Figure 89).⁸⁸ With acidic oxidative cross-coupling conditions (e.g., $\text{H}_4\text{PMo}_{11}\text{VO}_{40}$ ⁸⁴), these electron-rich heterocyclic arenes

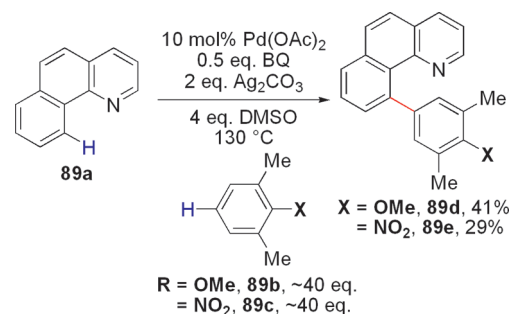


Figure 98. Competition study for Pd-catalyzed oxidative arylation of benzo[*h*]quinoline and 2-phenylpyridines.⁹⁰

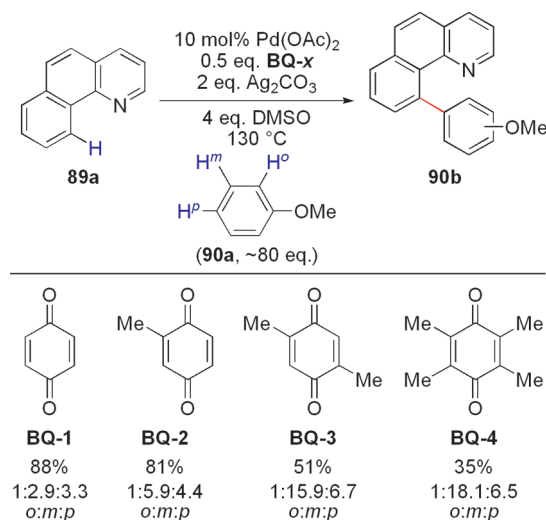


Figure 99. Ligand study for Pd-catalyzed oxidative arylation of benzo[*h*]quinoline and 2-phenylpyridines.⁹⁰

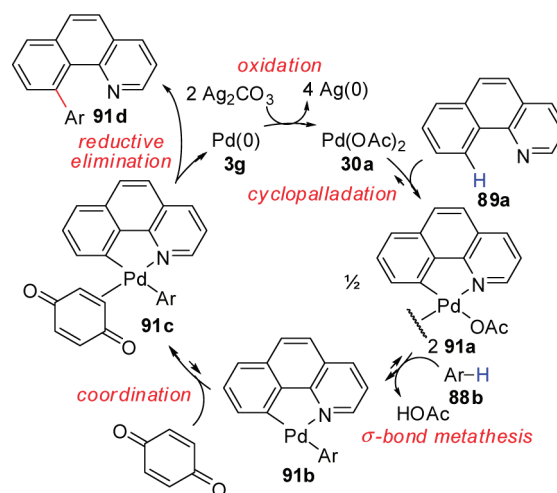


Figure 100. Proposed mechanism for Pd-catalyzed oxidative arylation of benzo[*h*]quinoline and 2-phenylpyridines.⁹¹

undergo decomposition; DeBoef's strategy to overcome this limitation involves modulating the acidity of the reaction medium by judicious selection of acid and base added (i.e., using a suitable buffer). Using catalytic quantities of palladium and stoichiometric amounts of pivalic acid and AgOAc (in slight

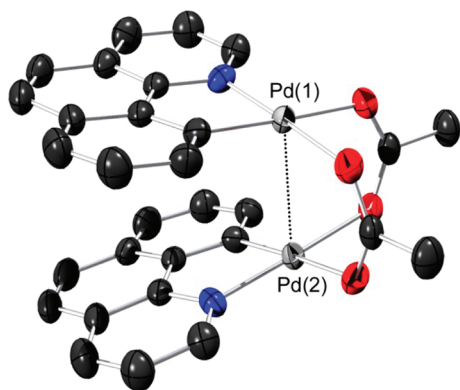


Figure 101. ORTEP plot of dimeric palladium complex resulting from the C–H activation of benzo[*h*]quinoline. All H atoms have been omitted for clarity. Anisotropic displacement ellipsoids are shown at the 50% probability level. The POV-Ray drawing was created from coordinates obtained from Powers and Ritter.⁹² Selected bond lengths (Å): Pd(1)–Pd(2) = 2.842. Legend: black = carbon, red = oxygen, blue = nitrogen, and silver = palladium.

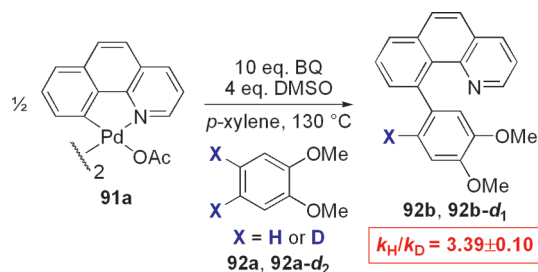


Figure 102. Kinetic isotope effect study for Pd-catalyzed oxidative arylation of benzo[*h*]quinoline and 2-phenylpyridines.⁹¹

excess to pivalic acid), a broad-scope oxidative C3 arylation of electron-rich *N*-protected indoles is possible. Azaindoles are also reactive under these reaction conditions.

DeBoef considered two possibilities for indole palladation: (1) electrophilic palladation⁶⁰ at C3, followed by palladium migration to C2, and (2) direct concerted metalation deprotonation²⁴ at the C2 position (Figure 90).⁸⁸ The authors conducted a competition study between 6-methoxy-*N*-[2-(trimethylsilyl)ethoxy]methylindole (**84a**), *N*-[2-(trimethylsilyl)ethoxy]methylindole (**84b**), and 6-nitro-*N*-[2-(trimethylsilyl)ethoxy]methylindole (**84c**, Figure 91). Kinetic analysis revealed that oxidative arylation occurs with pseudo-zero-order kinetics, which suggests that relative rates can be determined from reaction conversions directly. Electron-rich indole **84a** undergoes arylation at a faster rate than electron-neutral **84b** ($k_{84a}/k_{84b} = 1.34$), whereas **84b** arylates faster than electron-deficient **84c** ($k_{84b}/k_{84c} = 0.33$). Although electrophilic palladation can explain the higher reaction rates of methoxyindole **84a**, S_EAr of nitroindole **84c** leads to a benzylic cation intermediate that is destabilized by the electron-withdrawing 6-nitro group; this result is inconsistent with the high efficiencies reported. Hence, DeBoef favors concerted metalation deprotonation as a general mechanism for indole palladation, supported by computational studies highlighting that the electronic character of the indole exhibits the strongest impact on reactivity (i.e., more electron-rich indoles such as **84a** exhibit a stronger interaction with the Pd catalyst than less electron-rich analogues such as **84c**).

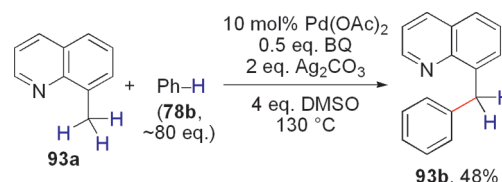


Figure 103. Pd-catalyzed oxidative phenylation of 8-methylquinoline.⁹⁰

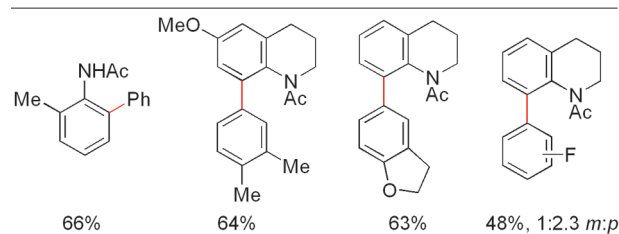
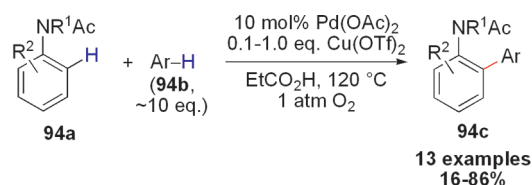


Figure 104. Pd-catalyzed oxidative *ortho*-arylation of anilides.⁹³

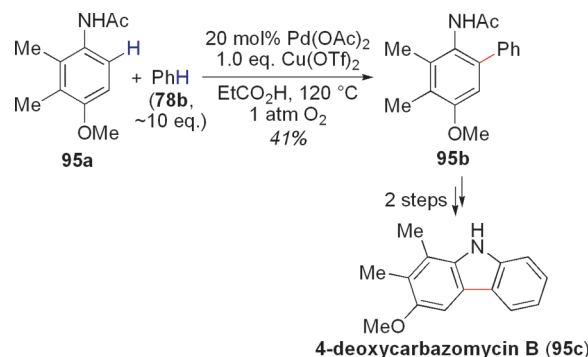


Figure 105. Total synthesis of 4-deoxycarbazomycin B (**95c**) via Pd-catalyzed oxidative *ortho*-phenylation of an anilide.⁹³

To probe the mechanism for arene palladation, a competition study between *o*-dichlorobenzene (**85a**) and *o*-dimethylbenzene (**85b**) revealed only a slight preference for the more electron-rich arene ($k_{85a}/k_{85b} = 1.1$, Figure 92).⁸⁸ An intramolecular competition study using 1-methyl-2-(trifluoromethyl)benzene (**86a**) also showed slight preference for arylation at the more electron-rich C–H bond (Figure 93). Observed kinetic isotope effects were large ($k_H/k_D = 4.1$ – 5.0 , Figure 94) and relatively invariant with the concentration of PivOH. This result led the authors to propose rate-limiting C–H bond activation of the simple arene via a CMD mechanism.²⁴ In DeBoef's system, both C–H palladation steps are believed to occur via acetate-assisted deprotonations.⁸⁸

Independently, the groups of Hu and You demonstrated that other classes of nitrogen-containing heterocycles (e.g., xanthines, imidazoles, benzimidazoles) undergo facile and regioselective arylation with stoichiometric amounts of $Cu(OAc)_2$ (Figure 95).⁸⁹ These compounds are prevalent in natural products, and hence, efficient strategies for synthesizing derivatives

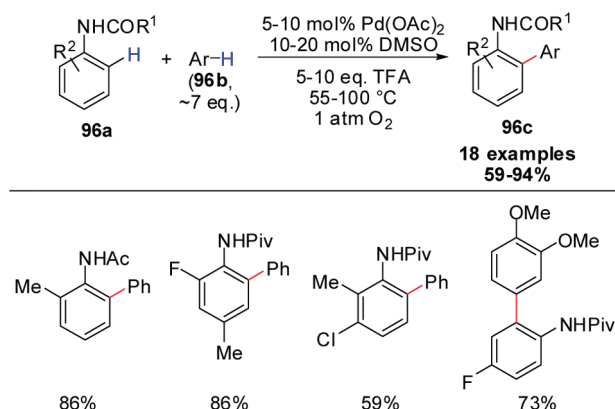


Figure 106. Pd-catalyzed, Cu-free oxidative *ortho*-arylation of anilides.⁹⁴

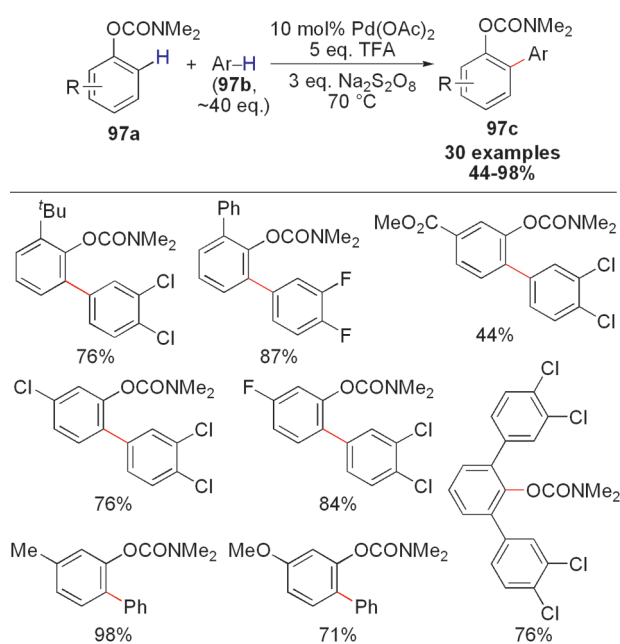


Figure 107. Pd-catalyzed oxidative *ortho*-arylation of *O*-phenyl-carbamates.⁹⁵

would be valuable to the drug-discovery process. Hu and You's reaction exhibits excellent functional group compatibility, tolerating unprotected aldehydes, ketones, and nitriles. A preliminary computational study using density functional theory (DFT) provided support for CMD mechanisms²⁴ for both C–H bond palladations (Figure 96). The lack of observed homocoupling was consistent with theoretical investigations.

In contrast to the Fagnou, DeBoef, and Hu and You strategies, Hull and Sanford used directing groups to achieve regioselective tandem arylation by mechanisms involving ligand-assisted cyclo-palladation (Figure 97).⁹⁰ Benzo[*h*]quinolines and 2-phenylpyridines (**78a**) undergo oxidative cross-coupling with simple arenes (**78b**) in the presence of Ag_2CO_3 . A range of electron-rich, -neutral, and -deficient arene coupling partners are suitable. DMSO is added to prevent both aggregation and precipitation of Pd(0). Homocoupling of either benzo[*h*]quinoline (**78a**) or arene (**78b**) partners is not observed under Sanford's optimized conditions. As highlighted in Figure 98, the authors conducted a competition experiment to demonstrate that electron-rich arenes

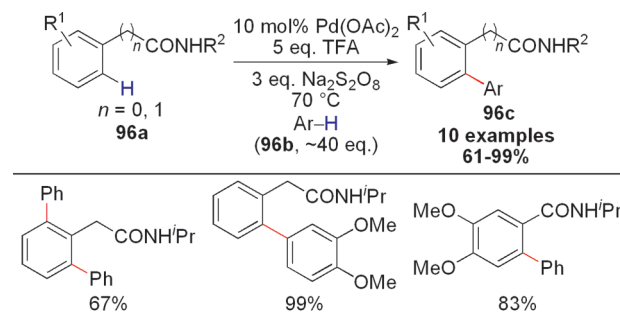


Figure 108. Pd-catalyzed oxidative *ortho*-arylation of phenylacetamides and benzamides.⁹⁶

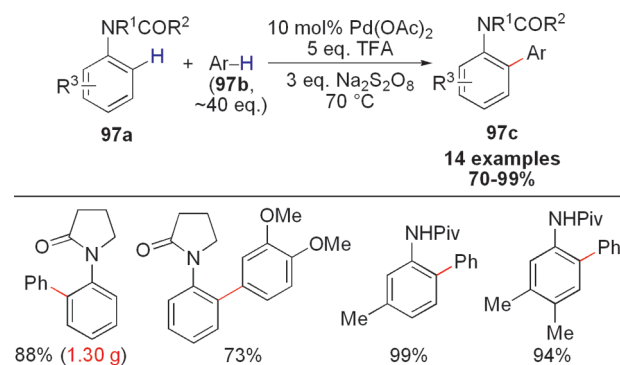


Figure 109. Pd-catalyzed oxidative *ortho*-arylation of anilides with $\text{Na}_2\text{S}_2\text{O}_8$.⁹⁶

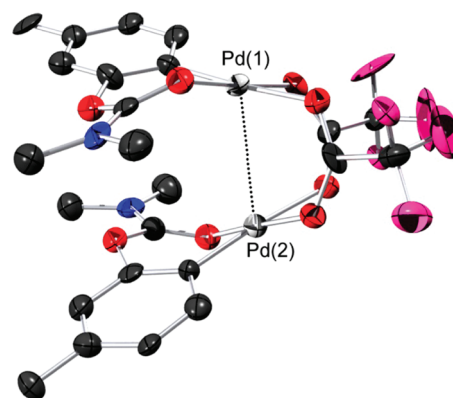


Figure 110. ORTEP plot of dimeric palladium complex resulting from C–H activation of *m*-tolyl dimethylcarbamate. All H atoms have been omitted for clarity. Anisotropic displacement ellipsoids are shown at the 50% probability level. The POV-Ray drawing was created from coordinates obtained from Zhao et al. Selected bond lengths (Å): Pd(1)–Pd(2) = 2.9163(10). Legend: black = carbon, red = oxygen, blue = nitrogen, pink = fluorine, and silver = palladium. Adapted with permission from ref 95. Copyright 2010 American Chemical Society.

exhibit slightly higher arylation rates than electron-deficient arenes, which suggests that chemoselectivities are primarily dependent on *steric* considerations. In dehydrogenative coupling with anisole (i.e., methoxybenzene, **80b**), the ratio between the *ortho*, *meta*, and *para* isomers is strongly influenced by the structure of the benzoquinone additive (Figure 99). Although this was initially attributed to a ligand effect, later studies suggest

that benzoquinone promotes reductive elimination of a diarylpalladium(II) complex (*vide infra*).

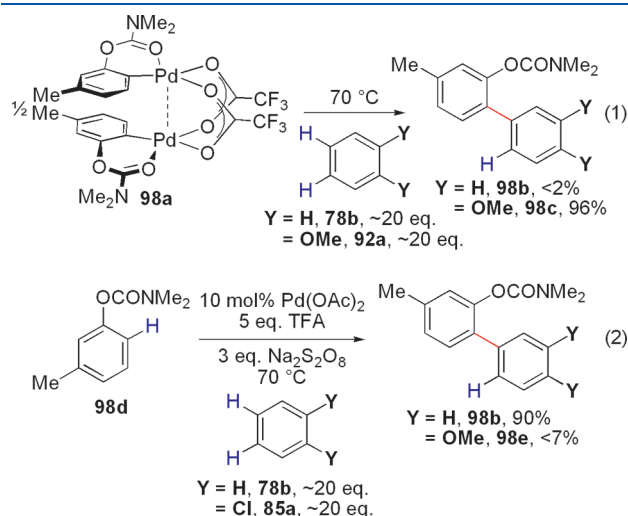


Figure 111. Competition study for Pd-catalyzed oxidative *ortho*-arylation of *O*-phenylcarbamates.⁹⁵

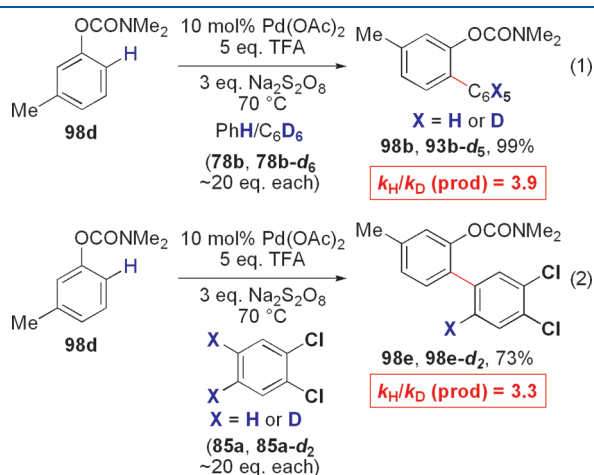


Figure 112. Kinetic isotope effect study for Pd-catalyzed oxidative *ortho*-arylation of *O*-phenylcarbamates.⁹⁵

The Sanford group proposed a mechanism involving a $\text{Pd}(\text{II}/0)$ catalytic cycle with the following steps: (1) C–H activation of benzo[*h*]quinoline **89a** by cyclopalladation to form **91a**,⁷⁸ (2) C–H activation of **88b** by σ -bond metathesis, (3) reductive elimination from **91c** to furnish the biaryl C–C bond, and (4) oxidation of $\text{Pd}(0)$ to $\text{Pd}(\text{II})$ in the presence of Ag_2CO_3 (Figure 100).⁹¹ Because electron-rich arenes react slightly faster than their electron-deficient counterparts, Sanford reasoned that CMD^{24} is not a viable pathway for the second C–H activation event. Additionally, the mild preference for electron-rich arenes appears inconsistent with a traditional electrophilic mechanism.⁶⁰ Thus, the authors propose a dissociative σ -bond metathesis mechanism⁷⁹ for reasons described below.

Sanford and co-workers prepared palladium dimer **91a**⁹² (by treatment of benzo[*h*]quinoline **89a** with $\text{Pd}(\text{OAc})_2$) to study the second C–H activation step (Figure 101).⁹¹ As shown in Figure 83, heating complex **91a** in the presence of arene, DMSO, and benzoquinone formed biaryl product **91d**. Kinetic analysis of this stoichiometric reaction displays half-order kinetics with dimer **91a**, first-order kinetics with arene **88b**, zero-order kinetics with DMSO, and inverse first-order kinetics with AcOH. Sanford's reaction exhibits saturation kinetics with benzoquinone. Subjecting **91a** to *o*-dimethoxybenzene (i.e., veratrole) in the presence of AcOH-d_4 results in deuteration of both 4- and 5-positions of the aromatic ring and is consistent with a reversible second C–H activation. Under saturating concentrations of benzoquinone, the authors observed a significant primary kinetic isotope effect for the simple arene (**92a**, **92a-d**, $k_{\text{H}}/k_{\text{D}} = 3.39$) (Figure 102). Thus, in the presence of excess benzoquinone, C–H palladation of **88b** is irreversible, is rate-limiting, and goes through dissociative σ -bond metathesis. On the other hand, with substoichiometric amounts of benzoquinone (or added AcOH), benzoquinone-promoted reductive elimination is rate-limiting.

Using a quinoline directing group in the presence of benzoquinone and Ag_2CO_3 , the Sanford group has achieved the only example of directing group facilitated sp^3 C–H bond arylation with simple arenes (Figure 103).⁹⁰

Shi and co-workers reported a complementary oxidative arene cross-coupling with amide directing groups (Figure 104).⁹³ Instead of stoichiometric silver salts, O_2 was used as a green oxidant for tandem direct arylation in conjunction with either catalytic or stoichiometric copper salts. *ortho*-Arylation of anilides (**94a**) proceeds smoothly with as little as 10 equiv of the

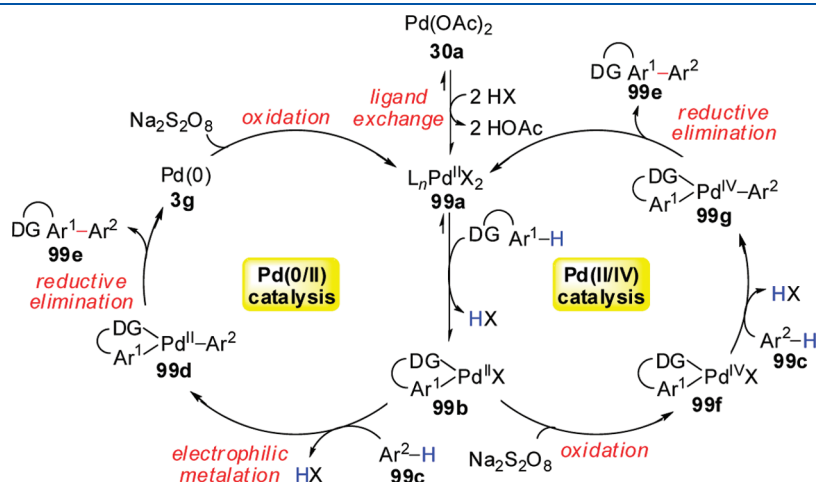
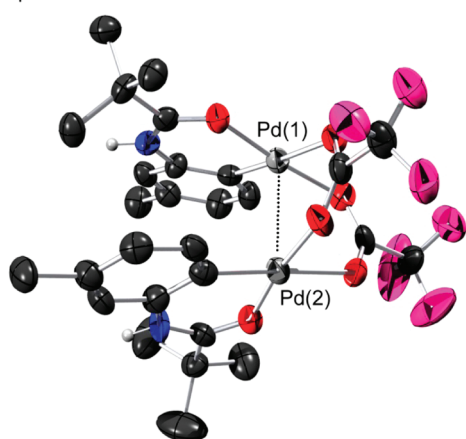


Figure 113. Proposed mechanism for Pd-catalyzed oxidative *ortho*-arylation of anilides with $\text{Na}_2\text{S}_2\text{O}_8$.⁹⁶ $\text{X} = \text{TFA}$.

a) Bimetallic Pd complex derived from *N*-(*m*-tolyl)-pivalanilide



b) Bimetallic Pd complex derived from *N*-phenylpyrrolidine

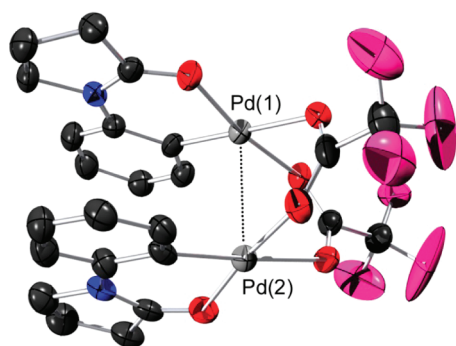


Figure 114. ORTEP plots of dimeric palladium complexes resulting from C–H activation of (a) *N*-(*m*-tolyl)pivalamide and (b) *N*-phenylpyrrolidine. All H atoms except the anilide N–H have been omitted for clarity. Anisotropic displacement ellipsoids are shown at the 50% probability level. The POV-Ray drawing was created from coordinates obtained from Yeung et al.⁹⁶ Selected bond lengths (Å): Pd(1)–Pd(2) = 2.9233(9) and 2.9515(9) for (a), and Pd(1)–Pd(2) = 2.8779(5) for (b). Legend: black = carbon, red = oxygen, blue = nitrogen, pink = fluorine, and silver = palladium. Adapted with permission from ref 96. Copyright 2010 Royal Society of Chemistry.

(typically electron-rich) unactivated arenes (**94b**). Additionally, this coupling can be conducted on a 10 mmol scale with moderate efficiencies (73%). Using 2,3-dihydrobenzofuran as the starting material, selective dehydrogenative coupling occurs without overoxidation of the arylation product to the corresponding benzofuran. Shi achieved a short synthesis of 4-deoxycarbazomycin B (**95c**) by this approach (Figure 105).

Shortly thereafter, Buchwald and co-workers described *ortho*-arylations using oxygen without the need for copper (Figure 106),⁹⁴ further reducing waste production. TFA was added to enhance the electrophilicity of the Pd catalyst and promote C–H activation. Buchwald's arylation works well with electron-rich arenes but not arenes bearing strong electron-withdrawing groups (e.g., trifluoromethyl-, nitro-, or ester-substituted arenes). Regioselective functionalization of the simple arene coupling partner occurs at the least sterically hindered C–H bond. In accord with Sanford's studies,⁹⁰ DMSO helps inhibit the formation of palladium black.⁹⁴ Although other oxidative arylation methods require a large excess of one arene,

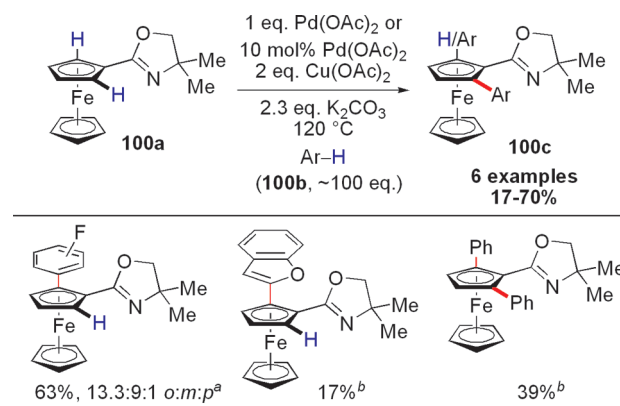


Figure 115. Pd-catalyzed oxidative *ortho*-arylation of ferrocenes.¹⁰³

^aStoichiometric in Pd(OAc)₂.

^bCatalytic in Pd(OAc)₂.

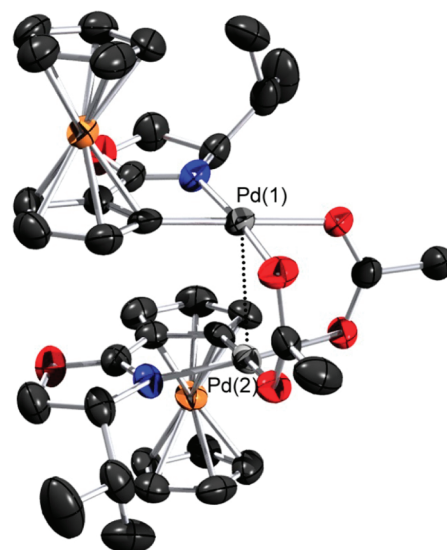


Figure 116. ORTEP plot of dimeric palladium complex resulting from C–H activation of ferrocene derivative. All H atoms have been omitted for clarity. Anisotropic displacement ellipsoids are shown at the 50% probability level. The POV-Ray drawing was created from coordinates obtained from Xia and You.¹⁰³ Selected bond lengths (Å): Pd(1)–Pd(2) = 2.858. Legend: black = carbon, red = oxygen, blue = nitrogen, orange = iron, and silver = palladium.

Buchwald's work demonstrates that highly selective arylation are possible with as little as 4–10 equiv of the simple arene.

Dong and co-workers reported catalytic conditions amenable to a relatively broad class of arenes, including *O*-carbamates, phenylacetamides, benzamides and anilides (Figures 107–109). Their *ortho*-arylations occurred under Fujiwara-type conditions using TFA in combination with Na₂S₂O₈, a relatively benign and inexpensive oxidant.^{95,96} The *ortho*-arylation of *O*-phenylcarbamates (**88a**) provides a way to make protected 2-arylphenol derivatives (**88c**, Figure 107).⁹⁵ Because of the high reactivity of the catalyst, *O*-phenylcarbamates bearing two reactive C–H bonds undergo facile diarylation in a 4-fold C–H functionalization process. Although used in large excess (~40 equiv), a wide range of electron-deficient, electron-neutral, and electron-rich arenes (**88b**) are well-suited for this process. In contrast, phenylacetamide and benzamide substrates undergo arylation

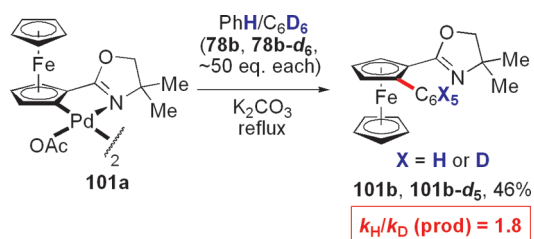


Figure 117. Kinetic isotope effect study for Pd-catalyzed oxidative *ortho*-arylation of ferrocenes.¹⁰³

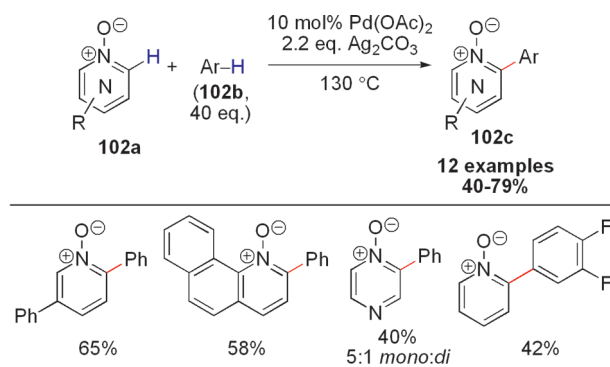


Figure 118. Pd-catalyzed oxidative 2-arylation of azine *N*-oxides.³⁰

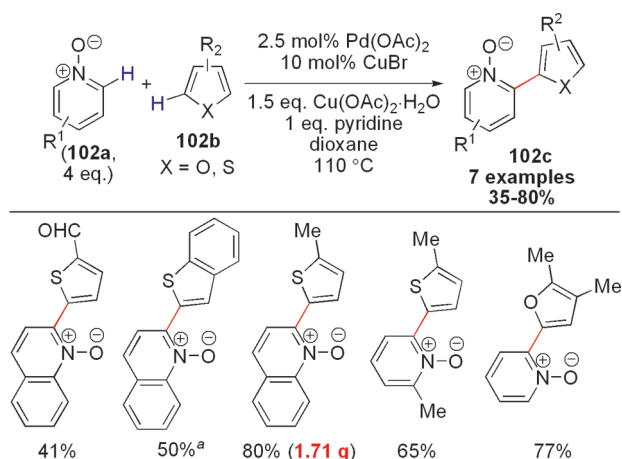


Figure 119. Pd-catalyzed oxidative 2-arylation of azine *N*-oxides.⁸⁹
^aConducted at 120 °C.

best with electron-neutral and electron-rich arenes (**89a**, Figure 108).⁹⁶ For benzamides, the presence of electron-donating groups, such as methoxy, is required to promote reactivity. Arylation of anilides exhibited reactivities and regioselectivities similar to that of Buchwald's⁹⁴ and could be conducted on a 1 g scale (88%, 1.30 g, Figure 109).⁹⁶

To study the mechanism of $\text{Na}_2\text{S}_2\text{O}_8$ oxidative coupling, Dong and co-workers prepared and characterized a cyclopalladate derived from an *O*-phenylcarbamate (Figure 110).^{95,97} Subjecting this bimetallic palladium complex to simple arenes in the *absence* of any external oxidant affords the *ortho*-arylation products in excellent yields. A series of competition studies revealed that electron-rich arenes react faster than electron-poor arenes (Figure 111). Both benzene (**78b**) and *o*-dichlorobenzene (**85a**) undergo cross-coupling in preference to their deuterated analogues (Figure 112). Together, these results are consistent with

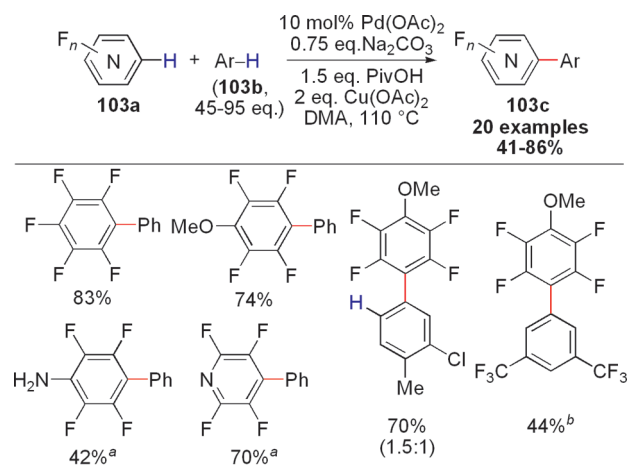


Figure 120. Pd-catalyzed oxidative arylation of perfluoroarenes.¹⁰⁴

^a20 mol % $\text{Pd}(\text{OAc})_2$ was used.

^b1 equiv Na_2CO_3 and 2 equiv PivOH were used.

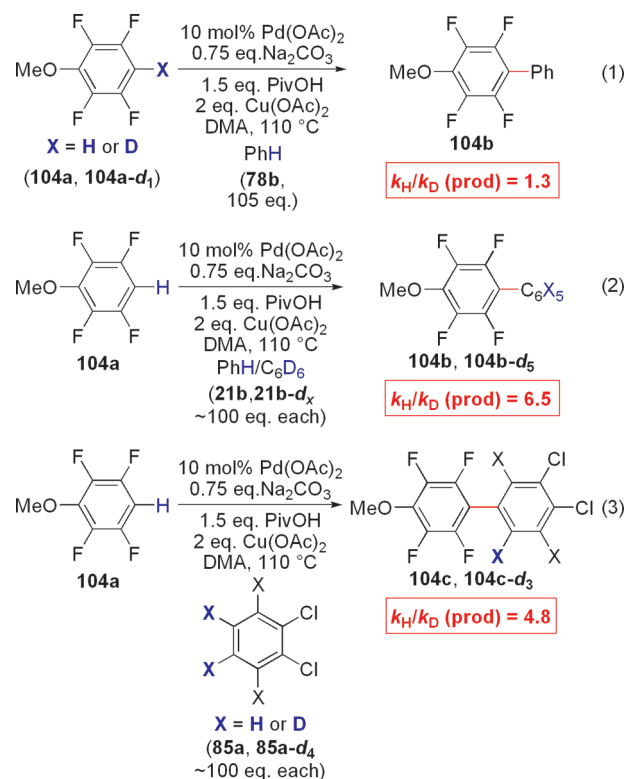


Figure 121. Kinetic isotope effect studies for Pd-catalyzed oxidative arylation of perfluoroarenes.¹⁰⁴

the $\text{Pd}(\text{II}/0)$ mechanism shown in Figure 113. Cyclopalladation generates palladacycle **99b** that can undergo electrophilic metalation with simple arene **99c**.⁶⁰ The authors note, however, that a concerted metalation deprotonation cannot be ruled out. In CMD mechanisms,²⁴ electron-deficient arenes typically react faster due to enhanced C–H acidity. However, Fagnou and Gorelsky's computational studies suggest that acidity is not the only critical parameter in (trifluoro)acetate-assisted deprotonations, and so the CMD mechanism may be more widespread than previously believed.

In related studies, the Dong group prepared palladium complexes derived from cyclopalladation with *N*-(*m*-tolyl)pivalamide

and *N*-phenylpyrrolidine (Figure 114).⁹⁶ In contrast to their previous work (vide supra), subjecting these bimetallic palladacycles to arenes does not give expected *ortho*-arylation product. Additives such as TFA and DMSO failed to effect cross-coupling. Yet, the addition of Na₂S₂O₈ results in smooth transformation to the final product. Because persulfate salts have a high redox potential (i.e., 2.01 eV)⁹⁸ and are thought to promote Pd(II/IV) catalytic manifolds,^{99,100} a mechanism involving oxidation of the bimetallic palladacycle (**99b**) to Pd(III)^{92,101} or Pd(IV)¹⁰² can be considered (Figure 113). These results emphasize that the mechanisms of oxidative cross-couplings may differ greatly depending on the type of directing group and oxidant involved.

The You group used oxazoline as a directing group for oxidative arylation of a ferrocene derivative **100a** (Figure 115).¹⁰³ The

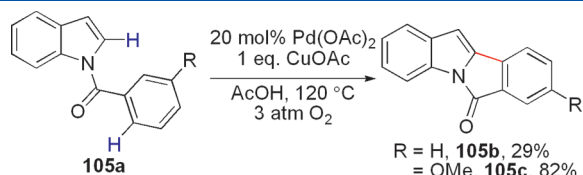


Figure 122. Pd-catalyzed intramolecular oxidative cyclization of *N*-benzoylindoles.⁸⁴

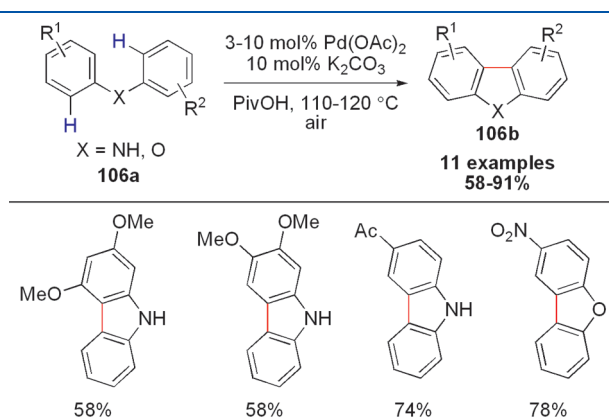


Figure 123. Pd-catalyzed intramolecular oxidative cyclization of diarylanilines and diarylethers.¹⁰⁶

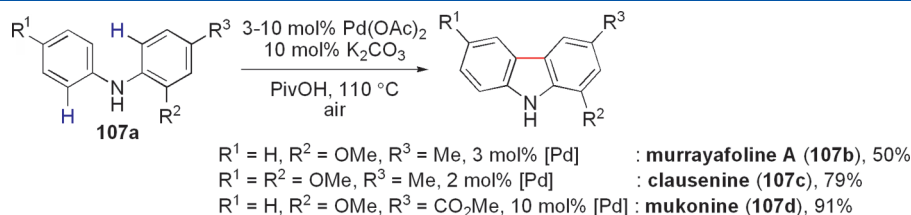


Figure 124. Total syntheses of murrayafoline A (**107b**), clausenine (**107c**), and mukonine (**107d**) via Pd-catalyzed intramolecular oxidative cyclization of diarylanilines.¹⁰⁶

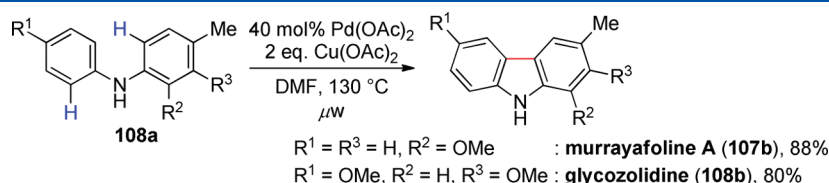


Figure 125. Total syntheses of murrayafoline A (**107b**) and glycozolidine (**108b**) via Pd-catalyzed oxidative cyclization.¹⁰⁷

stoichiometric version of this transformation proved more successful than the corresponding catalytic variant and accommodates electron-rich, -neutral, and -deficient arene coupling partners (**100b**, 26–70% yields). Isolating the palladium bimetallic complex (Figure 116) and subjecting it to a mixture of benzene and deuterated benzene (**78b**, **78b-d₆**) with an external base (i.e., K₂CO₃) reveals a primary product kinetic isotope effect. This result suggests that the second palladation step occurs with significant bond breaking of the arene C–H bond (i.e., $k_{\text{H}}/k_{\text{D}}$ (prod) = 1.8, Figure 117).

Other than *N*-protected indoles,^{82–84} pyrroles,⁸³ and benzofurans,⁸⁴ azine *N*-oxides can undergo intermolecular arene cross-couplings (Figure 118).³⁰ Chang and co-workers demonstrated that Ag₂CO₃ can effect the 2-arylation of pyridine *N*-oxides (**102a**) and other related heterocycles under Pd-catalyzed dehydrogenation. In another account, Hu, You, and co-workers developed conditions for catalytic arylation of heteroarenes (Figure 119).⁸⁹ Functionalization occurs regioselectively at the C2 position of electron-rich heteroaromatic rings. Hu and You's method can be performed on a gram scale without loss in reaction efficiency.

Next, the group of Su cross-coupled perfluorinated arenes with unfunctionalized arenes using Pd catalysts and stoichiometric Cu(OAc)₂ as the oxidant (Figure 120).¹⁰⁴ Silver salts, however, afforded lower yields of the desired biaryl product **103c**. This reaction tolerates sensitive and Lewis basic functionalities such as unprotected anilines. Su's arylations are highly regioselective, typically favoring the least sterically hindered C–H bond on the unactivated arene coupling partner (**103b**). In substrates bearing electronically differentiated C–H bonds exhibiting similar steric encumbrances, functionalization occurs at the more electron-rich site. Intermolecular competition studies suggest that palladation of the perfluoroarene is not the rate-limiting step ($k_{\text{H}}/k_{\text{D}}$ (prod) = 1.3), but rather it is C–H activation of the arene partner ($k_{\text{H}}/k_{\text{D}}$ (prod) = 4.8–6.5, Figure 121). A CMD mechanism²⁴ involving C–H deprotonation is likely.

3.2. Intramolecular Biaryl Bond Formation

Intramolecular oxidative arylation using palladium is a well-precedented process. In 1978, Shiotani and Itatani demonstrated that dibenzofurans could be derived from unsymmetrically

substituted diaryl ethers.¹⁰⁵ The first catalytic example of intramolecular oxidative arylation was developed by DeBoef and

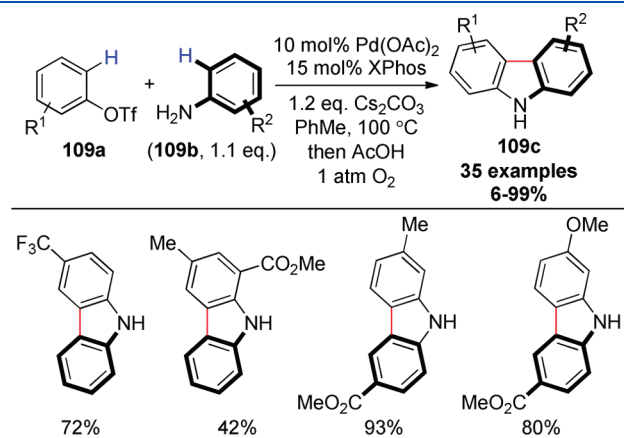


Figure 126. One-pot Pd-catalyzed synthesis of carbazoles from aryl triflates and anilines.¹⁰⁸

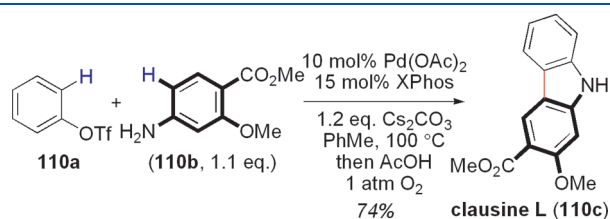


Figure 127. Total synthesis of clausine L (110c) via one-pot Pd-catalyzed synthesis of carbazoles from aryl triflates and anilines.¹⁰⁸

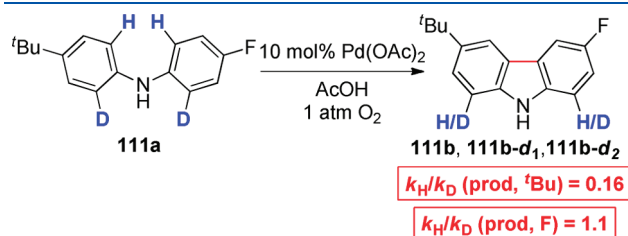


Figure 128. Intramolecular kinetic isotope effect study for one-pot Pd-catalyzed synthesis of carbazoles from aryl triflates and anilines.¹⁰⁸

co-workers in 2007 (Figure 122).⁸⁴ Using stoichiometric amounts of CuOAc under elevated pressures of O₂, cyclization of *N*-benzoylindoles (105a) affords the 6*H*-isoindolo[2,1-*a*]indol-6-ones (105b,c). The Fagnou group later extended this method to the ring closure of unsymmetrically substituted diarylanilines and diarylethers (106a) toward carbazoles and dibenzo[*b,d*]furans (106b), respectively (Figure 123).¹⁰⁶ Pivalic acid is a superior solvent to acetic acid and helps to improve reaction efficiency while minimizing byproduct formation. Fagnou synthesized murrayafoline A (107b), clausenine (107c), and mukonine (107d, Figure 124) by intramolecular tandem direct arylation. In combination with microwave technology, the total syntheses of alkaloids murrayfoline A (107b) and glycozolidine (108b) were later developed by Menéndez and co-workers (Figure 125).¹⁰⁷

The groups of Fujii and Ohno developed a one-pot carbazole synthesis that combines a Buchwald–Hartwig cross-coupling and intramolecular oxidative arylation (Figure 126).¹⁰⁸ In this transformation, Pd(0/II)-catalyzed coupling between an aryl triflate (109a) and an aniline derivative (109b) takes place to afford a diarylamine intermediate. Next, intramolecular C–C bond formation ensues in the presence of O₂ as the terminal oxidant, analogous to Fagnou and Menéndez's work. Many functionalities can be tolerated in Fujii and Ohno's reaction, including ketones and esters, and the total synthesis of clausine L (110c) was achieved by this method (Figure 127). Subjecting isotopically labeled diarylamine 111a produces carbazole product 111b but with significant loss of the deuterium label on the *tert*-butyl-substituted aromatic ring. This result suggests reversible *ortho*-palladation of diarylamine 111a. Additionally, a secondary kinetic isotope effect is observed for the fluorine-substituted aromatic ring (Figure 128). Overall, these investigations are consistent with a mechanism involving *carbopalladation* of the aromatic ring to give complex 112f, which undergoes β-H elimination to yield carbazole 109c (Figure 129). The mechanism bears resemblance to Heck couplings (see section 2). It is also reasonable to propose a pathway involving electrophilic metalation.⁶⁰

Synthesis of six-membered rings by Pd-catalyzed oxidative cyclization was first reported by Liégault and Fagnou.¹⁰⁹ Dong and co-workers developed a complementary strategy for anilides 110a via an intramolecular biaryl bond formation (Figure 130).⁹⁶ Direct synthesis of six-membered lactams (110b) can be achieved in the presence of Na₂S₂O₈. Electron-donating groups

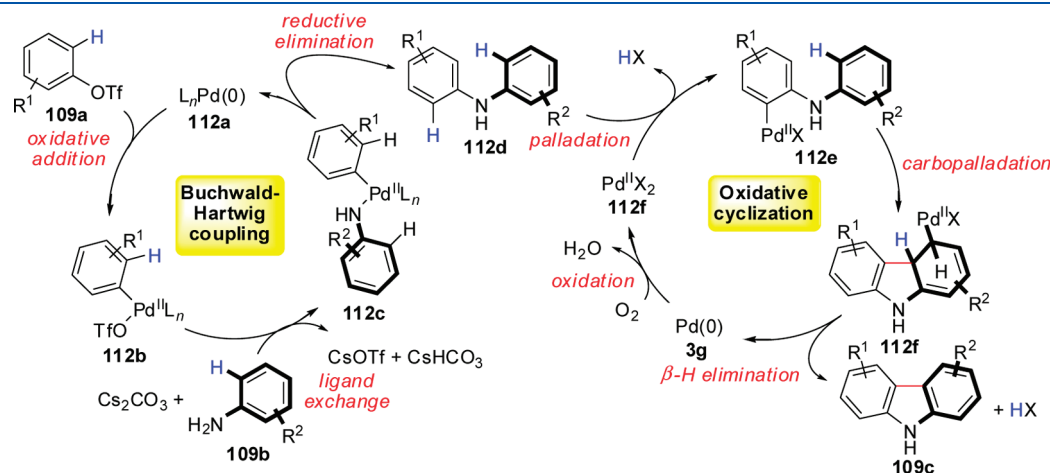


Figure 129. Proposed mechanism for one-pot Pd-catalyzed synthesis of carbazoles from aryl triflates and anilines.¹⁰⁸

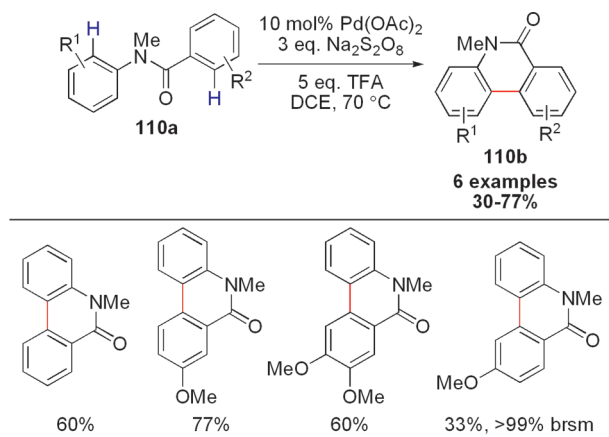


Figure 130. Pd-catalyzed oxidative cyclization of anilides.⁹⁶

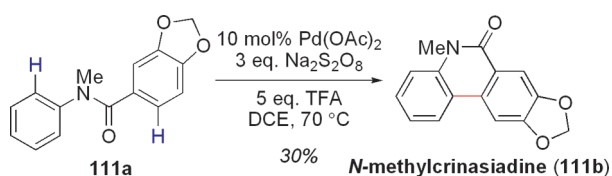


Figure 131. Total synthesis of *N*-methylcrinasiadine (111b) via Pd-catalyzed oxidative cyclization.⁹⁶

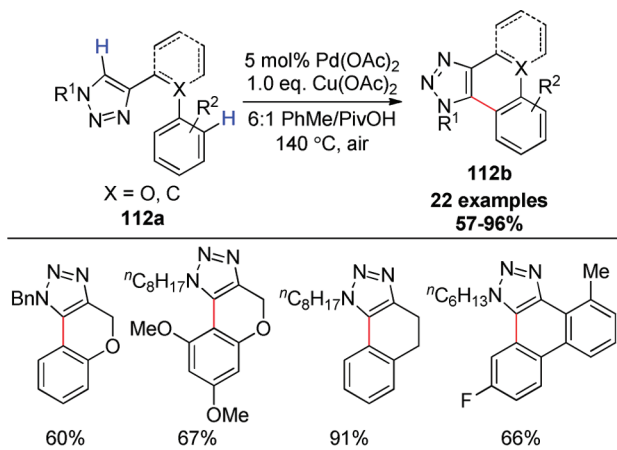


Figure 132. Pd-catalyzed intramolecular oxidative cyclization.¹¹⁰

on the benzamide ring are preferred. *N*-Methylcrinasiadine (110b), a natural product isolated from *Hippeastrum equestre* and *Lapiedra martinezii*, can be synthesized via this dehydrogenative reaction, albeit in low yield (Figure 131).

Ackermann and co-workers coupled a triazole sp² C–H bond with an arene sp² C–H bond using Pd(OAc)₂ and Cu(OAc)₂ (Figure 132).¹¹⁰ Neither air nor AgOAc was as effective as Cu(OAc)₂. On the basis of the observed regioselectivities, Ackermann proposes a mechanism involving triazole palladation followed by arene activation. This second C–H bond palladation may occur by a pathway distinct from base-assisted deprotonation (such as σ -bond metathesis or electrophilic metalation).

Intramolecular cyclization of *N*-pivaloyl pyrroles (111a) was reported by the Fagnou group, a reaction involving a rare sp²–sp³ coupling in air (Figure 133).¹⁰⁹ The use of other oxidants

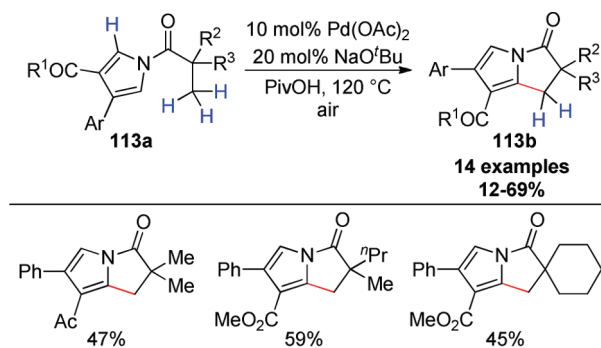


Figure 133. Pd-catalyzed oxidative intramolecular cyclization.¹⁰⁹

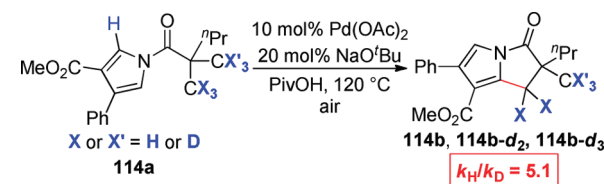


Figure 134. Kinetic isotope effect study on Pd-catalyzed oxidative intramolecular cyclization.¹⁰⁹

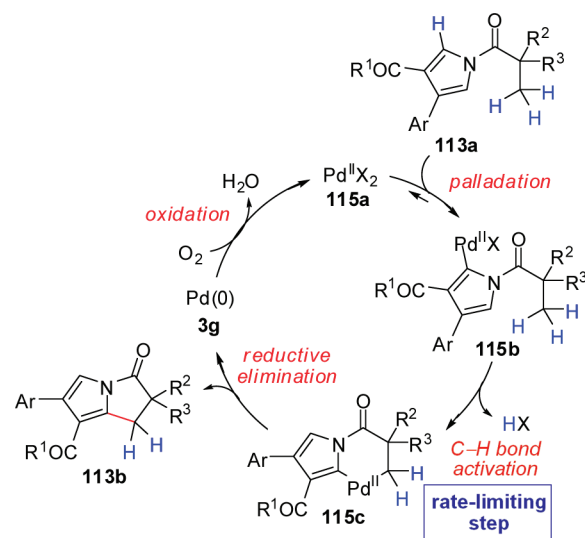


Figure 135. Proposed mechanism for Pd-catalyzed oxidative intramolecular cyclization.¹⁰⁹

(e.g., 1 atm dry O₂, Cu(OAc)₂, AgOAc) and bases (e.g., Na₂CO₃, CsOPiv, DABCO) decreased the overall reaction efficiency. Regioselectivity is high for the C–H bond adjacent to electron-withdrawing groups present on the pyrrole (113a). In the presence of deuterium-labeled pivalic acid, D atoms are incorporated in the isolated starting material (113a) and product (113b), which suggests reversible arene palladation. A large primary intramolecular kinetic isotope effect on the sp³ C–H bond reveals significant C–H or C–D bond breaking in the rate-limiting step (Figure 134). Thus, Fagnou proposes a mechanism involving reversible palladation of the arene as the first step, followed by rate-limiting sp³ C–H activation. Reductive elimination generates the desired product and liberates Pd(0), which undergoes oxidation by the O₂ present in air (Figure 135).

3.3. Miscellaneous Examples

Intramolecular 2-fold C–H activation has been coupled to alkyne carbopalladation in a domino sequence for the synthesis of quinolin-2(1*H*)-ones (**116c**) and 3-methyleneoxindoles (**116d**, Figure 136).¹¹¹ The Li group discovered that *N*-methyl-*N*-aryl-ynamides (**116a**) can undergo either 5-*exo*- or 6-*endo*-cyclization and arylation with an unactivated arene (**116b**) to afford the corresponding 5-membered and 6-membered *N*-containing heterocycles, quinolin-2(1*H*)-one (**116c**) and 3-methyleneoxindole (**116d**), respectively, with the former being favored in the presence of pivalic acid. *p*-Nitrobenzoic acid also performs the same task. Oxypalladation is a major byproduct when pivalic acid is present. On the basis of kinetic isotope effect data (Figure 137), Li and co-workers propose that C–H activation competes with alkyne oxypalladation but is favored in the presence of pivalic acid (Figure 138).

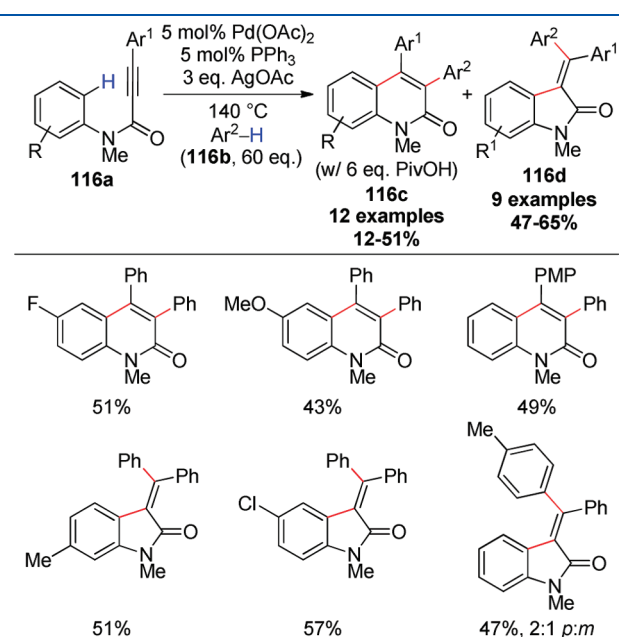


Figure 136. Pd-catalyzed synthesis of quinolin-2(1*H*)-ones and 3-methyleneoxindoles via C–H activation and tandem direct arylation.¹¹¹

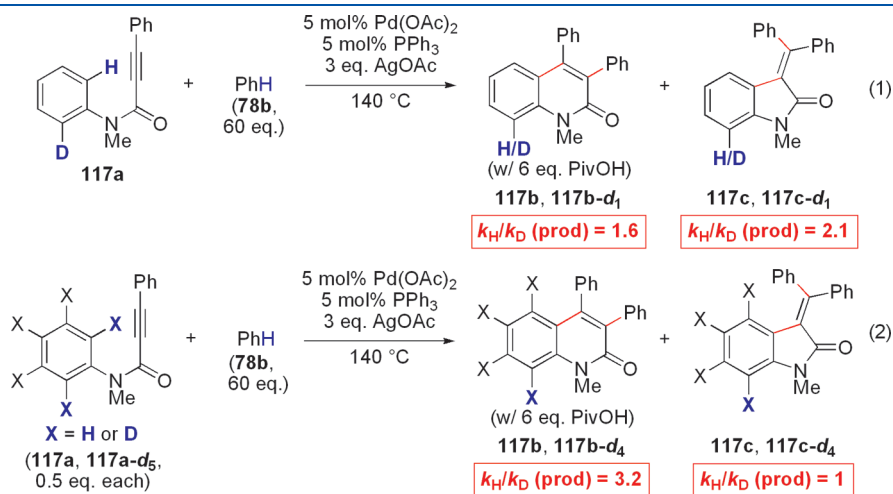


Figure 137. Kinetic isotope effect studies for Pd-catalyzed synthesis of quinolin-2(1*H*)-ones and 3-methyleneoxindoles via C–H activation and tandem direct arylation.¹¹¹

A domino intramolecular C–H activation/enolate arylation approach to phenanthrone derivatives (**119c**) was reported by the Cheng group,¹¹² and this method complements other oxidative enolate arylations (see section 5.2). Secondary alkylarylketone **119a** undergoes *ortho*-C–H arylation by direct coupling with aryl iodide **119b** to form an intermediate biphenylalkylketone, which then cyclizes (Figure 139). Catalytic amounts of Pd(OAc)₂ are optimal in the presence of an Ag₂O oxidant. A cyclopalladate derived from *ortho*-C–H activation of cyclohexylphenylketone (Figure 140) converts to the corresponding phenanthrone product when subjected to the reaction conditions. Hence, the proposed mechanism involves direct arylation (i.e., a C–H and C–I bond undergo cross-coupling)⁹ between the alkylarylketone (**119a**) and the iodoarene (**119b**) via cyclopalladation and may involve a Pd(II/IV) catalytic cycle.¹⁰⁰ Intermediate **120c** coordinates weakly to the Pd center and directs a second cyclopalladation on the distal aromatic ring. Seven-membered palladacycle **120d** undergoes deprotonation and, finally, reductive elimination to furnish cross-coupling product **119c** (Figure 141).¹¹² Using primary alkylarylketones, oxidative carbocyclization does not take place and the reaction halts after the direct arylation. An alternative mechanism involving a Lewis-acid catalyzed 6*π*-electrocyclization is also possible, because Ag₂O alone can promote conversion of **120c** to **119c**, albeit in reduced efficiencies.

4. CROSS-COUPLING VIA IONIC INTERMEDIATES

In sections 2 and 3, we described mechanistic strategies for dehydrogenative coupling involving Pd catalysis, which primarily involve the intermediacy of complexes containing Pd–C bonds via direct C–H bond activation. In a complementary approach, transition metals can promote oxidative C–C bond formation by polar bond formation between an electrophilic carbon species (e.g., a carbocation) and a carbon-based nucleophile (e.g., a carbanion, enamine, or heteroaromatic). Carbocations can be generated by C–H bond oxidation of a suitable precursor, whereas carbanions can be prepared by deprotonation of relatively acidic C–H bonds (Figure 142). Facile and mild oxidation of substrates including amines, ethers, and simple allylic and benzylic compounds and subsequent cross-coupling with a wide range of nucleophiles is possible (Figure 143). Ionic-type

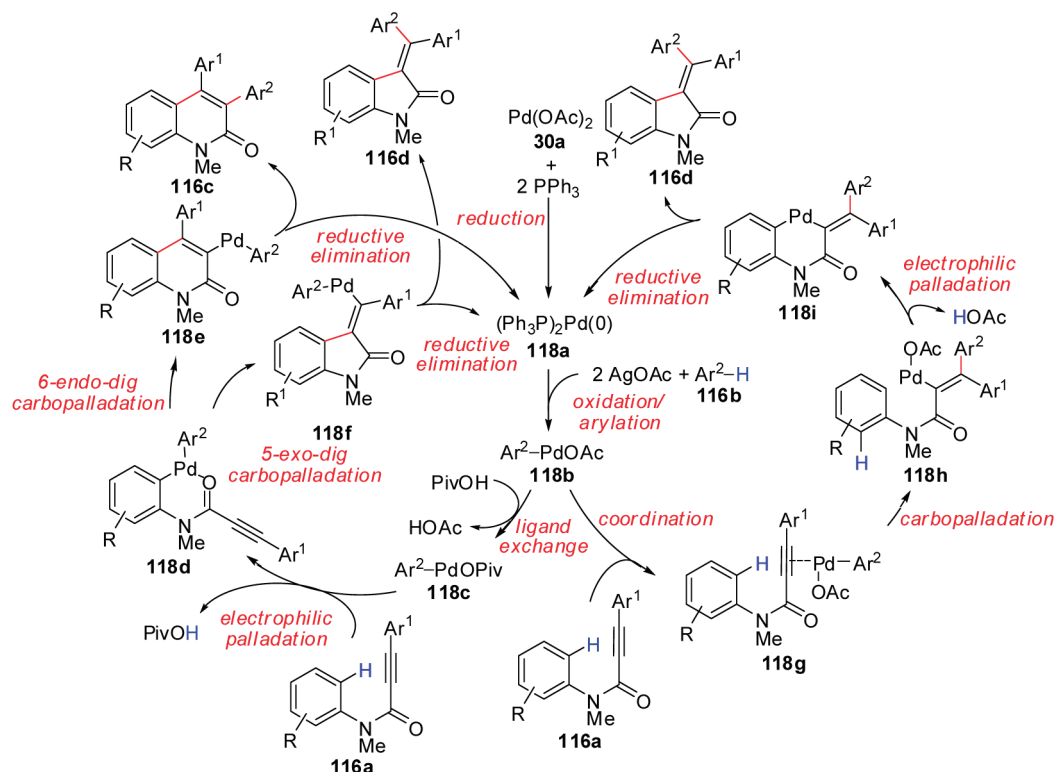


Figure 138. Proposed mechanism for Pd-catalyzed synthesis of quinolin-2(1H)-ones and 3-methyleneoxindoles via C–H activation and tandem direct arylation.¹¹¹

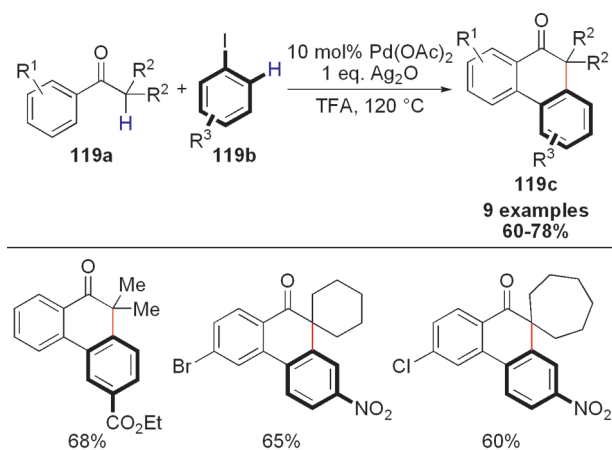


Figure 139. Pd-catalyzed synthesis of phenanthrones via cross-coupling of secondary alkylarylketones and iodoarenes.¹¹²

couplings generally occur with minimal homocoupling because the polarized intermediates (i.e., the carbocation or carbanion) have a greater propensity to react with each other instead of with themselves.

4.1. α -Functionalization of Amines

The electrochemical oxidation of alkylamines is a green process that generates iminium ions by using electrical energy to promote the loss of electrons.¹¹³ These iminium ions will react with various C-based nucleophiles to yield an overall dehydrogenative cross-coupling. To achieve efficient coupling, the iminium ions generated must react with a nucleophile faster than it undergoes decomposition.¹¹⁴ Oxidative C–C bond formations

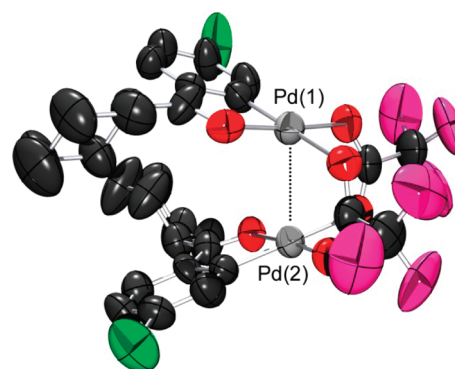


Figure 140. ORTEP plot of dimeric palladium complex resulting from the C–H activation of cyclohexylphenylketone. All H atoms have been omitted for clarity. Anisotropic displacement ellipsoids are shown at the 50% probability level. The POV-Ray drawing was created from coordinates obtained from Gandeepan et al.¹¹² Selected bond lengths (Å): Pd(1)–Pd(2) = 2.863. Legend: black = carbon, red = oxygen, green = chlorine, and silver = palladium.

via in situ generation of carbocations is challenging because the nucleophile (e.g., enolate) is susceptible oxidative degradation. The α -functionalization of amines (and also p -functionalization of arylamines¹¹⁵) with cyanide anions, however, has been known since the late 1960s using both anodic¹¹⁶ and chemical¹¹⁷ oxidation methods. This strategy can tolerate cyanide anions because cyanides exhibit higher oxidation potentials than other carbanions.¹¹⁴

In 2003, Murahashi and co-workers developed a general strategy for the α -cyanation of amines (139a) with HCN (139b) in the presence of Ru catalysts under nonelectrochemical

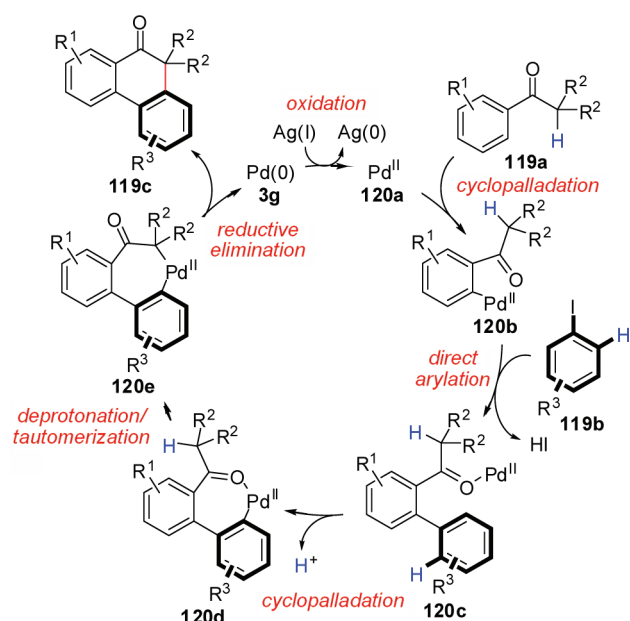


Figure 141. Proposed mechanism for Pd-catalyzed synthesis of phenanthrones via cross-coupling of secondary alkylarylketones and iodoarenes.¹¹²

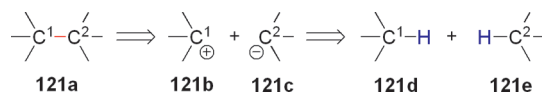
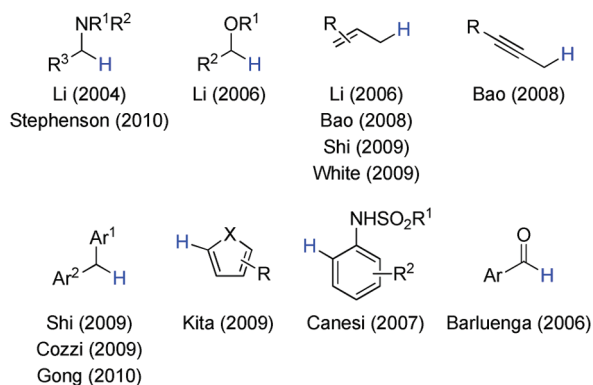


Figure 142. General scheme for cross-couplings via ionic intermediates.

Electrophiles



Nucleophiles

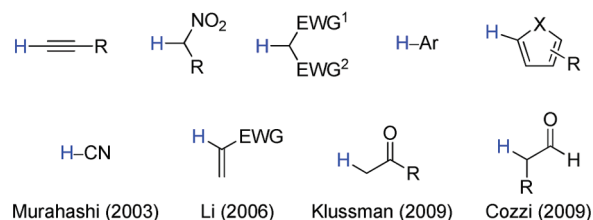


Figure 143. Overview of cross-couplings via ionic intermediates.

conditions (Figure 144).^{118,119} In this reaction, either H_2O_2 or O_2 act as the stoichiometric chemical oxidant and promote

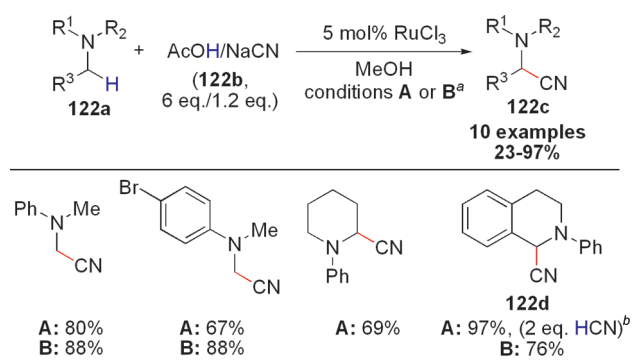


Figure 144. Ru-catalyzed α -cyanation of amines.^{118,119}
^aConditions A: 2.5 equiv H_2O_2 ; conditions B: 60 °C, 1 atm O_2 .
^bNeither AcOH nor NaCN were added to the reaction.

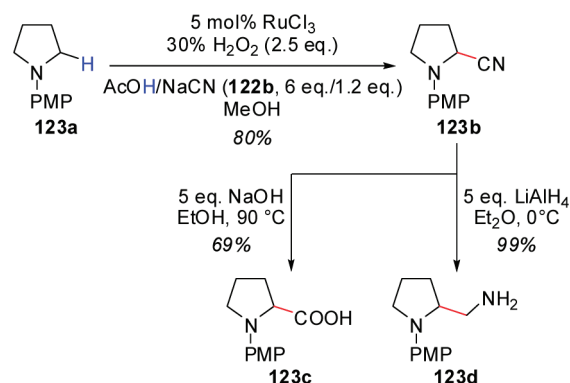


Figure 145. Synthesis of *N*-aryl amino acids and 1,2-diamines from α -cyanoamines.¹¹⁸

oxidation of the alkylamine starting material (139a) to the corresponding iminium cation. Nucleophilic addition of cyanide anions derived either from AcOH/NaCN or HCN directly quenches the positively charged intermediates, resulting in the formation of a new C–C bond. For the aerobic system, some ruthenium salts (e.g., $\text{K}_2[\text{RuCl}_5(\text{H}_2\text{O})]$, $\text{Ru}_2(\text{OAc})_4\text{Cl}$, $\text{RuCl}_2(\text{PPh}_3)_3$, $\text{Ru}(\text{bipy})_2\text{Cl}_2$, Pr_4NRuO_4 , RuO_2), as well as other metals (e.g., MnCl_2 , CuCl_2), demonstrated catalytic activity. For the H_2O_2 system, $\text{RuCl}_2(\text{PPh}_3)_3$ and Pr_4NRuO_4 are effective, but $\text{K}_4\text{Ru}(\text{CN})_6$ inhibits the desired α -functionalization. A Hammett study revealed $\rho = -3.35$ and -3.61 for O_2 - and H_2O_2 -mediated oxidations, respectively, supporting the existence of the proposed iminium cations. The α -cyanoamine products (140a) are useful building blocks for the synthesis of both *N*-aryl amino acids (140c) and 1,2-diamines (140d, Figure 145).

To expand the scope of nucleophiles that undergo oxidative α -C–C bond formation with aliphatic amines, iminium ions can be formed in a separate step. The Yoshida group pioneered the idea of “cation pools”, the generation of high concentrations of long-lived carbocations at low temperatures (-70°C).¹¹⁴ This method employs dichloromethane as the solvent and tetrabutylammonium tetrafluoroborate ($\text{N}^+\text{Bu}_4\text{BF}_4$) as the supporting electrolyte.^{114,120} Yoshida described the oxidative C–C cross-coupling between aliphatic carbamates (which are known to undergo oxidation to their corresponding *N*-acyliminium ions) and a variety of carbon nucleophiles using a graphitic anode (Figure 146).¹¹⁴ Reactive nucleophiles such as allylsilanes and silyl enol ethers were suitable, as well as coupling partners

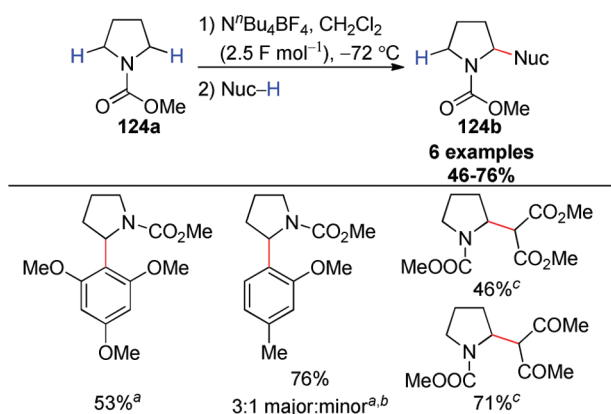


Figure 146. Electrochemical α -arylation and alkylation of methyl pyrrolidine-1-carboxylate (**124a**).¹¹⁴

^a1 equiv of the nucleophile was used.

^bThe product was isolated as a mixture of regioisomers.

^c20 equiv of the nucleophile was used at 0°C .

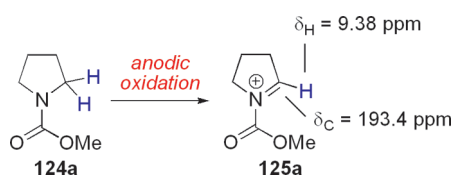


Figure 147. Electrochemical oxidation of methyl pyrrolidine-1-carboxylate (**124a**).¹¹⁴

including simple arenes and activated methylenes. The existence of electrochemically produced N -acyliminium ions was confirmed by NMR spectroscopy, which provides support for the proposed “cation pool” (Figure 147). With a robotic synthesizer, this method has been extended to solution-phase combinatorial synthesis¹¹⁴ and flow chemistry.¹²¹

Li and co-workers were among the first to realize ionic-type dehydrogenative couplings using chemical oxidants. In 2004, they achieved an α -alkynylation of N,N -dimethylanilines (**126a**) under neat conditions,¹²² a formal $\text{C}(\text{sp}^3)\text{--C}(\text{sp})$ cross-coupling (Figure 148). Both Cu(I) and Cu(II) halides are suitable catalysts, with CuBr giving the best results. *tert*-Butylhydroperoxide is the oxidant of choice, and aromatic alkynes (**126b**) are the best coupling partners. Functional groups including pyridines (36% yield) and aliphatic alcohols (40% yield) are tolerated despite the oxidative conditions. For N,N -dimethylbenzylamine (**127a**), alkynylation takes place selectively at the methyl C–H bond in preference to the benzylic C–H bond (Figure 149). Using tetrahydroisoquinolines as the substrates (**128a**), cross-coupling occurs at the benzylic position instead of the homo-benzylic carbon. In the presence of a chiral ligand (e.g., **PyBOx**), enantioenriched α -alkynyltetrahydroisoquinolines (**128c**) can be synthesized in up to 74% ee, a result that supports the existence of Cu-bound iminium ions (Figure 150).¹²³ Complementary to this work, Fu and co-workers described a NBS-mediated oxidative alkynylation under copper catalysis (Figure 151).¹²⁴

Li's proposed mechanism involves copper acetylide **130e** undergoing nucleophilic addition to iminium ion **130c**, which is generated by Cu-catalyzed oxidation of alkylamine **130b** (Figure 152).¹²² The authors noted that a peroxide may be a reactive intermediate (**131a**, Figure 153), although subjecting the peroxide to asymmetric oxidative coupling gave the desired

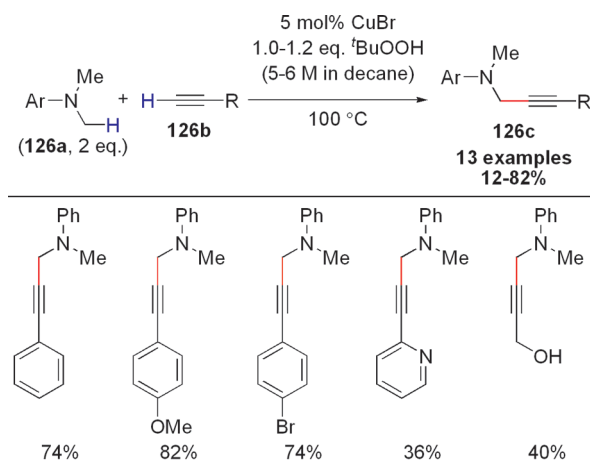


Figure 148. Cu-catalyzed α -alkynylation of amines.¹²² A decane solution of $t\text{BuOOH}$ is commercially available from Sigma-Aldrich.

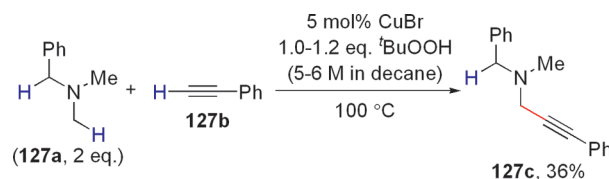


Figure 149. Site-selectivity in Cu-catalyzed α -alkynylation of amines.¹²²

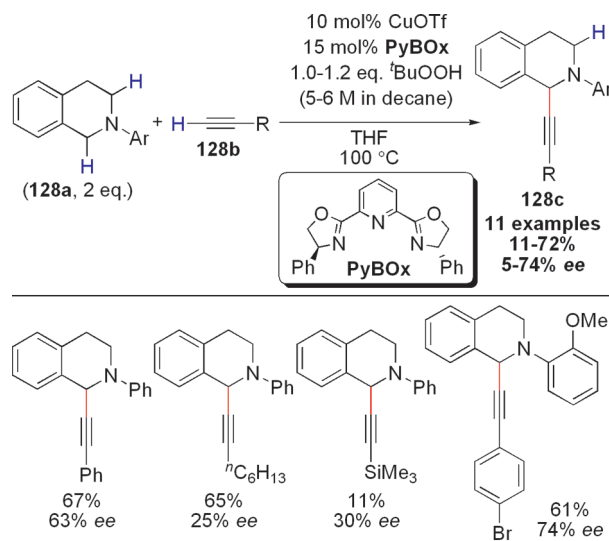
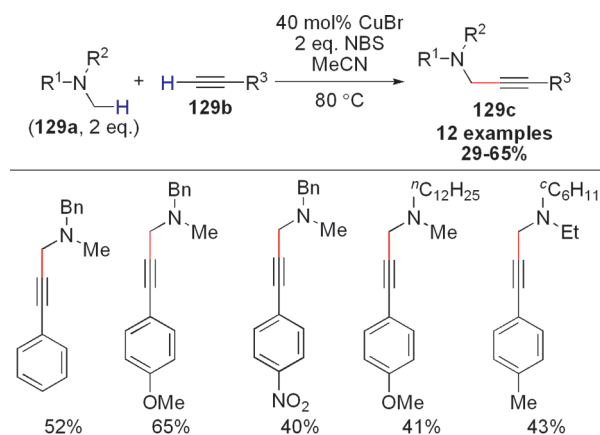
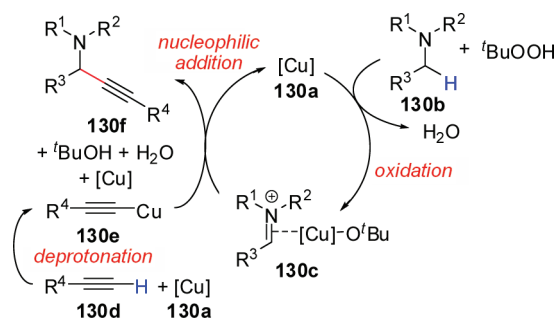
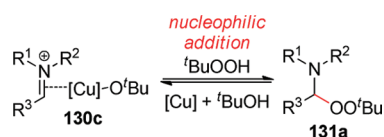
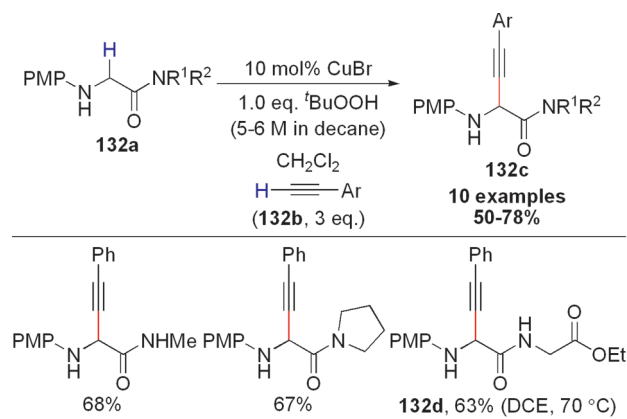


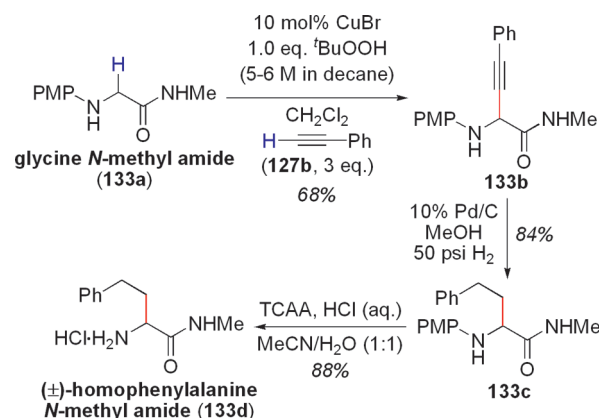
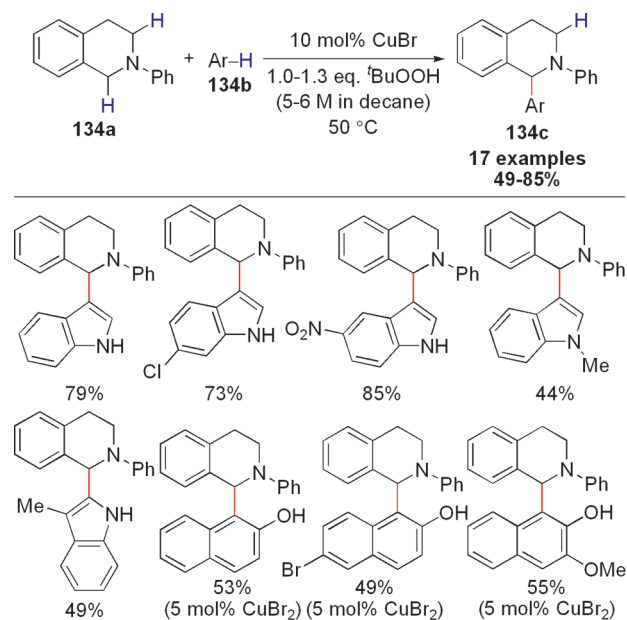
Figure 150. Enantioselective Cu-catalyzed α -alkynylation of tetrahydroisoquinolines.¹²³

product with decreased enantioselectivities.¹²³ The oxidation state and specific identity of the active copper complexes remains unknown. Cu-catalyzed (and -mediated) dehydrogenations may involve iminium radical cations in the mechanism and, hence, could be classified as radical C–C couplings (see section 5).

Amino acid amide derivatives can be prepared by oxidative α -alkynylation of protected glycines (**132c**, Figure 154).¹²⁵ Both secondary and tertiary amides are tolerated, but replacing the amide group with an ester functionality (i.e., an amino acid ester)

Figure 151. Cu-catalyzed α -alkynylation of amines with NBS.¹²⁴Figure 152. Proposed mechanism of Cu-catalyzed α -alkynylation of amines.¹²²Figure 153. Formation of peroxide intermediates in Cu-catalyzed α -alkynylation of amines.¹²²Figure 154. Cu-catalyzed α -alkynylation of glycine derivatives.¹²⁵

results in a loss of reactivity (e.g., **132d**). Li synthesized (\pm)-homophenylalanine *N*-methyl amide (**133d**) from glycine *N*-methyl amide (**133a**) in three steps, providing a straightforward and

Figure 155. Synthesis of (\pm)-homophenylalanine *N*-methyl amide (**133d**).¹²⁵Figure 156. Cu-catalyzed α -arylation of tetrahydroisoquinolines.^{4,126} CuBr was the optimal catalyst for indole alkylation, whereas CuBr₂ was optimal for 2-naphthol alkylation. Under optimized conditions, tetrahydroisoquinoline/indole = 1:1.2 and tetrahydroisoquinoline/naphthol = 2:1.

expedient route to this class of unnatural amino acid derivatives in racemic form (Figure 155).

Electron-rich aromatic rings (**134b**) are another class of carbon-based nucleophiles for amine α -functionalizations. Arenes, including indoles and naphthols, undergo amine α -arylations by a Friedel–Crafts-type mechanism (**134a**, Figure 156).^{4,126} With indoles (**134b**), C3 alkylation is typically predominant, as expected for an electrophilic aromatic substitution.⁴⁶ This reaction tolerates both *N*-H and *N*-alkylindoles, as well as other functional groups including chloro- (73% yield) and nitroaromatics (85% yield).¹²⁶ With naphthols (**134b**), derivatives of (\pm)-1-(α -aminobenzyl)-2-naphthol are produced, compounds commonly called Betti bases.¹²⁷ In these reactions, undesired oxidative homocoupling of 2-naphthol starting materials to BINOL derivatives can be observed in some cases,¹²⁶ analogous to many radical-type phenolic couplings (see section 5.1). The proposed mechanism

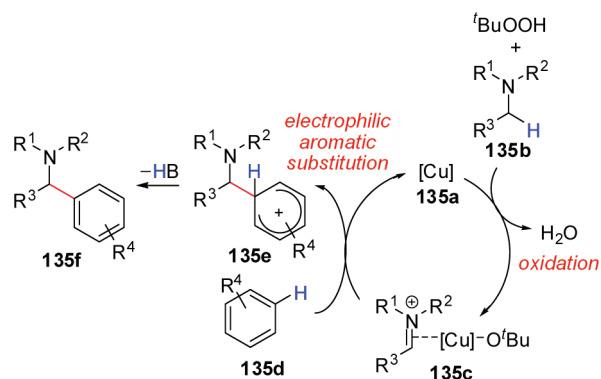


Figure 157. Proposed mechanism for Cu-catalyzed α -arylation of amines.

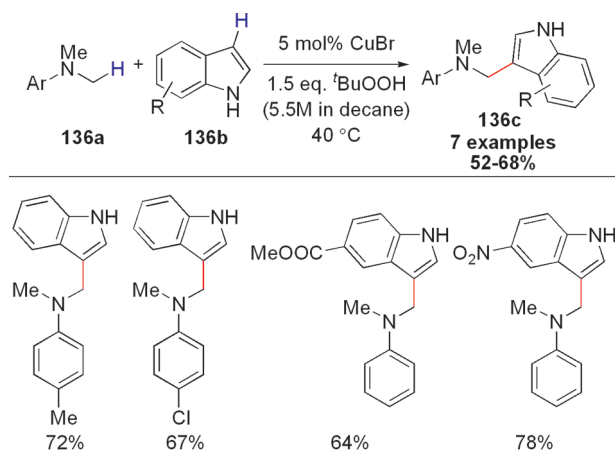


Figure 158. Cu-catalyzed α -arylation of *N,N*-dimethylanilines.¹²⁸

involves α -oxidation to generate an iminium ion intermediate 135c, followed by nucleophilic addition by the aromatic or heteroaromatic ring (135d) to yield a Wheland intermediate (135e, Figure 157).⁴⁶ Arenium cation 135e undergoes subsequent deprotonation and rearomatization to give product 135f.

Huang and co-workers demonstrated that *N,N*-dimethylanilines can undergo α -arylation under Cu catalysis (Figure 158),¹²⁸ whereas Itami and co-workers developed a Fe-catalyzed variant (Figure 159).¹²⁹ The Huang group observed regioselective C3 functionalization of indoles under copper catalysis with *tert*-butylhydroperoxide as the oxidant.¹²⁸ In Itami's method, FeCl₃/bipy is the best catalyst, but other iron halides (e.g., FeF₂, FeBr₂, FeI₂) and RuI₃ also promote the desired reaction.¹²⁹ In contrast to reports from the Li and Huang groups (vide supra), CuBr fails to generate the desired product. Pyridine *N*-oxide serves as the stoichiometric oxidant for this cross-coupling. Heterocycles including thiophenes, furans, indoles, and azaindoles are suitable substrates for Itami's tandem C–H bond dehydrogenation.

In a study by Tsuchimoto and Shirakawa's groups, coupling between electron-rich heteroaromatic rings (138c) and the 5-position of 1-methylpyrrolidin-2-one (138a) and 4-position of 3-methyloxazolidin-2-one (138b) was achieved with catalytic Zr(OTf)₄ (Figure 160).¹³⁰ Regioselectivity of the C–H bond alkylation depends on the coupling partner, with indoles favoring C3 alkylation and pyrroles and thiophenes favoring C2 alkylation. The authors propose that, under an aerobic atmosphere, the

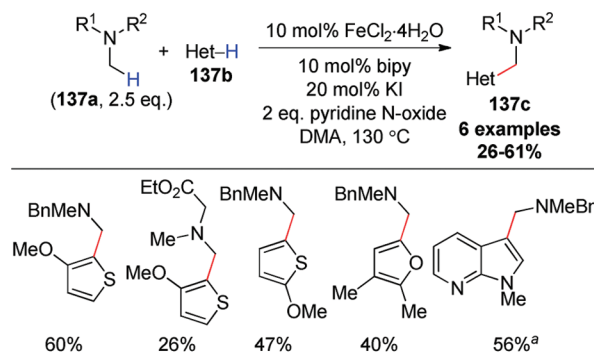


Figure 159. Fe-catalyzed α -arylation of amines with electron-rich heteroaromatics.¹²⁹

^aReaction conducted with 5 equiv 30% H₂O₂ (aq.) at 80 °C.

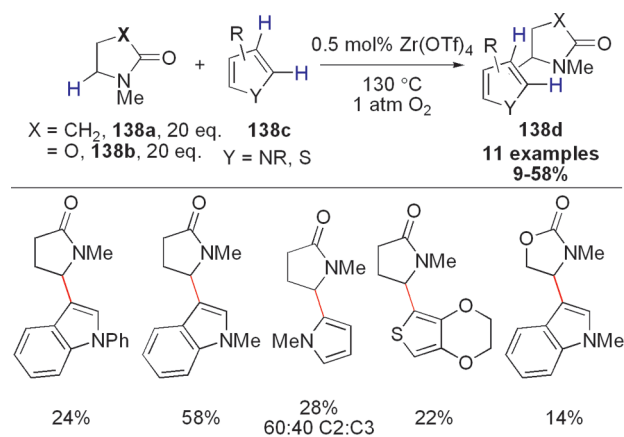


Figure 160. Zr-catalyzed arylation of 1-methylpyrrolidin-2-one (138a) and 3-methyloxazolidin-2-one (138b) with electron-rich heteroaromatics.¹³⁰

presence of the Lewis acid promotes oxidation of 138a and 138b to their corresponding *N*-acyliminium cations via cation radical intermediates. Indeed, 1 mol % of TEMPO, a radical scavenger, inhibits the reaction. Zr(OTf)₄ is believed to enhance the electrophilic aromatic substitution reaction that takes place between the heteroaromatic ring and the pyrrolidinone/oxazolidinone coupling partner.⁴⁶ Other Lewis acids (e.g., Sc(OTf)₃, In(OTf)₃) and also Brønsted acids (e.g., TfOH) are catalytically active.¹³⁰

Enolates undergo nucleophilic additions to iminium ions generated via α -oxidation of amines. The direct coupling between nitroalkanes (139b) and amines (139a) in the presence of a copper catalyst was described by Li and Li (Figure 161).¹³¹ This formal C(sp³)–C(sp³) coupling provides facile access to 1,2-diamines, a common motif found in natural products and chiral ligands.¹³² Although the nitroalkane starting material 139b is typically used as the solvent (~80 equiv), decreasing the amount to 1 equiv does not dramatically reduce reaction efficiency.¹³¹ When *N*-phenylpyrrolidine is subjected to catalysis, in addition to the monoalkylation product (139e, 53% yield), a side product resulting from two α -alkylations (i.e., difunctionalization) is observed (4% yield, not shown). This reaction can be conducted under aqueous conditions using oxygen to replace *tert*-butylhydroperoxide as the terminal electron acceptor.¹³³ Judicious choice of the oxidant is critical in controlling *mono*- over *didehydrogenation* (i.e., where the nitroalkane product is oxidized to its

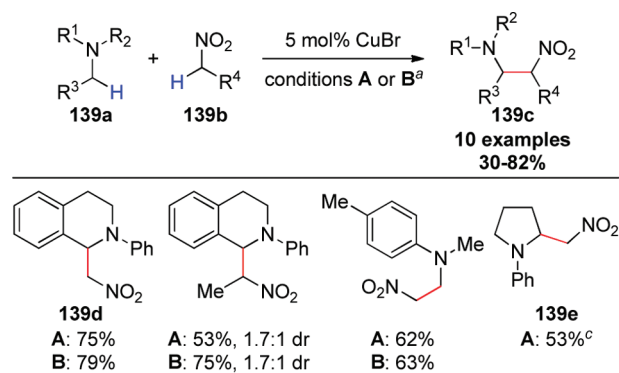


Figure 161. Cu-catalyzed α -alkylation of amines with nitroalkanes.^{131,133}

Conditions A: ~ 80 equiv nitroalkane, 1.0–1.2 equiv t BuOOH (5–6 M in decane); conditions B: 5 equiv nitroalkane, 1 atm O_2 , H_2O , 40–60 °C.

^b Additionally, a product resulting from two α -alkylation reactions was observed in 4% yield.

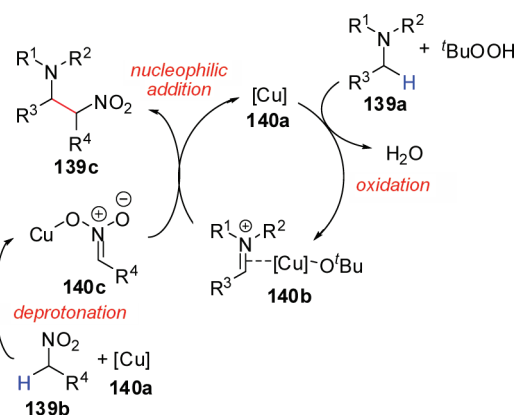


Figure 162. Proposed mechanism for Cu-catalyzed α -alkylation of amines with nitroalkanes.^{131,133}

corresponding nitroalkene). CuBr is critical for both amine (139a) oxidation and nitroalkane (139b) deprotonation/enolization steps (Figure 162).

The Stephenson group invented a photocatalytic version of this reaction using $Ir(ppy)_2(dtbbpy)PF_6$ (Figure 163).¹³⁴ They found that nitroalkanes (141b) and amines (141a) can undergo dehydrogenative cross-coupling with moderate to good yields. Removing either the Ir catalyst or light, however, leads to decreased efficiencies. Stephenson's oxidative C–C bond formation proceeds in the absence of O_2 and suggests that nitroalkane itself acts as an electron acceptor and visible light is simply used to initiate a sequence of single-electron transfer processes that culminates in the oxidation of the amine (136d) to its corresponding iminium cation (136g, Figure 164). The catalyst chosen is a variant of $Ru(bipy)_3Cl_2$, a complex known for its ability to undergo photoexcitation via metal-to-ligand charge transfer using light.¹³⁵ This Ru complex has also enabled new catalytic methods using visible light,¹³⁶ as described independently by the MacMillan¹³⁷ and Yoon groups.¹³⁸

Lessard, Li, and co-workers reported cross-dehydrogenative coupling between enolates and amines in the presence of ionic liquid (IL) $[BMIm][BF_4]$ (Figure 165).¹³⁹ The reaction

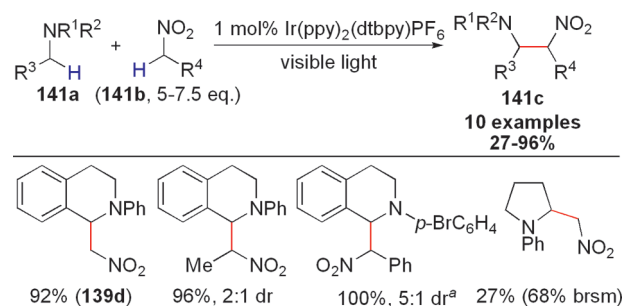


Figure 163. Ir-catalyzed photomediated α -alkylation of amines with nitroalkanes.¹³⁴

^a Reaction conducted in DMF. Conversion is based on 1H NMR.

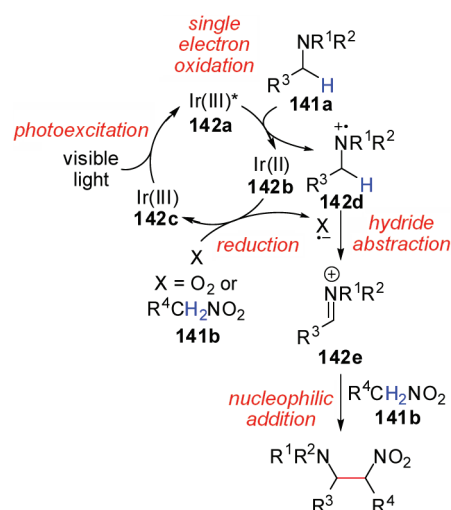


Figure 164. Proposed mechanism for Ir-catalyzed photomediated α -alkylation of amines with nitroalkanes.¹³⁴

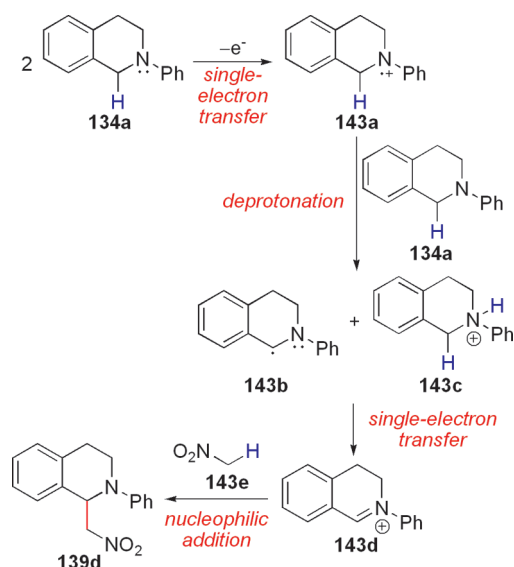


Figure 165. Proposed mechanism for oxidative α -alkylation of *N*-phenyltetrahydroisoquinoline (134a) with nitromethane.¹³⁹

between *N*-phenyltetrahydroisoquinoline (134a) and nitromethane yielding β -nitroamine 139d, for example, can be

recycled up to nine times without significant decreases in catalytic efficiency. Because of the robust nature of ILs and their ability to accommodate charged intermediates, the authors envisaged accomplishing dehydrogenative coupling electrochemically. Cyclic voltammetry experiments suggest that amine **134a** oxidation is a viable process. A two-step procedure was thus developed using a Pt electrode (Figure 166) and can be classified as a “cation pool”¹¹⁴ strategy. In this case, carbocations are generated electrochemically in the IL in the absence of nucleophiles.¹²⁰ Trapping the proposed cation **143d** with diethylphosphite resulted in a product from formal oxidative C–P bond formation via tandem oxidation of a C–H and P–H bond (not shown).¹³⁹ This work also provides support for the radical intermediates proposed in other Cu-catalyzed dehydrogenations.

Next, Li and co-workers extended ionic-type dehydrogenations to malonate nucleophiles (**144b**) under both neat¹⁴⁰ and aqueous¹³³ conditions (Figure 167). The mechanism proposed is analogous to that of nitroalkane–aminoalkane coupling. Cross-

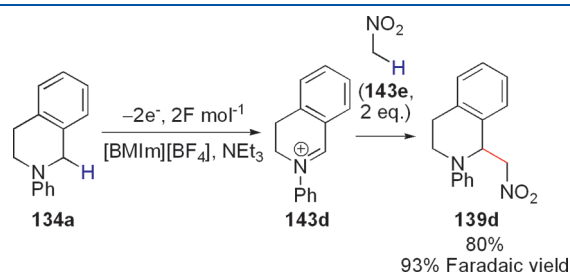


Figure 166. Electrochemical oxidative α -oxidation of *N*-phenyltetrahydroisoquinoline (**134a**) with nitromethane.¹³⁹

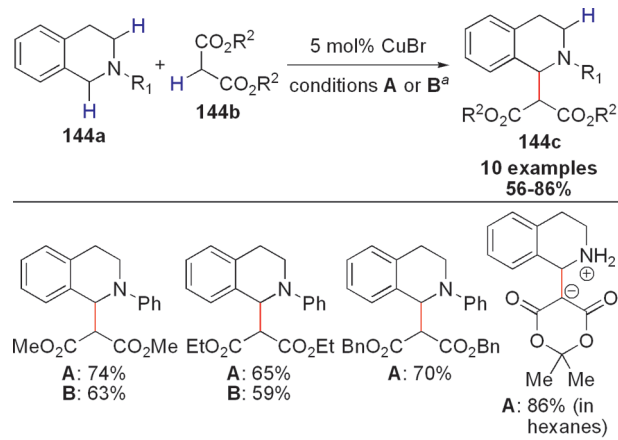


Figure 167. Cu-catalyzed α -alkylation of tetrahydroisoquinolines with malonates.^{4,133,140}

^aConditions A: 2.5 equiv H₂O₂; conditions B: 60 °C, 1 atm O₂, H₂O.

coupling *N*-phenyltetrahydroisoquinoline (**134a**) and malonitrile (**145a**) gives products derived from both the desired C–C bond formation (**145b**) and the competing α -cyanation (**145c**) depending on the amount of oxidant used (Figure 168). Additional equiv of **145a** also promote α -alkylation. The authors believe that oxidative degradation of malonitrile with Cu(II) to 2-oxomalonitrile and cyanide anions leads to the formation of this byproduct, in analogy to Murahashi's earlier work.^{118,119}

To achieve oxidative coupling between ketones and the α -carbon of an alkylamine, Klusmann and co-workers combined transition metal catalysis and organocatalysis. In 2009, VO(acac)₂ and *L*-proline were found to effect cross-coupling between simple ketones (**146b**) and amines such as tetrahydroisoquinolines and *N*-methylpyrrolidines (**146a**, Figure 169).¹⁴¹ VO(acac)₂ displays higher catalytic activity than Cu(acac)₂, Fe(acac)₃, and Co(acac)₂ salts. *L*-Proline is the optimal secondary amine catalyst for converting the ketone into an enamine nucleophile. In this reaction system, these two catalysts are mutually compatible and play independent roles. The proposed mechanism involves nucleophilic addition of enamine **147b** to iminium ion **147d**, which in turn is derived from amine **146a** (Figure 170). The authors mention that amine *N*-oxides are unreactive under the reaction conditions and are thus not likely intermediates. Oxidation of amine **146a** to iminium **147d**, however, may involve radical species because adding 2,6-di-*tert*-butylphenol inhibits catalysis. Although the organocatalyst used is enantiomerically pure, low levels of enantioinduction are observed (7% ee), possibly due to racemization of the β -aminoketone products under the reaction conditions. Regardless, this method provides a short route to (\pm)-hygrine (**148c**) (Figure 171). In a related account, Huang and co-workers reported a similar cross-dehydrogenative coupling between methyl ketones and *N,N*-dimethylanilines (Figure 172)¹²⁸ using copper and pyrrolidine/benzoic acid as catalysts. Although other copper and iron salts are also efficient metal catalysts for this transformation, the addition of the pyrrolidine cocatalyst is crucial.

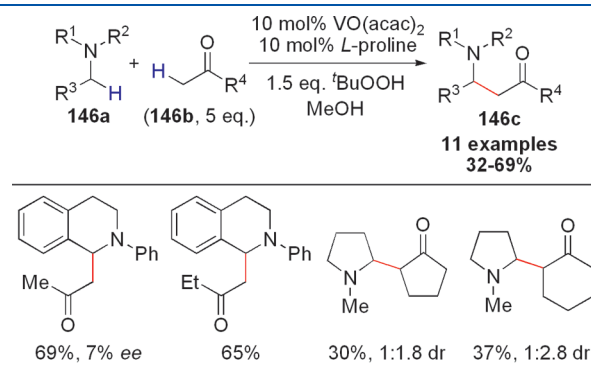


Figure 169. V- and proline-catalyzed α -alkylation of tetrahydroisoquinolines and *N*-methylpyrrolidines.¹⁴¹

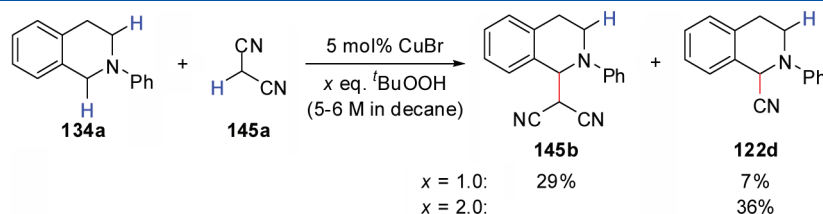


Figure 168. Cu-catalyzed α -alkylation and α -cyanation of tetrahydroisoquinolines with malonitrile.¹⁴⁰

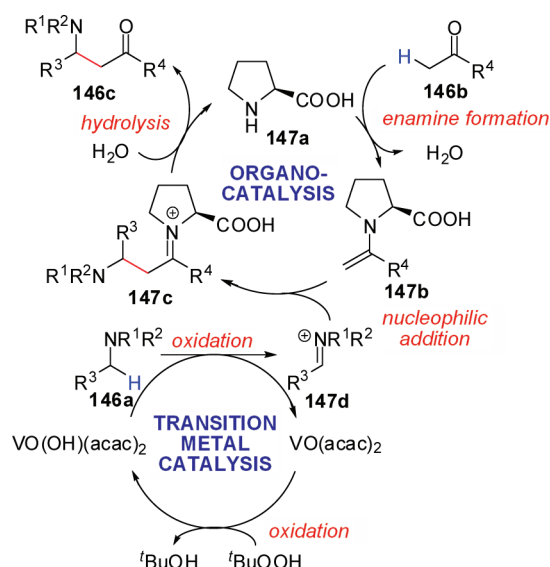


Figure 170. Proposed mechanism for V- and proline-catalyzed α -alkylation of tetrahydroisoquinolines and *N*-methylpyrrolidines.¹⁴¹

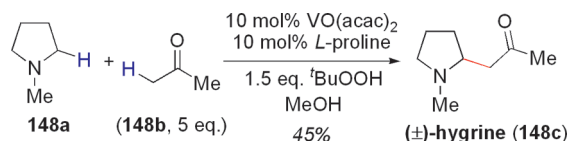


Figure 171. Total synthesis of (±)-hygrine (148c) via an oxidative α -alkylation of *N*-methylpyrrolidine.¹⁴¹

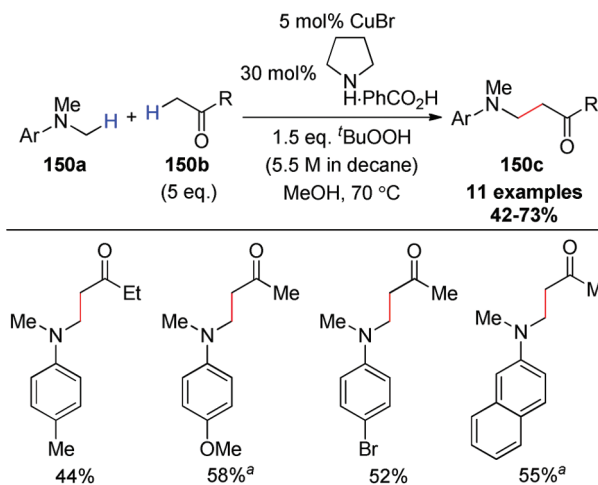


Figure 172. Cu- and pyrrolidine-catalyzed α -alkylation of *N,N*-dimethylanilines.¹²⁸

The Huang group applied this strategy to the synthesis of protected amino acid esters from glycine derivatives (Figure 173).¹⁴² Using a combined Cu/pyrrolidine catalytic system, oxidative C–C cross-coupling occurs with high yields (and diastereoselectivities where relevant). Using acetone (148b) as the starting material, dehydrogenative coupling is found to be optimal with *tert*-butylhydroperoxide, while for cyclic ketones, DDQ is preferred. In accordance with Klussman (vide supra), the authors note that replacing the organocatalyst pyrrolidine with *L*-proline derivatives provides the desired

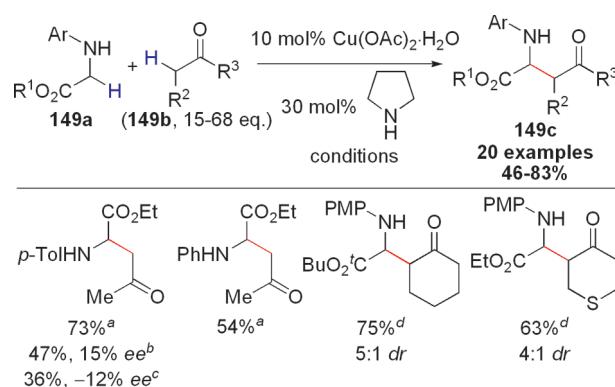


Figure 173. Cu- and pyrrolidine catalyzed α -alkylation of glycine derivatives.¹⁴²

^aConditions: 68 equiv acetone, 1.5 equiv *t*BuOOH (5.5 M in decane).

^bConditions: 30 mol % *L*-proline methyl ester was used, 1.5 equiv PhCOOH.

^cConditions: 30 mol % *L*-proline *n*-butylamide was used, 1.5 equiv PhCOOH.

^dConditions: 15 equiv ketone, 1 equiv DDQ, CHCl₃, 0 °C to rt.

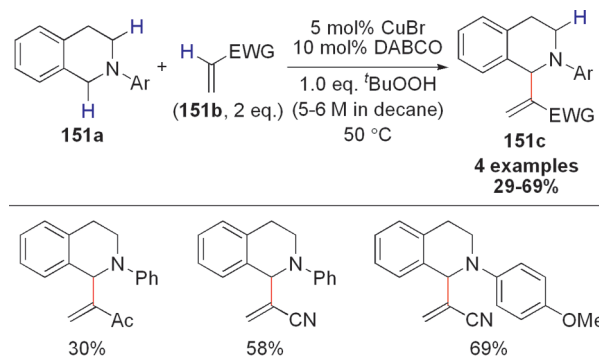


Figure 174. Cu-catalyzed α -vinylation of tetrahydroisoquinolines.⁴

coupling products with low levels of enantioinduction (<15% ee). This transformation is proposed to involve radicals because radical inhibitors (e.g., 2,6-di-*tert*-butyl-4-methylphenol) decreased yields significantly. For a related α -alkylation with dibenzylic cations, see section 5.4. For a related α -arylation under organo-SOMO catalysis, see section 5.2.

Li developed the α -vinylation of tetrahydroisoquinolines (151a) using an alternative transition metal catalysis and organocatalysis strategy (Figure 174).⁴ In this case, DABCO is the nucleophilic cocatalyst used to generate a reactive enolate that can subsequently undergo addition to the iminium cation, which is formed via Cu-catalyzed oxidation of the amine coupling partner 151a. This reaction is formally an aza-Morita–Baylis–Hillman reaction¹⁴³ with an alkylamine instead of an imine as the starting material. Other phosphine cocatalysts commonly used for these reactions, such as triphenylphosphine, are effective due to detrimental oxidation to their corresponding phosphine oxides.

4.2. α -Functionalization of Ethers

In analogy to the α -functionalization of amines, ionic-type oxidative C–C coupling is possible with benzylic ethers. In 2006, the Li group achieved the α -alkylation of ethers (152a) using a

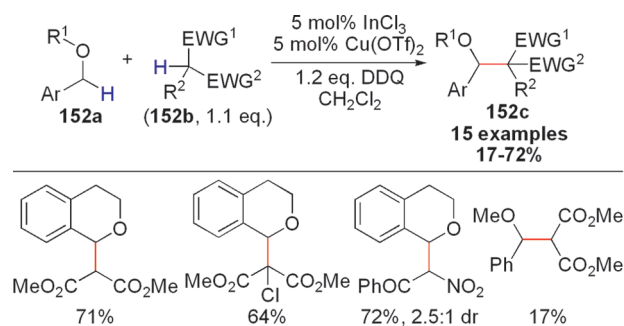


Figure 175. In- and Cu-catalyzed α -alkylation of benzylic ethers.¹⁴⁴

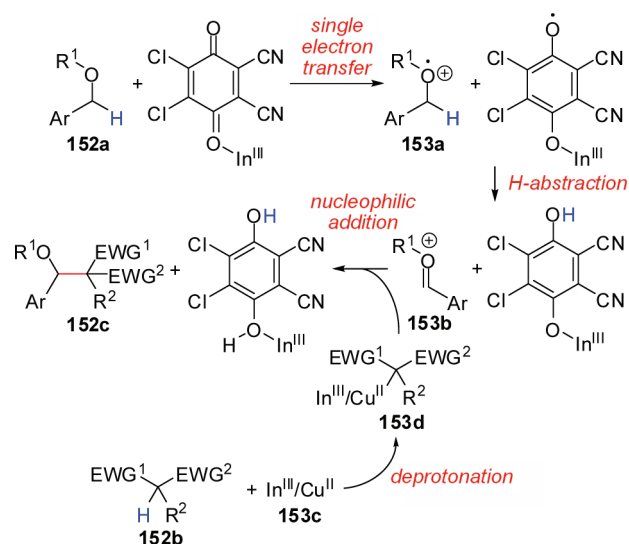


Figure 176. Proposed mechanism for In- and Cu-catalyzed α -alkylation of benzylic ethers.¹⁴⁴

combined In/Cu catalytic system in the presence of DDQ (Figure 175).¹⁴⁴ A number of different enolates can undergo cross-coupling with moderate to good yields. Sensitive functional groups such as alkyl chlorides remain intact under the optimized conditions. The authors found no reaction in the absence of either catalyst or oxidant. It is believed that the high oxidation potential of DDQ facilitates oxidation of the benzylic ether (152a) to the corresponding oxonium ion (153a) in the presence of InCl_3 (Figure 176). A copper or indium enolate (153d) is the proposed nucleophile. It was later discovered that a variant of this transformation could be achieved at elevated temperatures under neat conditions without a catalyst, which provides support for Li's mechanistic proposal:¹⁴⁴ a transition metal free oxidation of benzylic ethers to their corresponding oxonium ions (Figure 177).¹⁴⁵

4.3. Allylic C–H Bond Functionalization

Allylic C–H bonds, like α -C–H bonds of amines and ethers, can undergo functionalization by dehydrogenative cross-coupling. Because π -allyl intermediates have widespread use in organic synthesis, there is much interest in generating these reactive species by allylic C–H bond activation.¹⁴⁶ Li and Li discovered that the combination of copper and cobalt salts can catalyze coupling between simple allylic compounds (155a) and activated methylenes (155b, Figure 178).¹⁴⁷ Using *tert*-butylhydroperoxide as the sacrificial oxidant, five-, six-, and seven-

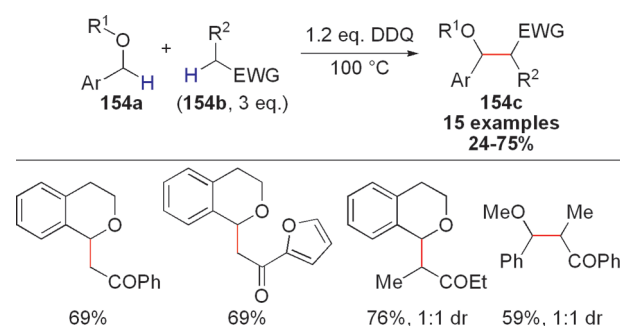


Figure 177. α -Alkylation of benzylic ethers mediated by DDQ.¹⁴⁵

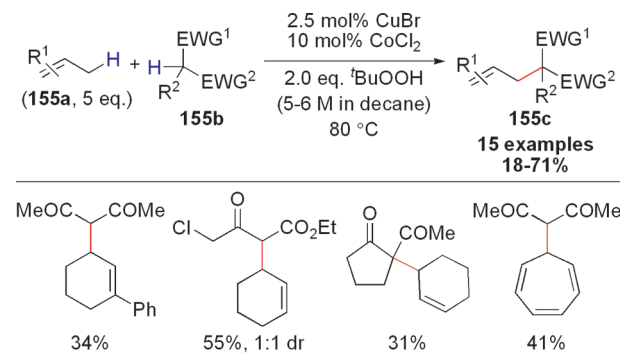


Figure 178. Cu- and Co-catalyzed allylic alkylation of activated methylenes with simple allyls.¹⁴⁷

membered cyclic alkenes (155a) undergo efficient C–C bond formation with a variety of stabilized carbanions. Functionalities that are typically reactive with carbon nucleophiles (e.g., alkyl chlorides) are tolerated. Whereas copper *improves* reaction efficiency, removal of cobalt leads to complete inhibition of the allylic alkylation. Li performed a deuterium labeling study to provide support for the intermediacy of a metal π -allyl complex (157b) and found that alkylation occurs at the both the vinylic and allylic carbons (i.e., generating formal $\text{S}_{\text{N}}2$ and $\text{S}_{\text{N}}2'$ products, Figure 179). On the basis of this mechanistic data, the Li group proposes a dehydrogenative coupling that involves allylic C–H bond abstraction, followed by nucleophilic substitution of the incoming nucleophile (Figure 180). The exact role of the added copper and cobalt salts and synergy between the two catalysts remains unknown.

The Shi group reported a complementary Pd-catalyzed allylic alkylation of simple allyls (158a) using benzoquinone as the sacrificial oxidant and 1,2-bis(phenylsulfinyl)ethane (BS) as the ligand under an aerobic atmosphere (Figure 181).¹⁴⁸ In intermolecular tandem C–H bond functionalization, the linear product dominates. In intramolecular dehydrogenation, cyclizations yielding five- and six-membered rings proceed efficiently and with excellent diastereoselectivity. Although Shi's reaction employs palladium salts as catalysts, aryl bromides and aryl chlorides are maintained under the reaction conditions. The authors confirmed that palladium was required because both benzoquinone and DDQ were ineffective in the absence of $\text{Pd}(\text{OAc})_2$. The addition of a radical inhibitor (e.g., 4-methoxyphenol) does not affect the observed reactivity, which provides evidence against single-electron transfer steps. Additionally, Wacker-type mechanisms¹⁴⁹ are ruled out based on the observation that 1-aryl-1-propenes could not act as suitable

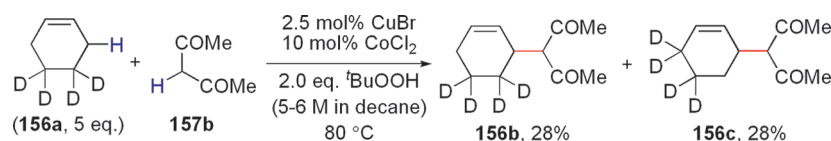


Figure 179. Deuterium labeling study for Cu- and Co-catalyzed allylic alkylation of activated methylenes.¹⁴⁷

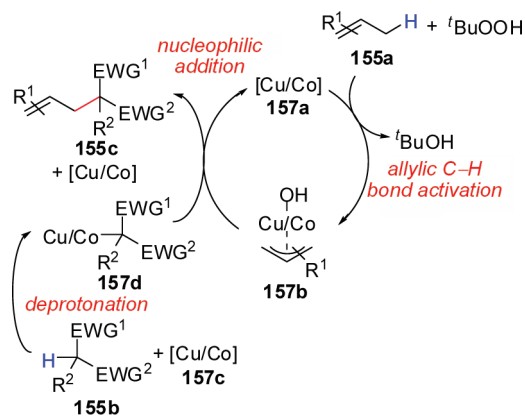


Figure 180. Proposed mechanism for Cu- and Co-catalyzed allylic alkylation of activated methylenes.¹⁴⁷

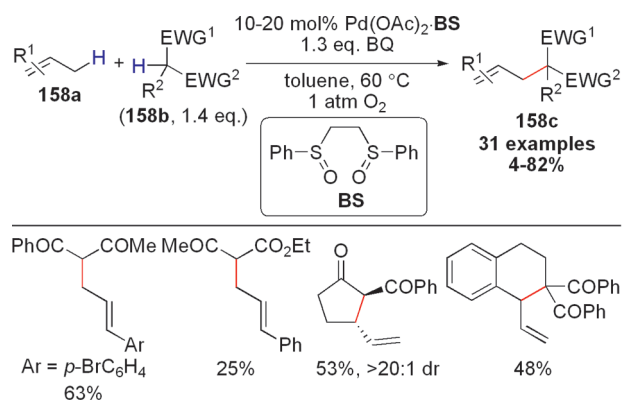


Figure 181. Pd-catalyzed allylic alkylation of activated methylenes with simple allyls.¹⁴⁸ BS is a mixture of *meso* and *racemic* isomers.

surrogates for allylarenes (although degenerate π -allyl intermediates would be formed). Indeed, a Pd π -allyl complex derived from allylbenzene can be detected by mass spectrometry (ESI-MS).¹⁴⁸ In contrast to traditional Tsuji–Trost reactions,¹⁴⁶ allylic acetate **152b** is unreactive under Shi's optimized conditions (Figure 182). A competition study between deuterated and undeuterated allylarenes (**160a**) revealed that allylic C–H activation is rate-limiting (Figure 183): $k_{\text{H}}/k_{\text{D}}$ (intramolecular) = 2.7 and $k_{\text{H}}/k_{\text{D}}$ (intermolecular) = 2.2. Thus, the mechanism proposed is rate-limiting sp^3 C–H bond activation of simple allyl **158a** to generate Pd π -allyl complex **161b**, followed by nucleophilic substitution with activated methylene **158b** and oxidation of the resulting Pd(0) to active Pd(II) catalyst (Figure 184). Although Pd(0) is formed during catalysis, aromatic C–Cl and C–Br (as well as allylic acetates) are maintained, likely because oxidative addition is not favored in the absence of phosphine ligands.

The White group concurrently discovered a similar allylic alkylation with exquisite selectivity for the linear isomer using the

same bis(sulfoxide) ligand BS (Figure 185).¹⁵⁰ With methylnitroacetate (**162b**) as the cross-coupling partner, a wide range of allylarenes (**162a**) can undergo allylic alkylation with excellent yields and functional group compatibility. Benzoylnitromethane and (phenylsulfonyl)nitromethane are also suitable coupling reagents. In contrast to other allylarenes, 3-allylindole undergoes dehydrogenative coupling with a minor preference for the branched isomer (1.2:1 dr). White isolated a Pd π -allyl complex resulting from C–H activation and examined its reactivity in stoichiometric experiments. DMSO is required for catalysis.

An analogous C3 alkylation of indoles **163b** with simple allyls **163a** was demonstrated by the Bao group (Figure 186).¹⁵¹ Catalytic PdCl₂ and stoichiometric DDQ are required to drive this reaction, but CuBr, NiCl₂, and ZrCl₄ also demonstrated some activity. This dehydrogenative coupling exhibits good functional group compatibility and accommodates reactive sp^2 C–Br bonds. Although direct allylic C–H palladation is a reasonable mechanism to consider, simple DDQ-mediated allylic cation formation is an alternative that is favored by the authors. Bao and co-workers propose a mechanism where Pd(II) acts as a templating agent by coordinating both allylic cation and indole and thereby promoting electrophilic aromatic substitution.⁴⁶ With 3-substituted indole substrates, alkylation of the C2 position is observed.¹⁵¹

Allylic alkylation with allylarenes is possible in the *absence* of transition metal catalysts and has been achieved with some success, as exemplified by Bao's discovery of cross-coupling between (*E*)-1,3-diarylprop-1-enes (**164a**) and activated methylenes (**164b**) with DDQ (Figure 187).¹⁵² The aromatic substituents on allylic partner **164a** impart a stabilizing effect that is crucial for reactivity. Bao's proposed mechanism for this coupling is analogous to Li's mechanism¹⁴⁴ for DDQ-mediated alkylation of benzylic ethers, namely, oxidation to a carbocation, followed by nucleophilic addition with a carbon enolate (Figure 188). A propargylic variant of this cross-coupling was later achieved by the same group (Figure 189).¹⁵³ In substrates where propargylic cross-coupling partner **166a** is unsymmetrical, alkylation takes place adjacent to the aromatic ring bearing an electron-releasing substituent (e.g., methoxy, chloro).

4.4. Benzylic C–H Bond Functionalization

On the basis of the known ability of allylic C–H bonds to undergo dehydrogenative C–C bond formation, the Shi group developed the first direct cross-coupling of benzylic C–H bonds in 2009. They discovered that an iron catalyst in combination with DDQ effects the direct arylation of diphenylmethanes (**167b**) with electron-rich arenes (**167a**), a reaction that has been termed “cross-dehydrogenative arylation” (CDA) (Figure 190).¹⁵⁴ DDQ is superior to other commonly used oxidants (e.g., ^tBuOO^tBu, dicumyl peroxide, ^tBuOOAc, and benzoquinone), and FeCl₂ promotes coupling with higher efficiency than other transition metal salts (e.g., NiCl₂, CoCl₂, PdCl₂, and CuCl₂). Shi's transformation exhibits excellent

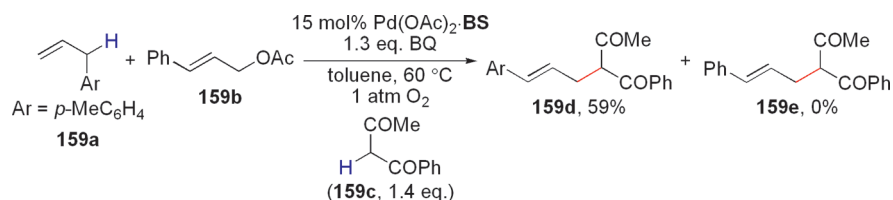


Figure 182. Crossover experiment for Pd-catalyzed allylic alkylation of activated methylenes.¹⁴⁸ BS is a mixture of *meso* and *racemic* isomers.

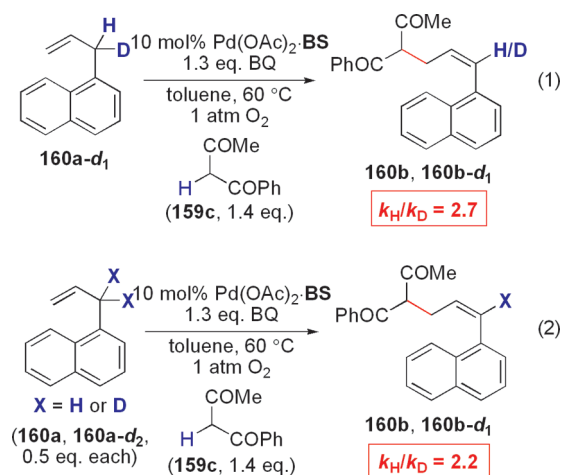


Figure 183. Kinetic isotope effect study for Pd-catalyzed allylic alkylation of activated methylenes.¹⁴⁸ BS is a mixture of *meso* and *racemic* isomers.

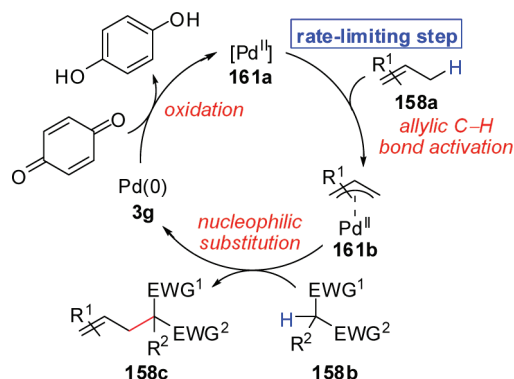


Figure 184. Proposed mechanism for Pd-catalyzed allylic alkylation of activated methylenes.¹⁴⁸

functional group compatibility and accommodates unprotected aldehydes, aryl halides, and thioethers.¹⁵⁴ The observed regioselectivity on the aromatic ring coupling partner **167a** favors alkylation ortho and para to electron-donating groups, which provides evidence for an S_EAr pathway.⁴⁶ Accordingly, electron-withdrawing aromatic substituents on diphenylmethane partner **167b** led to reduced reaction efficiencies in comparison to their electron-rich counterparts. Small amounts of a byproduct resulting from homocoupling of **167b** can be detected in some cases. Shi observed a large primary kinetic isotope effect for diphenylmethane (**168b**, $k_{\text{H}}/k_{\text{D}} = 6.0$), which suggests that benzylic C–H bond cleavage is the rate-limiting step (Figure 191). Although single-electron transfer steps are likely involved, the authors favor a mechanism involving

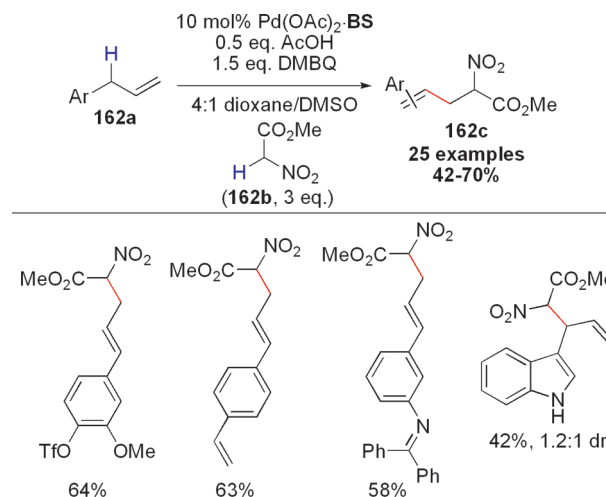


Figure 185. Pd-catalyzed allylic alkylation of methylnitroacetate.¹⁵⁰ BS is a mixture of *meso* and *racemic* isomers. DMBQ = 2,5-dimethylbenzoquinone.

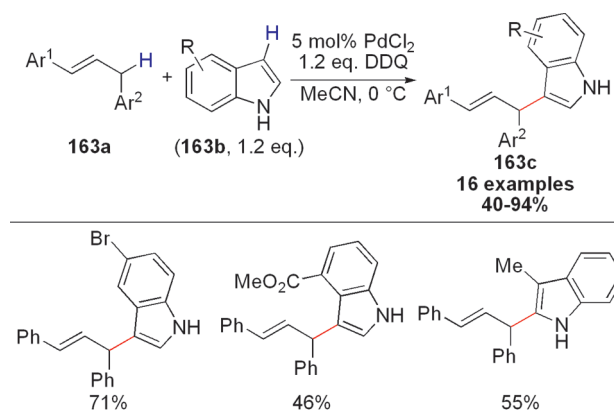
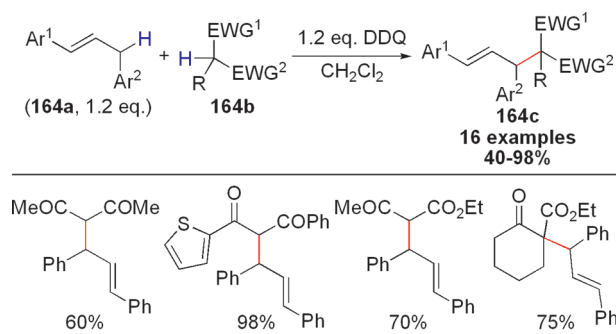
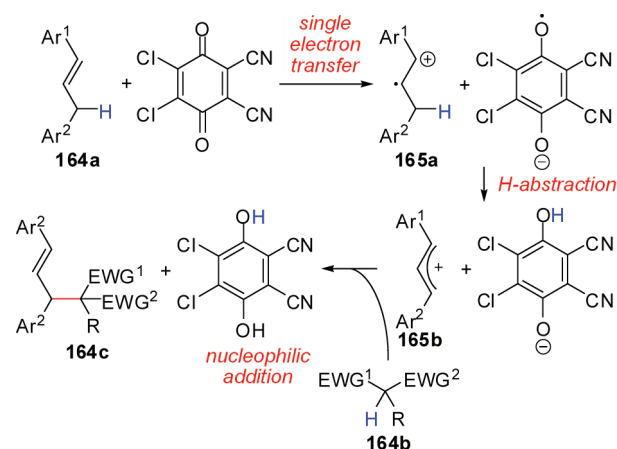
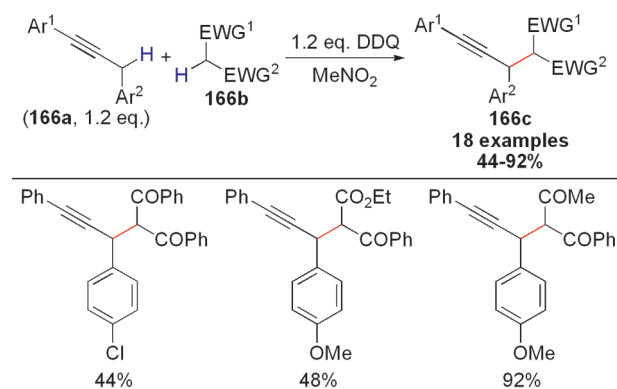


Figure 186. Pd-catalyzed C3 allylic alkylation of indoles.¹⁵¹

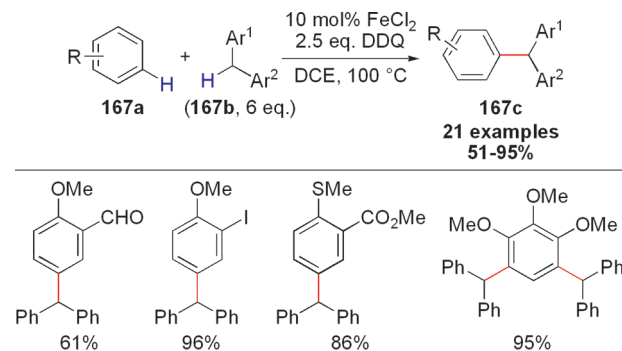
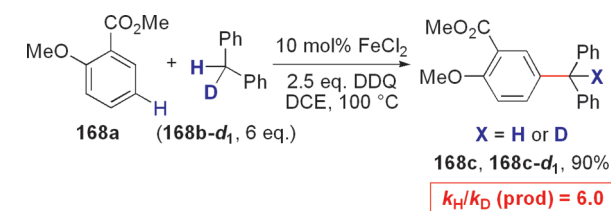
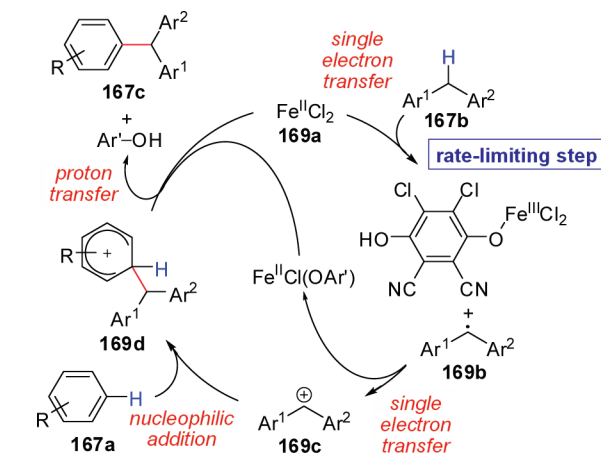
electrophilic aromatic substitution of dibenzylic cation **169c** (Figure 192). For a related study involving radical intermediates, see section 5.4.

An organocatalytic variant of this transformation was achieved by the group of Cozzi using a MacMillan imidazolidinone catalyst (**Im-1**) (Figure 193).¹⁵⁵ With DDQ as the terminal oxidant, α -alkylation of aldehydes (**170a**) with diarylmethanes (**170b**) is possible with moderate to good enantioselectivities. Cozzi's coupling tolerates a wide range of functional groups, including free N–H indoles, and exhibits moderate to good levels of both diastereo- and enantiocontrol. The proposed mechanism involves formation of enamine **171a**, followed by subsequent nucleophilic addition to dibenzylic cation **171b**, which in turn

Figure 187. DDQ-mediated allylic alkylation of activated methylenes.¹⁵²Figure 188. Proposed mechanism for DDQ-mediated allylic alkylation of activated methylenes.¹⁵²Figure 189. DDQ-mediated propargylic alkylation of activated methylenes.¹⁵³

results from DDQ oxidation of the diarylmethane starting material **170b** (Figure 194). Asymmetric induction is achieved by selective addition to the less-hindered face of the enamine as depicted in Figure 195. In addition to diarylmethanes, diallylic and allylbenzyl substrates **172b** undergo oxidative cross-coupling with aldehydes (**172a**, Figure 196). For a related enantioselective α -arylation of aldehydes under SOMO catalysis, see section 5.2.

Gong and co-workers developed a highly enantioselective Cu-catalyzed coupling between activated methylenes (**173b**) and 3-benzylindoles (**173a**) under Lewis acid catalysis (Figure 197).¹⁵⁶ Cu(OTf)₂ performs better than Mg(OTf)₂ or Zn(OTf)₂ in the

Figure 190. Fe-catalyzed arylation of diphenylmethanes.¹⁵⁴Figure 191. Kinetic isotope effect study for Fe-catalyzed arylation of diphenylmethanes.¹⁵⁴Figure 192. Proposed mechanism for Fe-catalyzed arylation of diphenylmethanes.¹⁵⁴ Ar¹OH represents reduced DDQ, i.e., 2,3-dichloro-5,6-dicyanohydroquinone.

presence of bis(oxazoline) (i.e., BOx) ligands. A large number of chiral indole products **173c** can be prepared via this strategy. Preliminary mechanistic studies suggest the intermediacy of dibenzylic cationic intermediates (**174b**, Figure 198), in agreement with Shi's original CDA reaction (vide supra). Stereoselective nucleophilic addition with chiral copper enolate **174c** is thought to be the enantiodetermining step, which results in the formation of a new C—C bond with enantiocontrol.

Shi and co-workers have demonstrated that Fe catalysis can be applied to an analogous oxidative functionalization of dibenzylic compounds with simple alkenes (**175a**); the olefin acts as a nucleophile for the carbocation formed from the oxidation of diphenylmethane (**168b**, Figure 199).¹⁵⁷ Although the product appears to arise from a formal Heck-type reaction, the mechanism invoked does not involve carbometalation and β -H elimination steps (see section 2).

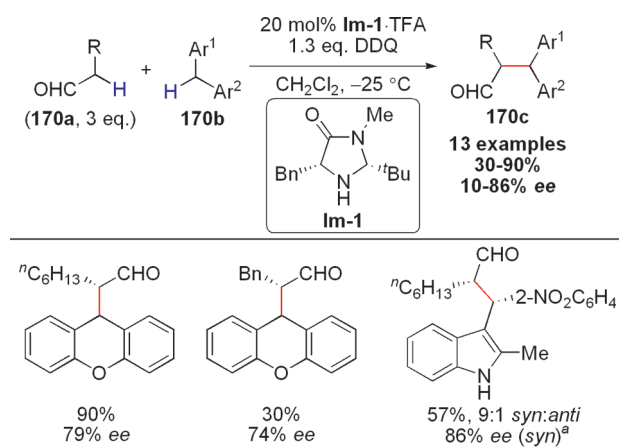


Figure 193. Enantioselective amine-catalyzed α -alkylation of aldehydes with diarylmethanes.¹⁵⁵

^aReaction is conducted with 2 equiv MeOH as an additive.

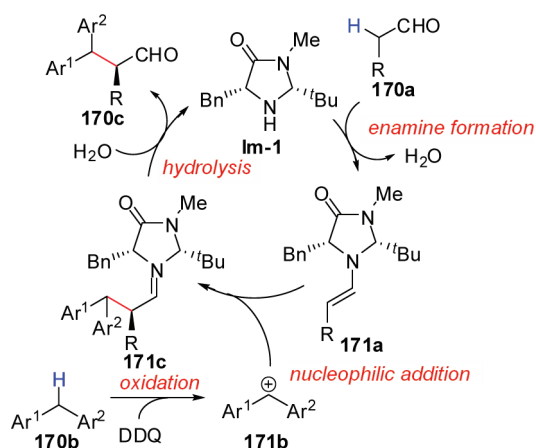


Figure 194. Proposed mechanism for enantioselective amine-catalyzed α -alkylation of aldehydes with diarylmethanes.¹⁵⁵

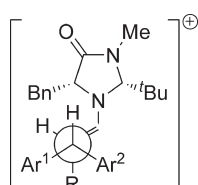


Figure 195. Model for enantioinduction in the enantioselective amine-catalyzed α -alkylation of aldehydes with diarylmethanes.¹⁵⁵

Complementary to enolate alkylations, alkyne alkylation by dehydrogenative coupling of dibenzyls (**176b**) is possible. The Li group reported CuOTf as a catalyst for oxidative C–C bond formation between terminal alkynes (**176a**) and dibenzyls (**176b**) in the presence of DDQ, a strong oxidant (Figure 200).¹⁵⁸ FeCl₂ did not demonstrate catalytic activity, and InCl catalyzed cross-coupling with reduced yields. The authors observed moderate to good reactivity for aromatic alkynes but could not extend this method to aliphatic variants.

4.5. Biaryl Bond Formation

Biaryl bond formation from two unactivated C–H bonds can be achieved via transition metal catalysis (see section 4) or phenolic type radical cross-couplings (see section 5.1). Direct

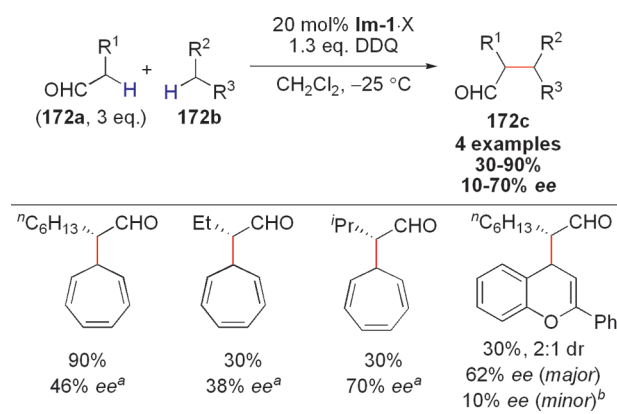


Figure 196. Enantioselective amine-catalyzed α -alkylation of aldehydes with diallylmethanes and allylbenzenes.¹⁵⁵

^aX = *p*-NO₂C₆H₄COOH.

^bX = TFA.

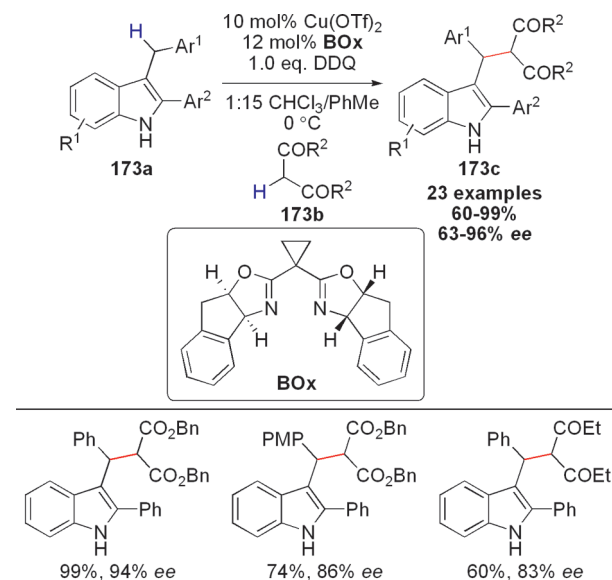


Figure 197. Cu-catalyzed enantioselective alkylation of activated methylenes.¹⁵⁶

arylations by mechanisms involving polar bond formation are an alternative strategy. In 2009, Kita et al. used Koser's reagent (i.e., PhI(OH)OTs) to couple heteroaromatic rings (**177a**) with other heteroaromatic rings or electron-rich arenes (**177b**, Figure 201).¹⁵⁹ This reaction was discovered based on the known ability of thiophenes and other electron-rich heterocycles to undergo 2-iodination in the presence of the hypervalent iodine(III) salts and fluorinated solvents (e.g., hexafluoro-2-propanol). TMSBr is required as an additive to promote the desired dehydrogenative C–C bond formation by exchanging the OTs ligand on the I(III) intermediate with a Br ligand, which reduces the electron density of the iodoarene intermediate. In light of these observations, Kita et al. propose a mechanism involving iodination of the heteroaromatic ring **177a** with Koser's reagent, ligand exchange with TMSBr, hydroarylation with unactivated arene **177b**, and subsequent elimination of PhI and HBr to liberate final product **177c** (Figure 202). In a stoichiometric study, the authors prepared the iodine(III) reagent (with either an OTs or Br ligand, i.e., **178a** or **178b**, respectively), subjected it

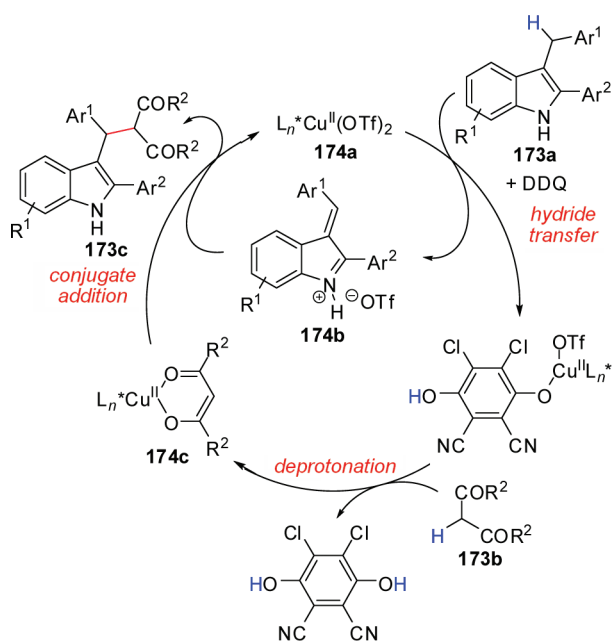


Figure 198. Proposed mechanism for Cu-catalyzed enantioselective alkylation of activated methylenes.¹⁵⁶

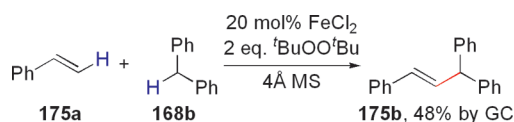


Figure 199. Fe-catalyzed styrenylation of diphenylmethane (175a).¹⁵⁷

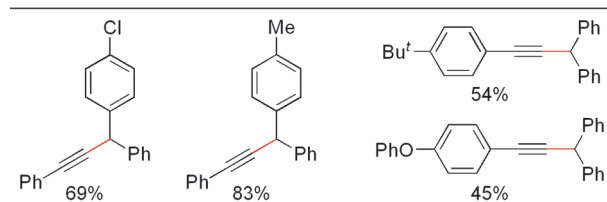
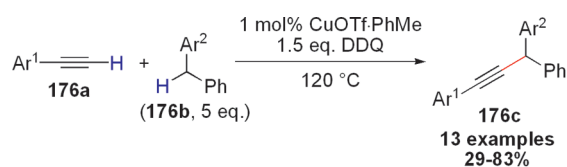


Figure 200. Cu-catalyzed alkylation of diphenylmethanes.¹⁵⁸

to the reaction conditions, and observed the cross-coupled product **177c** in excellent yields.

The group of Canesi used stoichiometric amounts of $\text{PhI}(\text{OAc})_2$ to achieve an oxidative C–C coupling between *p*-substituted anilides and phenols (**179a**) with thiophenes (**179b**, Figure 203).¹⁶⁰ Aliphatic alcohols, aryl chlorides, and aryl bromides are all tolerated under these reaction conditions, among many other functional groups. During the course of their studies, the authors identified a polycyclic byproduct believed to arise from a formal [4 + 3]-cycloaddition between an anilinium cation and thiophene. This observation supports a mechanistic proposal involving oxidation of anilide **179a** to anilinium cation **180a**, followed by nucleophilic addition of thiophene **179b**. Intermediate **180b** then follows one of two pathways. Either

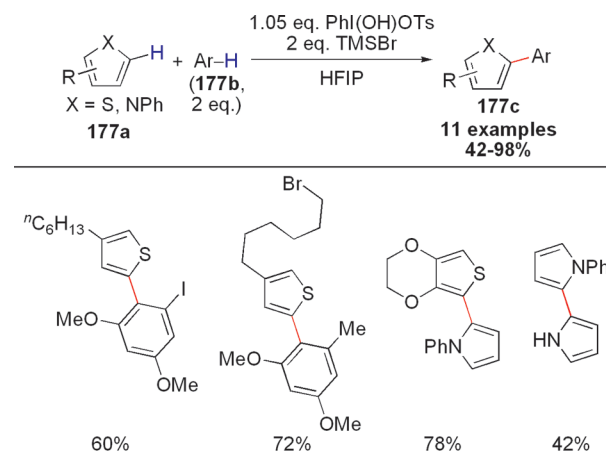


Figure 201. $\text{PhI}(\text{OH})\text{OTs}$ -mediated oxidative intermolecular biaryl C–C coupling.¹⁵⁹

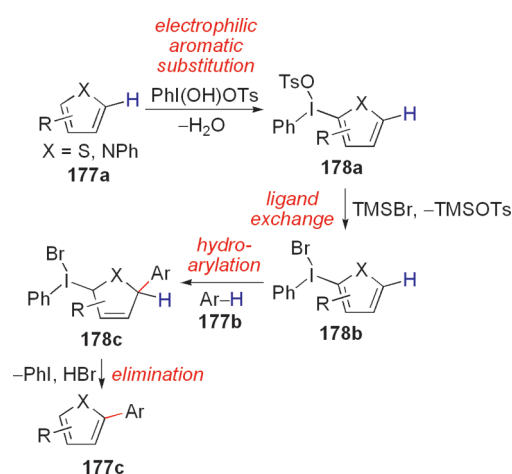


Figure 202. Proposed mechanism for $\text{PhI}(\text{OH})\text{OTs}$ -mediated oxidative intermolecular biaryl C–C coupling.¹⁵⁹

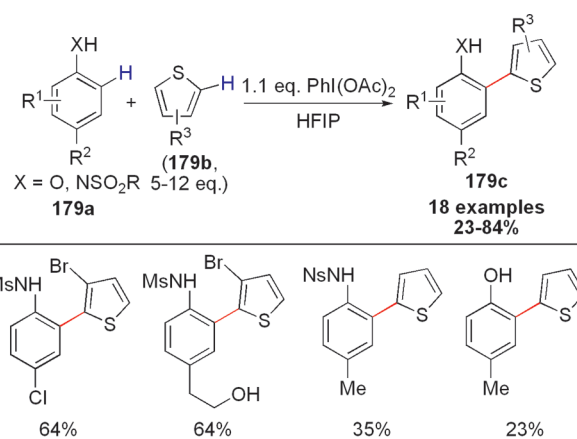


Figure 203. $\text{PhI}(\text{OAc})_2$ -mediated oxidative intermolecular biaryl C–C coupling.¹⁶⁰

direct proton transfer ensues, liberating the final biaryl product in one step (**180e**), or cyclization to furnish a new C–N bond, generating the aforementioned polycyclic byproduct, and subsequent rearrangement occurs (Figure 204). To improve reaction

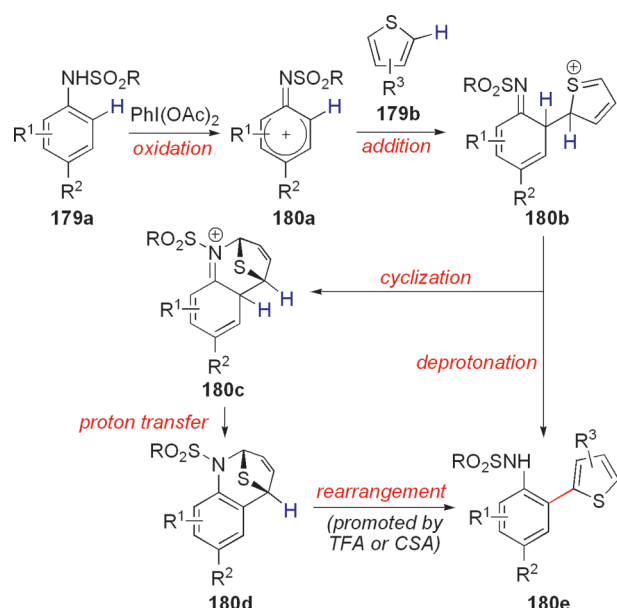


Figure 204. Proposed mechanism for $\text{PhI}(\text{OAc})_2$ -mediated oxidative intermolecular biaryl C–C coupling.¹⁶⁰

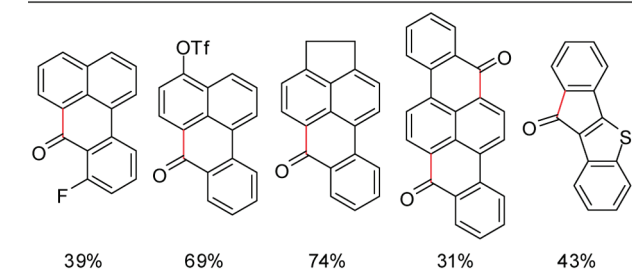
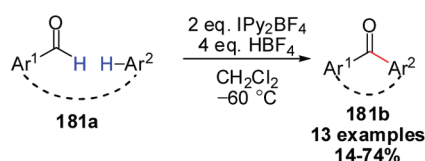


Figure 205. Intramolecular Friedel–Crafts acylation with aldehydes.¹⁶²

yields, protic acids such as trifluoroacetic acid or camphorsulfonic acid can be added to promote the final rearrangement step. This work parallels the well-known ability for polyphenylenes to undergo intramolecular oxidative C–C cross-coupling (i.e., the Scholl reaction¹⁶¹) via the action of appropriate Lewis acids and oxidants via Friedel–Crafts-type intermediates.⁴⁶

4.6. Miscellaneous Examples

An alternative and complementary method for oxidative C–C bond formation by ionic intermediates involves the direct coupling of an aldehydic C–H bond with an arene C–H bond via a Friedel–Crafts type mechanism. Barluenga and co-workers discovered an intramolecular reaction of polyaromatic aldehydes to yield ketone products using stoichiometric amounts of IPy_2BF_4 as an activating agent (Figure 205).¹⁶² This cyclization results in the formation of diarylketone products. Although the mechanistic understanding remains elusive, Barluenga proposes the intermediate of an iodonium-activated aldehyde (**182a**, Figure 206). This

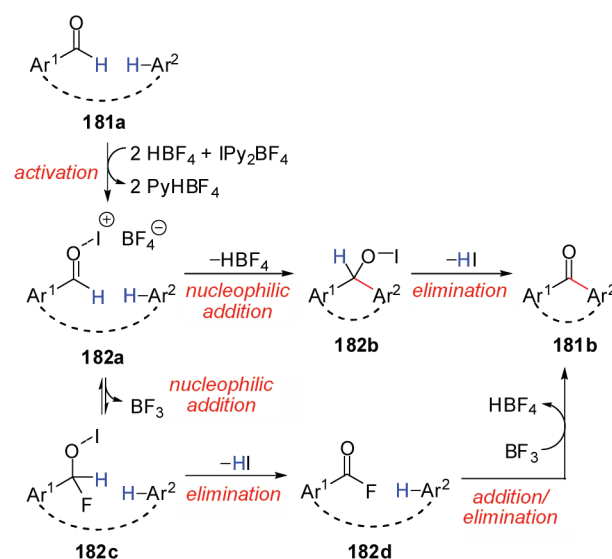


Figure 206. Proposed mechanism for intramolecular Friedel–Crafts acylation with aldehydes.¹⁶²

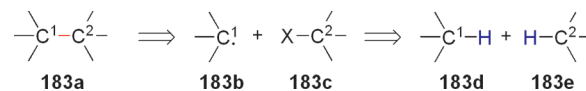


Figure 207. Generic scheme for cross-couplings via radical intermediates.

Substrates

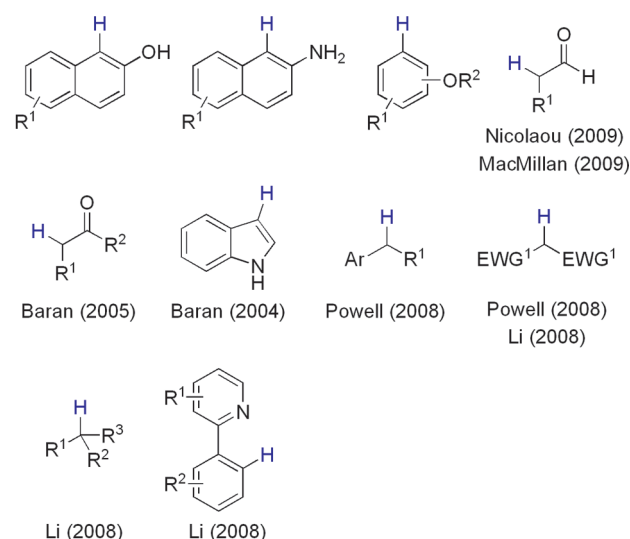


Figure 208. Overview of cross-couplings via radical intermediates.

activated electrophile is prone to nucleophilic attack of the nearby aromatic ring, followed by β -I elimination to afford final product **181b**. Alternatively, the BF_4^- anion may undergo addition to the iodonium-activated aldehyde **182a** to generate acyl fluoride intermediate **182d**, which liberates the desired product by a sequence of addition and elimination events.

5. CROSS-COUPLING VIA RADICAL INTERMEDIATES

Forming C–C bonds by using radical intermediates is relatively versatile because radicals can undergo couplings with

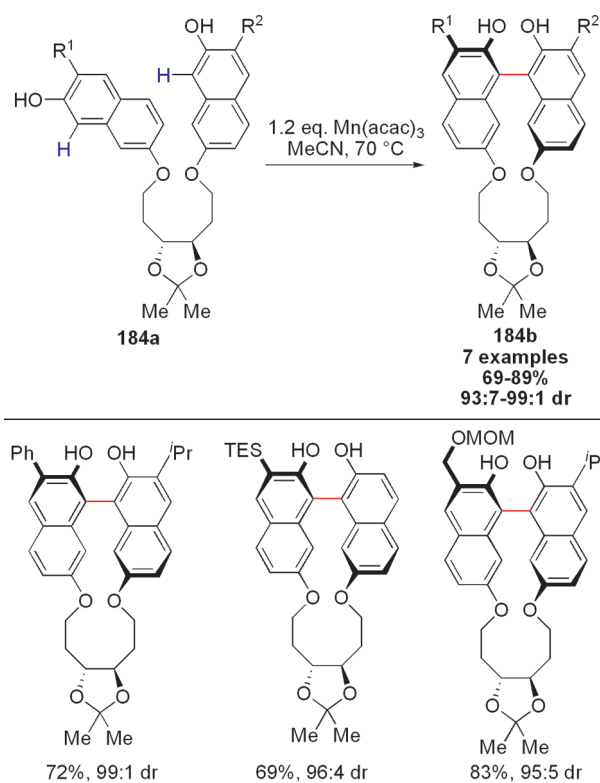


Figure 209. Mn-mediated intramolecular oxidative phenolic coupling toward *cyclo*-BINOLs.¹⁶⁷

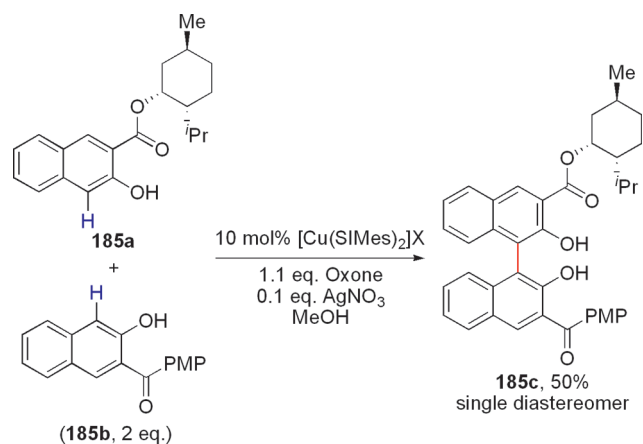


Figure 210. Cu-catalyzed diastereoselective intermolecular oxidative phenolic coupling.¹⁶⁸

carbocations, carbanions, and other radicals, as well as additions to C=C multiple bonds (Figure 207). In many cases, transition metals can be used to catalyze selective C–H bond oxidation to single-electron intermediates. Phenols, sp³ C–H bonds α- to carbonyl functionalities (e.g., aldehydes, ketones, and esters), electron-rich arenes (e.g., indoles and pyrroles), and simple benzylic compounds can all undergo oxidative radical C–C bond formation (Figure 208).

5.1. Biaryl Bond Formation

The cross-coupling between two phenols (or naphthols) yields valuable bisphenol (or binaphthol) products that make up a class of privileged ligands (e.g., BINOLs)¹⁶³ and natural

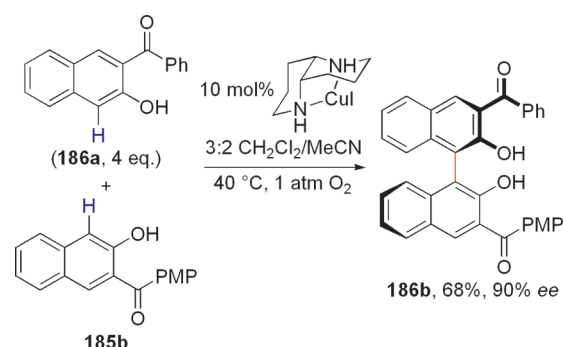


Figure 211. Cu-catalyzed enantioselective intermolecular oxidative phenolic coupling.¹⁶⁹ The carbonyl found *ortho* to the phenolic OH is essential for high enantiomeric excesses.

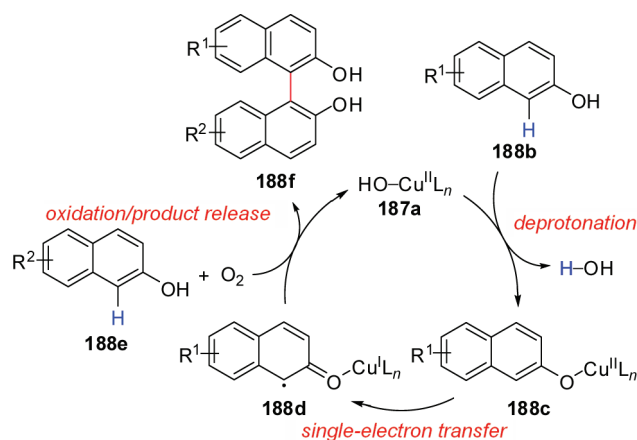


Figure 212. Proposed mechanism for Cu-catalyzed enantioselective intermolecular oxidative phenolic coupling.

products.¹⁶⁴ In general, to achieve oxidative cross-coupling between two distinct phenols, their oxidation potential must differ enough such that an oxidant will selectively oxidize one phenol and not the other; otherwise, competitive homocoupling occurs. In 1987, Yamamoto and co-workers reported the selective *cross-coupling* between naphthol and phenanthren-9-ol in the presence of stoichiometric amounts of a chiral Cu-DPEN complex,¹⁶⁵ and this method was later extended to include differentially substituted naphthols.¹⁶⁶ A diastereoselective intramolecular variant was developed by Lipshutz to make a new class of BINOL derivatives termed *cyclo-BINOLs* (**184b**, Figure 209).¹⁶⁷ Using a chiral tether (obtained in enantioenriched form by asymmetric dihydroxylation), excellent levels of diastereocontrol are possible. Lipshutz's reaction requires stoichiometric amounts of a Mn(acac)₃ oxidant, but catalytic quantities of CuCl(OH)·TMEDA (i.e., 8 mol %) in the presence of O₂ may be used instead. The Collins group developed an alternative Cu-catalyzed method using *N*-heterocyclic carbenes as ligands and Oxone as the terminal oxidant. A menthol auxiliary controls the biaryl coupling to provide chiral BINOL derivatives diastereoselectively (Figure 210).¹⁶⁸

Complementary to this work, the Kozłowski group reported a Cu-catalyzed enantioselective oxidative C–C bond formation between two different naphthols **181a** and **181b** using O₂ as the sole oxidant (Figure 211).¹⁶⁹ In cases where phenolic cross-coupling is favored over homocoupling, the authors propose a

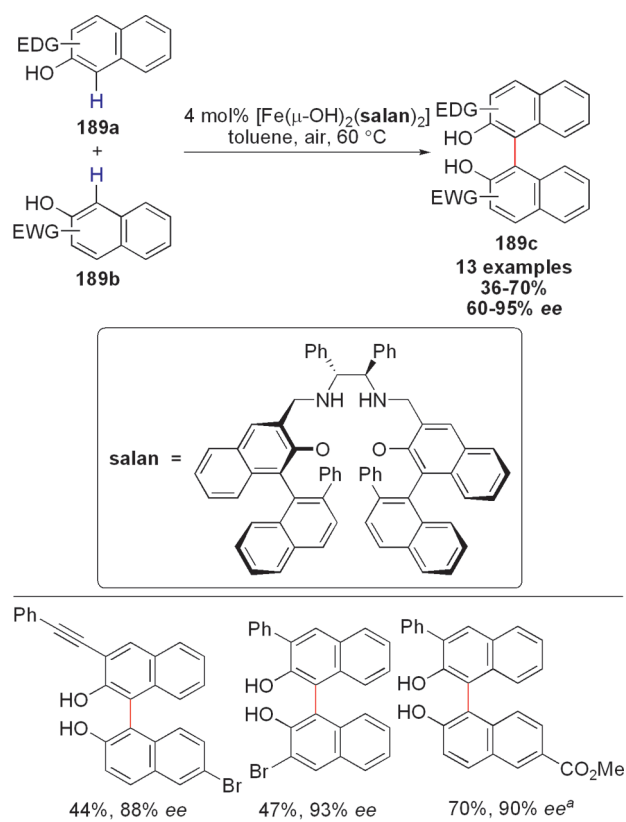


Figure 213. Fe-catalyzed enantioselective intermolecular oxidative phenolic coupling.¹⁷⁰

^aTwo equiv of coupling partner **189b** was used.

radical combination with a second equiv of the naphthol starting material as depicted in Figure 212. The Cu catalyst acts as an oxidizing agent that is itself reoxidized by an external sacrificial oxidant such as O₂. Single-electron transfer is more facile in the presence of electron-donating substituents on the naphthol cross-coupling partner. The authors suggest that the redox step from Cu(II) to Cu(I) is likely the slow step in the catalytic cycle.

The Katsuki group disclosed a highly stereoselective variant of this transformation under Fe catalysis (Figure 213).¹⁷⁰ Using a salan ligand, hydroxy-bridged iron dimer **190a** catalyzes oxidative cross-coupling of electronically differentiated 2-naphthols (i.e., an electron-rich naphthol **189a** with an electron-poor naphthol **189b**). The transformation favors cross-coupled binaphthol products **189c** with moderate to excellent selectivities (up to 20:1); both homocoupling (of the more electron-rich naphthol) and cross-coupling occurred with excellent levels of enantiocontrol (up to 96% ee). Catalytic homodimerization of 2-naphthols occurs with a first-order dependence on substrate concentration and partial pressure of O₂. Additionally, this reaction displayed a linear relationship between enantiomeric excesses of the catalyst and isolated product. As depicted in Figure 214, the proposed mechanism involves an Fe(III/IV) catalytic cycle for the phenolic cross-coupling, with ligand exchange, oxidation, nucleophilic coupling, and rearomatization as key steps. The mechanism likely involves radical cation intermediates and is related to biologically relevant oxidative couplings (see section 6). Electronic differentiation of the 2-naphthol starting materials affects two key parameters: (1) rate of oxidation by O₂ and (2) strength of coordination to the Fe center.

A related oxidative cross-coupling between naphthols and naphthylamines is possible¹⁷¹ and can be achieved enantioselectively.¹⁷² Although stoichiometric amounts of copper and chiral ligand (i.e., (*R*)- α -methylbenzylamine) are required, the Kočovský group found that coupling 2-naphthol (**191b**) and 2-naphthylamine (**191a**) results in fortuitous precipitation of the product enriched in (–)-isomer **191c**, while the mother liquor is enriched in the (+)-isomer **191d** (Figure 215).¹⁷² In another study, Lipshutz et al. used a tether approach to synthesize cyclic variants of these compounds, termed *cyclo*-NOBINS, via intramolecular dehydrogenation (**191b**, Figure 216).¹⁷³

Nonphenolic biaryl bond formation has previously been described (see sections 2.5 and 4). In 1973, using VOF₃ in TFA, Kupchan and co-workers were able to synthesize (±)-glaucine (**193b**) and (±)-*N*-formylnorglaucine by intramolecular biaryl coupling (**193d**, Figure 217).¹⁷⁴ Presumably, the more electron-rich aromatic ring undergoes oxidation to an arenium cation **194b** via a formal two-electron process that likely involves two single-electron transfer steps (Figure 218). Although the mechanistic details are unknown, we classify this C–C bond formation as a radical-type oxidative cross-coupling due to similarities to biological oxidations (see section 6). A photochemical variant of this transformation was disclosed in 1984 for the synthesis of (±)-cryptopleurine (**195c**, Figure 219).¹⁷⁵ Mechanistic understanding remains sparse, but it is believed that photochemical excitation generates intermediates with unpaired electrons. These species undergo cyclization by a sequence of radical addition and elimination steps to afford the product. Alternatively, a mechanism involving 6 π -electrocyclization may also be involved.

Prior to transition metal-catalyzed approaches to C–H activation, direct thallation and subsequent oxidative cross-coupling provided a strategy for direct C–C bond formation.¹⁷⁶ Syntheses of (±)-ocotene (**196b**), also known as (±)-thalicimine;¹⁷⁷ (±)-3-methoxy-*N*-acetylnornantenine (**196d**, a nonbasic noraporphine alkaloid from the heartwood of *Liriodendron tulipifera*); (±)-kreysigine (**196f**, an alkaloid from *Kreysigia multiflora*); (±)-*O*-methylkreysigine (**196h**);¹⁷⁸ and (±)-deoxytylophorinine (**196j**)¹⁷⁹ were achieved via oxidative biaryl coupling in the presence of stoichiometric amounts of Tl(TFA)₃ (Figure 220). Electrophilic thallation of the electron-rich aromatic ring occurs via single-electron oxidations and forms radical cation intermediates that undergo subsequent cyclization and finally oxidation to liberate the biaryl product.¹⁷⁸ Another possible mechanism involving electron-transfer steps that do not involve C–Tl bond cannot be ruled out.

An Fe-mediated dehydrogenative cyclization was developed by the Wang group for the total synthesis of (±)-deoxytylophorinine (**196j**) and (±)-antofine (**197c**, Figure 221).¹⁸⁰ A mixture of *E* and *Z* isomers of the starting materials **197a** and **197d** provides the desired phenanthrene products (**197b** and **197e**, respectively) with high efficiency. The authors propose a radical mechanism for this cyclization based on ESR spectroscopic studies on their related catalytic studies ($g = 2.0025$) with *m*-CPBA as the terminal oxidant (Figure 222).¹⁸¹

Most intramolecular oxidative biaryl C–C couplings result in six-membered ring formation. Larger rings, however, can be formed by this dehydrogenative approach. Kita and co-workers observed selective formation of seven- and eight-membered rings using phenyliodine bis(trifluoroacetate) (PIFA) as an oxidant (Figure 223).¹⁸² BF₃·OEt₂ is added to promote the desired intramolecular coupling by rendering PIFA more reactive.

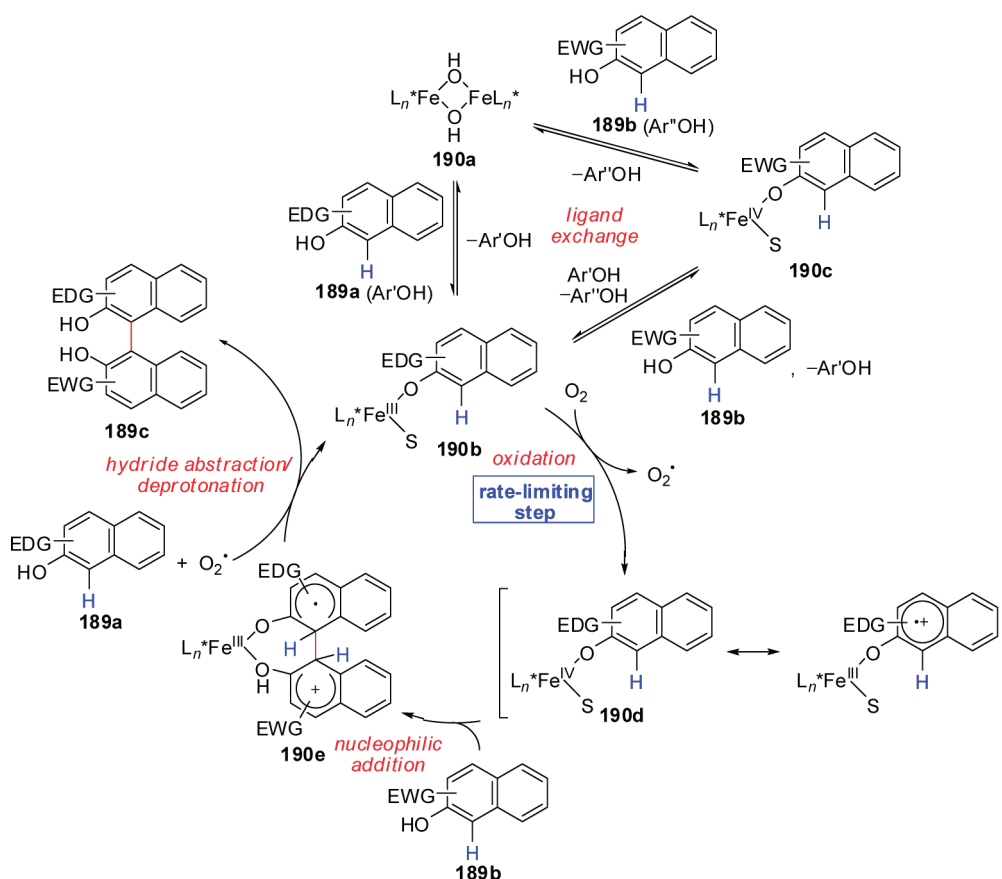


Figure 214. Proposed mechanism for Fe-catalyzed enantioselective intermolecular oxidative phenolic coupling.¹⁷⁰

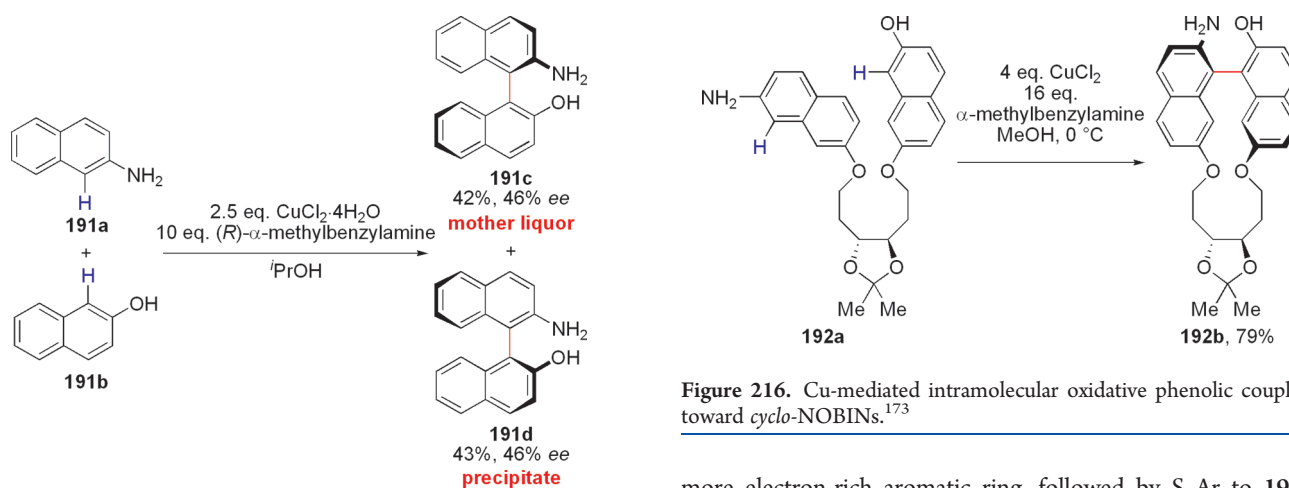


Figure 215. Cu-mediated enantioselective intermolecular oxidative coupling between 2-naphthol and 2-naphthylamine.¹⁷² The precipitate isolated from the reaction is enriched in (–)-isomer **191c**, whereas the mother liquor is enriched in the (+)-isomer **191d**.

Cyclization to form eight-membered rings is difficult, and oxidation to the corresponding quinone byproduct competes.¹⁸³ In Kita's reaction, the desired C–C bond-forming event can be favored by choosing substituents on the starting material that favor cyclization over overoxidation to quinones. As such, the proposed mechanism involves single-electron oxidation of the

Figure 216. Cu-mediated intramolecular oxidative phenolic coupling toward *cyclo*-NOBINs.¹⁷³

more electron-rich aromatic ring, followed by S_EAr to **199c**, oxidation to arenium cation **199d**, and finally ring-expansion to give the desired product **199f** (Figure 224).

An intermolecular PIFA-mediated biaryl coupling between arenes (**200a**) and mesitylene derivatives (**200b**) has been achieved by the Kita group (Figure 225).¹⁸⁴ The Koser reagent, $PhI(OH)OTf$, can be a substitute, but using other metal salts, including $FeCl_3$ and $Tl(TFA)_3$, leads to significantly reduced reaction efficiencies. Other common oxidants, including DMP, DDQ , and CAN , give no desired cross-coupled product (**200c**). The Kita group found that naphthalenes, thiophenes, and anisole derivatives (**200a**) are suitable cross-coupling partners. Conceptually related but mechanistically distinct strategies for oxidative

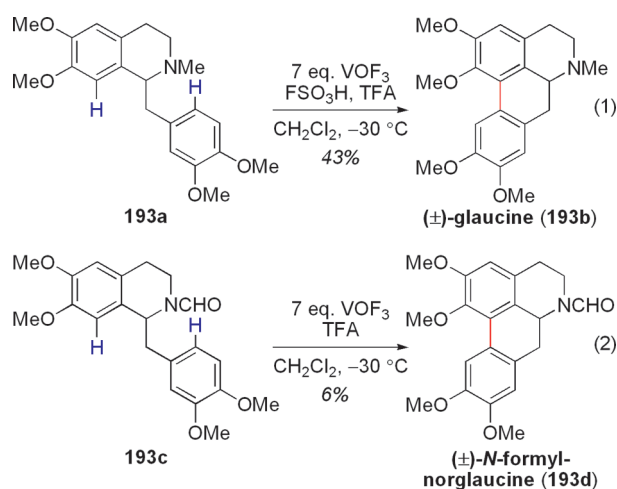


Figure 217. Total syntheses of (±)-glaucine (193b) and (±)-N-formyl-norglaucine (193d) via oxidative intramolecular biaryl C–C coupling.¹⁷⁴

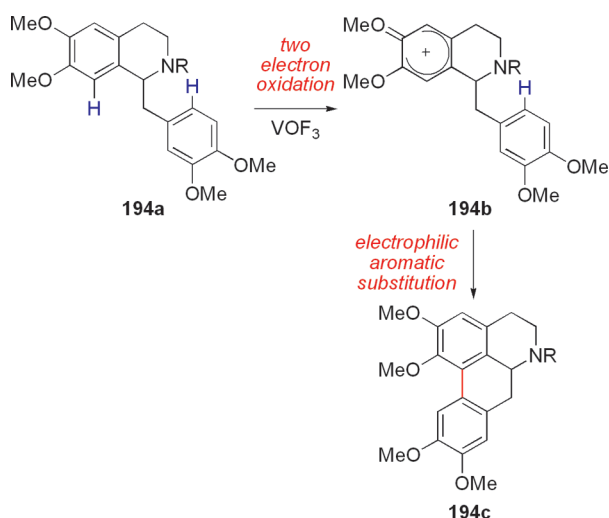


Figure 218. Proposed mechanism for intramolecular oxidative biaryl bond formation via oxidative intramolecular biaryl C–C coupling.¹⁷⁴

C–C cross-coupling using Koser's reagent or iodobenzene diacetate between electron-rich heteroarenes and electron-rich arenes were discussed in section 2.5.

5.2. α -Arylation of Aldehydes by Organo-SOMO Catalysis

Organocatalysis enables enantioselective oxidative coupling via radical intermediates. In 2009, the groups of Nicolaou¹⁸⁵ and MacMillan¹⁸⁶ independently reported the enantioselective α -arylation of aldehydes (201a, 202a) by organo-SOMO catalysis.¹⁸⁷ With an amine catalyst and an appropriate oxidant (e.g., CAN or [Fe(phen)₃]PF₆), high levels of enantioinduction are possible (Figures 226 and 227).^{185,186} In general, electron-rich aromatic rings undergo efficient oxidative C–C bond formation. Using this approach, Nicolaou and co-workers achieved the total synthesis of (–)-demethyl calamenene (206c, Figure 228),¹⁸⁵ while MacMillan and co-workers prepared (–)-tashiromine (207c, Figure 229).¹⁸⁶

While Nicolaou suggested a Friedel–Crafts mechanism involving ionic intermediates⁴⁶ (see section 4),¹⁸⁵ MacMillan and

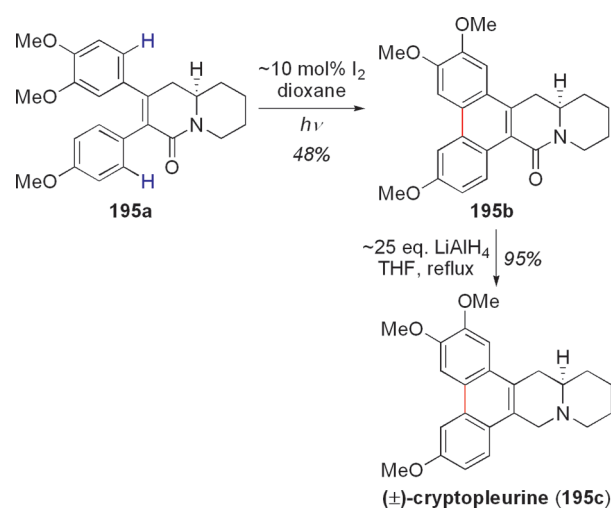


Figure 219. Total syntheses of (±)-cryptopleurine (195c) via photochemical oxidative intramolecular biaryl C–C coupling.¹⁷⁵

co-workers proposed an alternative radical-based pathway. On the basis of related studies on SOMO catalysis,¹⁸⁷ MacMillan favors a mechanism involving formation of iminium ion 208b, which undergoes a one-electron oxidation to enammonium radical cation 208c, which then cyclizes to afford an arenium radical cation 208d (Figure 230).¹⁸⁸ 208d undergoes a second one-electron oxidation to arenium cation 208e, followed by rearomatization (by deprotonation) and hydrolysis to regenerate the amine catalyst (Im-2). In a collaborative study, MacMillan and Houk supported the existence of open-shell radical intermediates in this intramolecular dehydrogenative coupling by DFT calculations. The best theoretical description of prochiral enammonium radical cation 208c was determined to be an alkyl radical stabilized by an adjacent iminium ion. MacMillan and Houk's calculations support ortho-selective cyclization via a tightly ordered six-membered transition state (Figure 231); in contrast, a Friedel–Crafts mechanism would favor *para*-selective alkylation.

5.3. Enolate–Enolate Cross-Coupling

Two different enolates can undergo cross-coupling at their α -positions to provide direct access to 1,4-dicarbonyl compounds by dehydrogenative C–C bond formation. Dienolate *homocoupling* was first reported in 1971.¹⁸⁹ As early as 1975, oxidative coupling from two enolates was reported using CuCl₂ as the stoichiometric oxidant, presumably occurring via radical intermediates. Typically, one enolate coupling partner is used in excess to minimize competitive homocoupling. With this approach, expeditious syntheses of several natural products, including dihydrojasnone (209c), *cis*-jasnone (209f), allylrethron (209i), and ipomeanine (209k), were realized (Figure 232).¹⁹⁰ Regioselectivity of these dehydrogenation reactions is dictated by the inherent reactivities of the α -C–H bonds (i.e., formation of a kinetic versus thermodynamic enolate by selective deprotonation). Concurrent with this work, cross-coupling between two ester enolates was developed.¹⁹¹

Baran and co-workers were first to apply oxidative dienolate coupling to complex molecule total synthesis in their synthesis of the stephacidins, a family of alkaloids that exhibit potent *in vitro* cytotoxicity against a number of human tumor cell lines (Figure 233).^{192–194} Intramolecular coupling between the α -carbons of an amide and an ester afforded the basic polycyclic

framework required for *ent*-(−)-stephacidin A (**210c**, 61%, 66% brsm). $\text{Fe}(\text{acac})_3$ was the optimal oxidant, and Cp_2FePF_6 , FeCl_3 , CuCl_2 , $\text{Cu}(\text{OTf})_2$, and $\text{Cu}(\text{2-ethylhexanoate})_2$ ($\text{Cu}(\text{2-EH})_2$) gave lower yields. Carefully tuning the oxidation potential is necessary to promote the desired oxidation over competing ones.

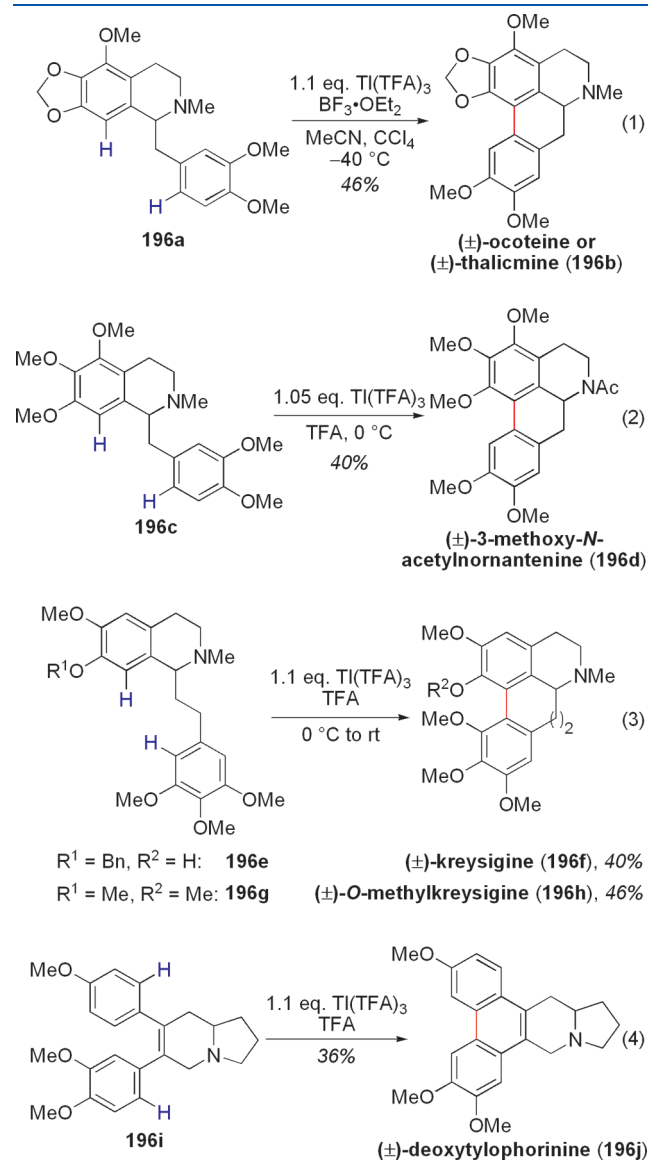


Figure 220. Total syntheses of (±)-ocoteine (**196b**), (±)-3-methoxy-N-acetylnornantennine (**196d**), (±)-kreysigine (**196f**), (±)-O-methylkreysigine (**196h**), and (±)-deoxytylophorinine (**196j**) via Ti-mediated oxidative biaryl C–C coupling.^{177–179}

By repeating the same sequence with the opposite enantiomer of the starting reagents, (+)-stephacidin A (**210c**) was prepared and ultimately transformed into (−)-avrainvillamide (**211a**, Figure 234) and subsequently (+)-stephacidin B (not shown).

Overman and co-workers used a similar oxidative ketone–ester cross-coupling to achieve the first total synthesis of (±)-actinophyllic acid (**212c**), an indole alkaloid obtained from *Alstonia actinophylla* that demonstrates promising inhibition of carboxypeptidase U (Figure 235).¹⁹⁵ In the presence of excess amounts of strong base, indole derivative **212a** underwent chemo- and stereoselective intramolecular oxidative C–H bond cross-coupling to afford polycyclic compound **212b** in a single step. The authors identified $[\text{Fe}(\text{DMF})_3\text{Cl}_2][\text{FeCl}_4]$ ¹⁹⁶ as the best oxidant for this dehydrogenative cyclization. Product **212b** was subsequently converted to (±)-actinophyllic acid hydrochloride (**212c**) in four steps.¹⁹⁵ In a subsequent account, enantioenriched (+)-actinophyllic acid was prepared from commercially available γ -aminobutyric acid in a total synthesis

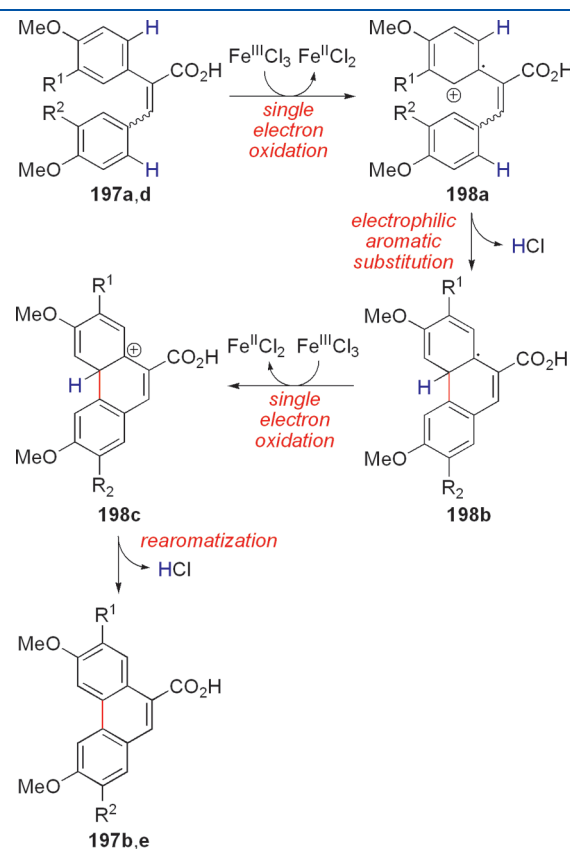


Figure 222. Proposed mechanism for Fe-mediated oxidative arylation.

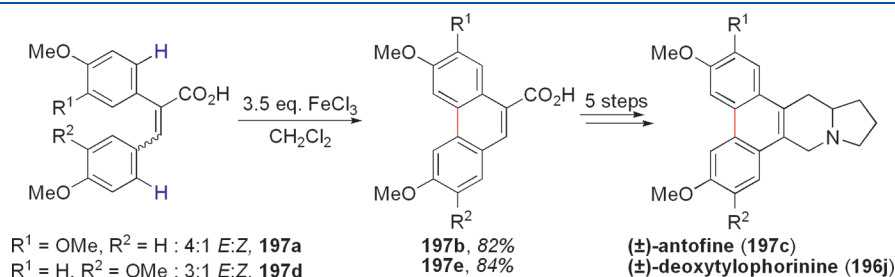


Figure 221. Total syntheses of (±)-antofine (**197c**) and (±)-deoxytylophorinine (**196j**) via oxidative phenolic coupling.¹⁸⁰

featuring an asymmetric hydrogenation.¹⁹⁷ The Overman group used this approach toward *Strychnos* alkaloids (+)-condylocarpine (**212d**), (+)-isocondylocarpine (**212e**), and (+)-tubotaiwine (**212f**).

Baran and co-workers have conducted an in-depth study on their intermolecular oxidative dienolate cross-coupling reaction (Figure 236).^{198,199} Distinct diastereomers can be generated by varying the oxidant (i.e., Fe(III) or Cu(II)). Using this method, (–)-burshehennin (**214d**), a lignan lactone that exhibits antitumor activity, was synthesized using a chiral auxiliary to control the absolute stereochemistry (Figure 237).

Baran performed radical clock experiments to support the existence of radical intermediates (Figure 238).^{198,199} Whereas the Cu(II)-mediated coupling leads to ring-opening of the adjacent cyclopropane ring (i.e., suggesting radical character at the α -carbon), the analogous Fe(III)-mediated reaction does not. A Hammett analysis on both the oxazolidinone and propio-

phenone components identified linear relationships for Fe(III)-mediated oxidations for both partners ($\rho_{\text{oxazolidinone}} = -0.63$; $\rho_{\text{propiophenone}} = -0.25$), which provides support for partial loss of electrons during the course of the reaction. For Cu(II), an inverse parabolic relationship is observed for both partners, which

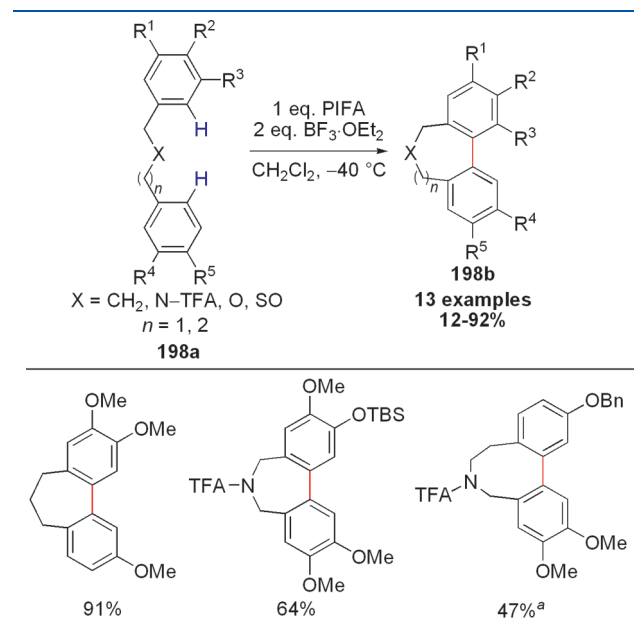


Figure 223. PIFA-mediated oxidative intramolecular biaryl C–C coupling.¹⁸²

^a1.1 equiv PIFA in TFE at -40°C with no $\text{BF}_3 \cdot \text{OEt}_2$.

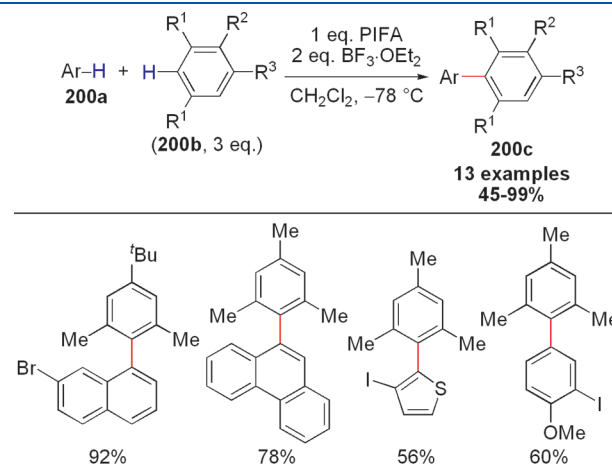


Figure 225. PIFA-mediated oxidative intermolecular biaryl C–C coupling.¹⁸⁴

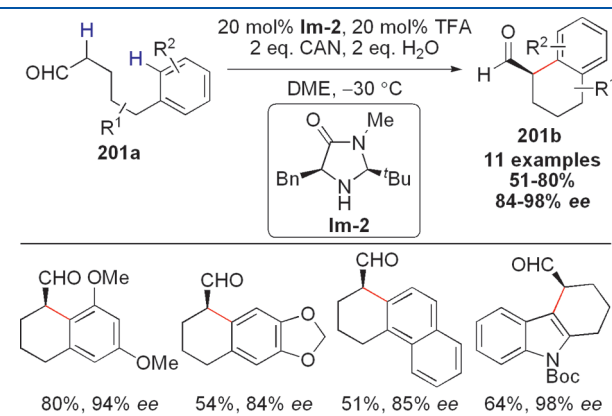


Figure 226. Nicolaou's amine-catalyzed enantioselective α -arylation of aldehydes.¹⁸⁵

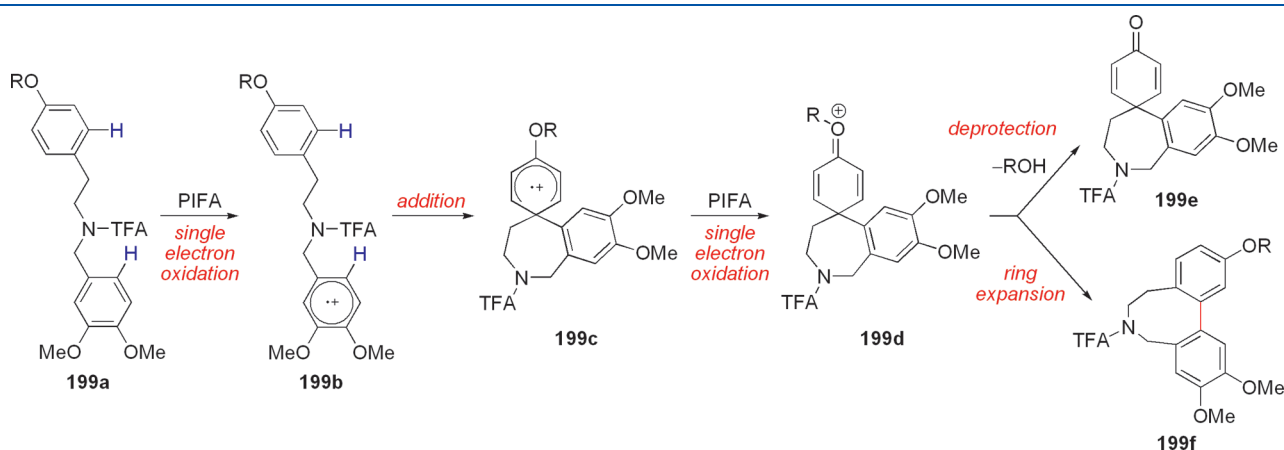


Figure 224. Proposed mechanism for PIFA-mediated oxidative intramolecular biaryl C–C coupling.¹⁸²

indicates a change in rate-determining step. The mechanistic intricacies of both Cu(II)- and Fe(III)-mediated dehydrogenative enolate cross-coupling warrant further investigation both experimentally and theoretically.

Extending the scope of enolate cross-coupling, Baran and co-workers reported a novel indole–enolate heterocoupling for the expeditious synthesis of (+)-hapalindole Q (**216d**), (–)-*ent*-12-*epi*-hapalindole D (**216e**), and (–)-12-*epi*-fischerindole U isothiocyanate (**216f**, Figure 239).^{199–201} A brief examination of reaction conditions revealed that indole (**216a**) undergoes dehydrogenative C–C bond formation with (*R*)-carvone (**216b**) in the presence of Pb(OAc)₄, FeCl₃, TiCl₄, Mn(acac)₃, and CAN, with Cu(2-ethylhexanoate)₂ being the optimal stoichiometric oxidant. Using a more advanced coupling partner, (–)-*ent*-12-*epi*-fischerindole G (**217c**), (–)-12-*epi*-fischerindole I (**217d**), and (+)-welwitindolinone A (**217e**) can also be accessed (Figure 240). Similarly, (+)-acremonoxin A (**218c**), a plant growth inhibitor, and (+)-oxazin C (**218f**) can be prepared by this route (Figure 241).²⁰¹ These tandem C–H bond

oxidations typically occur with excellent levels of diastereoselectivity and can be applied to a wide range of ketone and ester enolates (Figure 242). Functionalizing the α -position of ketones (**219a**) with indole (**216a**) yields structural motifs that are present in many naturally occurring compounds and may be a useful tool for the drug-discovery process.

To study the oxidative coupling between indoles and enolates, Baran constructed a series of Hammett plots for C5- and C6-substituted indoles.²⁰¹ For C5-substituted indole coupling partners, a nonlinear relationship between the observed reaction rate and σ is observed. The reactivity trend, however, dictates that electron-withdrawing substituents enhance coupling. On the other hand, for C6-substituted indoles, a negative linear correlation is observed (with $\rho = -0.61$). Thus, Baran can conclude significant anionic character at both C3 and N1 positions in the transition state. Dimerization of indole itself does not occur in the absence of the ketone, which suggests that oxidation of the ketone takes place first. Because free N–H indoles are

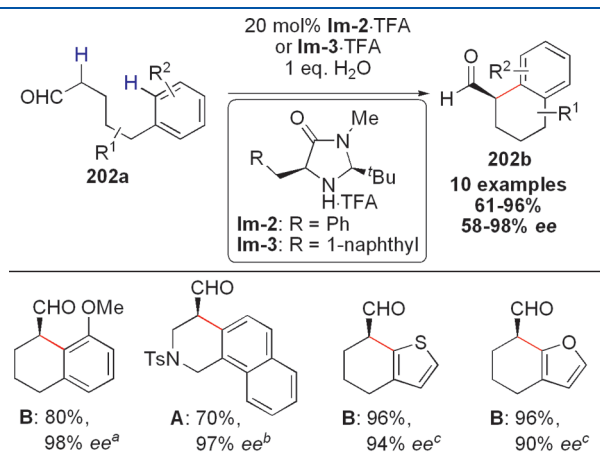


Figure 227. MacMillan's amine-catalyzed enantioselective α -arylation of aldehydes.¹⁸⁶

^a2.5 equiv [Fe(phen)₃]PF₆, 5 equiv NaHCO₃, MeCN, –20 °C.

^b2.5 equiv [Fe(phen)₃]PF₆, 1 equiv Na₂HPO₄, acetone, –30 °C.

^c2 equiv CAN, 2 equiv NaHCO₃, 2 equiv NaTFA, acetone, –30 °C.

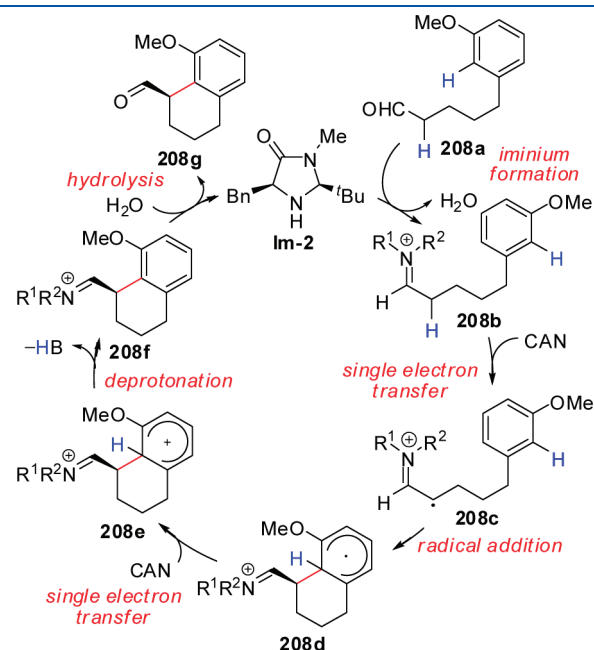


Figure 230. Proposed mechanism for amine-catalyzed enantioselective α -arylation of 5-(3-methoxyphenyl)pentanal (**208a**).

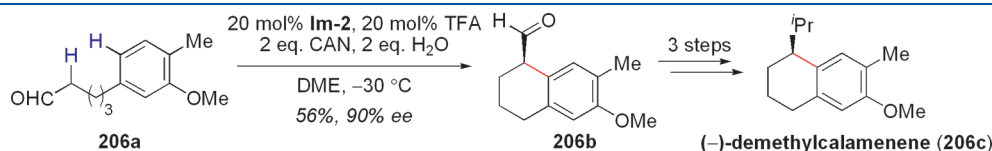


Figure 228. Total synthesis of (–)-demethyl calamenene (**206c**) via oxidative enantioselective α -arylation of aldehydes.¹⁸⁵

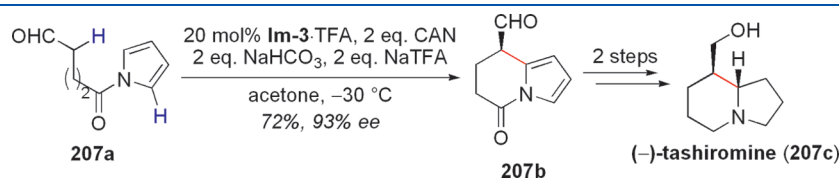


Figure 229. Total synthesis of (–)-tashiromine (**207c**) via oxidative enantioselective α -arylation of aldehydes.¹⁸⁶

required for the C–C bond formation, the authors favor a radical anion mechanism involving a templated radical addition that may help to explain the excellent diastereocontrol observed (Figure 243).

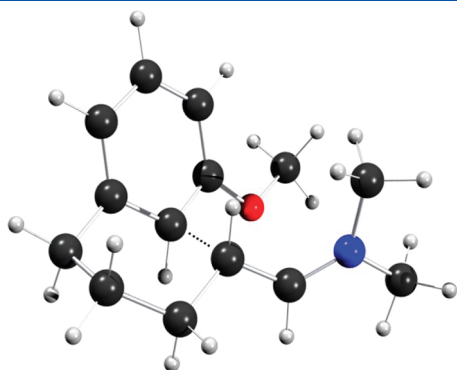


Figure 231. Transition state model for amine-catalyzed enantioselective α -arylation of aldehyde 5-(3-methoxyphenyl)pentanal. The POV-Ray drawing was created from coordinates obtained from Um et al.¹⁸⁸ Legend: black = carbon, red = oxygen, blue = nitrogen, and white = hydrogen.

Ma and co-workers used an intramolecular indole–enolate dehydrogenative coupling in the synthesis of (–)-communesin F (**221d**, Figure 244).²⁰² In contrast to work from the Baran group (vide supra), this reaction proceeds with I_2 as the stoichiometric oxidant in the absence of transition metals. Although the mechanistic details for this oxidative cross-coupling remain elusive, model studies suggest that oxidative cyclization occurs selectively between the C3 position of the indole and the α -carbon of an amide. The reaction efficiency depends on the pK_a of the α -proton, with nitro-substituted phenylacetamides being the best substrates. Ma used indole derivative **221a** substituted with a TBS-protected (*S*)-phenylglycinol to synthesize compound **221b**, which upon reduction of the aromatic nitro group liberated pentacyclic compound **221c** with good levels of diastereoselectivity. The chiral auxiliary tethered to the amide N induced *stereoselectivity* in the C–C bond coupling. The Ma group transformed compound **221c** to (–)-communesin F (**221d**) in 13 steps.

Extending dehydrogenative cross-coupling to the C2 alkylation of pyrroles (**222b**) was demonstrated by the Baran lab (Figure 245).^{201,203} Although pyrroles bearing electron-deficient substituents are inefficient in oxidative coupling, electron-rich pyrroles participate in efficient oxidative C–C bond formation to yield products containing highly sterically congested quaternary

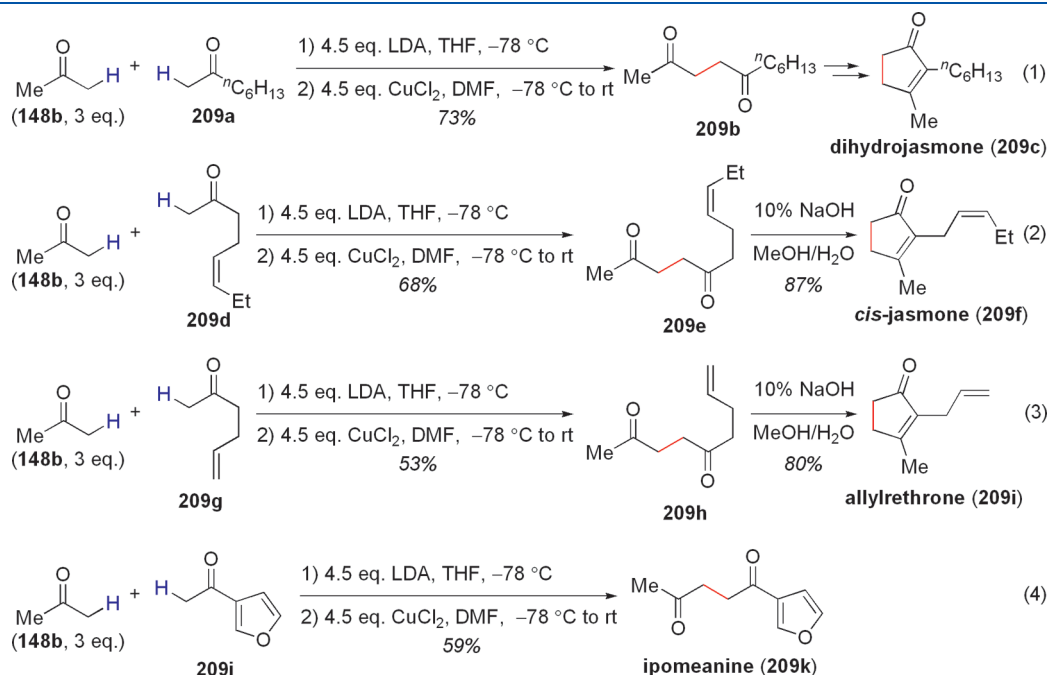


Figure 232. Formal synthesis of dihydrojasmonone (**209c**) and total syntheses of *cis*-jasmonone (**209f**), allylrethronone (**209i**), and ipomeanine (**209k**) via oxidative ketone dienolate cross-coupling.¹⁹⁰

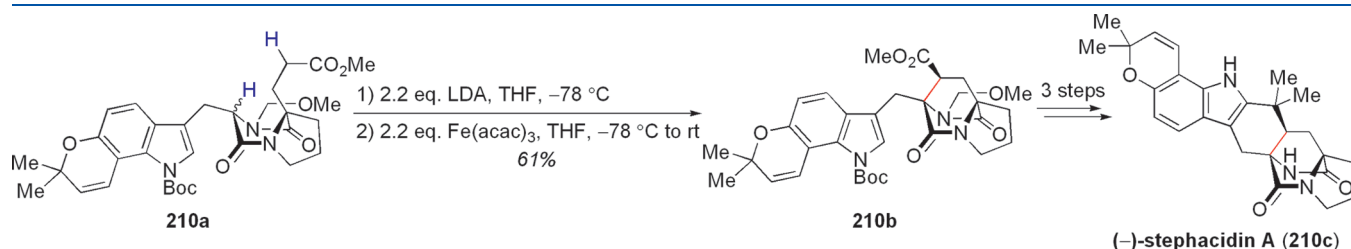


Figure 233. Total synthesis of (–)-stephacidin A (**210c**) via oxidative ester–amide dienolate cross-coupling.^{192–194}

carbons. Baran used this approach in his synthesis of (*S*)-ketorolac (**223c**) with a ferrocenium hexafluorophosphate oxidant (Figure 246). As in the case of indole–enolate heterocouplings and enolate cross-couplings, Baran proposes a radical mechanism that involves an outer-sphere single-electron transfer process from the Fe center.

5.4. Functionalization of Simple Alkanes

Benzylic radical formation can provide an alternative route for oxidative C–C cross-coupling (see section 2.4 for benzylic cation formation). In 2008, Powell and co-workers demonstrated that C–H bonds adjacent to aromatic rings undergo dehydrogenative alkylation with activated methylene compounds (**224b**) under copper catalysis in the presence of a *t*-BuOOBz oxidant (Figure 247).²⁰⁴ In this reaction, bathophenanthroline (BP) was the ligand of choice. A primary intramolecular kinetic isotope effect was observed for the diphenylmethane partner ($k_H/k_D = 1.6$) (Figure 248). Because 1-phenylethyl benzoate undergoes smooth conversion

to the desired product under the reaction conditions, the authors propose a mechanism involving two distinct steps: (1) C–H bond oxygenation, followed by (2) nucleophilic substitution (Figure 249).

In contrast to transition metal-catalyzed C–H activation and ion formation, radicals derived from simple unfunctionalized alkanes can undergo selective oxidative C–C bond formation. Zhang and Li reported an Fe-catalyzed alkylation of activated methylenes (**227a**) using simple cycloalkanes (**227b**) as the coupling partners in the presence of di-*tert*-butylperoxide

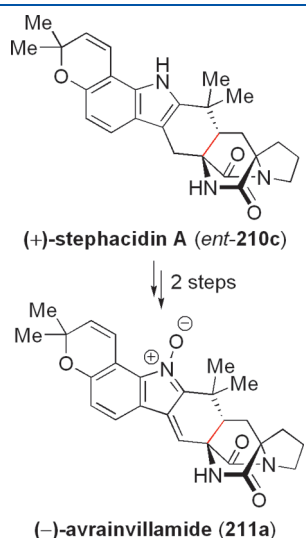


Figure 234. Total synthesis of (–)-avrainvillamide (**211a**) via oxidative ester–amide dienolate cross-coupling.^{193,194}

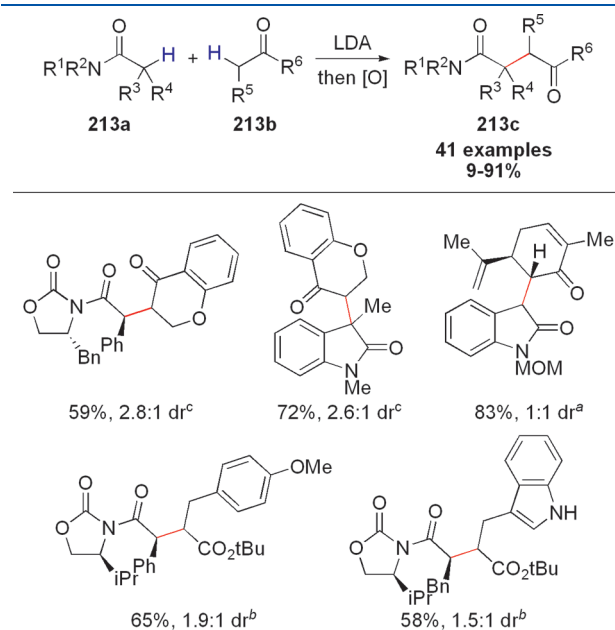


Figure 236. Oxidative intermolecular ester–amide dienolate cross-coupling.^{198,199}

^a2.1 equiv LDA, THF, –78 °C to rt, then 2.0 equiv Fe(*t*-BuCOCHMe)₃.

^b3 equiv LDA, 5 equiv LiCl, toluene, –78 °C to rt, then 2.75 equiv Cu(2-EH)₂ with 1.75 equiv **213b**.

^c2.1 equiv LDA, THF, –78 °C to rt, then 2.0 equiv Fe(acac)₃.

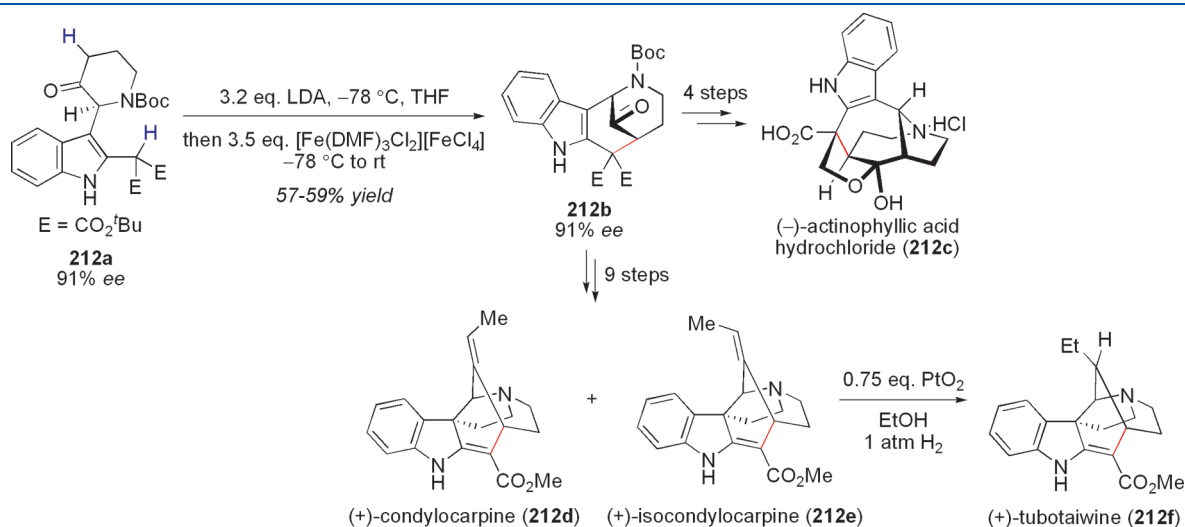


Figure 235. Total syntheses of (–)-actinophyllic acid (**212c**), (+)-condylocarpine (**212d**), (+)-isocondylocarpine (**212e**), and (+)-tubotaiwine (**212f**) via oxidative ketone–ester dienolate cross-coupling.¹⁹⁵

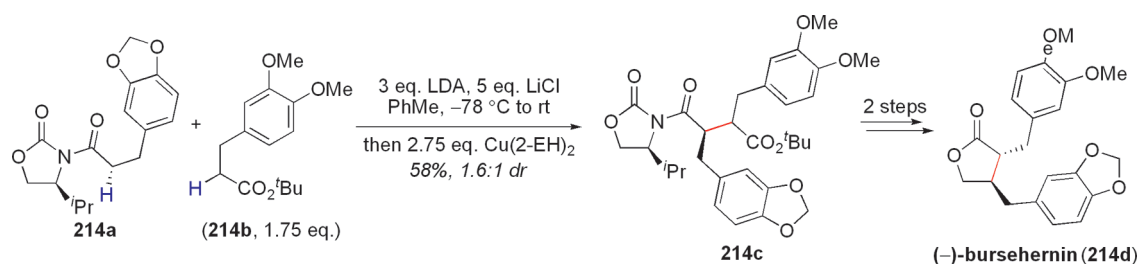


Figure 237. Total syntheses of (–)-burschernin (**214d**) via oxidative intermolecular ester–amide dienolate cross-coupling.^{198,199}

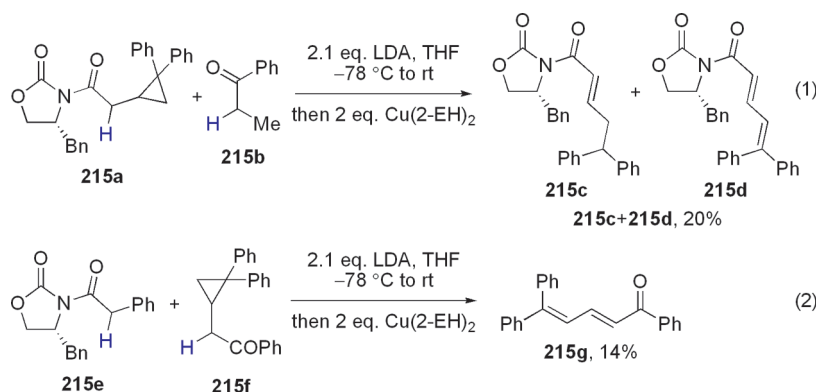


Figure 238. Radical probe experiments for oxidative intermolecular ester–amide dienolate cross-coupling.^{198,199}

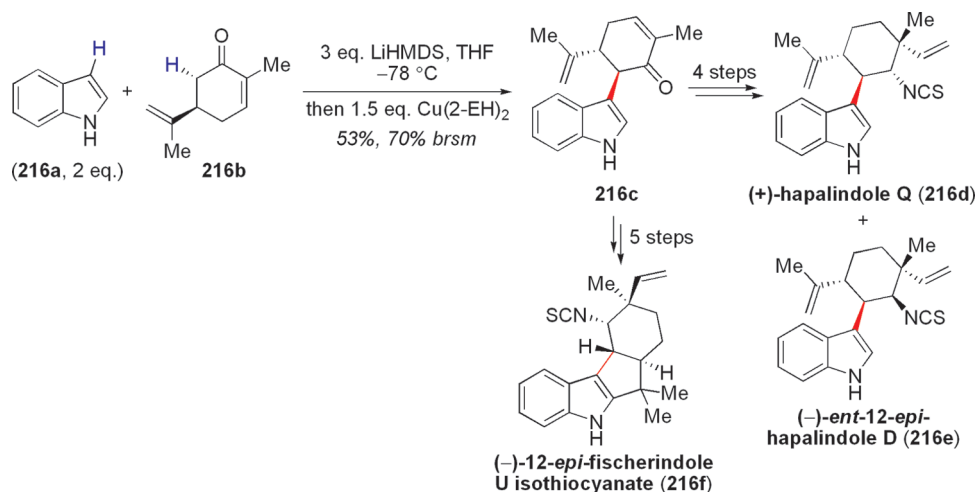


Figure 239. Total syntheses of (+)-hapalindole Q (**216d**), (–)-*ent*-12-*epi*-hapalindole D (**216e**), and (–)-12-*epi*-fischerindole U isothiocyanate (**216f**) via oxidative indole–enolate cross-coupling.^{199–201}

(Figure 250).²⁰⁵ Of the metal salts screened (e.g., FeBr_2 , FeCl_3 , $\text{FeCl}_2 \cdot x\text{H}_2\text{O}$, $\text{Fe}(\text{NO}_3)_3 \cdot 9\text{H}_2\text{O}$, $\text{Fe}(\text{acac})_3$, $\text{CuCl} \cdot 5\text{H}_2\text{O}$, $\text{Cu}(\text{OAc})_2$, $\text{CuSO}_4 \cdot 5\text{H}_2\text{O}$, CuCl_2), FeCl_2 is optimal. Presumably, the reaction involves the combination of an $\text{Fe}(\text{III})$ enolate (**228b**) with an unstabilized alkyl radical (**228c**, Figure 251).

In another study, Li and co-workers developed an oxidative cross-coupling between arenes bearing directing groups (**229a**) and cycloalkanes (**229b**, Figure 252).²⁰⁶ Using $[\text{Ru}(p\text{-cymene})\text{Cl}_2]_2$ as the catalyst and di-*tert*-butylperoxide as the oxidant, a number of 2-phenylpyridine derivatives (**229a**) can undergo *mono*- and *dialkyl*ation with unfunctionalized cyclic alkanes (**229b**). Functional groups such as ethers and esters are well accommodated in this dehydro-

genative C–C bond formation. Selectivities for *monoalkylation* over *dialkyl*ation are typically higher if the aryl ring of **229a** is substituted at either the *meta* or *para* positions. The proposed mechanism involves directed sp^2 C–H bond activation (i.e., cycloruthenation), followed by sp^3 C–H bond activation of the cyclic alkane (**229b**) in the presence of di-*tert*-butylperoxide. The resulting alkylaryl ruthenium complex (**230c**) undergoes reductive elimination to liberate the product (**229c**, Figure 253).

An alternative Cu-mediated intramolecular oxidative C–C bond formation between an enolate C–H bond and an aromatic C–H bond via radical intermediates was independently described by Jia and Kündig²⁰⁷ and Taylor and co-workers²⁰⁸ (Figures 254 and 255, respectively). The Kündig group found

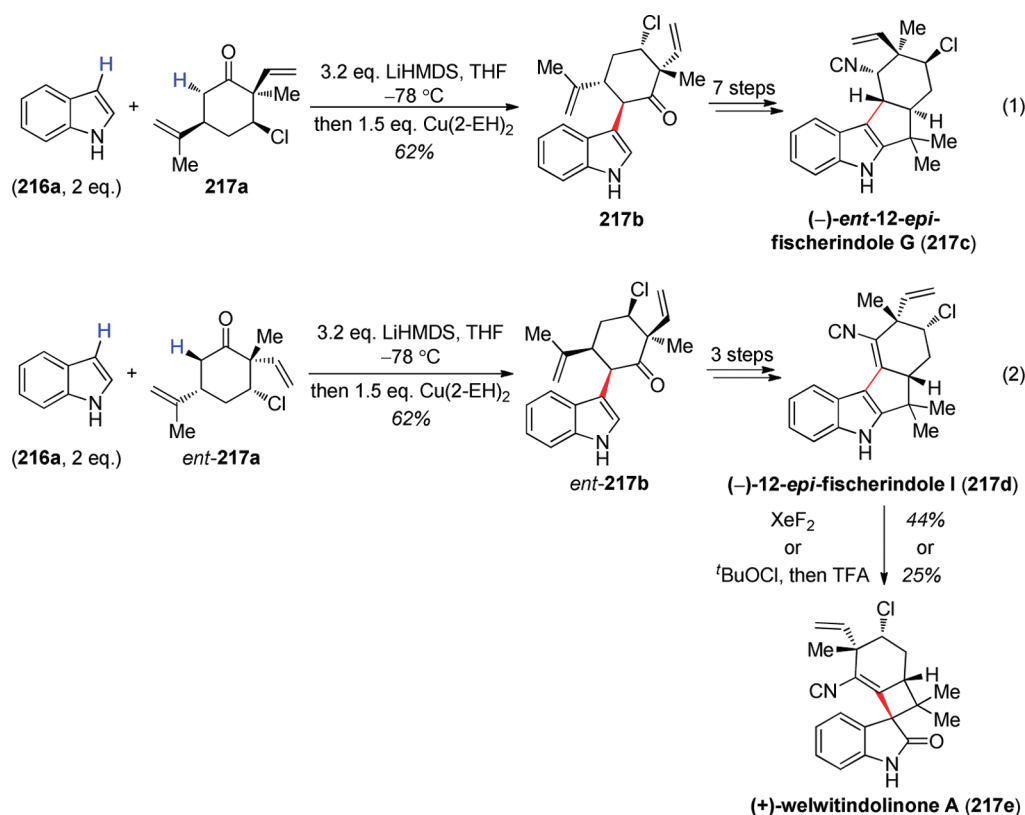


Figure 240. Total syntheses of (-)-ent-12-epi-fischerindole G (217c), (-)-12-epi-fischerindole I (217d), and (+)-welwitindolinone A (217e) via oxidative indole-enolate cross-coupling.^{199–201}

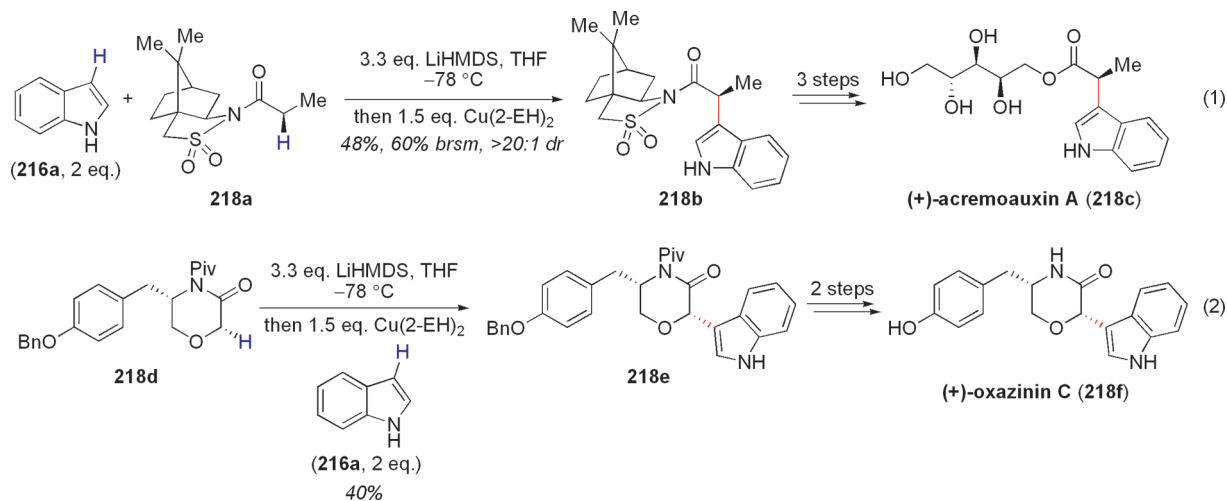


Figure 241. Total syntheses of (+)-acremauxin A (218c) and (+)-oxazin C (218f) via oxidative indole-enolate cross-coupling.²⁰¹

that oxidants including inorganic salts (e.g., CuBr_2 , $\text{Cu}(\text{OTf})_2$, Ag_2O , and $\text{Mn}(\text{OAc})_3$) and organic reagents (e.g., benzoquinone) could be used, although CAN and $\text{K}_2\text{S}_2\text{O}_8$ were ineffective (Figure 254).²⁰⁷ In Taylor's system, the presence of an electron-withdrawing group adjacent to the amide carbonyl group was crucial and provided a synthetic handle for further manipulations, particularly for oxindole synthesis via decarboxylation (Figure 255).²⁰⁸ To probe the mechanism, the Taylor group prepared a substrate bearing a cyclopropane α to the amide (233a) and subjected this compound to the copper salt.

Because the authors observed ring-opening under the reaction conditions (Figure 256), they favor an open-shell pathway (Figure 257).

Taylor has extended this cross-coupling methodology to a catalytic variant using air as the terminal oxidant (Figure 258).²⁰⁹ The pH of the reaction mixture is independent of reaction conversion, which suggests that dehydrogenation liberates H_2O instead of H^+ . Using this approach, a formal synthesis of (\pm)-horsfiline (236c) was achieved (Figure 259). Taylor and co-workers favor a mechanism

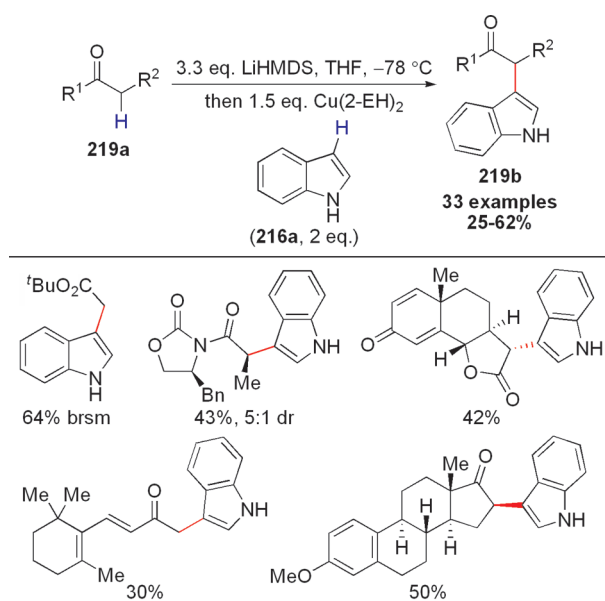


Figure 242. Oxidative indole-enolate cross-coupling.^{199–201}

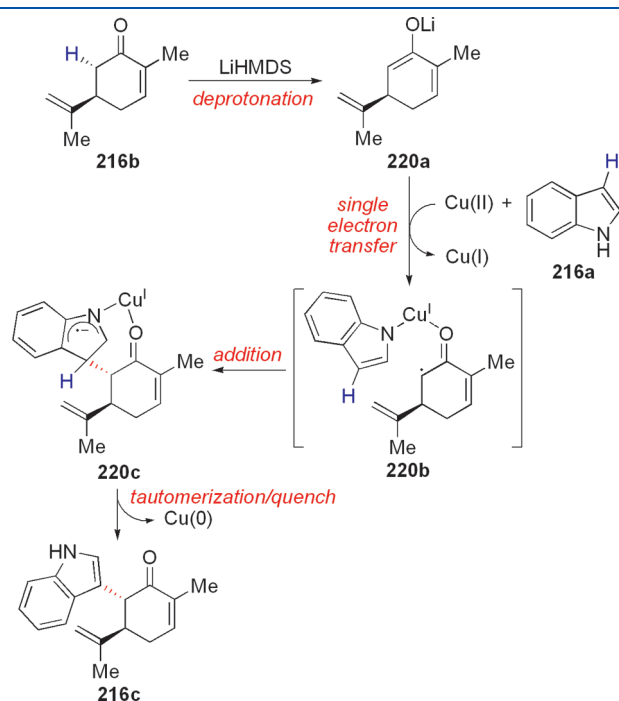


Figure 243. Proposed mechanism for oxidative indole-(*R*)-carvone cross-coupling.²⁰¹

analogous to the corresponding stoichiometric C–C coupling (vide supra).

6. ENZYME-CATALYZED OXIDATIVE COUPLING

Biological dehydrogenative C–C bond-forming reactions primarily involve catalysis promoted by cytochrome P450 (CYP) enzymes²¹⁰ in the presence of O_2 as the terminal oxidant. Perhaps the most common class of oxidative couplings in nature are those involved in the synthesis of secondary metabolites containing the bisphenol functionality,¹⁶⁴ particularly those involving tyrosine residues. These enzymatic C–C couplings occur via the intermediacy of radicals (see section 5). Typically, heme-dependent phenolic couplings in natural product biosynthesis involve a cytochrome P450 monooxygenase, a class of enzymes that contain a porphyrin ligated to an iron center. During *cross*-coupling, oxidation of either the iron center or the porphyrin ligand can occur. The mechanism involves several one-electron transfer steps that result in the formation of Fe(IV)oxo/porphyrin radical cation **237b**, a high-energy intermediate capable of abstracting a H atom from an otherwise unreactive C–H bond (Figure 260). The intricate details of this mechanism remain sparse and are an active topic of debate.

Phenolic coupling by tandem C–H bond oxidation is an important process in the biosynthesis of many natural products, including alkaloids (e.g., (–)-isoboldine (**238a**)²¹¹) and glycopeptides (e.g., vancomycin (**238b**)¹⁶⁴) (Figure 261). In addition, tyrosine residues are known to undergo dehydrogenative coupling reactions as a response to oxidative stress (e.g., ionizing and ultraviolet radiation) resulting from reactive oxygen species (ROS),²¹² including hydroxyl radicals and superoxide radical anions, and are particularly important in cross-linking and repair

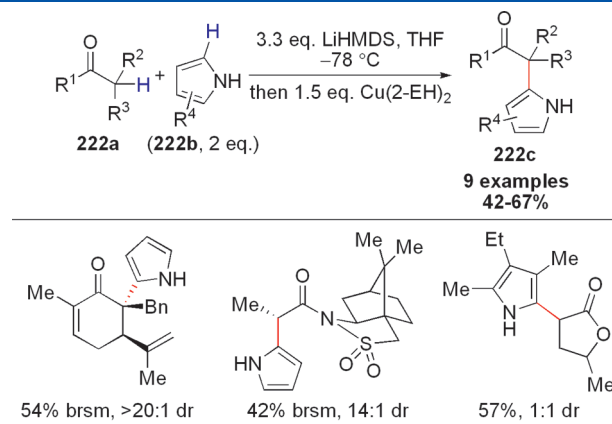


Figure 245. Oxidative pyrrole-enolate cross-coupling.^{201,203}

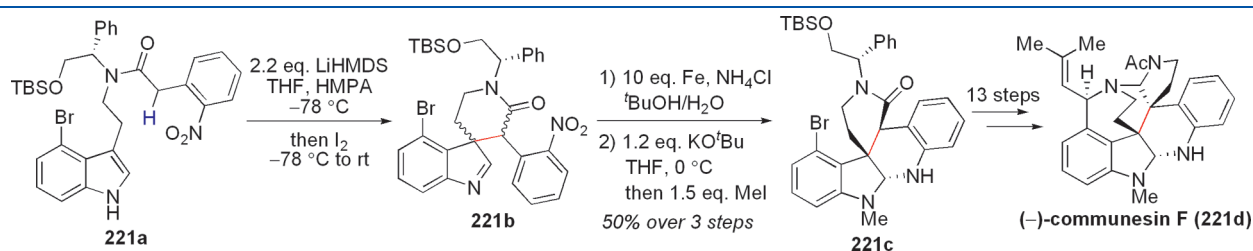


Figure 244. Total synthesis of (–)-communesin F via intramolecular oxidative amide-indole cross-coupling.²⁰²

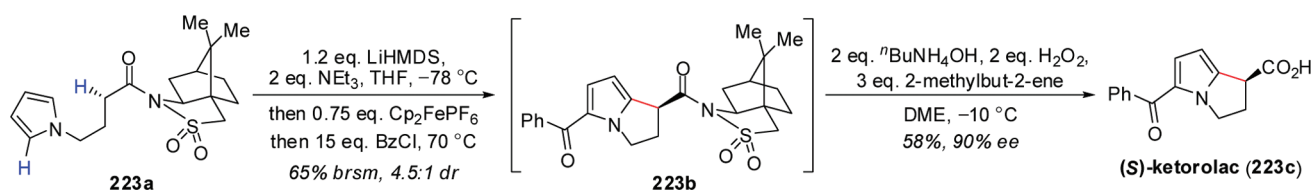


Figure 246. Total synthesis of (S)-ketorolac (223c) via intramolecular oxidative pyrrole-enolate cross-coupling.^{201,203}

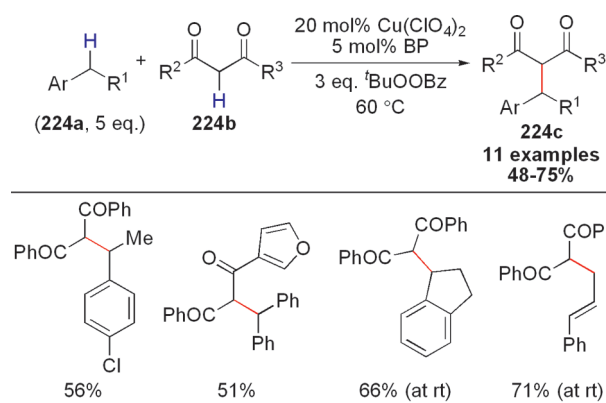


Figure 247. Cu-catalyzed benzylation of activated methylenes with simple benzyls.²⁰⁴

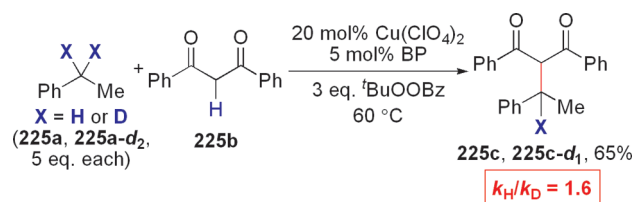


Figure 248. Kinetic isotope effect study for Cu-catalyzed benzylation of activated methylenes with simple benzyls.²⁰⁴

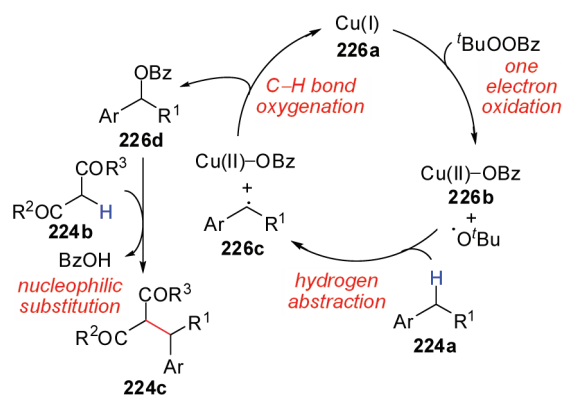


Figure 249. Proposed mechanism for Cu-catalyzed benzylation of activated methylenes with simple benzyls.²⁰⁴

processes.²¹³ For instance, tyrosine is known to trimerize to yield unsymmetrical products, including pulcherosine (238c)²¹⁴ and isotrityrosine (238d).²¹⁵ A similar type of oligomerization has been reported for ferulic acid, yielding 4-O-8',5',5''-dehydrotriferulic acid (238e), a metabolite isolated from maize bran.²¹⁶ Oxidative cross-linking between phenolic C-H bonds and nucleotides have also been observed, exemplified by model

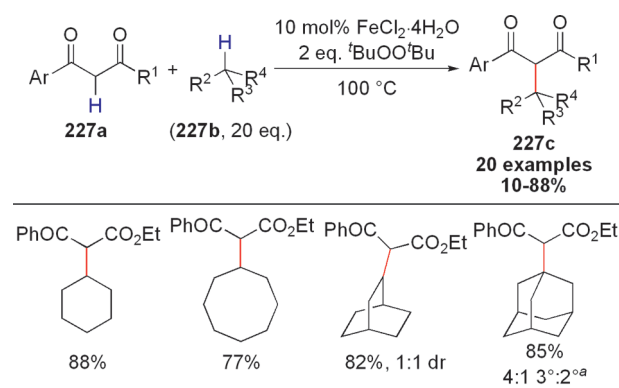


Figure 250. Fe-catalyzed alkylation of activated methylenes with simple alkanes.²⁰⁵

^aUsing benzene as the solvent.

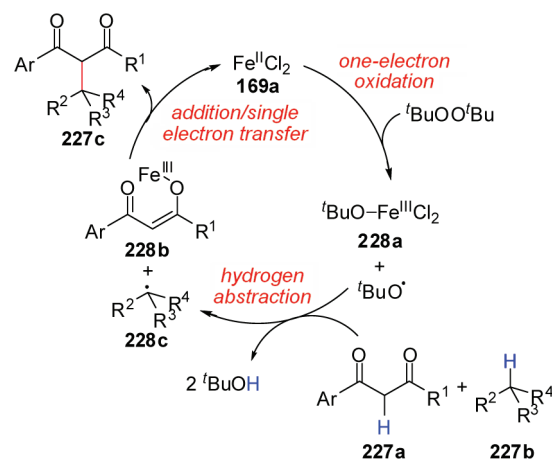


Figure 251. Proposed mechanism for Fe-catalyzed alkylation of activated methylenes with simple alkanes.²⁰⁵

compounds 238f-h shown in Figure 261. DFT calculations suggest radical pathways for cross-coupling reactions of tyrosine residues.²¹⁷

Other than bisphenols, certain pyrrole alkaloids are biosynthesized by dehydrogenative C-C bond formation. For example, oxidative cyclization is proposed to be a key step in the enzymatic synthesis of the prodiginines, a class of pyrrole alkaloids exhibiting antibacterial, antifungal, and anticancer properties (Figure 262).²¹⁸ In addition, butyl-*meta*-cycloheptylprodiginine (or streptorubin B, 239c) is thought to arise from a formal two-electron oxidation via site-selective C-H activation of undecylprodiginine (240a, Figure 263).²¹⁹ An enzyme can achieve this large-size ring-closure with efficiency and selectivity that is unrivaled by synthetic systems.

The Challis group studied the prodiginosine biosynthesis gene cluster of *Streptomyces coelicolor* A3(2) and discovered an enzyme

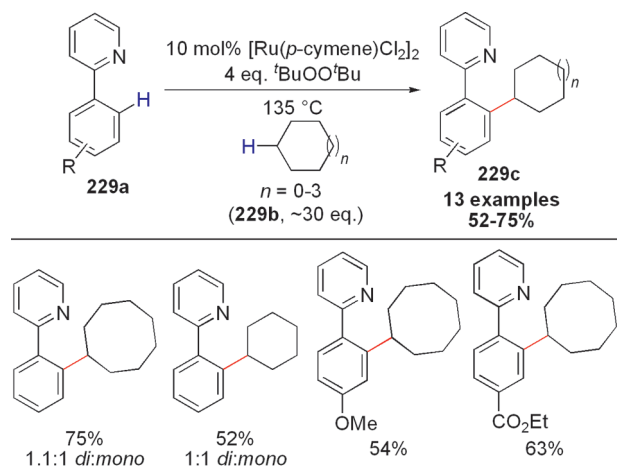


Figure 252. Ru-catalyzed *ortho*-alkylation of 2-phenylpyridines with cycloalkanes.²⁰⁶

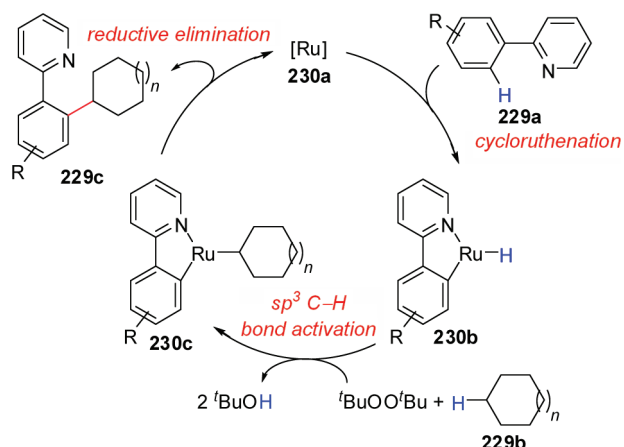


Figure 253. Proposed mechanism for Ru-catalyzed *ortho*-alkylation of 2-phenylpyridines with cycloalkanes.²⁰⁶

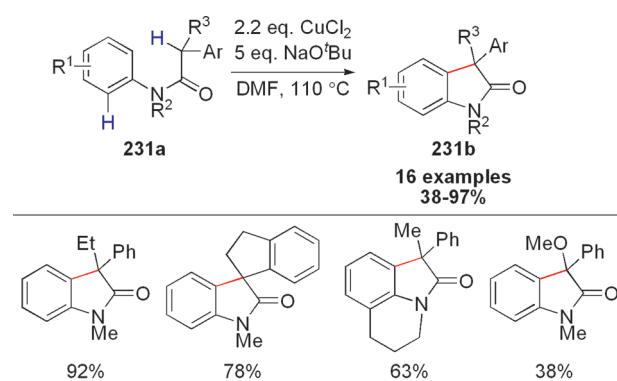


Figure 254. Kündig's Cu-mediated synthesis of oxindoles from anilides.²⁰⁷

redG that may effect the oxidative cyclization of undecylprodigine (**240a**) to butyl-*meta*-cycloheptylprodiginine (**239c**).²¹⁹ The mechanism of this transformation remains unknown and *RedG* has not been fully characterized, but evidence suggests that the active enzyme is a nonheme iron-dependent dioxygenase²¹⁰ (e.g., Rieske dioxygenase). Dioxygenases are typically exemplified

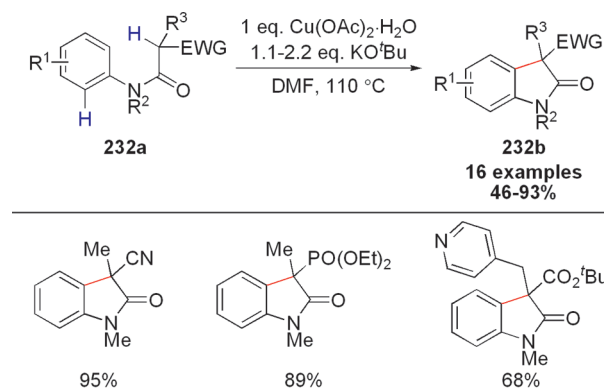


Figure 255. Taylor's Cu-mediated synthesis of oxindoles from anilides.²⁰⁸

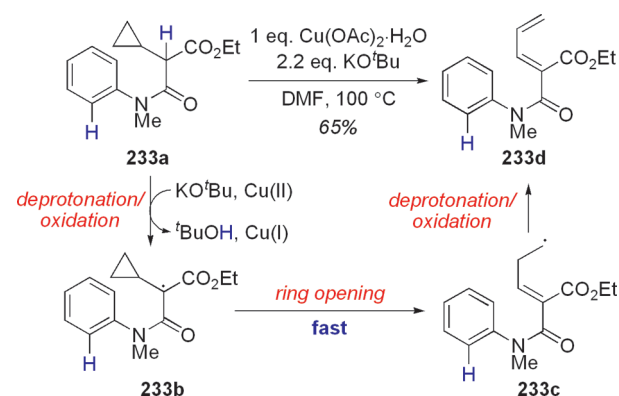


Figure 256. Radical clock experiment for Cu-mediated synthesis of oxindoles from anilides.²⁰⁸

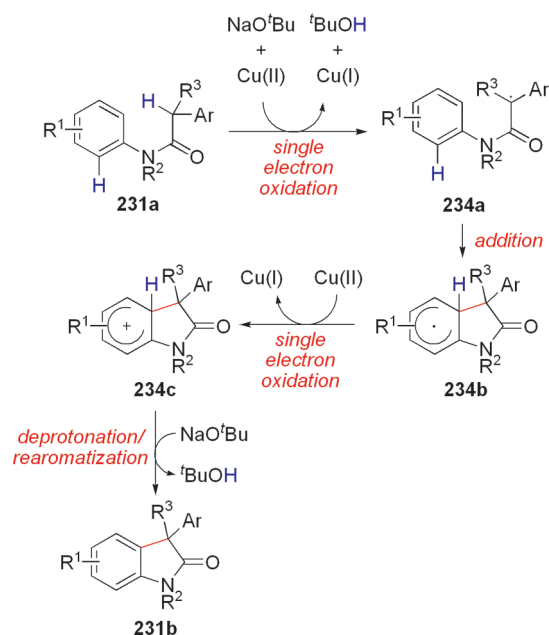


Figure 257. Proposed mechanism for Cu-mediated synthesis of oxindoles from anilides.²⁰⁸

by Fe_2S_2 -clusters (i.e., a ferredoxin) and universally conserved His and Asp Fe-binding residues and act via radical pathways. On the basis of the known chemistry of this class of enzymes, the

authors suggest that *RedG* could interact directly with molecular O_2 to achieve the regioselective removal of a H atom²¹⁹ via either radical or cationic intermediates. The pyrrole ring then intercepts the alkyl radical/cation, furnishing the new C–C bond. Site-selective C–H functionalization is controlled by the active site of the enzyme.

7. OTHER MECHANISMS FOR CROSS-COUPLING

7.1. Indole Synthesis by Intramolecular Coupling

Indoles are biologically relevant motifs, and many methods for making indoles have been pursued,²²⁰ from Fischer's synthesis (using arylhydrazines and aldehydes or ketones)²²¹ to Larock's catalytic reaction (with *ortho*-iodoanilines and disubstituted alkynes).²²² Glorius and co-workers have invented a novel indole synthesis by Pd-catalyzed intramolecular oxidative dehydrogenation of *N*-arylenamines (Figure 264).²²³ In this reaction, C–C bond formation occurs between alkenyl and aryl sp^2 C–H bonds. The optimal oxidant is $Cu(OAc)_2$; Ag_2CO_3 promotes the coupling in dramatically reduces yields. The addition of ligands (e.g., PPh_3) reduces catalytic efficiencies, although other additives, including NaCl, have minimal impact. Glorius' reaction tolerates electron-rich, electron-neutral, and electron-poor *N*-arylenamines and a wide range of functional groups, such as ketones, esters, and nitriles. The Pd-catalyzed synthesis of methyl 2-methyl-1*H*-indole-3-carboxylate (**242d**) can be accomplished in a one-pot, two-step procedure from aniline and methyl acetoacetate (Figure 265). A competition study revealed that electron-rich *N*-arylenamines undergo cyclization at faster rates than electron-deficient *N*-arylenamines. Additionally, a kinetic isotope effect investigation demonstrated that *ortho*-C–H bond cleavage is involved in the rate-limiting step (k_H/k_D (prod) = 4.6, Figure 266). Thus, Glorius proposes a mechanism involving

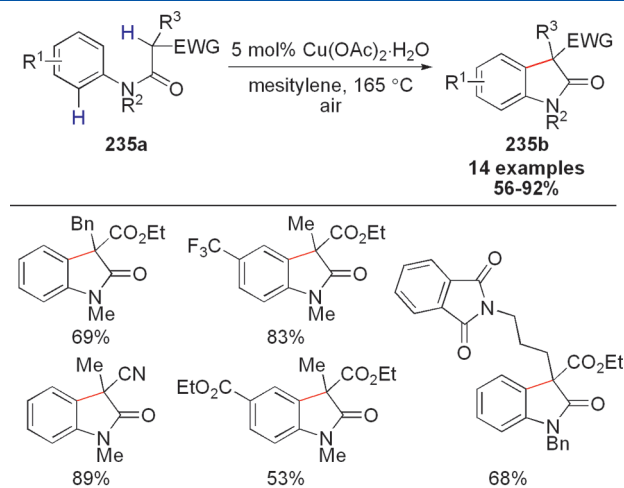


Figure 258. Cu-catalyzed synthesis of oxindoles from anilides.²⁰⁹

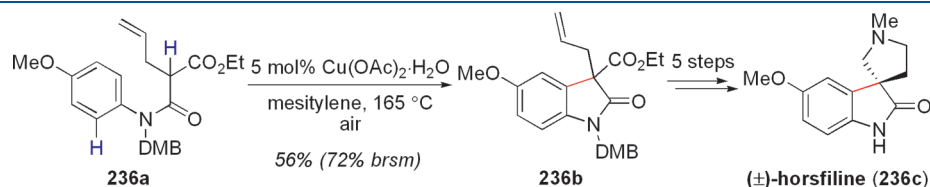


Figure 259. Formal synthesis of (±)-horsfiline (**236c**) via Cu-catalyzed synthesis of oxindoles from anilides.²⁰⁹

alkene palladation followed by arene functionalization via σ -bond metathesis or base-assisted deprotonation (Figure 267). In contrast to Heck-type processes (see section 2), this pathway does not include directing-group-promoted cyclopalladation of the arene as the first step.

A Cu-catalyzed variant was subsequently described by Cacchi and co-workers (Figure 268).²²⁴ In this reaction, an unprotected N–H indole (**245b**) can be prepared via oxidative cyclization of *N*-arylenamines (**245a**). Surprisingly, this reaction does not require O_2 to proceed—the reaction can be conducted under completely anaerobic conditions without loss in reaction efficiencies. In a study using D-labeled anilide starting material, Cacchi observed no significant kinetic isotope effect (**246a**, Figure 269). Thus, the proposed mechanism involves base-assisted cupration of enaminone **245a**, followed by intramolecular nucleophilic addition by the adjacent arene ring. Isomerization and rearomatization liberate alkenylaryl copper intermediate **247d**, which then undergoes reductive elimination. The active

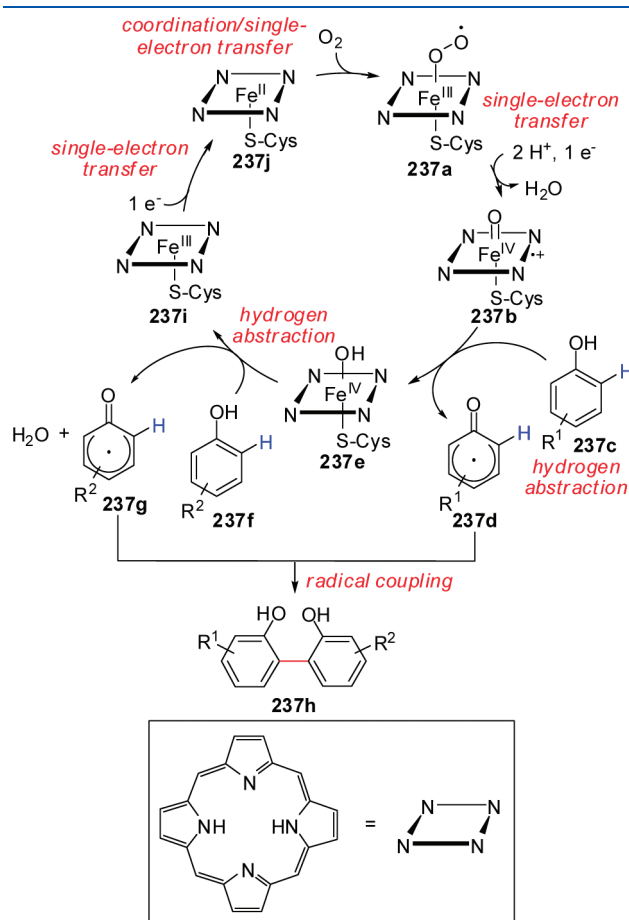


Figure 260. Proposed mechanism for enzyme-mediated oxidative phenolic coupling.²¹⁰

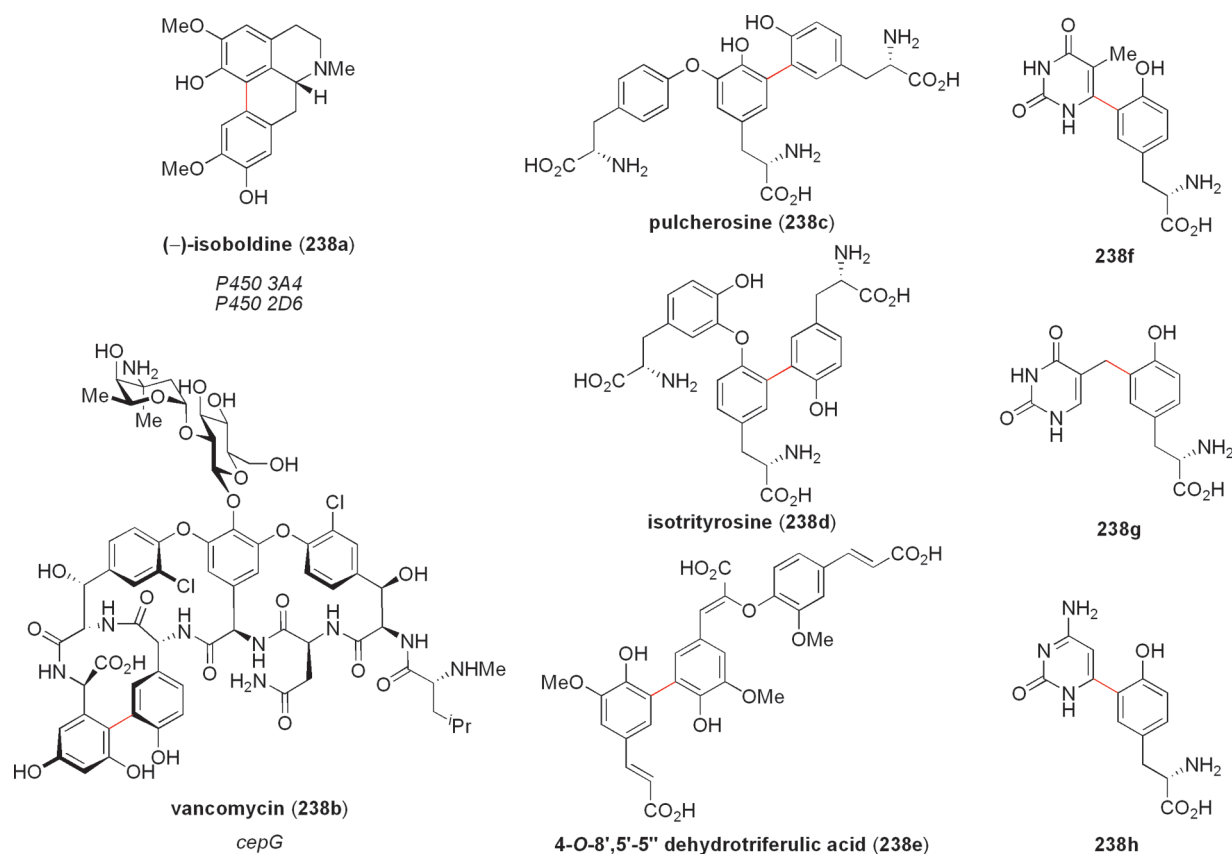


Figure 261. Representative natural products synthesized in nature via oxidative phenolic coupling.

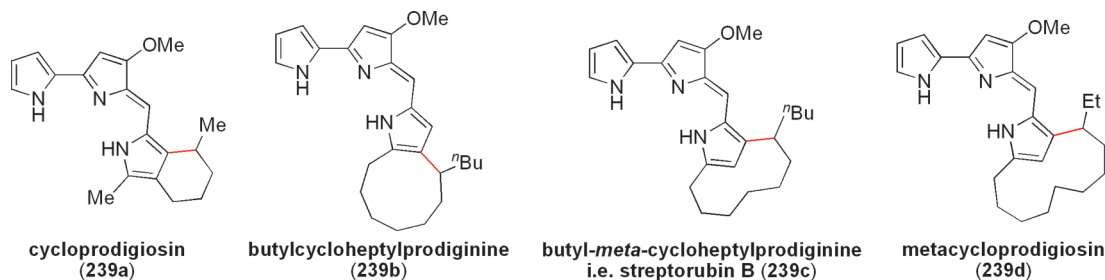


Figure 262. Representative members of the prodiginine family with macrocycles.²¹⁸

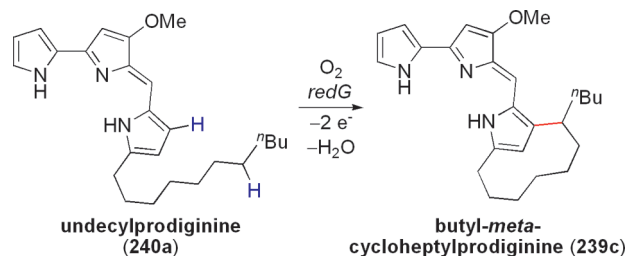


Figure 263. Proposed biosynthesis of butyl-*meta*-cycloheptylprodiginine (239c).²¹⁹

catalyst **247a** is generated by loss of H₂ (Figure 270). This reaction is a dehydrogenative C–C bond formation because H₂ is generated as the only byproduct.

Liang and co-workers discovered a complementary Fe-catalyzed dehydrogenative cyclization of *N*-arylenamines (**248a**,

Figure 271).²²⁵ In the presence of catalytic FeCl₃ (>99.99% purity) and stoichiometric Cu(OAc)₂·CuCl₂, indole formation occurs with moderate to good yields. This strategy, in accordance with Cacchi's work (vide supra), also tolerates functionalities traditionally reactive under Pd catalysis (e.g., aryl bromides and aryl iodides). Although the mechanistic details have not been elucidated, the authors propose intramolecular nucleophilic addition of the electron-rich aromatic ring to the pendant electron-deficient olefin coordinated to FeCl₃ (Figure 272). This step is a formal 5-*endo*-trig cyclization. The Fe catalyst is thought to act as a Lewis acid to promote cyclization by coordination to the Lewis basic ester; the copper oxidant, on the other hand, is believed to form a covalent linkage with the substrate by deprotonating the N–H bond of the enamine. On the basis of this mechanism, Liang's cyclization can be classified as an ionic-type oxidative dehydrogenation.

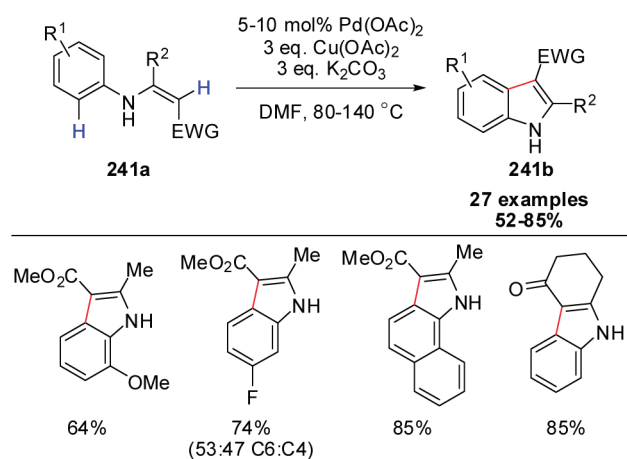


Figure 264. Pd-catalyzed indole synthesis from *N*-arylenamines.²²³

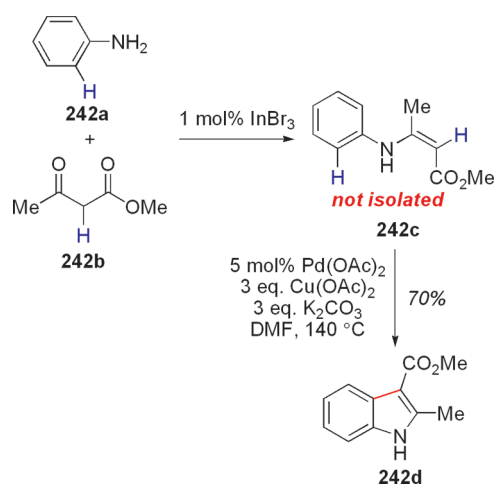


Figure 265. One-pot, two-step synthesis of methyl 2-methyl-1H-indole-3-carboxylate by Pd catalysis.²²³

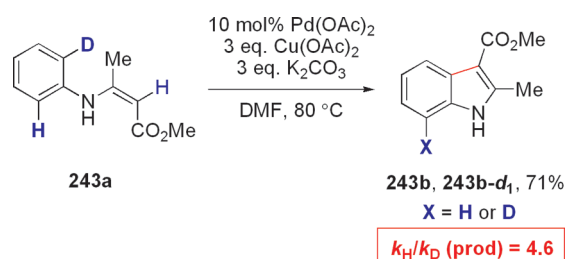


Figure 266. Kinetic isotope effect study for Pd-catalyzed indole synthesis from *N*-arylenamines.²²³

In a related account, Zhao and co-workers were able to completely eliminate the need for transition metals for oxidative indole formation from *N*-arylenamines.²²⁶ Using $\text{PhI}(\text{OAc})_2$ as the sacrificial oxidant, dehydrogenative C–C coupling affords the desired cyclic products **250b** in moderate to good yields (Figure 273). PIFA was found to be a suitable surrogate for iodobenzene diacetate, but cryogenic conditions (–78 °C) were required. Zhao's transformation tolerates nitriles, nitroaromatics, and aryl halides. This reaction resembles Liang's Fe-catalyzed coupling (vide supra), because $\text{PhI}(\text{OAc})_2$ can form a covalent

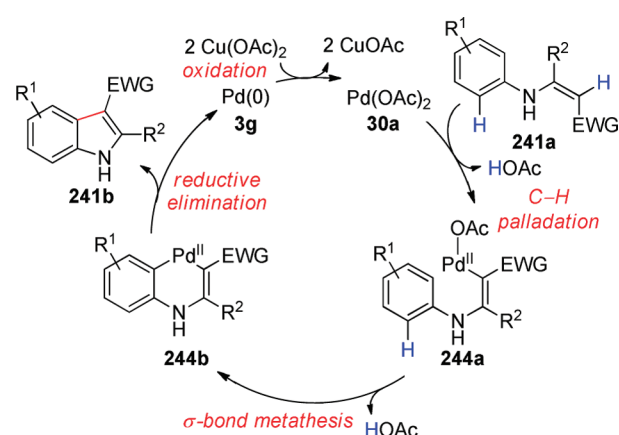


Figure 267. Proposed mechanism for Pd-catalyzed indole synthesis from *N*-arylenamines.²²³

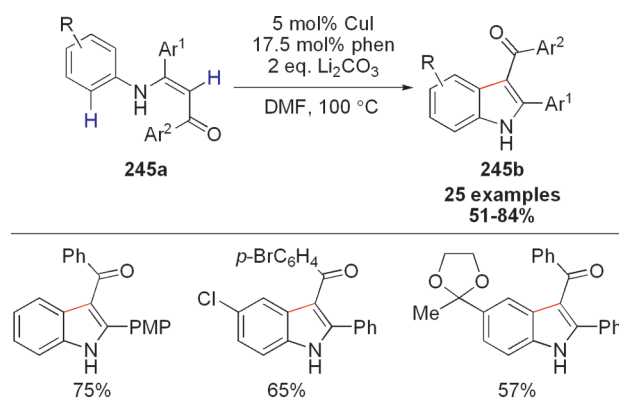


Figure 268. Cu-catalyzed indole synthesis from *N*-arylenamines.²²⁴

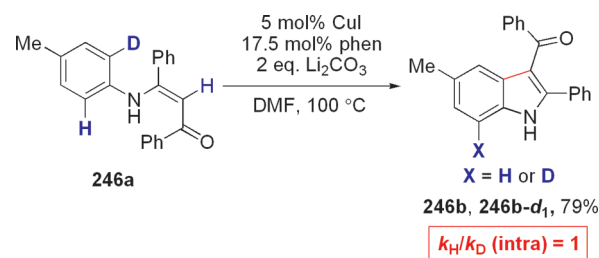


Figure 269. Kinetic isotope effect study for Cu-catalyzed indole synthesis from *N*-arylenamines.²²⁴

complex with substrate **250a**, followed by intramolecular $\text{S}_{\text{E}}\text{Ar}$,⁴⁶ and subsequent rearomatization by deprotonation and tautomerization (Figure 274). As such, Zhao's $\text{PhI}(\text{OAc})_2$ -mediated intramolecular coupling can also be considered a dehydrogenative reaction involving ionic intermediates (see section 4).

7.2. Sonogashira-Type Cross-Coupling

On the basis of known biaryl bond formations via tandem direct arylation and oxidative alkene–alkene cross-couplings via Heck-type processes, a modern variant of the Sonogashira coupling²²⁷ using terminal alkynes bearing sp^2 -hybridized C–H bonds instead of traditional C–X bonds was described by Li and co-workers (Figure 275).²²⁸ By subjecting an *N*-protected

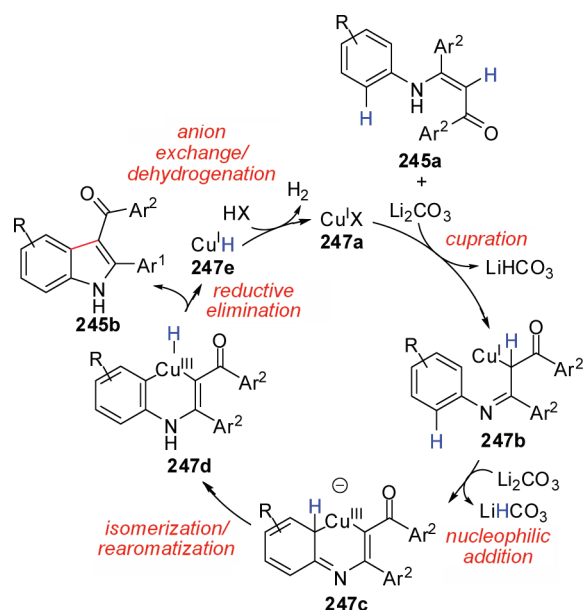


Figure 270. Proposed mechanism for Cu-catalyzed indole synthesis from *N*-arylenamines.²²⁴

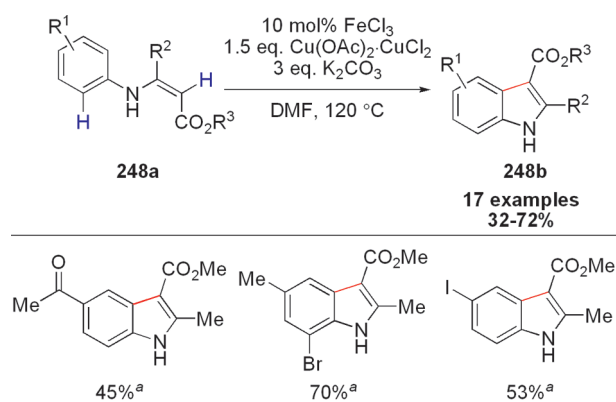


Figure 271. Fe-catalyzed indole synthesis from *N*-arylenamines.²²⁵
^a2 equiv ^tBu₄Cl was added.

indole (**252a**) to a Pd catalyst, base, and pivalic acid under aerobic conditions, oxidative C–C bond formation is possible. Aryl- and silylacetylenes are superior to alkylacetylenes in their ability to undergo cross-coupling. The authors propose a mechanism involving electrophilic palladation of the alkyne starting material (**252b**) to Pd–acetylide **253b**, followed by a second palladation of the indole coupling partner (**252a**) to afford alkynylaryl palladium intermediate **253c** (Figure 276). This complex is subject to reductive elimination that liberates product **252c**.

Intermolecular catalytic alkynylation of perfluoroarenes (**234a**) was reported by the Su group (Figure 277).²²⁹ This Cu-catalyzed transformation can accommodate many functional groups, including acetals, amines, thiophenes, and pyridines, among others. A strong base, LiO^tBu, is required and may serve to deprotonate either the alkyne (**254b**), the perfluoroarene (**254a**), or both. Adding catalytic amounts of DDQ improves reaction efficiency, possibly due to its ability to serve as a single-electron mediator during the oxidant-induced reductive elimination step. Su

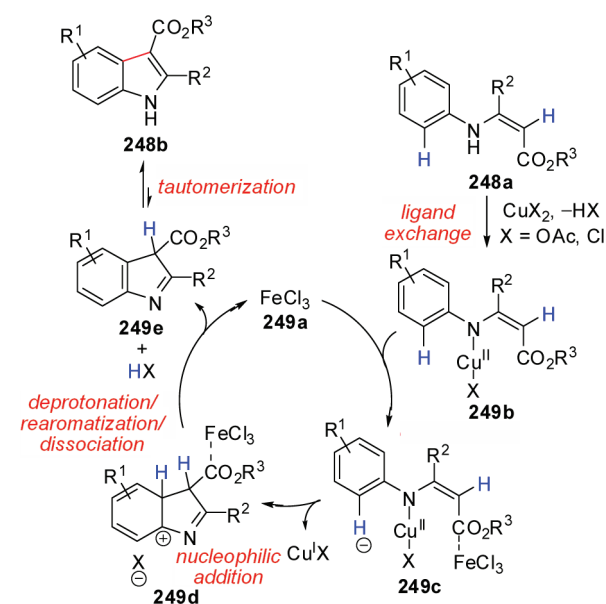


Figure 272. Proposed mechanism for Fe-catalyzed indole synthesis from *N*-arylenamines.²²⁵

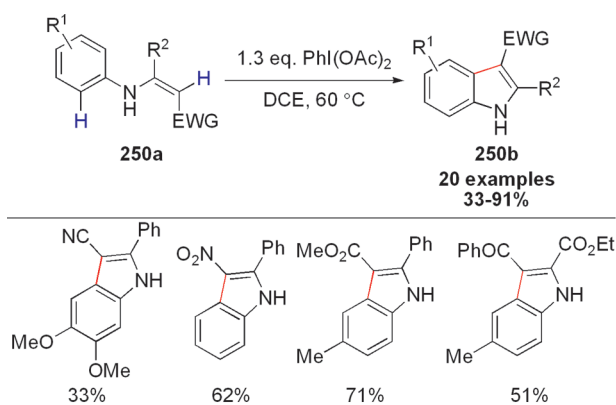


Figure 273. PhI(OAc)₂-mediated indole synthesis from *N*-arylenamines.²²⁶

proposes a mechanism involving cupric halide **255a** undergoing sequential substitution with either lithiated alkyne or perfluoroarene to generate an alkynylaryl cuprate **255c** (Figure 278). Complex **255c** undergoes reductive elimination to furnish the desired C–C bond. In a related study, Miura and co-workers also published catalytic alkynylation of perfluoroarenes using Cu(OTf)₂ instead of CuCl₂ (**256a**, Figure 279).²³⁰

In analogy to indole and perfluoroarene alkynylation, Cu-mediated and -catalyzed alkynylation of azoles (e.g., oxazoles, oxadiazoles, **257a**) has been achieved (Figure 280).²³¹ Miura's group later disclosed a variant of this transformation using Ni catalysts (i.e., NiBr₂·diglyme) and extended the substrate scope to encompass benzoxazoles and benzthiazoles as well (Figure 281).²³⁰ The mechanism of both of these transformations is believed to parallel that of perfluoroarene alkynylation (i.e., a sequential alkynylation of the catalytic Cu and Ni complexes).

de Haro and Nevado described a related and complementary Au-catalyzed oxidative C–C cross-coupling of alkynes.²³² Using Ph₃PAuCl in the presence of an PhI(OAc)₂ oxidant, catalytic

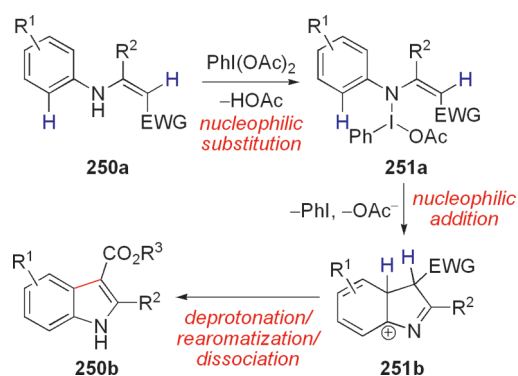


Figure 274. Proposed mechanism for $\text{PhI}(\text{OAc})_2$ -mediated indole synthesis from *N*-arylenamines.²²⁶

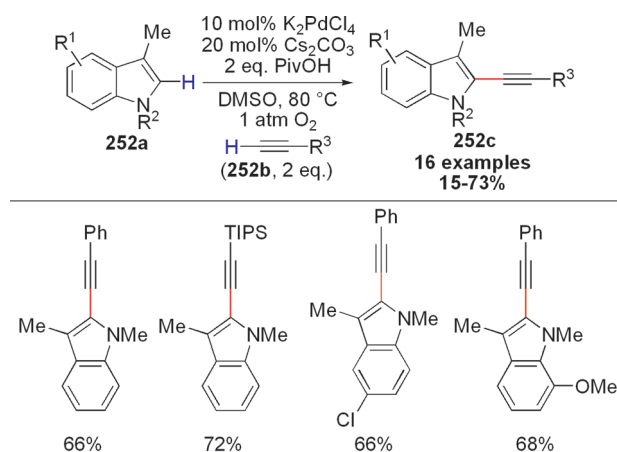


Figure 275. Pd-catalyzed C2-alkynylation of *N*-protected indoles with alkynes.²²⁸

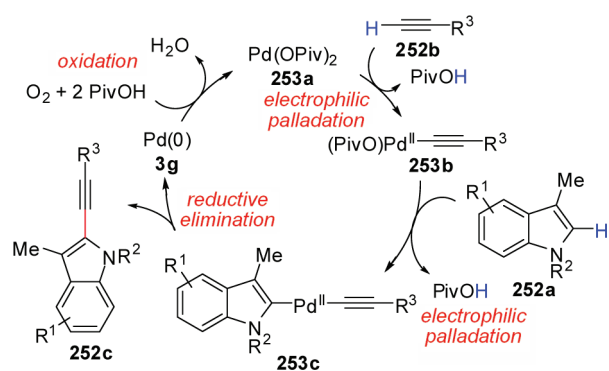


Figure 276. Proposed mechanism for Pd-catalyzed C2-alkynylation of *N*-protected indoles with alkynes.²²⁸

alkynylation of electron-rich arenes and heteroarenes (**259a**) was reported (Figure 282). The substrates chosen for alkyne coupling have a known propensity to undergo C–H bond auration in the presence of Au complexes. In particular, cationic Au complexes (e.g., $\text{Ph}_3\text{PAuNTf}_2$ and Ph_3PAuOTf) demonstrated inferior reactivity in comparison to the neutral Ph_3PAuCl salt. Other metals, including Pd(II) and Cu(I), failed to produce the desired products. $\text{PhI}(\text{OAc})_2$ is optimal and cannot be replaced with other oxidants, such as Selectfluor or $t\text{BuOOH}$. To

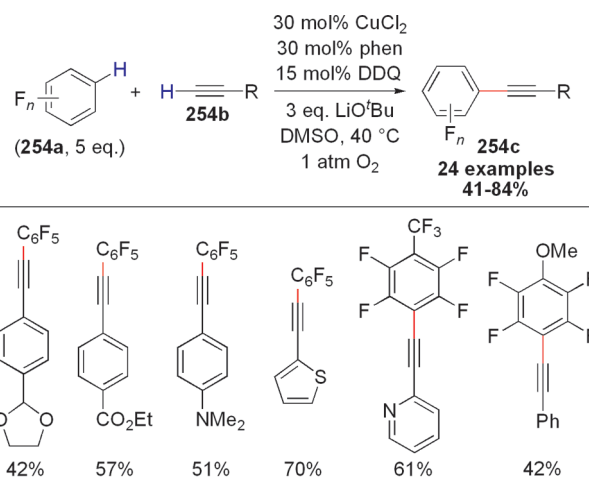


Figure 277. Cu-catalyzed alkynylation of perfluoroarenes.²²⁹

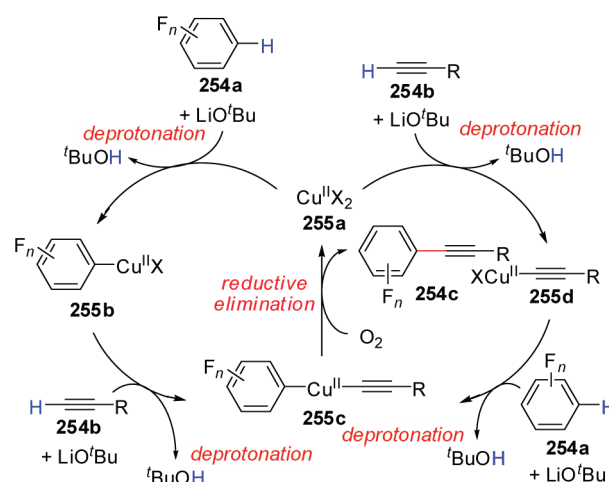


Figure 278. Proposed mechanism for Cu-catalyzed alkynylation of perfluoroarenes.²²⁹

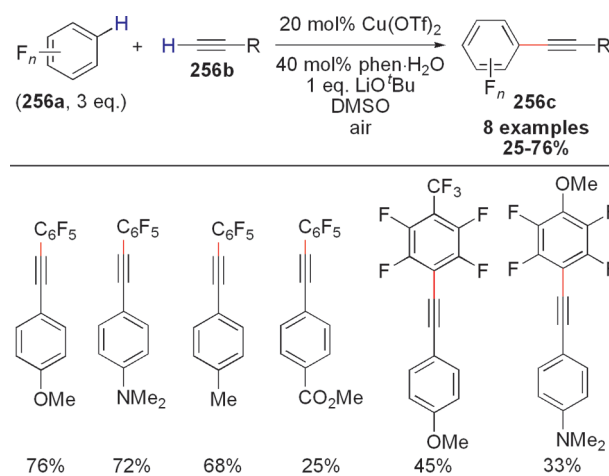


Figure 279. Cu-catalyzed alkynylation of perfluoroarenes.²³⁰

understand the mechanism, the authors confirmed the existence of Au(I)–acetylide intermediates by ^{31}P NMR spectroscopy and also conducted preliminary kinetic analysis. The reaction rate of Nevado's arene–alkyne coupling is first order in both alkyne

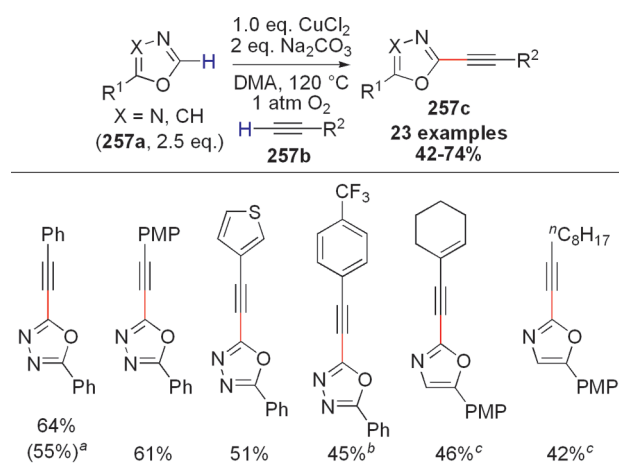


Figure 280. Cu-mediated and -catalyzed alkylation of azoles.²³¹
^a25 mol % CuCl₂, 50 mol % DMEDA, 2 equiv Na₂CO₃, DMA, 120 °C, 1 atm O₂.
^b1.5 equiv Na₂CO₃.
^c2.4 equiv Na₂CO₃, DMSO, 150 °C.

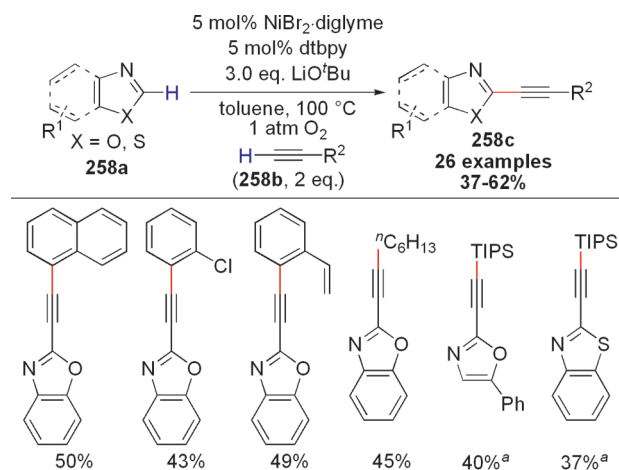


Figure 281. Ni-catalyzed alkylation of azoles.²³⁰
^aReaction conducted at 120 °C.

259b and arene 259a starting materials. Studies on deuterium-labeled analogues revealed, however, negligible kinetic isotope effects on both cross-coupling partners ($k_{\text{H}}/k_{\text{D}}$ (alkyne) = 0.92; $k_{\text{H}}/k_{\text{D}}$ (arene) = 1.15, Figure 283). Hence, two mechanisms are possible (Figure 284): (1) a PhI(OAc)₂-mediated oxidation of an Au(I)–acetylide (261b), electrophilic auration, and reductive elimination, or (2) iodination,²³³ aryl-auration, and subsequent β -elimination (although this step is unprecedented). Nevado's conditions are also applicable to *alkenes* (262a)—oxidative bond formation between an sp² and sp carbon is possible (Figure 285).²³²

Two different terminal alkynes (263a,b) can undergo oxidative cross-coupling, as described by Lei and co-workers in 2009 (Figure 286).²³⁴ This reaction is a modern variant of the Glaser coupling (i.e., homocoupling of a terminal alkyne).⁵ Lei's dehydrogenative alkyne cross-coupling requires catalytic amounts of both nickel and copper salts.²³⁴ Reaction efficiencies are good to excellent, and the system tolerates many functional groups, including free OH, basic tertiary amines, and sp² C–Br and

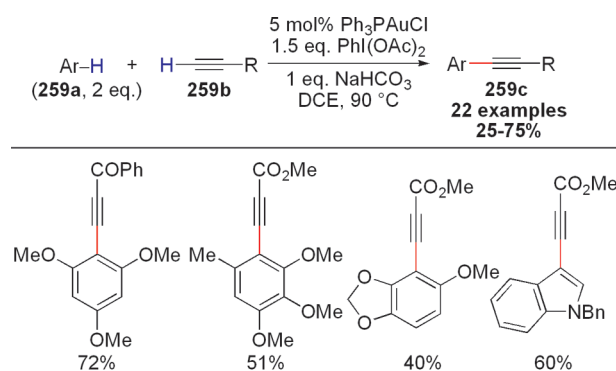


Figure 282. Au-catalyzed alkylation of electron-rich arenes and heteroarenes.²³²

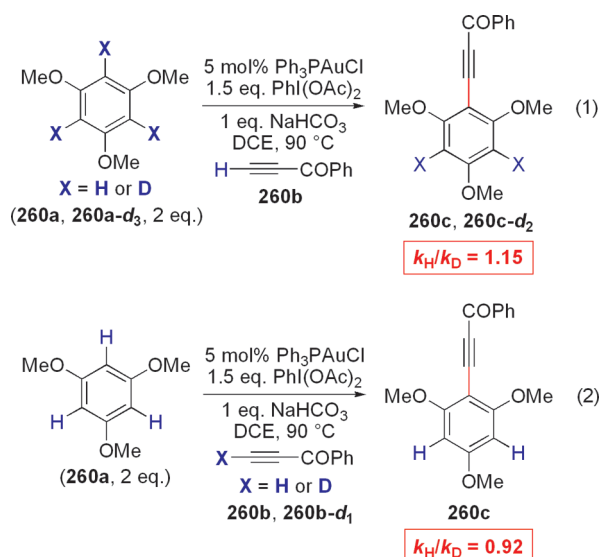


Figure 283. Kinetic isotope effect study for Au-catalyzed alkylation of electron-rich arenes and heteroarenes.²³²

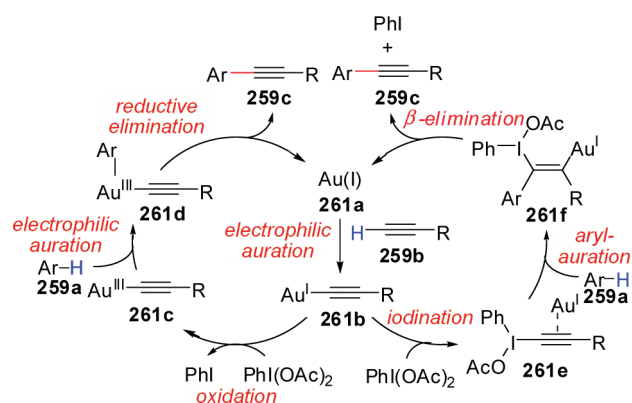


Figure 284. Proposed mechanism for Au-catalyzed alkylation of electron-rich arenes and heteroarenes.²³²

C–I bonds. The authors propose a mechanism where copper acetylides 264c and 264d are generated from the alkyne starting materials 263a and 263b, respectively, in analogy to the traditional Sonogashira reaction (Figure 287). Next, these copper acetylides (264c,d) undergo transmetalation to Ni(II), followed by subsequent reductive elimination to the 1,3-butadiyne products (263c).

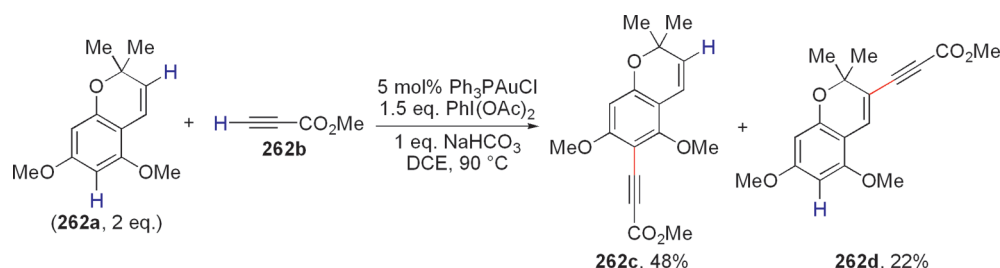


Figure 285. Au-catalyzed alkyne-alkene cross-coupling.²³²

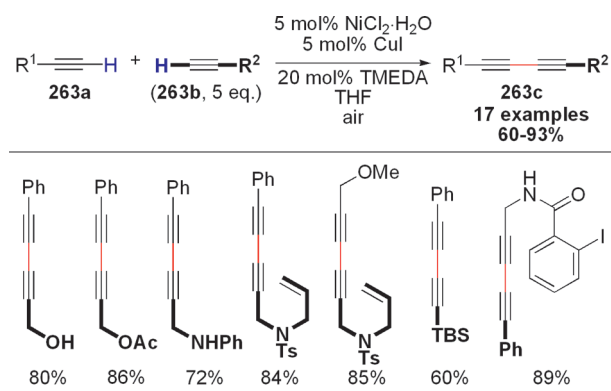


Figure 286. Ni- and Cu-catalyzed alkyne-alkyne cross-coupling.²³⁴

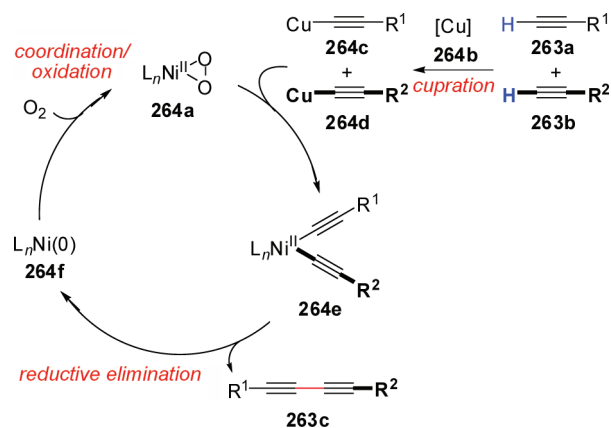


Figure 287. Proposed mechanism for Ni- and Cu-catalyzed alkyne-alkyne cross-coupling.²³⁴

The fate of the resulting Cu salt remains unknown. Chemoselectivities for differentially substituted 1,3-butadiene products **263c** over the corresponding homocoupling reactions are achieved by using one of the alkyne starting materials in excess.

7.3. Cross-Coupling Aldehydic C–H Bonds

Transition metals are known to activate aldehydic C–H bonds,²³⁵ and this type of C–H activation has been used in oxidative coupling to make ketones. In section 4.6, we covered Barluenga's work on Friedel–Crafts-type intramolecular cyclization of aldehydes to yield diarylketones.¹⁶² Complementary to this work, the Li group developed a Cu-catalyzed cyclization of formyl-*N*-arylformamides (**265a**) for the synthesis of indoline-2,3-diones (**265b**, Figure 288).²³⁶ Under an atmosphere of either O₂ or air, heterocyclic products **265b** are obtained in moderate to

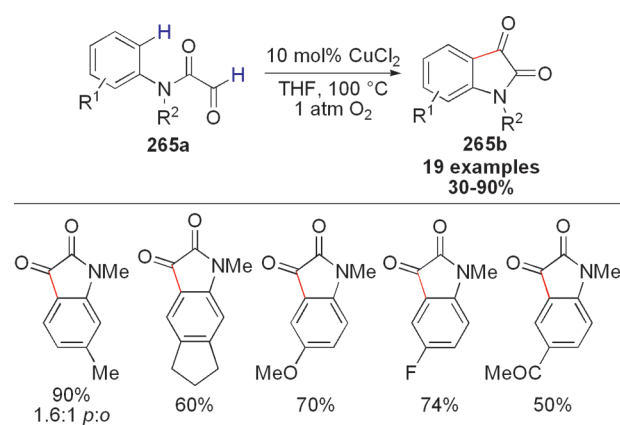


Figure 288. Cu-catalyzed intramolecular oxidative aldehyde–arene cross-coupling toward indoline-2,3-diones.²³⁶

good yields. The best catalyst is CuCl₂; using CuOTf or Cu(OTf)₂ gives a product resulting from intramolecular Friedel–Crafts addition to the C=O of the aldehyde (i.e., an α -hydroxyamide), a byproduct that does not transform to the desired indoline-2,3-dione. Functional groups including ketones and thiophenes are tolerated under the reaction conditions. Li and co-workers suggest a novel chelation-assisted dual C–H activation mechanism (Figure 289) based on FTIR spectroscopy, ESI-MS, and kinetic isotope effect studies (k_H/k_D (aldehyde) = 2.4; k_H/k_D (intramolecular, arene) = 1.5; k_H/k_D (intermolecular, arene) = 1.5) (Figure 290). Furthermore, the authors demonstrated that the addition of radical inhibitors such as 1,1-diphenylethylene and TEMPO had no effect on the reaction, which rules out radical pathways. In contrast to Barluenga's experiments, the use of IPy₂BF₄ did not produce the desired product **265b**.

Cheng and co-workers reported an aldehyde sp² C–H functionalization involving an alternative mechanism (Figure 291).²³⁷ Using Pd catalysts, arenes bearing a directing group (e.g., pyridine, oxazole, **268a**) undergo *ortho*-arylcyclization with air as the terminal oxidant. Cheng's conditions are compatible with functional groups, including aryl bromides and nitriles. Preliminary mechanistic studies revealed a large intramolecular primary kinetic isotope effect when using a deuterated pyridine partner (**269a-d**, Figure 292), a result that suggests a slow cyclopalladation step. The authors synthesized a palladacycle derived from 2-phenylpyridine (**269a**) and found that it is a competent catalyst for this coupling. The proposed mechanism involves (1) rate-limiting cyclopalladation of arene with the directing group **268a**, (2) carbopalladation of the C=O bond of the aldehyde **268b**, (3) β -H elimination, and (4) oxidation of Pd(0) to Pd(II) (Figure 293).

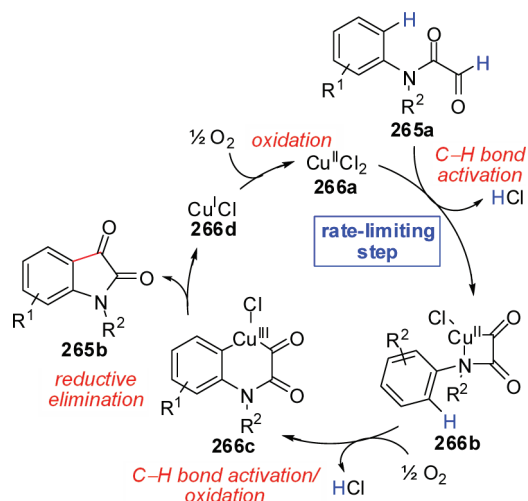


Figure 289. Proposed mechanism for Cu-catalyzed intramolecular oxidative aldehyde-arene cross-coupling toward indoline-2,3-diones.²³⁶

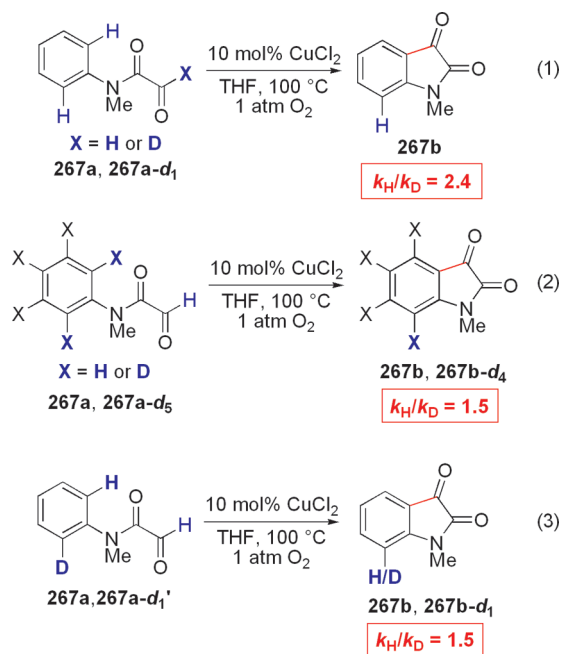


Figure 290. Kinetic isotope effect studies for Cu-catalyzed intramolecular oxidative aldehyde-arene cross-coupling toward indoline-2,3-diones.²³⁶

A related coupling between aryloximes (**271a**) and aldehydes (**271b**) was reported by the Yu group (Figure 294).²³⁸ Among Pd catalysts examined, Pd(OAc)₂ was optimal, although decent reactivity was observed for PdCl₂(PhCN)₂ and PdCl₂(PPh₃)₂. Like Cheng's reaction (vide supra), aryloxime-aldehyde cross-coupling occurs with good functional group tolerance, and substrates bearing Lewis basic thiophenes and reactive sp² C-Br bonds undergo oxidative C-C bond formation with moderate to good efficiencies. The products generated in Yu's reaction exhibit a 1,4-relationship between C=O groups and, hence, can be transformed into phthalazines (not shown), structural motifs common in organic materials and anticancer drugs. In studying the mechanism, Yu and co-workers observed dramatic decreases

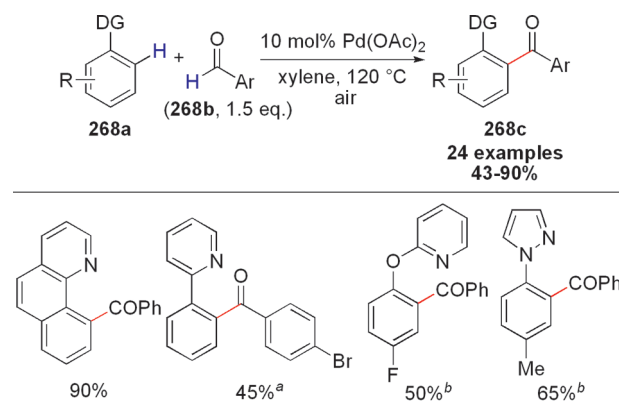


Figure 291. Pd-catalyzed *ortho*-arylcarbonylation of arenes with aldehydes.²³⁷

^a1 equiv of **268a** was used instead of 1.5 equiv.

^bReaction was conducted at 130 °C.

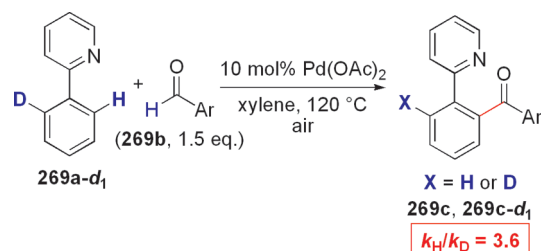


Figure 292. Kinetic isotope effect study for Pd-catalyzed *ortho*-arylcarbonylation of arenes with aldehydes.²³⁷

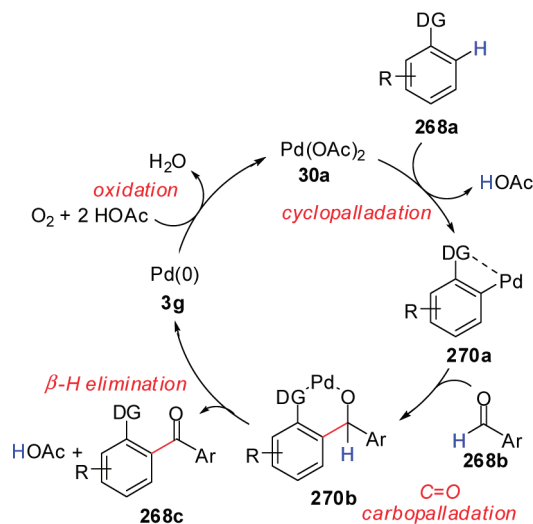


Figure 293. Proposed mechanism for Pd-catalyzed *ortho*-arylcarbonylation of arenes with aldehydes.²³⁷

in reaction yields when radical scavengers (e.g., ascorbic acid) are added. Hence, a radical pathway involving hydrogen abstraction from the aldehyde (**271b**) is proposed (Figure 295). Presumably, oxidation of palladacycle **270c** with a carbon-centered carbonyl radical **270e** forms a putative Pd(III) or Pd(IV) complex **270f**. This intermediate then undergoes reductive elimination to regenerate the active Pd(II) catalyst. On the basis of the similarity to Cheng's system (vide supra), however, it is possible that an alternative C=O carbopalladation/ β -H

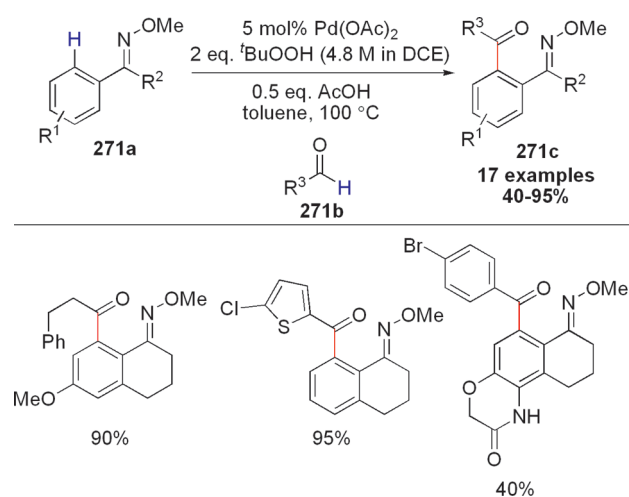


Figure 294. Pd-catalyzed *ortho*-arylcyclization of aryloximes with aldehydes.²³⁸

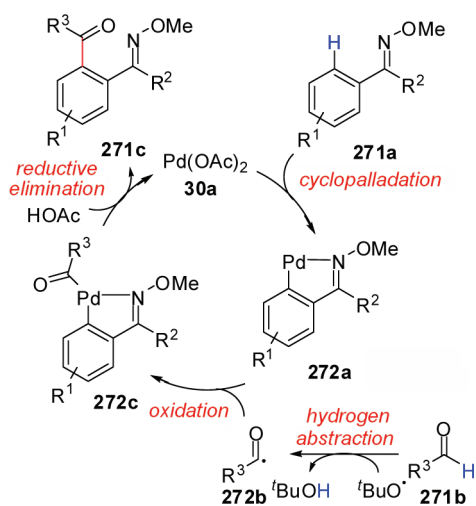


Figure 295. Proposed mechanism for Pd-catalyzed *ortho*-arylcyclization of aryloximes with aldehydes.²³⁸

elimination sequence may be involved as described previously in Figure 293.

7.4. Miscellaneous Examples

Oxidative cross-couplings may occur via a wide array of pathways. In 2010, dehydrogenative cyclization of allenes involving Au catalysis was demonstrated by Gouverneur and co-workers (Figure 296).²³⁹ In this reaction, allene (273a) cyclization to produce a butenolide equivalent is combined with intramolecular oxidative C–C bond formation with a nearby arene C–H bond. This reaction uses Selectfluor as the sacrificial oxidant, although no F atom is incorporated into the final product. While *N*-fluorobenzenesulfonimide (NFSI) and Oxone also afforded small amounts of the product (273b), other oxidants, such as $\text{PhI}(\text{OAc})_2$ and Ph_2SO , failed to promote the desired cyclization completely. In Gouverneur's studies, chiral tricyclic alkene 273c arising from the corresponding chiral allene starting material can be formed under the reaction conditions without loss of stereochemical information. Although the mechanistic details of this transformation are unclear, the authors demonstrated that a butenolide bearing an olefinic

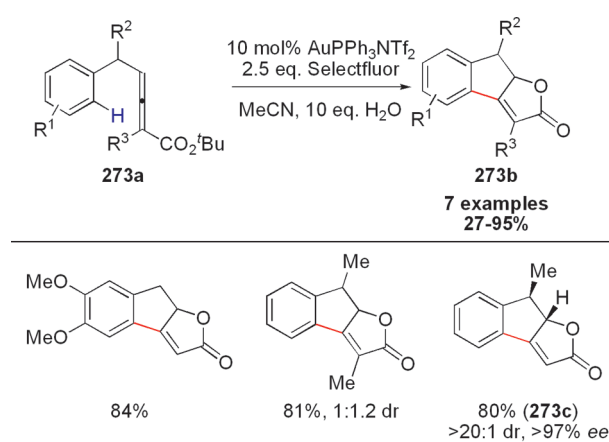


Figure 296. Au-catalyzed tandem cyclization/oxidative arene alkenylation.²³⁹

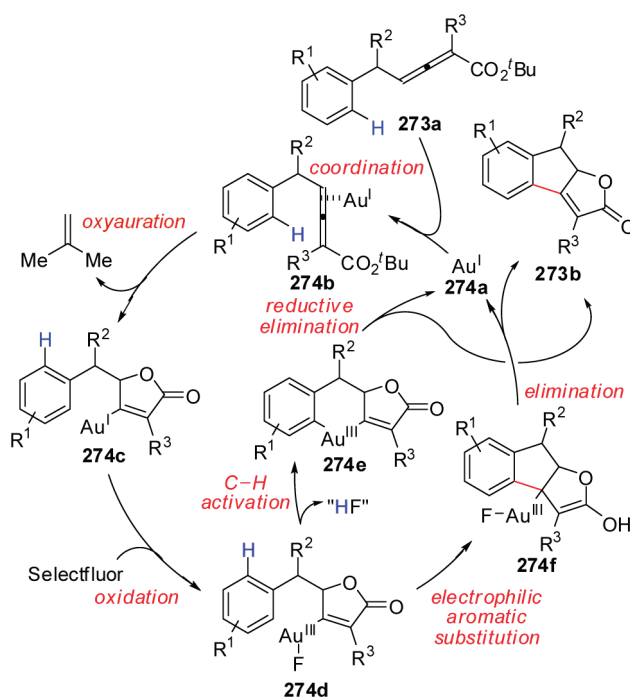


Figure 297. Proposed mechanism for Au-catalyzed tandem cyclization/oxidative arene alkenylation.²³⁹

sp^2 C–F bond is not a viable reaction intermediate. Hence, a mechanism involving coordination and oxyauration is proposed, followed by oxidation to Au(III) (274d, Figure 297). This Au complex (274d) can undergo subsequent C–C bond formation by either C–H activation or electrophilic aromatic substitution⁴⁶ pathways.

8. CONCLUSIONS AND OUTLOOK

There is a growing interest and appreciation for inventing chemical technologies that are green and sustainable.¹ As a result, the oxidative Fujiwara–Heck and enolate cross-couplings (first reported in the late 1960s and early 1970s) have received a renewed interest in recent years. On the basis of

improved mechanistic understanding, useful variants of these transformations have been invented and applied in natural product synthesis. In addition, novel strategies such as Li's cross-dehydrogenative coupling⁴ and catalytic tandem direct arylation⁸ have been devised. Overall, oxidative coupling complements its well-established counterparts, such as Heck reactions, organometallic additions, and Suzuki cross-couplings. Although using simple and inexpensive building blocks is an attractive alternative to consuming more functionalized and costly reagents, chemo- and regioselectivity remain issues that limit the broad usage of these methods. In addition, many current dehydrogenative couplings require stoichiometric oxidants, such as silver or copper salts. Practical approaches to C–H bond oxidation using reagents that are more environmentally friendly, such as oxygen, electricity, and visible light, are desirable and are being developed.²⁴⁰

There remains ample opportunity for discovering versatile catalysts, useful transformations, and new mechanistic manifolds for catalytic dehydrogenative cross-coupling. While many mechanisms are proposed, few are supported by detailed studies (e.g., characterization of intermediates, kinetic investigations, computational studies). In terms of asymmetric catalysis, enantioselective C–C bond formation by C–H bond oxidation is still in its infancy, although ligand-accelerated transition metal catalysis and organocatalysis has enabled some growth. Future advances in oxidative cross-coupling depend on designing chiral ligand scaffolds and catalysts specific for oxidation chemistry. Dehydrogenative couplings have the potential to provide bulk and fine chemicals from simple and/or sustainable feedstocks. For example, the oxidation of methane to ethane, once achieved, would be a green way to make alkanes²⁴¹—without using petroleum cracking or steam reforming (i.e., synthesis from syngas). Finally, practitioners in total synthesis will further demonstrate how these methods can be used to make structurally complex and biologically relevant molecules.

AUTHOR INFORMATION

Corresponding Author

*E-mail: vdong@chem.utoronto.ca.

BIOGRAPHIES



Charles S. Yeung obtained his B.Sc. (Honours) degree in 2006 at the University of British Columbia, where he worked with

Professor Laurel Schafer on asymmetric hydroamination. Charles is pursuing doctoral studies with Professor Vy Dong at the University of Toronto, where he holds a Julie Payette NSERC Scholarship and André Hamer Postgraduate Prize. His research interests include low-valent transition metal activation of carbon dioxide and catalytic oxidative arene cross-couplings.



Vy M. Dong received her bachelor's degree in chemistry at the University of California at Irvine, where she completed an honors thesis with Professor Larry Overman. She completed her doctorate with Professor David MacMillan at the California Institute of Technology, where she studied sigmatropic rearrangements and macrolide total synthesis. As an NIH postdoctoral fellow, she pursued organometallic and supramolecular chemistry with Professors Robert Bergman and Kenneth Raymond at the University of California at Berkeley. Vy began her independent career at the University of Toronto in July 2006 and was promoted to Associate Professor in July 2010. Professor Dong's recent awards include an Alfred P. Sloan Fellowship and Arthur C. Cope Scholar Award. The Dong Group focuses on inventing green strategies for asymmetric catalysis and natural product synthesis.

ACKNOWLEDGMENT

Funding is provided by the University of Toronto, Canada Foundation for Innovation, Ontario Research Fund, Boehringer Ingelheim Ltd. (Canada), Amgen Inc., and Hoffman-La Roche, American Chemical Society Petroleum Research Fund, and the Natural Sciences and Engineering Research Council (NSERC) of Canada. V.M.D. is grateful for an Alfred P. Sloan Fellowship and Arthur C. Cope Scholar Award; C.S.Y. is grateful for the NSERC André Hamer Award and the Julie Payette Research Scholarship. We thank other members of the Dong Group for helpful suggestions.

ABBREVIATIONS

Ac	acetyl
acac	acetoacetate
aq	aqueous
Ar	aryl
Ar _F	perfluoroaryl
Asp	aspartic acid
BEMP	2-tert-butylimino-2-diethylamino-1,3-dimethylperhydro-1,3,2-diazaphosphorine
BINOL	1,1'-bi-2-naphthol

bipy	2,2'-bipyridine	H ₂ [O]	reduced form of an oxidant
BMim	1-butyl-3-methylimidazolium tetrafluoroborate	IL	ionic liquid
Bn	benzyl	Ile	isoleucine
Boc	<i>tert</i> -butoxycarbonyl	Im	imidazolidinone
BOx	bis(oxazoline)	IPr	<i>N,N'</i> -bis-(2,6-di-iso-propylphenyl)imidazolyl carbene
BP	bathophenanthroline, 4,7-diphenyl-1,10-phenanthroline	IPy ₂ BF ₄	bis(pyridine)iodonium(I) tetrafluoroborate
BQ	<i>p</i> -benzoquinone	<i>k</i> _H / <i>k</i> _D	kinetic isotope effect
brsm	based on recovered starting material	<i>k</i> _H / <i>k</i> _D (inter)	intermolecular kinetic isotope effect
BS	bis(sulfoxide)	<i>k</i> _H / <i>k</i> _D (intra)	intramolecular kinetic isotope effect
Bz	benzoyl	<i>k</i> _H / <i>k</i> _D (prod)	product kinetic isotope effect
CA	cinchona alkaloid	L	ligand
CAN	ceric(IV) ammonium nitrate	LDA	lithium di-isopropylamide
CDC	cross-dehydrogenative coupling	LiHMDS	lithium hexamethyldisilazide, lithium bis-(trifluoromethyl)silylamide
chloranil	2,3,5,6-tetrachlorobenzoquinone	L _n	ligand
CMD	concerted metalation deprotonation	<i>m</i>	meta
COE	cyclooctene	<i>m</i> -CPBA	<i>meta</i> -chloroperoxybenzoic acid
Cp	cyclopentadiene	MOM	methoxymethyl
Cp*	1,2,3,4,5-pentamethylcyclopentadiene	<i>mono</i>	monofunctionalization product
CSA	camphorsulfonic acid	MS	molecular sieves
<i>p</i> -cymene	1-methyl-4-(1-methylethyl)benzene	NBE	norbornene
Cys	cysteine	NBS	<i>N</i> -bromosuccinimide
CYP	cytochrome P450	NHC	<i>N</i> -heterocyclic carbene
DABCO	1,4-diazabicyclo[2.2.2]octane	NMP	<i>N</i> -methyl-2-pyrrolidinone
dba	dibenzylideneacetone	NMR	nuclear magnetic resonance
DCE	1,2-dichloroethane	NOBIN	2'-amino-1,1'-binaphthyl-2-ol
DDQ	2,3-dichloro-5,6-dicyanobenzoquinone	NSAIDs	nonsteroidal anti-inflammatory drugs
DFT	density functional theory	NTf ₂	bis(trifluoromethylsulfonyl)amide
DG	directing group	<i>o</i>	ortho
<i>di</i>	difunctionalization product	<i>σ</i>	Hammett substituent constant
diglyme	bis(2-methoxyethyl) ether	[O]	oxidant
DIPP	2,6-di-iso-propylphenyl	ORTEP	Oak Ridge thermal ellipsoid plot
DMA	<i>N,N</i> -dimethylacetamide	OTf	trifluoromethanesulfonate, triflate (i.e., CF ₃ SO ₂)
DMB	2,4-dimethoxybenzyl	organo	organocatalytic
DMBQ	2,5-dimethylbenzoquinone	Oxone	potassium peroxymonosulfate (i.e., KHSO ₅ · 1/2 KHSO ₄ · 1/2 K ₂ SO ₄)
DME	1,2-dimethoxyethane	<i>p</i>	para
DMEDA	<i>N,N'</i> -dimethylethylenediamine	<i>ρ</i>	Hammett reaction constant
DMF	<i>N,N</i> -dimethylformamide	<i>p</i> -cymene	1-methyl-4-(1-isopropyl)benzene
DMP	Dess–Martin periodinane	phen	1,10-phenanthroline
DMSO	dimethylsulfoxide	PIFA	phenyliodine(III) bis(trifluoroacetate)
DPEN	1,2-diphenylethylenediamine	Piv	pivaloyl (i.e., <i>tert</i> -butylcarbonyl)
<i>dr</i>	diastereomeric ratio	PMP	<i>para</i> -methoxyphenyl (i.e., <i>p</i> -OMeC ₆ H ₄)
dtbpy	4,4'-di- <i>tert</i> -butyl-2,2'-bipyridine	POV-Ray	Persistence of Vision Raytracer
ee	enantiomeric excess	ppy	2-phenylpyridyl
2-EH	2-ethylhexanoate	<i>p</i> -Ts	<i>para</i> -toluenesulfonyl (i.e., <i>p</i> -MeC ₆ H ₄ SO ₂)
<i>ent</i>	enantiomeric	PTS	polyoxyethanyl α-tocopheryl sebacate
<i>epi</i>	epimer	Pyr	pyridine
eq	equivalents (in figures)	PyBOx	pyridine bis(oxazoline)
equiv	equivalents	PyOx	pyridine oxazoline
ESI-MS	electrospray-mass spectrometry	ROS	reactive oxygen species
ESR	electron-spin resonance	rt	room temperature
EWG	electron-withdrawing group	SOMO	singly occupied molecular orbital
F ₆ -acac	hexafluoroacetylacetonate	Selectfluor	1-chloromethyl-4-fluoro-1,4-diazoniabicyclo-[2.2.2]octane bis(tetrafluoroborate)
FePc	iron phthalocyanine	SEM	2-trimethylsilylethoxymethyl
FePc _{ox}	iron phthalocyanine, oxidized form	SIMes	<i>N,N'</i> -bis(2,4,6-trimethylphenyl)-4,5-dihydroimidazolyl carbene
FePc _{red}	iron phthalocyanine, reduced form	sp.	species
Fmoc	fluorenylmethyloxycarbonyl	^t Am	<i>tert</i> -amyl (i.e., 2,2-dimethylpropyl)
FTIR	Fourier transform infrared	^t Bu	<i>tert</i> -butyl
HFIP	1,1,1,3,3,3-hexafluoro-2-propanol		
His	histidine		
HIV	human immunodeficiency virus		

TBS	<i>tert</i> -butyldimethylsilyl
TCAA	trichloroisocyanuric acid
TEMPO	2,2,6,6-tetramethylpiperidine-1-oxyl
TES	triethylsilyl
TSE	2-trimethylsilylethyl
TFA	trifluoroacetate, trifluoroacetic acid
TFE	trifluoroethanol
THF	tetrahydrofuran
TIPS	tri-isopropylsilyl
TMEDA	tetramethylethylenediamine
TMS	trimethylsilyl
TON	turnover number
μ w	microwave
Val	valine
XPhos	2-dicyclohexylphosphino-2',4',6'-tri-isopropylbiphenyl

REFERENCES

- (1) For reviews on green chemistry, see: (a) Li, C.-J.; Trost, B. M. *Proc. Natl. Acad. Sci. U.S.A.* **2008**, *105*, 13197. (b) Anastas, P. T.; Warner, J. C. *Green Chemistry: Theory and Practice*; Oxford University Press: New York, 1998.
- (2) Corey, E. J.; Cheng, X. M. *The Logic of Chemical Synthesis*; John Wiley & Sons: New York, 1989.
- (3) For reviews on the ideal chemical synthesis, see: (a) Newhouse, T.; Baran, P. S.; Hoffmann, R. W. *Chem. Soc. Rev.* **2009**, *38*, 3010. (b) Gaich, T.; Baran, P. S. *J. Org. Chem.* **2010**, *75*, 4657. (c) Hendrickson, J. B. *J. Am. Chem. Soc.* **1975**, *97*, 5784.
- (4) For reviews on Li's cross-dehydrogenative couplings, see: (a) Li, C.-J. *Acc. Chem. Res.* **2009**, *42*, 335. (b) Li, Z.; Bohle, D. S.; Li, C.-J. *Proc. Natl. Acad. Sci. U.S.A.* **2006**, *103*, 8928. (c) Li, C.-J.; Li, Z. *Pure Appl. Chem.* **2006**, *78*, 935. (d) Yoo, W.-J.; Li, C.-J. *Top. Curr. Chem.* **2010**, *292*, 281. For a review on other recent developments, see: (e) Scheuermann, C. J. *Chem.—Asian J.* **2010**, *5*, 436.
- (5) The Glaser coupling is one example of oxidative homocoupling. For a review, see: Siemsen, P.; Livingston, R. C.; Diederich, F. *Angew. Chem., Int. Ed.* **2000**, *39*, 2632.
- (6) Many mechanisms are proposed for cross-dehydrogenative couplings. Detailed studies on these transformations are relatively rare in the literature (e.g., kinetics investigations, DFT calculations). For the purposes of this review, we will cover plausible reaction pathways proposed by the authors. Designation of the rate-limiting (or turnover-limiting) step and reversibility of each elementary reaction are based on the experimental data provided in combination with relevant literature references. Our descriptions are not intended to suggest that these mechanistic proposals are fully supported by detailed investigations.
- (7) For reviews on Pd-catalyzed oxidative Heck-type alkenylations, see: (a) Beccalli, E. M.; Broggini, G.; Martinelli, M.; Sottocornola, S. *Chem. Rev.* **2007**, *107*, 5318. (b) For a review on transition metal catalyzed addition to C=C bonds, see: Ritleng, V.; Sirlin, C.; Pfeffer, M. *Chem. Rev.* **2002**, *102*, 1731.
- (8) For reviews on tandem direct arylation, see: (a) Ashenhurst, J. A. *Chem. Soc. Rev.* **2010**, *39*, 540. (b) McGlacken, G. P.; Batemann, L. M. *Chem. Soc. Rev.* **2009**, *38*, 2447. (c) You, S.-L.; Xia, J.-B. *Top. Curr. Chem.* **2010**, *292*, 165.
- (9) For reviews on Pd-catalyzed direct arylation, see: (a) Lyons, T. W.; Sanford, M. S. *Chem. Rev.* **2010**, *110*, 1147. (b) Ackermann, L.; Vicente, R.; Kapdi, A. *Angew. Chem., Int. Ed.* **2009**, *48*, 9792. (c) Li, B.-J.; Yang, S.-D.; Shi, Z.-J. *Synlett* **2008**, 949. For a review on transition metal-catalyzed direct arylation, see: (d) Alberico, D.; Scott, M. E.; Lautens, M. *Chem. Rev.* **2007**, *107*, 174.
- (10) For reviews on Heck alkenylations, see: (a) *Handbook of Organopalladium Chemistry for Organic Synthesis*; John Wiley & Sons, Inc.: New York, 2002; Vol. 1, Chapter IV.2. (b) Wu, X.-F.; Anbarasan, P.; Neumann, H.; Beller, M. *Angew. Chem., Int. Ed.* **2010**, *49*, 9047. (c) Crisp, G. T. *Chem. Soc. Rev.* **1998**, *27*, 427. (d) Beletskaya, I. P.; Cheprakov, A. V. *Chem. Rev.* **2000**, *100*, 3009. (e) de Vries, J. G. *Can. J. Chem.* **2001**, *79*, 1086. (f) de Meijere, A.; Meyer, F. E. *Angew. Chem., Int. Ed. Engl.* **1995**, *33*, 2379.
- (11) Moritani, I.; Fujiwara, Y. *Synthesis* **1973**, 524.
- (12) For a discussion on the mechanism of oxidation of Pd(0) to Pd(II), see: (a) Piera, J.; Bäckvall, J.-E. *Angew. Chem., Int. Ed.* **2008**, *47*, 3506. (b) Gligorich, K. M.; Sigman, M. S. *Angew. Chem., Int. Ed.* **2006**, *45*, 6612. (c) Muzart, J. *Chem. Asian J.* **2006**, *1*, 508.
- (13) Beck, E. M.; Gaunt, M. J. *Top. Curr. Chem.* **2010**, *292*, 85.
- (14) Boele, M. D. K.; van Strijdonck, G. P. F.; de Vries, A. H. M.; Kamer, P. C. J.; de Vries, J. G.; van Leeuwen, P. W. N. M. *J. Am. Chem. Soc.* **2002**, *124*, 1586.
- (15) Nishikata, T.; Lipshutz, B. H. *Org. Lett.* **2010**, *12*, 1972.
- (16) Houlden, C. E.; Bailey, C. D.; Ford, J. G.; Gagné, M. R.; Lloyd-Jones, G. C.; Booker-Milburn, K. I. *J. Am. Chem. Soc.* **2008**, *130*, 10066.
- (17) Li, J.-J.; Mei, T.-S.; Yu, J.-Q. *Angew. Chem., Int. Ed.* **2008**, *47*, 6452.
- (18) For reviews on isoquinoline synthesis, see: (a) Chrzanowska, M.; Rozwadowska, M. D. *Chem. Rev.* **2004**, *104*, 3341. (b) Szawkalo, J.; Czarnocki, Z. *Monatsh. Chem.* **2005**, *136*, 1619.
- (19) For selected examples of late-stage C—H oxidations, see: (a) Chen, M. S.; White, M. C. *Science* **2007**, *318*, 783. (b) Vermeulen, N. A.; Chen, M. S.; White, M. C. *Tetrahedron* **2009**, *65*, 3078. (c) Stang, E. M.; White, M. C. *Nature Chem.* **2009**, *1*, 547. (d) Chen, K.; Baran, P. S. *Nature* **2009**, *459*, 824. (e) Wender, P. A.; Hilinski, M. K.; Mayweg, A. V. W. *Org. Lett.* **2005**, *7*, 79.
- (20) Wang, D.-H.; Engle, K. M.; Shi, B.-F.; Yu, J.-Q. *Science* **2010**, *327*, 315.
- (21) Engle, K. M.; Wang, D.-H.; Yu, J.-Q. *Angew. Chem., Int. Ed.* **2010**, *49*, 6169.
- (22) Engle, K. M.; Wang, D.-H.; Yu, J.-Q. *J. Am. Chem. Soc.* **2010**, *132*, 14137.
- (23) Davies, D. L.; Donald, S. M. A.; Macgregor, S. A. *J. Am. Chem. Soc.* **2005**, *127*, 13754.
- (24) For a discussion of concerted metalation deprotonation, see: (a) Lafrance, M.; Rowley, C. N.; Woo, T. K.; Fagnou, K. *J. Am. Chem. Soc.* **2006**, *128*, 8754. (b) Gorelsky, S. I.; Lapointe, D.; Fagnou, K. *J. Am. Chem. Soc.* **2008**, *130*, 10848. (c) Sun, H.-Y.; Gorelsky, S. I.; Stuart, D. R.; Campeau, L.-C.; Fagnou, K. *J. Org. Chem.* **2010**, *75*, 8180.
- (25) Shi, B.-F.; Zhang, Y.-H.; Lam, J. K.; Wang, D.-H.; Yu, J.-Q. *J. Am. Chem. Soc.* **2010**, *132*, 460.
- (26) Zhang, Y.-H.; Shi, B.-F.; Yu, J.-Q. *J. Am. Chem. Soc.* **2009**, *131*, 5072.
- (27) For a review on *meta*-selective C—H bond functionalization, see: (a) Zhou, Y.; Zhao, J.; Liu, L. *Angew. Chem., Int. Ed.* **2009**, *48*, 7126. (b) Park, J.-W.; Jun, C.-H. *ChemCatChem* **2009**, *1*, 69. For selected examples of *meta*-selective C—H bond functionalization, see: (c) Phipps, R. J.; Gaunt, M. J. *Science* **2009**, *323*, 1593. (d) Duong, H. A.; Gilligan, R. E.; Cooke, M. L.; Phipps, R. J.; Gaunt, M. J. *Angew. Chem., Int. Ed.* **2010**, *50*, 463.
- (28) For selected examples of catalytic C—H functionalization of perfluoroarenes, see: (a) Ref 24a. (b) Lafrance, M.; Shore, D.; Fagnou, K. *Org. Lett.* **2006**, *8*, 5097. (c) Do, H.-Q.; Daugulis, O. *J. Am. Chem. Soc.* **2008**, *130*, 1128. (d) Nakao, Y.; Kashiwara, N.; Kanyiva, K. S.; Hiyama, T. *J. Am. Chem. Soc.* **2008**, *130*, 16170.
- (29) Zhang, X.; Fan, S.; He, C.-Y.; Wan, X.; Min, Q.-Q.; Yang, J.; Jiang, Z.-X. *J. Am. Chem. Soc.* **2010**, *132*, 4506.
- (30) Cho, S. H.; Hwang, S. J.; Chang, S. J. *J. Am. Chem. Soc.* **2008**, *130*, 9254.
- (31) Wu, J.; Cui, X.; Chen, L.; Jiang, G.; Wu, Y. *J. Am. Chem. Soc.* **2009**, *131*, 13888.
- (32) Wasa, M.; Engle, K. M.; Yu, J.-Q. *J. Am. Chem. Soc.* **2010**, *132*, 3680.
- (33) Balavoine, G.; Clinet, J. C. *J. Organomet. Chem.* **1990**, *390*, C84.
- (34) For selected examples of Pd-catalyzed oxidative Heck-type alkenylations of heteroaromatics, see: (a) Shue, R. S. *J. Chem. Soc. D, Chem. Commun.* **1971**, 1510. (b) Shue, R. S. *J. Catal.* **1972**, *26*, 112. (c) Maruyama, O.; Yoshidomi, M.; Fujiwara, Y.; Taniguchi, H. *Chem. Lett.*

- 1979, 1229. (d) Fujiwara, Y.; Maruyama, O.; Yoshidomi, M.; Taniguchi, H. *J. Org. Chem.* **1981**, *46*, 851. (e) Itahara, T.; Ikeda, M.; Sakakibara, T. *J. Chem. Soc., Perkin Trans. 1* **1983**, 1361. (f) Tsuji, J.; Nagashima, H. *Tetrahedron* **1984**, *40*, 2699. (g) Itahara, T.; Kawasaki, K.; Ouseto, F. *Synthesis* **1984**, 236. (h) Itahara, T.; Kawasaki, K.; Ouseto, F. *Bull. Chem. Soc. Jpn.* **1984**, *57*, 3488. (i) Itahara, T. *J. Org. Chem.* **1985**, *50*, 5546. (j) Pindur, U.; Adam, R. *Helv. Chim. Acta* **1990**, *73*, 827. (k) Melnyk, P.; Legrand, B.; Gasche, J.; Ducrot, P.; Thal, C. *Tetrahedron* **1995**, *51*, 1941. (l) Grimster, N. P.; Gauntlett, C.; Godfrey, C. R. A.; Gaunt, M. J. *Angew. Chem., Int. Ed.* **2005**, *44*, 3125. (m) Capito, E.; Brown, J. M.; Ricci, A. *Chem. Commun.* **2005**, 1854. (n) Beck, E. M.; Grimster, N. P.; Hatley, R.; Gaunt, M. J. *J. Am. Chem. Soc.* **2006**, *128*, 2528. (o) Aouf, C.; Thiery, E.; Bras, J. L.; Muzart, J. *Org. Lett.* **2009**, *11*, 4096.
- (35) Yokoyama, Y.; Matsumoto, T.; Murakami, Y. *J. Org. Chem.* **1995**, *60*, 1486.
- (36) For selected examples of intramolecular Pd-catalyzed oxidative Heck-type alkenylations, see: (a) Iida, H.; Yuasa, Y.; Kibayashi, C. *J. Org. Chem.* **1980**, *45*, 2938. (b) Ferreira, E. M.; Stoltz, B. M. *J. Am. Chem. Soc.* **2003**, *125*, 9578. (c) Abbiati, G.; Beccalli, E. M.; Brogini, G.; Zoni, C. *J. Org. Chem.* **2003**, *68*, 7625. (d) Zhang, H.; Ferreira, E. M.; Stoltz, B. M. *Angew. Chem., Int. Ed.* **2004**, *43*, 6144. (e) Beccalli, E. M.; Brogini, G.; Martinelli, M.; Paladino, G. *Tetrahedron* **2005**, *61*, 1077. (f) Kong, A.; Han, X.; Lu, X. *Org. Lett.* **2006**, *8*, 1339.
- (37) Baran, P. S.; Corey, E. D. *J. Am. Chem. Soc.* **2002**, *124*, 7904.
- (38) Garg, N. K.; Caspi, D. D.; Stoltz, B. M. *J. Am. Chem. Soc.* **2004**, *126*, 9552.
- (39) Beck, E. M.; Hatley, R.; Gaunt, M. J. *Angew. Chem., Int. Ed.* **2008**, *47*, 3004.
- (40) Bowie, A. L., Jr.; Trauner, D. *J. Org. Chem.* **2009**, *74*, 1581.
- (41) (a) Schiffner, J. A.; Machotta, A. B.; Oestreich, M. *Synlett* **2008**, 2271. (b) Schiffner, J. A.; Wöste, T. H.; Oestreich, M. *Eur. J. Org. Chem.* **2010**, 75, 174.
- (42) Itahara, T. *J. Chem. Soc., Chem. Commun.* **1981**, 859.
- (43) Itahara, T. *J. Org. Chem.* **1985**, *50*, 5546.
- (44) (a) Knölker, H.-J.; Fröhner, W. *J. Chem. Soc., Perkin Trans. 1* **1998**, 173. (b) Knölker, H.-J.; Reddy, K. R.; Wagner, A. *Tetrahedron Lett.* **1998**, *39*, 8267. (c) Knölker, H.-J.; Fröhner, W.; Reddy, K. R. *Synthesis* **2002**, 557.
- (45) (a) Pirrung, M. C.; Park, K.; Li, Z. *Org. Lett.* **2001**, *3*, 365. (b) Pirrung, M. C.; Deng, L.; Li, Z.; Park, K. *J. Org. Chem.* **2002**, *67*, 8374.
- (46) For a discussion of electrophilic aromatic substitution, see: Carey, F. A.; Sundberg, R. J. *Advanced Organic Chemistry, Part B: Reactions and Synthesis*, 5th ed.; Springer: New York, 2007; p 1004.
- (47) Yadav, J. S.; Reddy, B. V. S.; Swamy, T. *Tetrahedron Lett.* **2003**, *44*, 9121.
- (48) Pirrung, M. C.; Liu, Y.; Deng, L.; Halstead, D. K.; Li, Z.; May, J. F.; Wedel, M.; Austin, D. A.; Webster, N. J. G. *J. Am. Chem. Soc.* **2005**, *127*, 4609.
- (49) Zhang, H.-B.; Liu, L.; Chen, Y.-J.; Wang, D.; Li, C.-J. *Adv. Synth. Catal.* **2006**, *348*, 229.
- (50) (a) Bogle, K. M.; Hirst, D. J.; Dixon, D. J. *Tetrahedron* **2010**, *66*, 6399. (b) Bogle, K. M.; Hirst, D. J.; Dixon, D. J. *Org. Lett.* **2007**, *9*, 4901.
- (51) Harrison, C. R.; Hodge, P. *J. Chem. Soc., Perkin Trans. 1* **1982**, 509.
- (52) Hong, P.; Yamazaki, H. *Chem. Lett.* **1979**, 1335.
- (53) (a) Matsumoto, T.; Yoshida, H. *Chem. Lett.* **2000**, 1064. (b) Matsumoto, T.; Periana, R. A.; Taube, D. J.; Yoshida, H. *J. Catal.* **2002**, *206*, 272.
- (54) Sasaki, K.; Sakakura, T.; Tokunaga, Y.; Wada, K.; Tanaka, M. *Chem. Lett.* **1988**, 685.
- (55) Ueura, K.; Satoh, T.; Miura, M. *Org. Lett.* **2007**, *9*, 1407.
- (56) Wang, F.; Song, G.; Li, X. *Org. Lett.* **2010**, *12*, 5430.
- (57) Umeda, N.; Hirano, K.; Satoh, T.; Miura, M. *J. Org. Chem.* **2009**, *74*, 7094.
- (58) Patureau, F. W.; Glorius, F. *J. Am. Chem. Soc.* **2010**, *132*, 9982.
- (59) Weissman, H.; Song, X.; Milstein, D. *J. Am. Chem. Soc.* **2001**, *123*, 337.
- (60) For a discussion of electrophilic metalation, see: (a) Carey, F. A.; Sundberg, R. J. *Advanced Organic Chemistry, Part B: Reactions and Synthesis*, 5th ed.; Springer: New York, 2007; p 1026. (b) Ryabov, A. D. *Chem. Rev.* **1990**, *90*, 403. (c) Davidson, J. M.; Triggs, C. *J. Chem. Soc. A* **1968**, 1324.
- (61) Yi, C. S.; Yun, S. Y.; Guzei, I. A. *Organometallics* **2004**, *23*, 5392.
- (62) DeBoef, B.; Pastine, S. J.; Sames, D. *J. Am. Chem. Soc.* **2004**, *126*, 6556.
- (63) Hirota, K.; Isobe, Y.; Kitade, Y.; Maki, Y. *Synthesis* **1987**, 495.
- (64) Cheng, D.; Gallagher, T. *Org. Lett.* **2009**, *11*, 2639.
- (65) Hatamoto, Y.; Sakaguchi, S.; Ishii, Y. *Org. Lett.* **2004**, *6*, 4623.
- (66) Xu, Y.-H.; Lu, J.; Loh, T.-P. *J. Am. Chem. Soc.* **2009**, *131*, 1372.
- (67) Yu, H.; Jin, W.; Sun, C.; Chen, J.; Du, W.; He, S.; Yu, Z. *Angew. Chem., Int. Ed.* **2010**, *49*, 5792.
- (68) Bee, C.; Leclerc, E.; Tius, M. A. *Org. Lett.* **2003**, *5*, 4927.
- (69) For a review of the Nazarov reaction, see: Frontier, A. J.; Collison, C. *Tetrahedron* **2005**, *61*, 7577.
- (70) Rönn, M.; Andersson, P. G.; Bäckvall, J.-E. *Tetrahedron Lett.* **1997**, *38*, 3603.
- (71) Pei, T.; Wang, X.; Widenhoefer, R. A. *J. Am. Chem. Soc.* **2003**, *125*, 648.
- (72) Liu, C.; Wang, X.; Pei, T.; Widenhoefer, R. A. *Chem.—Eur. J.* **2004**, *10*, 6343.
- (73) Yip, K.-T.; Li, J.-H.; Lee, O.-Y.; Yang, D. *Org. Lett.* **2005**, *7*, 5717.
- (74) Wang, X.; Widenhoefer, R. A. *Chem. Commun.* **2004**, 660.
- (75) Franzén, J.; Bäckvall, J.-E. *J. Am. Chem. Soc.* **2003**, *125*, 6056.
- (76) Piera, J.; Närhi, K.; Bäckvall, J.-E. *Angew. Chem., Int. Ed.* **2006**, *45*, 6914.
- (77) For reviews of transition metal-catalyzed cross-coupling reactions, see: (a) Corbet, J.-P.; Mignani, G. *Chem. Rev.* **2006**, *106*, 2651. (b) Hassan, J.; Sévignon, M.; Gozzi, C.; Schulz, E.; Lemaire, M. *Chem. Rev.* **2002**, *102*, 1359. (c) Ref 9d.
- (78) For a review on palladacycles, see: Dupont, J.; Consorti, C. S.; Spencer, J. *Chem. Rev.* **2005**, *105*, 2527.
- (79) For a discussion of σ -bond metathesis, see: (a) Labinger, J. A.; Bercaw, J. E. *Nature* **2002**, *417*, 507. (b) Balcells, D.; Clot, E.; Eisenstein, O. *Chem. Rev.* **2010**, *110*, 749. (c) Boutadla, Y.; Davies, D. L.; Macgregor, S. A.; Poblador-Bahamonde, A. I. *Dalton Trans.* **2009**, 5820. (d) Ref 23.
- (e) Shilov, A. E.; Shul'pin, G. B. *Chem. Rev.* **1997**, *97*, 2879.
- (80) Li, R.; Liang, L.; Lu, W. *Organometallics* **2006**, *25*, 5973.
- (81) TFA is known to facilitate the formation of Pd(II) σ -aryl intermediates. See: (a) Jia, C.; Piao, D.; Oyamada, J.; Lu, W.; Kitamura, T.; Fujiwara, Y. *Science* **2000**, *287*, 1992. (b) Jia, C.; Lu, W.; Oyamada, J.; Kitamura, T.; Matsuda, K.; Irie, M.; Fujiwara, Y. *J. Am. Chem. Soc.* **2000**, *122*, 7252.
- (82) Stuart, D. R.; Fagnou, K. *Science* **2007**, *316*, 1172.
- (83) Stuart, D. R.; Villemure, E.; Fagnou, K. *J. Am. Chem. Soc.* **2007**, *129*, 12072.
- (84) Dwight, T. A.; Rue, N. R.; Charyk, D.; Josselyn, R.; DeBoef, B. *Org. Lett.* **2007**, *9*, 3137.
- (85) Potavathri, S.; Dumas, A. S.; Dwight, T. A.; Naumiec, G. R.; Hammann, J. M.; DeBoef, B. *Tetrahedron Lett.* **2008**, *49*, 4050.
- (86) (a) Sloan, O. D.; Thornton, P. *Inorg. Chim. Acta* **1986**, *120*, 173. (b) Brandon, R. W.; Claridge, D. V. *Chem. Commun.* **1968**, 677.
- (87) Joucla, L.; Djakovitch, L. *Adv. Synth. Catal.* **2009**, *351*, 673.
- (88) Potavathri, S.; Pereira, K. C.; Gorelsky, S. I.; Pike, A.; LeBris, A. P.; DeBoef, B. *J. Am. Chem. Soc.* **2010**, *132*, 14676.
- (89) Xi, P.; Yang, F.; Qin, S.; Zhao, D.; Lan, J.; Gao, G.; Hu, C.; You, J. *J. Am. Chem. Soc.* **2010**, *132*, 1822.
- (90) Hull, K. L.; Sanford, M. S. *J. Am. Chem. Soc.* **2007**, *129*, 11904.
- (91) Hull, K. L.; Sanford, M. S. *J. Am. Chem. Soc.* **2009**, *131*, 9651.
- (92) Powers, D. C.; Ritter, T. *Nature Chem.* **2009**, *1*, 302.
- (93) Li, B.-J.; Tian, S.-L.; Fang, Z.; Shi, Z.-J. *Angew. Chem., Int. Ed.* **2008**, *47*, 1115.
- (94) Brasche, G.; García-Fortanet, J.; Buchwald, S. L. *Org. Lett.* **2008**, *10*, 2207.

- (95) Zhao, X.; Yeung, C. S.; Dong, V. M. *J. Am. Chem. Soc.* **2010**, *132*, 5837.
- (96) (a) Yeung, C. S.; Borduas, N.; Zhao, X.; Dong, V. M. *Chem. Sci.* **2010**, *1*, 331. For a recent mechanistic study on intramolecular oxidative coupling with Na₂S₂O₈, see: (b) Borduas, N.; Lough, A. J.; Dong, V. M. *Inorg. Chim. Acta* **2011**, DOI: 10.1016/j.ica.2011.01.059.
- (97) Xiao, B.; Fu, Y.; Xu, J.; Gong, T.-J.; Dai, J.-J.; Yi, J.; Liu, L. *J. Am. Chem. Soc.* **2010**, *132*, 468.
- (98) Killian, P. F.; Bruell, C. J.; Liang, C.; Marley, M. C. *Soil Sediment Contam.* **2007**, *16*, 523.
- (99) For selected examples, see: (a) Desai, L. V.; Malik, H. A.; Sanford, M. S. *Org. Lett.* **2006**, *8*, 1141. (b) Wang, G.-W.; Yuan, T.-T.; Wu, X.-L. *J. Org. Chem.* **2008**, *73*, 4717. (c) Thu, H.-Y.; Yu, W.-Y.; Che, C.-M. *J. Am. Chem. Soc.* **2006**, *128*, 9048. (d) Liu, Y.-K.; Lou, S.-J.; Xu, D.-Q.; Xu, Z.-Y. *Chem.—Eur. J.* **2010**, *16*, 13590.
- (100) For reviews of Pd(II/IV) catalysis, see: (a) Xu, L.-M.; Li, B.-J.; Yang, Z.; Shi, Z.-J. *Chem. Soc. Rev.* **2010**, *39*, 712. (b) Sehnal, P.; Taylor, R. J. K.; Fairlamb, I. J. S. *Chem. Rev.* **2010**, *110*, 824.
- (101) Powers, D. C.; Geibel, M. A. L.; Klein, J. E. M. N.; Ritter, T. *J. Am. Chem. Soc.* **2009**, *131*, 17050.
- (102) Deprez, N. R.; Sanford, M. S. *J. Am. Chem. Soc.* **2009**, *131*, 11234.
- (103) Xia, J.-B.; You, S.-L. *Organometallics* **2007**, *26*, 4869.
- (104) Wei, Y.; Su, W. *J. Am. Chem. Soc.* **2010**, *132*, 16377.
- (105) Shiotani, A.; Itatani, H. *Angew. Chem., Int. Ed. Engl.* **1978**, *13*, 471.
- (106) Liégault, B.; Lee, D.; Huestis, M. P.; Stuart, D. R.; Fagnou, K. *J. Org. Chem.* **2008**, *73*, 5022.
- (107) Sridharan, V.; Martín, M. A.; Menéndez, J. C. *Eur. J. Org. Chem.* **2009**, 4614.
- (108) Watanabe, T.; Oishi, S.; Fujii, N.; Ohno, H. *J. Org. Chem.* **2009**, *74*, 4720.
- (109) Liégault, B.; Fagnou, K. *Organometallics* **2008**, *27*, 4841.
- (110) Ackermann, L.; Jeyachandran, R.; Potukuchi, H. K.; Novák, P.; Büttner, L. *Org. Lett.* **2010**, *12*, 2056.
- (111) Tang, D.-J.; Tang, B.-X.; Li, J.-H. *J. Org. Chem.* **2009**, *74*, 6749.
- (112) Gandeepan, P.; Parthasarathy, K.; Cheng, C.-H. *J. Am. Chem. Soc.* **2010**, *132*, 8569.
- (113) Murahashi, S.-I. *Angew. Chem., Int. Ed. Engl.* **1995**, *34*, 2443.
- (114) Yoshida, J.-i.; Suga, S.; Suzuki, S.; Kinomura, N.; Yamamoto, A.; Fujiwara, K. *J. Am. Chem. Soc.* **1999**, *121*, 9546.
- (115) Yoshida, K.; Fueno, T. *J. Org. Chem.* **1972**, *37*, 4145.
- (116) (a) Andreades, S.; Zahnow, E. W. *J. Am. Chem. Soc.* **1969**, *91*, 4181. (b) Chiba, T.; Takata, Y. *J. Org. Chem.* **1977**, *42*, 2973.
- (117) Chen, C.-K.; Hortmann, A. G.; Marzabadi, M. R. *J. Am. Chem. Soc.* **1988**, *110*, 4829.
- (118) Murahashi, S.-I.; Komiya, N.; Terai, H. *Angew. Chem., Int. Ed.* **2005**, *44*, 6931.
- (119) (a) Murahashi, S.-I.; Nakae, T.; Terai, H.; Komiya, N. *J. Am. Chem. Soc.* **2008**, *130*, 11005. (b) Murahashi, S.-I.; Komiya, N.; Terai, H.; Nakae, T. *J. Am. Chem. Soc.* **2003**, *125*, 15312.
- (120) Yoshida, J.-i.; Suga, S. *Chem.—Eur. J.* **2002**, *8*, 2650.
- (121) Suga, S.; Okajima, M.; Fujiwara, K.; Yoshida, J.-i. *J. Am. Chem. Soc.* **2001**, *123*, 7941.
- (122) Li, Z.; Li, C.-J. *J. Am. Chem. Soc.* **2004**, *126*, 11810.
- (123) (a) Li, Z.; Li, C.-J. *Org. Lett.* **2004**, *6*, 4997. (b) Li, Z.; MacLeod, P. D.; Li, C.-J. *Tetrahedron: Asymmetry* **2006**, *17*, 590.
- (124) Niu, M.; Yin, Z.; Fu, H.; Jiang, Y.; Zhao, Y. *J. Org. Chem.* **2008**, *73*, 3961.
- (125) Zhao, L.; Li, C.-J. *Angew. Chem., Int. Ed.* **2008**, *47*, 7075.
- (126) Li, Z.; Li, C.-J. *J. Am. Chem. Soc.* **2005**, *127*, 6968.
- (127) Cardellicchio, C.; Ciccarella, G.; Naso, F.; Schingaro, E.; Scordari, F. *Tetrahedron: Asymmetry* **1998**, *9*, 3667.
- (128) Yang, F.; Li, J.; Xie, J.; Huang, Z.-Z. *Org. Lett.* **2010**, *12*, 5214.
- (129) Ohta, M.; Quick, M. P.; Yamaguchi, J.; Wünsch, B.; Itami, K. *Chem. Asian J.* **2009**, *4*, 1416.
- (130) Tsuchimoto, T.; Ozawa, Y.; Negoro, R.; Shirakawa, E.; Kawakami, Y. *Angew. Chem., Int. Ed.* **2004**, *43*, 4231.
- (131) Li, Z.; Li, C.-J. *J. Am. Chem. Soc.* **2005**, *127*, 3672.
- (132) For reviews on vicinal diamines, see: (a) Lucet, D.; Le Gall, T.; Mioskowski, C. *Angew. Chem., Int. Ed.* **1998**, *37*, 2580. (b) Cardona, F.; Goti, A. *Nature Chem.* **2009**, *1*, 269. (c) Kotti, S. R. S. S.; Timmons, C.; Li, G. *Chem. Biol. Drug Design* **2006**, *67*, 101.
- (133) Baslé, O.; Li, C.-J. *Green Chem.* **2007**, *9*, 1047.
- (134) Condé, A. G.; González-Gómez, J. C.; Stephenson, C. R. J. *J. Am. Chem. Soc.* **2010**, *132*, 1464.
- (135) For reviews on Ru(bipy)₃Cl₂, see: (a) Kalyanasundaram, K. *Coord. Chem. Rev.* **1982**, *46*, 159. (b) Juris, A.; Balzani, V.; Barigelli, F.; Campagna, S.; Belser, P.; von Zelewsky, A. *Coord. Chem. Rev.* **1988**, *84*, 85. (c) Campagna, S.; Puntoriero, F.; Nastasi, F.; Bergamini, G.; Balzani, V. *Top. Curr. Chem.* **2007**, *280*, 117.
- (136) For reviews on visible light photocatalysis, see: (a) Yoon, T. P.; Ischay, M. A.; Du, J. *Nature Chem.* **2010**, *2*, 527. (b) Narayanam, J. M. R.; Stephenson, C. R. J. *Chem. Soc. Rev.* **2011**, *40*, 102.
- (137) Nicewicz, D.; MacMillan, D. W. C. *Science* **2008**, *322*, 77.
- (138) Ischay, M. A.; Anzovino, M. E.; Du, J.; Yoon, T. P. *J. Am. Chem. Soc.* **2008**, *130*, 12886.
- (139) Baslé, O.; Borduas, N.; Dubois, P.; Chapuzet, J. M.; Chan, T.-H.; Lessard, J.; Li, C.-J. *Chem.—Eur. J.* **2010**, *16*, 8162.
- (140) Li, Z.; Li, C.-J. *Eur. J. Org. Chem.* **2005**, 3173.
- (141) Sud, A.; Sureshkumar, D.; Klussmann, M. *Chem. Commun.* **2009**, 3169.
- (142) Xie, J.; Huang, Z.-Z. *Angew. Chem., Int. Ed.* **2010**, *49*, 10181.
- (143) For reviews on the Morita–Baylis–Hillman reaction, see: (a) Basavaiah, D.; Reddy, B. S.; Badsara, S. S. *Chem. Rev.* **2010**, *110*, 5447. (b) Basavaiah, D.; Rao, K. V.; Reddy, R. J. *Chem. Soc. Rev.* **2007**, *36*, 1581. (c) Basavaiah, D.; Rao, A. J.; Satyanarayana, T. *Chem. Rev.* **2003**, *103*, 811. (d) Basavaiah, D.; Rao, P. D.; Hyma, R. S. *Tetrahedron* **1996**, *52*, 8001.
- (144) Zhang, Y.; Li, C.-J. *Angew. Chem., Int. Ed.* **2006**, *45*, 1949.
- (145) Zhang, Y.; Li, C.-J. *J. Am. Chem. Soc.* **2006**, *128*, 4242.
- (146) For a review on allylic alkylation reactions with simple allyls, see: (a) Jensen, T.; Fristrup, P. *Chem.—Eur. J.* **2009**, *15*, 9632. (b) For a review on Pd-catalyzed Tsuji–Trost reactions, see: *Handbook of Organopalladium Chemistry for Organic Synthesis*; John Wiley & Sons, Inc.: New York, 2002; Vol. 1, Chapter V.2.
- (147) Li, Z.; Li, C.-J. *J. Am. Chem. Soc.* **2006**, *128*, 56.
- (148) Lin, S.; Song, C.-X.; Cai, G.-X.; Wang, W.-H.; Shi, Z.-J. *J. Am. Chem. Soc.* **2008**, *130*, 12901.
- (149) For a review on Wacker reactions, see: *Handbook of Organopalladium Chemistry for Organic Synthesis*; John Wiley & Sons, Inc.: New York, 2002; Vol. 1, Chapter V.3.
- (150) Young, A. J.; White, M. C. *J. Am. Chem. Soc.* **2008**, *130*, 14090.
- (151) Mo, H.; Bao, W. *Adv. Synth. Catal.* **2009**, *351*, 2845.
- (152) Cheng, D.; Bao, W. *Adv. Synth. Catal.* **2008**, *350*, 1263.
- (153) Cheng, D.; Bao, W. *J. Org. Chem.* **2008**, *73*, 6881.
- (154) Li, Y.-Z.; Li, B.-J.; Lu, X.-Y.; Lin, S.; Shi, Z.-J. *Angew. Chem., Int. Ed.* **2009**, *48*, 3817.
- (155) Benfatti, F.; Gapdevila, M. G.; Zoli, L.; Benedetto, E.; Cozzi, P. G. *Chem. Commun.* **2009**, 5919.
- (156) Guo, C.; Song, J.; Luo, S.-W.; Gong, L.-Z. *Angew. Chem., Int. Ed.* **2010**, *49*, 5558.
- (157) Song, C.-X.; Cai, G.-X.; Farrell, T. R.; Jiang, Z.-P.; Li, H.; Gan, L.-B.; Shi, Z.-J. *Chem. Commun.* **2010**, 6002.
- (158) Correia, C. A.; Li, C.-J. *Adv. Synth. Catal.* **2010**, *352*, 1446.
- (159) Kita, Y.; Morimoto, K.; Ito, M.; Ogawa, C.; Goto, A.; Dohi, T. *J. Am. Chem. Soc.* **2009**, *131*, 1668.
- (160) Jean, A.; Cantat, J.; Bérard, D.; Bouchu, D.; Canesi, S. *Org. Lett.* **2007**, *9*, 2553.
- (161) For seminal work on the Scholl reaction, see: (a) Scholl, R.; Seer, C. *Liebigs Ann. Chem.* **1912**, 394, 111. (b) For a recent account, see: King, B. T.; Kroulík, J.; Robertson, C. R.; Rempala, P.; Hilton, C. L.; Korinek, J. D.; Gortari, L. M. *J. Org. Chem.* **2007**, *72*, 2279.
- (162) Barluenga, J.; Trincado, M.; Rubio, E.; González, J. M. *Angew. Chem., Int. Ed.* **2006**, *45*, 3140.

- (163) For a review on BINOL ligands, see: (a) Brunel, J. M. *Chem. Rev.* **2005**, *105*, 857. (b) Chen, Y.; Yekta, S.; Yudin, A. K. *Chem. Rev.* **2003**, *103*, 3155.
- (164) For a review of natural products containing biphenols and binaphthols, see: Hubbard, B. K.; Walsh, C. T. *Angew. Chem., Int. Ed.* **2003**, *42*, 730.
- (165) Yamamoto, K.; Yumioka, H.; Okamoto, Y.; Chikamatsu, H. *J. Chem. Soc., Chem. Commun.* **1987**, 168.
- (166) (a) Hovorka, M.; Günterová, J.; Závada, J. *Tetrahedron Lett.* **1990**, *31*, 413. (b) Hovorka, M.; Ščigel, R.; Gunterová, J.; Tichý, M.; Závada, J. *Tetrahedron* **1992**, *48*, 9503. (c) Hovorka, M.; Závada, J. *Tetrahedron* **1992**, *48*, 9517.
- (167) Lipshutz, B. H.; Shin, Y.-J. *Tetrahedron Lett.* **1998**, *39*, 7017.
- (168) Grandbois, A.; Mayer, M.-E.; Bédard, M.; Collins, S. K.; Michel, T. *Chem.—Eur. J.* **2009**, *15*, 9655.
- (169) Li, X.; Hewgley, J. B.; Mulrooney, C. A.; Yang, J.; Kozlowski, M. C. *J. Org. Chem.* **2003**, *68*, 5500.
- (170) Egami, H.; Matsumoto, K.; Oguma, T.; Kunisu, T.; Katsuki, T. *J. Am. Chem. Soc.* **2010**, *132*, 13633.
- (171) (a) Smrčina, M.; Lorenc, M.; Hanuš, V.; Kočovský, P. *Synlett* **1991**, 231. (b) Smrčina, M.; Vyskočil, S.; Máca, B.; Polásek, M.; Claxton, T. A.; Abbott, A. P.; Kočovský, P. *J. Org. Chem.* **1994**, *59*, 2156.
- (172) Smrčina, M.; Lorenc, M.; Hanuš, V.; Sedmera, P.; Kočovský, P. *J. Org. Chem.* **1992**, *57*, 1917.
- (173) Lipshutz, B. H.; Buzard, D. J.; Olsson, C.; Noson, K. *Tetrahedron* **2004**, *60*, 4443.
- (174) Kupchan, S. M.; Liepa, A. J.; Kameswaran, V.; Bryan, R. F. *J. Am. Chem. Soc.* **1973**, *95*, 6861.
- (175) Iida, H.; Watanabe, Y.; Tanaka, M.; Kibayashi, C. *J. Org. Chem.* **1984**, *49*, 2412.
- (176) (a) McKillop, A.; Hunt, J. D.; Zelesko, M. J.; Fowler, J. S.; Taylor, E. C.; McGillivray, G.; Kienzle, F. *J. Am. Chem. Soc.* **1971**, *93*, 4841. (b) Taylor, E. C.; Kienzle, F.; Robey, R. L.; McKillop, A.; Hunt, J. D. *J. Am. Chem. Soc.* **1971**, *93*, 4845. (c) Larock, R. C.; Fellows, C. A. *J. Am. Chem. Soc.* **1982**, *104*, 1900.
- (177) Taylor, E. C.; Andrade, J. G.; McKillop, A. *J. Chem. Soc., Chem. Commun.* **1977**, 538.
- (178) Taylor, E. C.; Andrade, J. G.; Rall, G. J. H.; McKillop, A. *J. Am. Chem. Soc.* **1980**, *102*, 6513.
- (179) Cragg, J. E.; Herbert, R. B.; Jackson, F. B.; Moody, C. J.; Nicolson, I. T. *J. Chem. Soc., Perkin Trans. 1* **1982**, 2477.
- (180) Wang, K.-L.; Lü, M.-Y.; Wang, Q.-M.; Huang, R.-Q. *Tetrahedron* **2008**, *64*, 7504.
- (181) Wang, K.; Lü, M.; Yu, A.; Zhu, X.; Wang, Q. *J. Org. Chem.* **2009**, *74*, 935.
- (182) (a) Kita, Y.; Takada, T.; Gyoten, M.; Tohma, H.; Zenk, M. H.; Eichhorn, J. *J. Org. Chem.* **1996**, *61*, 5857. (b) Kita, Y.; Gyoten, M.; Ohtsubo, M.; Tohma, H.; Takada, T. *Chem. Commun.* **1996**, 1481. (c) Takada, T.; Arisawa, M.; Gyoten, H.; Hamada, R.; Tohma, H.; Kita, Y. *J. Org. Chem.* **1998**, *63*, 7698.
- (183) For reviews on medium-sized ring formation, see: (a) Yet, L. *Chem. Rev.* **2000**, *100*, 2963. (b) Molander, G. A. *Acc. Chem. Res.* **1998**, *31*, 603. (c) Illuminati, G.; Mandolini, L. *Acc. Chem. Res.* **1981**, *14*, 95.
- (184) Dohi, T.; Ito, M.; Morimoto, K.; Iwata, M.; Kita, Y. *Angew. Chem., Int. Ed.* **2008**, *47*, 1301.
- (185) Nicolaou, K. C.; Reingruber, R.; Sarlah, D.; Bräse, S. *J. Am. Chem. Soc.* **2009**, *131*, 2086.
- (186) Conrad, J. C.; Kong, J.; Laforteza, B. N.; MacMillan, D. W. C. *J. Am. Chem. Soc.* **2009**, *131*, 11640.
- (187) For seminal work on organocatalytic SOMO catalysis, see: (a) Beeson, T. D.; Mastracchio, A.; Hong, J.-B.; Ashton, K.; MacMillan, D. W. C. *Science* **2007**, *316*, 582. (b) Rendler, S.; MacMillan, D. W. C. *J. Am. Chem. Soc.* **2010**, *132*, 5027. (c) Jui, N. T.; Lee, E. C. Y.; MacMillan, D. W. C. *J. Am. Chem. Soc.* **2010**, *132*, 10015. (d) Devery, J. J., III; Conrad, C. J.; MacMillan, D. W. C.; Flowers, R. A., II. *Angew. Chem., Int. Ed.* **2010**, *49*, 6106. (e) Graham, T. H.; Jones, C. M.; Jui, N. T.; MacMillan, D. W. C. *J. Am. Chem. Soc.* **2008**, *130*, 16494. (f) Ref 185. (g) Ref 186.
- (188) Um, J. M.; Guitierrez, O.; Schoenebeck, F.; Houk, K. N.; MacMillan, D. W. C. *J. Am. Chem. Soc.* **2010**, *132*, 6001.
- (189) Rathke, M. W.; Lindhert, A. *J. Am. Chem. Soc.* **1971**, *93*, 4605.
- (190) (a) Ito, Y.; Konoike, T.; Saegusa, T. *J. Am. Chem. Soc.* **1975**, *97*, 2912. (b) Ito, Y.; Konoike, T.; Harada, T.; Saegusa, T. *J. Am. Chem. Soc.* **1977**, *99*, 1487.
- (191) Tokuda, M.; Shigei, T.; Itoh, M. *Chem. Lett.* **1975**, *4*, 621.
- (192) Baran, P. S.; Guerrero, C. A.; Ambhaikar, N. B.; Hafenstein, B. D. *Angew. Chem., Int. Ed.* **2005**, *44*, 606.
- (193) Baran, P. S.; Guerrero, C. A.; Hafenstein, B. D.; Ambhaikar, N. B. *Angew. Chem., Int. Ed.* **2005**, *44*, 3892.
- (194) Baran, P. S.; Hafenstein, B. D.; Ambhaikar, N. B.; Guerrero, C. A.; Gallagher, J. D. *J. Am. Chem. Soc.* **2006**, *128*, 8678.
- (195) Martin, C. L.; Overman, L. E.; Rohde, J. M. *J. Am. Chem. Soc.* **2008**, *130*, 7568.
- (196) Tobinaga, S.; Kotani, E. *J. Am. Chem. Soc.* **1972**, *94*, 309.
- (197) Martin, C. L.; Overman, L. E.; Rohde, J. M. *J. Am. Chem. Soc.* **2010**, *132*, 4894.
- (198) DeMartino, M. P.; Chen, K.; Baran, P. S. *J. Am. Chem. Soc.* **2008**, *130*, 11546.
- (199) Richter, J. M.; Ishihara, Y.; Masuda, T.; Whitefield, B. W.; Llamas, T.; Pohjakallio, A.; Baran, P. S. *J. Am. Chem. Soc.* **2008**, *130*, 17938.
- (200) Baran, P. S.; Richter, J. M. *J. Am. Chem. Soc.* **2004**, *126*, 7450.
- (201) Richter, J. M.; Whitefield, B. W.; Maimone, T. J.; Lin, D. W.; Castroviejo, M. P.; Baran, P. S. *J. Am. Chem. Soc.* **2007**, *129*, 12857.
- (202) Zuo, Z.; Xie, W.; Ma, D. *J. Am. Chem. Soc.* **2010**, *132*, 13226.
- (203) Baran, P. S.; Richter, J. M.; Lin, D. W. *J. Am. Chem. Soc.* **2005**, *127*, 609.
- (204) Borduas, N.; Powell, D. A. *J. Org. Chem.* **2008**, *73*, 7822.
- (205) Zhang, Y.; Li, C.-J. *Eur. J. Org. Chem.* **2008**, 4654.
- (206) Deng, G.; Zhao, L.; Li, C.-J. *Angew. Chem., Int. Ed.* **2008**, *47*, 6278.
- (207) Jia, Y.-X.; Kündig, E. P. *Angew. Chem., Int. Ed.* **2009**, *48*, 1636.
- (208) (a) Perry, A.; Taylor, R. J. K. *Chem. Commun.* **2009**, 3249. (b) Pugh, D. S.; Klein, J. E. M. N.; Richard, A. P.; Taylor, J. K. *Synlett* **2010**, 934.
- (209) Klein, J. E. M. N.; Perry, A.; Pugh, D. S.; Taylor, R. J. K. *Org. Lett.* **2010**, *12*, 3446.
- (210) For reviews on cytochrome P450s, see: (a) Bugg, T. D. H. *Introduction to Enzyme and Coenzyme Chemistry*, 2nd ed.; Blackwell Publishing Ltd.: Oxford, U.K., 2004; Chapter 6. (b) Silverman, R. B. *The Organic Chemistry of Enzyme-Catalyzed Reactions*, 2nd ed.; Academic Press: San Diego, 2002; Chapters 3–6. (c) Denisov, I. G.; Makris, T. M.; Sligar, S. G.; Schlichting, I. *Chem. Rev.* **2005**, *105*, 2253.
- (211) Grobe, N.; Zhang, B.; Fisinger, U.; Kutchan, T. M.; Zenk, M. H.; Guengerich, F. P. *J. Biol. Chem.* **2009**, *284*, 24425.
- (212) For a review on ROS, see: Novo, E.; Parola, M. *Fibrogen. Tissue Rep.* **2008**, *1*, 5.
- (213) For a review on oxidative couplings involving tyrosine residues, see: Fry, S. C. *Phytochem. Rev.* **2004**, *3*, 97.
- (214) (a) Brady, J. D.; Sadler, I. H.; Fry, S. C. *Phytochemistry* **1998**, *47*, 349. (b) Nomura, K.; Suzuki, N.; Matsumoto, S. *Biochemistry* **1990**, *29*, 4525.
- (215) Fujimoto, D.; Horiuchi, K.; Hiram, M. *Biochem. Biophys. Res. Commun.* **1981**, *99*, 637.
- (216) (a) Rouau, X.; Cheynier, V.; Surget, A.; Gloux, D.; Barron, C.; Meudec, E.; Louis-Montero, J.; Criton, M. *Phytochemistry* **2003**, *63*, 899. (b) Bunzel, M.; Ralph, J.; Funk, C.; Steinhart, H. *Eur. Food Res. Technol.* **2003**, *217*, 128.
- (217) (a) Ban, F.; Lundqvist, M. J.; Boyd, R. J.; Eriksson, L. A. *J. Am. Chem. Soc.* **2002**, *124*, 2753. (b) Mitrassinovic, P. M. *Bioconjugate Chem.* **2005**, *16*, 588. (c) Shamovsky, I. L.; Riopelle, R. J.; Ross, G. M. *J. Phys. Chem. A* **2001**, *105*, 1061.
- (218) For reviews on prodiginines, see: (a) Williamson, N. R.; Fineran, P. C.; Leeper, F. J.; Salmond, G. P. C. *Nature Rev. Microbiol.* **2006**, *4*, 887. (b) Fürstner, A. *Angew. Chem., Int. Ed.* **2003**, *42*, 3582.

- (219) (a) Cerdeño, A. M.; Bibb, M. J.; Challis, G. L. *Chem. Biol.* **2001**, *8*, 817. (b) For a recent stereochemical elucidation of streptorubin B, see: Haynes, S. W.; Sydor, P. K.; Corre, C.; Song, L.; Challis, G. L. *J. Am. Chem. Soc.* **2011**, *133*, 1793.
- (220) For reviews on modern indole syntheses, see: (a) Cacchi, S.; Fabrizi, G. *Chem. Rev.* **2005**, *105*, 2873. (b) Gribble, G. W. *J. Chem. Soc., Perkin Trans. 1* **2000**, 1045. (c) Campo, J.; García-Valverde, M.; Maraccini, S.; Rojo, M. J.; Torroba, T. *Org. Biomol. Chem.* **2006**, *4*, 757. (d) For selected examples, see: Hsieh, T. H. H.; Dong, V. M. *Tetrahedron* **2009**, *65*, 3062. (e) Stokes, B. J.; Dong, H.; Leslie, B. E.; Pumphrey, A. L.; Driver, T. G. *J. Am. Chem. Soc.* **2007**, *129*, 7500. (f) Shi, Z.; Zhang, C.; Li, S.; Pan, D.; Ding, S.; Cui, Y.; Jiao, N. *Angew. Chem., Int. Ed.* **2009**, *48*, 4572. (g) Fang, Y.-Q.; Lautens, M. *Org. Lett.* **2005**, *7*, 3549. (h) Kumar, M. P.; Liu, R.-S. *J. Org. Chem.* **2006**, *71*, 4951. (i) Taber, D. F.; Tian, W. *J. Am. Chem. Soc.* **2006**, *128*, 1058. (j) Penoni, A.; Palmisano, G.; Broggini, G.; Kadowaki, A.; Nicholas, K. M. *J. Org. Chem.* **2006**, *71*, 823. (k) Yue, D.; Yao, T.; Larock, R. C. *J. Org. Chem.* **2006**, *71*, 62.
- (221) For reviews on the Fischer indole synthesis, see: (a) Robinson, B. *Chem. Rev.* **1963**, *63*, 373. (b) Robinson, B. *Chem. Rev.* **1969**, *69*, 227.
- (222) Larock, R. C.; Yum, E. K.; Refvik, M. D. *J. Org. Chem.* **1998**, *63*, 7652.
- (223) Würtz, S.; Rakshit, S.; Neumann, J. J.; Dröge, T.; Glorius, F. *Angew. Chem., Int. Ed.* **2008**, *47*, 7230.
- (224) Bernini, R.; Fabrizi, G.; Sferazza, A.; Cacchi, S. *Angew. Chem., Int. Ed.* **2009**, *48*, 8078.
- (225) Guan, Z.-H.; Yan, Z.-Y.; Ren, Z.-H.; Liu, X.-Y.; Liang, Y.-M. *Chem. Commun.* **2010**, *46*, 2823.
- (226) Yu, W.; Du, Y.; Zhao, K. *Org. Lett.* **2009**, *11*, 2417.
- (227) For a review of the Sonogashira coupling, see: Chinchilla, R.; Najera, C. *Chem. Rev.* **2007**, *107*, 874.
- (228) Yang, L.; Zhao, L.; Li, C.-J. *Chem. Commun.* **2010**, *46*, 4184.
- (229) Wei, Y.; Zhao, H.; Kan, J.; Su, W.; Hong, M. *J. Am. Chem. Soc.* **2010**, *132*, 2522.
- (230) Matsuyama, N.; Kitahara, M.; Hirano, K.; Satoh, T.; Miura, M. *Org. Lett.* **2010**, *12*, 2358.
- (231) Kitahara, M.; Hirano, K.; Tsurugi, H.; Satoh, T.; Miura, M. *Chem.—Eur. J.* **2010**, *16*, 1772.
- (232) de Haro, T.; Nevado, C. *J. Am. Chem. Soc.* **2010**, *132*, 1512.
- (233) For a related account, see: Brand, J. P.; Charpentier, J.; Waser, J. *Angew. Chem., Int. Ed.* **2009**, *48*, 9346.
- (234) Yin, W.; He, C.; Chen, M.; Zhang, H.; Lei, A. *Org. Lett.* **2009**, *11*, 709.
- (235) For reviews on aldehydic C—H bond activation, see: (a) Garralda, M. A. *Dalton Trans.* **2009**, 3635. (b) Willis, M. C. *Chem. Rev.* **2010**, *110*, 725. (c) Jun, C.-H.; Park, Y. J. *Acc. Chem. Res.* **2008**, *41*, 222. (d) Jun, C.-H.; Moon, C. W.; Lee, D.-Y. *Chem.—Eur. J.* **2002**, *8*, 2422. (e) For selected recent examples, see: Coulter, M. M.; Kou, K. G. M.; Galligan, B.; Dong, V. M. *J. Am. Chem. Soc.* **2010**, *132*, 16330. (f) Phan, D. H. T.; Kou, K. G. M.; Dong, V. M. *J. Am. Chem. Soc.* **2010**, *132*, 16354. (g) Shibata, Y.; Tanaka, K. *J. Am. Chem. Soc.* **2009**, *131*, 12552. (h) Mora, G.; Darses, S.; Genet, J.-P. *Adv. Synth. Catal.* **2007**, *349*, 1180. (i) Qin, C.; Chen, J.; Wu, H.; Cheng, J.; Zhang, Q.; Zuo, B.; Su, W.; Ding, J. *Tetrahedron Lett.* **2008**, *49*, 1884.
- (236) Tang, B.-X.; Song, R.-J.; Wu, C.-Y.; Liu, Y.; Zhou, M.-B.; Wei, W.-T.; Deng, G.-B.; Yin, D.-L.; Li, J.-H. *J. Am. Chem. Soc.* **2010**, *132*, 8900.
- (237) Jia, X.; Zhang, S.; Wang, W.; Luo, F.; Cheng, J. *Org. Lett.* **2009**, *11*, 3120.
- (238) Chan, C.-W.; Zhou, Z.; Chan, A. S. C.; Yu, W.-Y. *Org. Lett.* **2010**, *12*, 3926.
- (239) Hopkinson, M. N.; Tessier, A.; Salisbury, A.; Giuffredi, G. T.; Combettes, L. E.; Gee, A. D.; Gouverneur, V. *Chem.—Eur. J.* **2010**, *16*, 4739.
- (240) Oxidative cross-coupling is a rapidly advancing field. During the review process, the following accounts appeared in the literature: (a) Feng, C.; Loh, T.-P. *J. Am. Chem. Soc.* **2010**, *132*, 17710. (b) Faggi, E.; Sebastián, R. M.; Pleixats, R.; Vallibera, A.; Shafir, A.; Rodríguez-Gimeno, A.; Ramírez de Arellano, C. *J. Am. Chem. Soc.* **2010**, *132*, 17980. (c) Shirakawa, E.; Ichiyama, N.; Hayashi, T. *J. Org. Chem.* **2011**, *76*, 25. (d) Tsai, A. S.; Brasse, M.; Bergman, R. G.; Ellman, J. A. *Org. Lett.* **2011**, *13*, 540. (e) Patureau, F. W.; Besset, T.; Glorius, F. *Angew. Chem., Int. Ed.* **2011**, *50*, 1064. (f) Han, W.; Mayer, P.; Ofial, A. R. *Angew. Chem., Int. Ed.* **2011**, DOI: 10.1002/anie.201006208. (g) Schrittwieser, J. H.; Resch, V.; Sattler, J. H.; Lienhart, W.-D.; Durchschein, K.; Winkler, A.; Gruber, K.; Macheroux, P.; Kroutil, W. *Angew. Chem., Int. Ed.* **2011**, *50*, 1068. (h) Ueyama, T.; Mochida, S.; Fukutani, T.; Hirano, K.; Satoh, T.; Miura, M. *Org. Lett.* **2011**, *13*, 706. (i) Rakshit, S.; Grohmann, C.; Besset, T.; Glorius, F. *J. Am. Chem. Soc.* **2011**, DOI: 10.1021/ja109676d. (j) Hackeloer, K.; Schnakenburg, G.; Waldvogel, S. R. *Org. Lett.* **2011**, DOI: 10.1021/ol102969k. (k) Zhu, C.; Falck, J. R. *Org. Lett.* **2011**, DOI: 10.1021/ol200093f. (l) Huang, L.; Niu, T.; Wu, J.; Zhang, Y. *J. Org. Chem.* **2011**, DOI: 10.1021/jo1023975. (m) Yang, Y.; Chen, L.; Zhang, Z.; Zhang, Y. *Org. Lett.* **2011**, DOI: 10.1021/ol200025k. (n) Jessing, M.; Baran, P. S. *Heterocycles* **2011**, *82*, 1739. (o) Malakar, C. C.; Schmidt, D.; Conrad, J.; Beifuss, U. *Org. Lett.* **2011**, DOI: 10.1021/ol200065s.
- (241) For a review on alkane metathesis, see: (a) Basset, J.-M.; Copéret, C.; Soulivong, D.; Taoufik, M.; Thivolle-Cazat, J. *Angew. Chem., Int. Ed.* **2006**, *45*, 6082. (b) For selected examples, see: Goldman, A. S.; Roy, A. H.; Huang, Z.; Ahuja, R.; Schinski, W.; Brookhart, M. *Science* **2006**, *312*, 257. (c) Vidal, V.; Théolier, A.; Thivolle-Cazat, J.; Basset, J.-M. *Science* **1997**, *276*, 99. (d) Basset, J. M.; Copéret, C.; Lefort, L.; Maunders, B. M.; Maury, O.; Le Rouz, E.; Saggio, G.; Soignier, S.; Soulivong, D.; Sunley, G. J.; Taoufik, M.; Thivolle-Cazat, J. *J. Am. Chem. Soc.* **2005**, *127*, 8604. (e) Ahuja, R.; Kundu, S.; Goldman, A. S.; Brookhart, M.; Vicente, B.; Scott, S. L. *Chem. Commun.* **2008**, 253. (f) Joubert, J.; Delbecq, F.; Sautet, P. *J. Catal.* **2007**, *251*, 507. (g) Ito, T.; Wang, J.-X.; Lin, C.-H.; Lunsford, J. H. *J. Am. Chem. Soc.* **1985**, *107*, 5062. (h) Burnett, R. L.; Hughes, T. R. *J. Catal.* **1973**, *31*, 55.